INFORMATION TO USERS

This manuscript has been reproduced from the microfilm master. UMI films the text directly from the original or copy submitted. Thus, some thesis and dissertation copies are in typewriter face, while others may be from any type of computer printer.

The quality of this reproduction is dependent upon the quality of the copy submitted. Broken or indistinct print, colored or poor quality illustrations and photographs, print bleedthrough, substandard margins, and improper alignment can adversely affect reproduction.

In the unlikely event that the author did not send UMI a complete manuscript and there are missing pages, these will be noted. Also, if unauthorized copyright material had to be removed, a note will indicate the deletion.

Oversize materials (e.g., maps, drawings, charts) are reproduced by sectioning the original, beginning at the upper left-hand corner and continuing from left to right in equal sections with small overlaps.

ProQuest Information and Learning
300 North Zeeb Road, Ann Arbor, MI 48106-1346 USA
800-521-0600

Sc

CONTROLLED POTENTIAL STUDIES ON THE KOLBE REACTION

by

A.K. Vijh

A thesis submitted in partial fulfillment
of the requirements for the degree of
Doctor of Philosophy
in the
Department of Chemistry
University of Ottawa
Ottawa, Canada
February, 1966

B.E. Conway
Professor of Chemistry
Research Supervisor

A.K. Vijh
Ph.D. Candidate

PREFACE

The phenomenological aspects of organic electrode reactions, including the Kolbe reaction, have been extensively examined for several decades from the point of view of preparative organic chemistry. However, only relatively superficial investigations have, until recently, been available on the electrochemical kinetic and related aspects of these reactions. The Kolbe reaction is a relatively simple example of an organic electrode process; however, as a class, such processes are usually quite complex. Electrode-kinetic aspects of this reaction have been the subject of investigations at the University of Newcastle on Tyne and previously in this Department.

Previous experimental work from this laboratory and that reported in the literature led to the conclusion that the Kolbe reaction merited further investigation by use of recently developed controlled potential techniques and modern approaches regarding kinetics of consecutive reactions. Accordingly, the present project was undertaken in order to examine the mechanism of the Kolbe reaction at platinum and gold in several non-aqueous and aqueous solutions. In the present work, mechanistic investigations on the Kolbe reaction have been conducted with special reference to the following matters.

(i) The kinetic behaviour of the Kolbe reaction under potentiostatic and potentiodynamic conditions. Such approaches yield more significant experimental information than do the galvanostatic techniques used previously for reasons discussed in the text of this thesis.

(ii) The role of surface oxides that might be co-adsorbed with the Kolbe species on the electrode in the presence of traces or excess of water in the solutions examined. This information, it will be shown, is indispensable in the comparative examination of the reaction mechanisms in non-aqueous and aqueous solutions to be discussed in the present thesis.

(iii) The Kolbe reaction as an example of the special class of heterogeneous reactions, "electrode processes". This approach has involved a kinetic analysis of a scheme of consecutive processes that may be involved in the overall Kolbe reaction; the related problem of pseudo-capacity and charge associated with the adsorbed intermediates and the potential dependence of these quantities has also been examined, and correlations between these quantities and the reaction mechanisms have been proposed.

For the sake of convenience and brevity, Naperian Tafel slopes have been referred to in the text, whereas in the graphs and tables etc., decadic (Briggsian) Tafel slopes have been employed in the representation of the numerical data.

ACKNOWLEDGEMENTS

The author wishes to express his thanks to Professor B.E. Conway, under whose direction and constant supervision this work was carried out. Throughout the course of this research, as well as in the preparation of the manuscript, Professor Conway was always prepared to give freely of his time and advice. Professor Conway's contagious enthusiasm and patient approach helped the author in many less tangible ways whenever difficulties arose.

The author is also indebted to the Ontario Government for the award of a Graduate Fellowship for the year 1963-1964, and to the Sprague Electric Company, North Adams, Mass., U.S.A. for the award of a Fellowship for the years 1964-1966. Financial support for part of this research project was also provided by the National Research Council of Canada.

Thanks are also due to Dr. D. Gilroy for numerous critical discussions and for permission to quote some of his original results which are in course of publication. The assistance of Mr. E. Rudd with the vapour phase charomatographic measurements and of Mrs. J. Rudd in typing the manuscript is gratefully acknowledged.

TABLE OF CONTENTS

Page No.

CHAPTER II

EXPERIMENTAL

LIST OF FIGURES

LIST OF TABLES

ABSTRACT

The mechanism of the Kolbe reaction has been examined (a) on Pt and Au in "very anhydrous", "nominally anhydrous" and aqueous 1M KTFA/TFA solutions, (b) on Pt in "very anhydrous" 1M CH_3COOK/CH_3COOH solution (in vacuo) and in aqueous (1M CH_3COOK + 1M CH_3COOH) solution, and (c) on Au in "nominally anhydrous" 1M CH_3COOK/CH_3COOH solution and in aqueous (1M CH_3COOK + 1M CH_3COOH) solution. Controlled potential techniques have been used and both steady-state and non-steady state measurements have been carried out. These measurements have been conducted in order to seek information on the steady-state kinetics of the reaction under controlled potential conditions and on the identity and extent of adsorption of the intermediates that may be present on the electrode surface. The potential dependence of the pseudo-capacity and charge associated with the ad-species has also been discussed and its significance has been examined. Previous data on the characterisation of the products of electrolyses have been qualitatively checked and confirmed. Several types of correlations and derived plots have been discussed which illustrate the significance of the experimental data in relation to the derivation of the mechanisms of the electrode reaction under various conditions. On the basis of these data and treatments, mechanisms are proposed for the

Kolbe reaction on platinum and gold in the various types of solutions studied.

In general, high Tafel slopes have been observed in most of the cases studied. The presence of traces or excess of water in solutions seems to result in the co-adsorption of surface oxide together with the Kolbe ad-species both on platinum and gold. The co-adsorbed oxide has been shown to be an inhibiting species in all cases where its presence is indicated experimentally.

In the case of gold in aqueous (1M CH_3COOK + 1M CH_3COOH) solution, the Kolbe reaction has been shown to be completely inhibited, probably by surface oxides, so that the oxygen evolution reaction is predominant, in agreement with the conclusions of previous workers. In the case of the Kolbe reaction on platinum in very anhydrous 1M KTFA/TFA solutions, it has been concluded that the reaction proceeds on a "barrier-layer" film of "electro-inactive" ad-species, $CF_3^{\bullet}$. In the case of very anhydrous 1M CH_3COOK/CH_3COOH solutions, it is believed that the Kolbe reaction on platinum proceeds by initial discharge of the CH_3COO^- ion as the rate-determining step (r.d.s.). In all other cases, it appears that the Kolbe reaction proceeds on a film (which is effectively a barrier-layer) of adsorbed $RCOO^{\bullet}$ (with or without co-adsorbed oxide, depending on whether or not some

water is present in the solution) across which a part of the total metal-solution potential drop is regarded as operating and which is hence not available for assisting the activation controlled charge transfer process. This would result in a diminution of the values of the effective symmetry factor β and hence lead to high Tafel slopes, which indeed are experimentally observed. In all these cases, electrochemical desorption of the $RCOO^{\bullet}$ species has been suggested as the rate-determining step (r.d.s.).

An hypothesis has been presented which seems to provide a plausible explanation for a number of important general characteristics associated with the Kolbe electrosynthesis, e.g., the inhibition of oxygen evolution in aqueous media. A brief discussion of recent related work has also been presented.

CHAPTER I

INTRODUCTION

1. GENERAL

The study of electrode processes has been the subject of intensive investigation since 1833 when Faraday reported the first semi-quantitative experiments on the electrolysis of aqueous solutions (1), including acetic acid. Most of the early effort in the field of electrode kinetics was directed to the investigation of the hydrogen and oxygen evolution reactions and in more recent years to the study of metal deposition or electro-crystallisation. Electrode processes involving organic species have received relatively little attention from a basic electrochemical mechanistic point of view and are hence much less understood. However, many synthetic reactions have been carried out by electrochemical means.

The Kolbe reaction, which is the subject of the present investigation, has been extensively studied by organic chemists interested in synthetic applications of the reaction. Recently (2,3) there have also been some investigations the purpose of which has been the elucidation of the electrochemical kinetics of the Kolbe reaction. However, these studies have usually been made under galvanostatic conditions (i.e. constant current conditions) which fail to control effectively the most important variable in the kinetics of electrode processes, namely, the potential of the working electrode. While in

most cathodic processes it is usually found that the galvanostatic and potentiostatic methods give essentially the same results, in anodic reactions where non-linear log [current] - potential behaviour often arises, use of the potentiostatic method is quite essential for the full study of the electrochemical kinetic characteristics of the reaction. In the present investigation, techniques employing potential-controlling devices, which were not easily available until relatively recently, have been used. Use of potentiostatic or potentiodynamic techniques yields results which are more valid and significant in the interpretation of electrochemical kinetics of the processes involved at the electrode in the Kolbe reaction, than those obtainable by galvanostatic procedures. The electrochemical significance of the controlled-potential techniques will be discussed in detail in section C of this chapter.

In the present investigation, particular attention has been paid to a comparative study of the kinetics of the Kolbe reaction, from a mechanistic point of view, in completely non-aqueous media, in media containing traces of water and finally in solutions where excess of water was deliberately added. This approach was adopted in order to seek information on the role of surface oxides in the Kolbe reaction, and this has constituted a principal aspect of the present work.

2. KOLBE REACTION

(i) Phenomenology

(a) Organic Chemical Aspects

The production of a hydrocarbon at the anode upon electrolysis of an acetate solution (or, in general, aliphatic carboxylates), generally known as the Kolbe reaction, was, it seems, first observed by Faraday in 1834 (4). However, detailed results were not obtained until 1849 by Kolbe who showed that electrolysis of an alkali metal acetate led to the formation of a hydrocarbon subsequently known as ethane, together with two volumes of carbon dioxide (5). More generally, the Kolbe reaction refers to an anodic reaction involving a carboxylate structure, producing carbon dioxide together with a hydrocarbon or a corresponding hydrocarbon derivative. The overall anodic reaction can be written as

$$2RCOO^- \longrightarrow 2CO_2 + R\text{-}R + 2e$$

where R is an aliphatic alkyl function or an alkyl residue substituted in certain ways.

A considerable amount of work has been carried out on this reaction with regard to its use in preparative organic chemistry. Several attempts have also been made at elucidating the mechanism of this reaction using mostly the techniques and principles of synthetic and mechanistic organic chemistry. Since a number of excellent reviews and bibliographies have already been published on the organic chemistry of this reaction (see references 6, 18, 25) a further review of this aspect of the problem is not justified in the present thesis.

(b) Electrochemical Aspects

The experimental conditions used in much of the earlier work cannot be considered ideal in relation to modern techniques available for the investigation of electrode processes.

Measurements of electrode potentials over a range of current densities have been carried out by several investigators (2,3,7-11) for the acetate case and for higher homologues and plots of anode potential versus log [current density] have in all cases shown discontinuities in the curves, corresponding to a sudden increase in the anode potential at a particular current density and vice versa. Analysis of products over a range of current densities has shown that in acidic solutions (9-15) (for a series of alkali metal carboxylic acid salts and/or corresponding acids from acetic to heptanoic), the major product at low current densities was oxygen together with a variety of oxidative degradation products derived from the entity R. As a critical current density and associated potential is approached, the yields of carbon dioxide and the Kolbe product R_2 begin to become appreciable, while the rate of production of oxygen decreases. At and above the critical current density, the major products are as expected for the Kolbe electrosynthesis together with negligible amounts, if any, of oxygen. Under alkaline solution conditions, Hofer and Moest (16) have shown that methyl alcohol is formed instead of ethane during the electrolysis of acetates, particularly at Au.

The range of so-called critical potentials in aqueous solutions lies in the region 2.1-2.2 volts (with respect to the potential of the normal hydrogen electrode). In non-aqueous solutions, Glasstone and Hickling (17) have shown that the critical potential for the electrolysis of acetates and/or acetic acid was similar to that observed (viz. 2.14V) for aqueous solutions (17), and that the current efficiencies for ethane production were quantitatively similar in the two types of system.

Recently Conway and Dzieciuch (2) have established that the Kolbe reaction occurs on an electrode to some extent covered by adsorbed intermediates (R$^{\bullet}$, RCOO$^{\bullet}$ etc.) and that a part of the total metal-solution potential drop operates across this adsorbed layer and is hence not utilised for the normal activation-controlled discharge process occurring across the ionic double-layer. Thus, it is only an unusually small fraction (< 0.5) of the total metal-solution potential drop which assists the discharge of the reactant species from its initial state to the activated state, i.e.,there is a consequent decrease in the effective value of the symmetry factor β (which, in the absence of such adsorbed layers, normally has a value close to 0.5 for many reactions), so that high Tafel slopes arise.

All the investigations summarised above were carried out under galvanostatic conditions, i.e., current was controlled

as the independent variable in obtaining the current-potential relations.

(ii) Proposed Mechanisms for the Kolbe Reaction

Numerous early theories were proposed for the mechanism of the Kolbe synthesis; almost all of them were based on the analysis of the end products of the reaction and in some cases the conclusions were supplemented by electrochemical considerations based on scanty and electrochemically unsound experimental evidence with little theoretical analysis. A brief review of these theories, some of them essentially of historical interest only, will be presented here. Details of these theories as well as the criticisms to which they were subject, have been omitted since full reviews have already been published (6,18).

(a) The Acyl Peroxide Theory

This was originally proposed by Schall (19) and subsequently developed by Fichter (20,21). These investigators proposed the view that the acetate ions were discharged at the anode, and the resulting acetoxyl radicals reacted to form diacetyl peroxide, which then decomposed to form alkyl radicals and thence the hydrocarbon. Their mechanism may be summarised in the following scheme:

$$\left.\begin{array}{l} CH_3COO^- \longrightarrow CH_3COO^{\bullet} \\ CH_3COO^- \longrightarrow CH_3COO^{\bullet} \end{array}\right] \longrightarrow \begin{array}{l} CH_3COO \\ | \\ CH_3COO \end{array} \longrightarrow 2CO_2 + C_2H_6$$

If this mechanism were valid, it would be expected that diacetyl peroxide would be detectable under the normal conditions of electrolysis; positive results were obtained only under very special experimental conditions (low temperature and streaming of the electrolyte) when diacetyl peroxide was detected in very small amounts (22,23). Even under these circumstances, it cannot be concluded that diacetyl peroxide is a true intermediate in the consecutive series of reactions which are involved and not a side product arising from the rather special conditions used. This, among other observations, is a major objection to this theory.

(b) Hydrogen Peroxide Theory

This theory was proposed by Glasstone and Hickling, (7,17,24). According to these authors, in the electrolysis of aqueous acetate solutions, hydrogen peroxide is first formed at the anode from adsorbed hydroxyl radicals. The hydrogen peroxide thus formed, or the hydroxyl radicals themselves prior to their recombination in pairs, then react with the acetate ions to form acetate radicals. These then combine, possibly with the intermediate formation of diacetyl peroxide, to yield ethane and carbon dioxide, according to the scheme:

$$2CH_3COO^- + 2OH^\bullet \longrightarrow 2CH_3COO^\bullet + 2OH^-$$

or

$$2CH_3COO^- + H_2O_2 \longrightarrow 2CH_3COO^\bullet + 2OH^-, \text{ followed by:}$$

$$2CH_3COO^\bullet \longrightarrow (CH_3COO)_2 \longrightarrow CH_3\text{-}CH_3 + 2CO_2$$

Numerous criticisms have been raised against this mechanism, the most serious of them are:

(α) that addition of concentrated hydrogen peroxide to acetate solutions produces only trace amounts of hydrocarbon (7,24);

(β) that attempts to detect even trace amounts of hydrogen peroxide during, and following Kolbe electrolysis have not been successful (18,25);

(γ) that this mechanism also fails to account for the fact that the Kolbe synthesis takes place with high efficiency in non-aqueous media (2,8,25) where H_2O_2 could not be involved.

(c) <u>The Free Radical Theory</u>

This was originally proposed by Crum-Brown and Walker (26) and supported by Walker and co-workers (14,27). The important steps in the proposed mechanisms are the direct electrochemical oxidation of the carboxylate ion and subsequent decomposition of the radicals formed. The consecutive steps in the reaction can be written as:

$$2RCOO^- \longrightarrow 2RCOO^\bullet + 2e$$

$$2RCOO^\bullet \longrightarrow 2R^\bullet + 2CO_2$$

$$R^\bullet + R^\bullet \longrightarrow R\text{-}R$$

Although it was not specifically discussed in the early work on this theory, the presumption must be made that the radicals $RCOO^{\bullet}$ and $R^{\bullet}$ in the above scheme are specifically, or chemisorbed, at sites upon the metal electrode surface acting as an electrocatalyst for the reaction.

Although each of the above proposed mechanisms was postulated as occurring through several steps, no mention was made by the authors concerning which step might be rate-determining nor what current-potential behaviour would limitingly be associated with each step. Such an analysis, however, has been given by Conway and Dzieciuch (2) in an attempt to elucidate the rate-determining step for Tafel regions of galvanostatic current-potential curves for the Kolbe reaction.

A number of elegant investigations have been reported which tend to favour the free radical mechanism for the Kolbe reaction. Such studies include the work of (α) Clusius and co-workers (28,29,30) who used isotopic tracer techniques; (β) Wilson and Lippincott (31) who reported kinetic studies of the anodic oxidation of carboxylic acids by a periodic polarisation technique; (γ) Fieser, Clapp and Daudt (32) who showed that trinitrotoluene can be methylated in the anode compartment during an electrolysis of an aqueous solution of acetate; (δ) also acetylation and acetoxylation of certain substrates can be achieved (18).

All these investigations, which support the free-radical mechanism for the Kolbe reaction, have been recently reviewed (6) and hence do not merit further examination here.

Pande and Shukla (11) have also reported investigations supporting the free-radical theory of the Kolbe reaction.

Dickinson and Wynne-Jones (3) have made an interesting study of the Kolbe electrosynthesis on Pt, Ir, and Au in aqueous acetate solutions; they examined galvanostatic current-potential behaviour and galvanostatic charging curves under a variety of experimental conditions. The conclusions of these authors give further support, with some modifications, to the free-radical mechanism suggested by Walker and co-workers.

The recent investigations of Conway and Dzieciuch (2,6) involving examination of intermediates that might be adsorbed on the electrode give further direct support to a free-radical mechanism for the Kolbe reaction.

A critical assessment of the recent work on the electrochemical aspects of the Kolbe reaction (2,3,11,60) will be presented in Chapter IV of the thesis.

3. EXPERIMENTAL APPROACHES FOR INVESTIGATING ELECTRODE PROCESSES

In general, the study of electrode processes must usually be conducted complementarily by a number of related methods. In the present work on the Kolbe reaction, several approaches have been used which will be described below together with their respective limitations.

(1) Steady-State Current-Potential Relations

The classical approach for the study of electrode reactions involves measurements of current-potential relations, in which the rate is measured directly in terms of current i as a function of potential V. In a number of cases, including the Kolbe reaction examined here, the rate of the reaction must be related to the current passing by means of experimental studies of coulombic or Faradaic yields of reaction products. In the hydrogen or oxygen evolution reactions, however, this procedure is usually unnecessary, since H_2 or O_2 are the only chemical products.

Under limiting conditions of surface coverage ($\theta \rightarrow 0$ or $\theta \rightarrow 1$) by possible adsorbed reaction intermediates, limiting values of the Tafel slope can be deduced and compared with experiment and in a number of favourable cases* can be shown to be characteristic of the reaction mechanism (33,34).

These current-potential relations can be obtained under two kinds of experimental conditions:

---

*There has thus been some tendency to over-emphasise this approach at the expense of other complementary approaches, e.g., in some of the early work of Bockris and co-workers.

(a) Galvanostatic. Here current is controlled as the independent variable and corresponding values of potential at given currents, under steady-state conditions, are recorded.

(b) Potentiostatic. Here potential is controlled as the independent variable, and the values of the current at given controlled potentials, after the steady-state has been established, are recorded.

Both these methods give identical results for electrode reactions where only a simple linear Tafel region is observed. In more complex cases, where a Tafel region follows a well-defined transition region, e.g., in the Kolbe and other anodic oxidation reactions, the potentiostatic method is to be preferred as it reveals the detailed structure of the transition region in a way which is not accessible under galvanostatic current control. Hence in cases where the transition region is of interest because of the possibility of inhibition or passivation effects, or other complications due to co-adsorbed species, the potentiostatic method is quite essential for full interpretation and study of the electrochemical kinetic behaviour of the reaction. The Kolbe reaction is an example of a complex system of this type, especially in aqueous solutions where application of the potentiostatic method is necessary for elucidation of the kinetic behaviour.

The necessity of control of electrode potential rather than the rate (i.e., current) in organic electrode processes

has to be emphasised for a variety of other reasons. Apart from determining the coverage of some electrodes by adsorbed H or O containing species (e.g., in aqueous solutions of organic salts), potential will also be of importance in determining the adsorption of the organic reactant itself. The adsorption will depend on the electrode potential in relation to the potential of zero charge. It has not been widely appreciated in work on organic electrochemical reactions, that adsorption on the working electrode (determined, of course, by the potential of the latter in relation to that of zero charge) is one of the two most important single factors which distinguish electrode processes from other heterogeneous processes (the second factor is the potential-dependent free energy of activation). Again, effects of electrode potential are often highly specific. In the reduction of nitro-benzene, for example, various steps are possible and their occurrence is sensitive to the electrode potential; thus in the scheme

$$C_6H_5NO_2 \xrightarrow{2e} C_6H_5NO \xrightarrow{2e} C_6H_5NH.OH \xrightarrow{2e} C_6H_5NH_2$$

the effective terminal stage depends on the reduction potential and the nature of the electrode metal. This reaction has recently been studied potentiostatically by Wynne-Jones and co-workers (35).

The basic kinetic equation relating current density and electrode potential (measured either galvanostatically or potentiostatically) for a reaction proceeding at a metal/solution interface is given by

$$i_a = i_o' (1-\theta) \exp -[\alpha\eta ZF/RT] = i_o \exp -[\alpha\eta ZF/RT] \quad (1)$$

where i_a is the anodic current density, i_o the exchange current density, that is the current at $\eta = o$, and i_o' the exchange current corrected for coverage*, η , the overpotential defined by $\eta = E - E_r$, where E_r is the value of the metal-solution potential E when the reaction at the metal-solution interface is at thermodynamic equilibrium; α is the transfer coefficient determining the dependence of rate upon potential and is a parameter the magnitude of which depends upon the mechanism of the reaction and the extent of coverage of the electrode by adsorbed reaction intermediates; θ is the fraction of the electrode surface covered with intermediates produced in the ionic discharge (and subsequent) reactions; Z is the number of electrons involved in the discharge step and will be assumed to be equal to one; the remaining terms have their usual significance (36,37).

---

*Here the expression for the current is written in such a way as to include a coverage term $(1-\theta)$ which may or may not be potential dependent. This expression and the corresponding definition of i_o' differ from that usually used (viz. $i_a = i_o \exp -[\alpha\eta F/RT]$) which includes the coverage term in i_o. This expression [1], suggested by Devanathan and Selvaratnam (35a), is to be preferred on account of its greater generality.

The Tafel parameters i_o and $RT/\alpha F$ (or b) are readily evaluated from experimental logarithmic current-potential curves if the reversible potential for the reaction can be established experimentally or calculated from appropriate experimental data. The experimentally determined values of b, for limitingly low or high coverage of the surface by possible intermediates, can be characteristic of the reaction mechanism (33,34,37). The degree of coverage θ can be estimated from galvanostatic charging or discharging data (38-41) when θ is significant (e.g., $\theta > 0.1$), i.e. when the rate-determining step is not the initial ionic discharge reaction, or else the coverage is determined by some other process, e.g., surface oxide formation (see below).

The applicability of the galvanostatic or potentiostatic d.c. polarisation studies for the determination of the Tafel slope b, and hence the transfer coefficient α, is, however, limited to ranges of current density where errors due to solution resistance, local heating effects, diffusion control, etc. can be minimized. In practice, this means that the upper limit of the current density for reactant concentrations expressed as normality N is $i_{max.} \doteq 0.1N$. A more fundamental difficulty arises when the surface condition of the electrode changes with time on account of the formation of surface films. This is particularly important in anodic processes where the degree of surface oxidation of the electrode may have a direct

bearing on the reaction mechanism and the relation between electrode potential and current density (43).

(ii) Non-Steady-State Measurements

A variety of non-steady-state measurements, which yields information on the nature of adsorbed intermediates, has been used in the study of electrode processes. The results obtained by the non-steady-state techniques may be used in a complementary way to those obtained by steady-state current-potential curves for interpreting the mechanisms of electrode reactions. The various non-steady-state techniques used in the present investigation are described below.

(a) Potentiodynamic Current-Potential Relations

This procedure consists of subjecting the electrode to a repetitive "triangular" or single "ramp" voltage-time sweep usually by feeding a reference signal of this form into a potentiostat and observing by means of an oscilloscope, the time- and hence potential-dependent current which passes during the voltage sweep. The currents which are measured are composite and contain components due to non-Faradaic, (double-layer charging), pseudo-Faradaic [a term which it is convenient to use to refer to currents arising from charging or discharging adsorption capacitances associated with potential-dependence of coverage by adsorbed intermediates in the reactions (40,54,55,56)], and Faradaic currents passing during the voltage sweep. If any processes are diffusion

controlled*, further complications arise; diffusion controlled processes can be distinguished from activation controlled ones by plotting the peak current density in the sweep vs. $[dV/dt]^{\frac{1}{2}}$, when a straight line passing through the origin indicates a diffusion controlled process. This criterion is, of course, useful when one of the two types of reactions has a predominantly higher rate; when both diffusion controlled and activation controlled reactions are of comparable rates, only complex results are obtained. The technique is thus a kind of polarographic sweep method except that in most applications which have been recently made (45), the surface charging processes observed are not usually diffusion controlled. The transient currents which pass during the sweep are determined in part by a quantity $C_{ads}d\eta/dt$ and it is the quantity $d\eta/dt$ taking periodically positive and negative constant values which can be varied in this technique from run to run. Here, C_{ads} is the pseudo-capacitance associated with the adsorbed species on the electrode and $d\eta/dt$ is the rate of change of the potential or overpotential of the electrode. The transient currents which pass in various potential regions of the sweep may be integrated with respect to time to give approximate estimates of the charge associated with formation or removal of the intermediates, except at potentials where a

*The development of this method was first made for diffusion controlled reactions in polarography and the theory was worked out by Sevcik (44). For most of the recent applications, however, his treatment will not be applicable.

net overall (or real Faradaic) reaction begins to be predominant or if diffusion effects are significant. Since the adsorption pseudo-capacitance usually varies with the rate at which it is measured due to non-equilibrium effects, the potential sweep method can give capacitances associated with oxidation or reduction peaks which depend on the sweep rate (46). The current peaks determined by $C_{ads}d\eta/dt$ will thus not necessarily be proportional to $d\eta/dt$ in sweeps taken at various rates. Also, if with increasing potential in a sweep, a potential region is passed through in which the capacitance has a maximum value, the transitory current-time relation will exhibit a maximum. This will not generally be distinguishable from current maxima which arise for kinetically different reasons in passivation or inhibition processes. In such cases, however, the current maxima will also be observed in very slow (i.e. steady-state) potentiostatic scanning and will be connected with the steady-state kinetics of the overall Faradaic process (62); in the other type of case, current maxima arise from a pseudo-Faradaic process and have a different origin. Previously, little critical distinction has been made with regard to the effects that can arise in applications of this method. However, for an electrochemical adsorption peak where the currents are pseudo-Faradaic, the $\int idt$ area under the peak, proportional to the charge passed in forming or removing a

layer of adsorbed intermediates, should ideally be independent of sweep rate.

The method has, however, the advantage of providing a rapid technique for observing the qualitative features of complex reactions but it must be pointed out that rather little quantitative information can at present be deduced since the method lacks any firm theoretical foundation as applied to successive non-diffusion controlled processes. From the point of view of electrochemical kinetics, the method is somewhat difficult to develop quantitatively for successive reactions, since the electrode process takes place under conditions where neither steady current nor steady-state kinetics apply and potentials are time dependent.

Will and Knorr (42) were the first workers to apply the potentiodynamic method to a simple charging reaction. They studied the hydrogen ionisation reaction in some detail by this method and experimentally examined the dependence of the potential of the current maximum and of current itself on dV/dt. This reaction, however, is a relatively reversible one and hence the problems involved here in the interpretation of results are not quite as complex as in some organic oxidations, e.g., the Kolbe reaction or formate oxidation.

Recently, Conway, Gileadi, and Kozlowska (46) have developed the essential non-steady state theory of this method. However, the equations deduced by them are difficult to test

experimentally without simplyfying them by resorting to approximations; even then the experimental data can be tested only in a semi-quantitative way.

A typical potentiodynamic profile is shown schematically in Fig. 1 for Pt in H_2SO_4. In this profile, a potentiodynamic sweep scanning the range of potential between that for the process of hydrogen evolution (cathodic potential) and that for oxygen evolution (anodic potential) has been represented. At the extreme cathodic potential side in this profile is a Faradaic current-potential relation for the H_2 evolution reaction. When the potential of the electrode is made gradually more anodic, two small pseudo-Faradaic current peaks for the ionisation of adsorbed H are observed in the potential region somewhat anodic to the potential of the reversible hydrogen electrode. These two peaks are followed by a non-Faradaic double-layer charging region which in turn is followed by an extended pseudo-Faradaic current peak for oxide formation at more anodic potentials. This oxide formation peak is followed at still more anodic potentials by a region for Faradaic oxygen evolution.

After reaching the extreme anodic end of the sweep, the potential bias is reversed in direction resulting in a gradual decrease in anodic potential (i.e., a gradual relative increase in cathodic potential) of the electrode. The first principal peak encountered in this reversed-bias condition is

Figure 1

Schematic representation of potentiodynamic current-potential profile for the Pt/H_2SO_4 system.

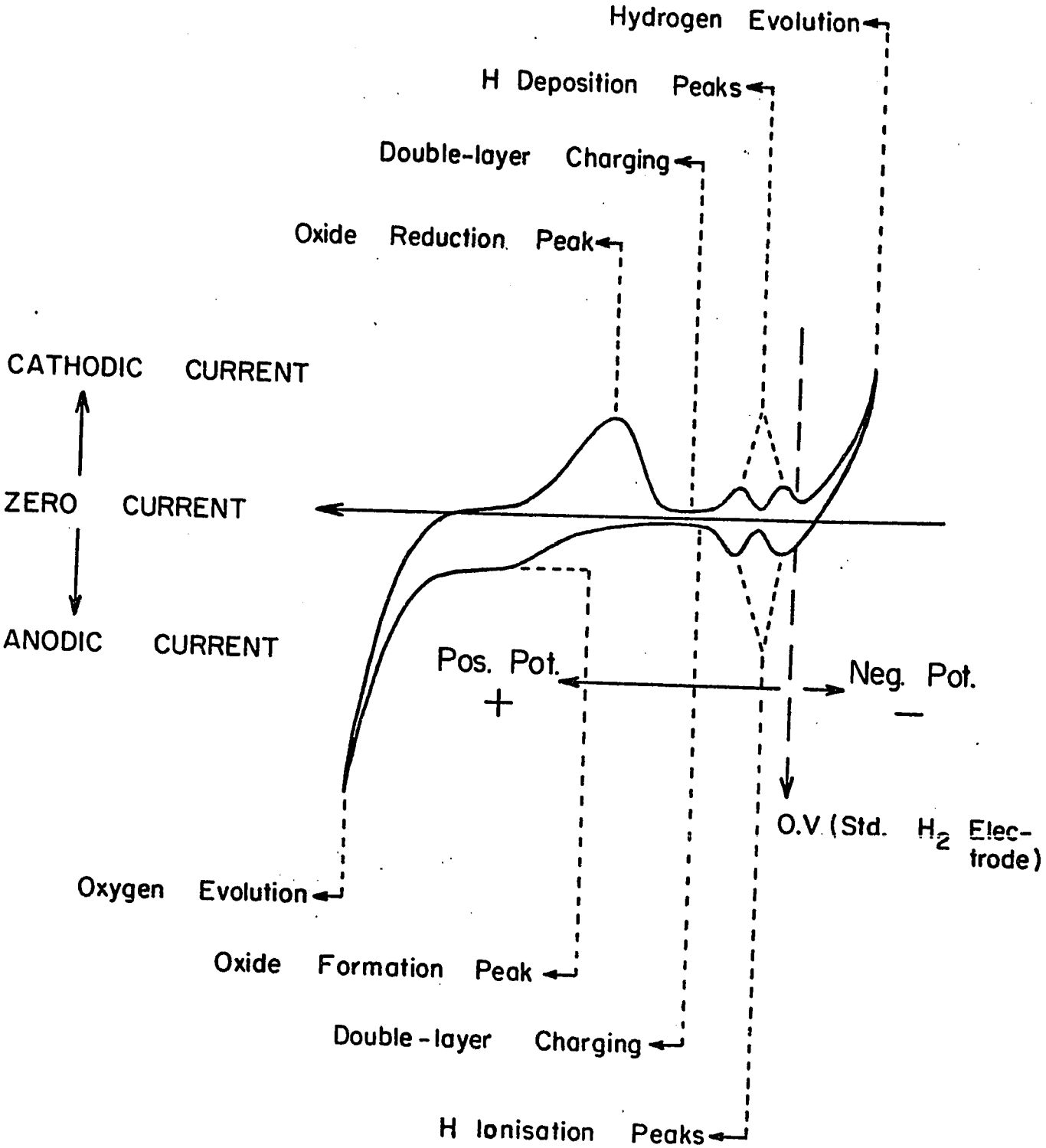
Hydrogen Evolution
H Deposition Peaks
Double-layer Charging
Oxide Reduction Peak
CATHODIC CURRENT
ZERO CURRENT
ANODIC CURRENT
Pos. Pot.
+
Neg. Pot.
−
O.V (Std. H_2 Electrode)
Oxygen Evolution
Oxide Formation Peak
Double-layer Charging
H Ionisation Peaks

the one for the pseudo-Faradaic process of reduction of oxide formed previously on the electrode when its potential was increasing anodically. After the oxide is completely reduced, there follows another non-Faradaic double-layer (dis-) charging region (cathodic) on the bare electrode. At still less anodic (or more cathodic) potentials, two small pseudo-Faradaic current peaks for H atom deposition are observed, beyond which on the more cathodic side of the reversible hydrogen potential, a region associated with the Faradaic process of hydrogen evolution arises. In an ideal case, as shown schematically in this profile, potentiodynamic scanning reveals quite clearly the regions associated with non-Faradaic, Faradaic, and pseudo-Faradaic processes, both anodic and cathodic, which can occur on the electrode. It will also be noted that in Fig. 1 the potential range for oxide reduction is displaced to more cathodic potentials than that for formation of the oxide at Pt in the anodic direction of the potential sweep. This phenomenon which has been observed by many workers, is basic to the understanding of the hysteresis exhibited in the kinetics of anodic oxidation at Pt for changes of potential in anodic and cathodic directions.

(b) Open-Circuit e.m.f. Decay

In the present investigation, information on the

nature of adsorbed intermediates has also been obtained by evaluating pseudo-capacity from the rate of decay of potential of the working electrode on open-circuit following steady-state polarization. In this case, the potential of the electrode is allowed to change by a self-discharge process without external control of potential or current. Thus the rate of decay of overpotential will be a function of time, but will always be determined by the intrinsic electrochemical time constant RC of the reaction comprised of an equivalent capacitor and a resistor in parallel (47). The current density flowing internally in the system at any potential will usually be equal to the steady-state current density measured at the same potential (48). It is assumed that the electrode reaction is studied in the potential range where the initial ion discharge step can effectively be regarded as being at quasi-equilibrium, and the pseudo-capacity obtained by any method based on open-circuit decay of potential will thus represent the true equilibrium value.

The essential calculations involved in this method proceed as follows, e.g., for an anodic process.

Let the capacitance involved be C where C may be a function of η. On interruption of a current i, the initial polarising current, the electrode process continues on open-

circuit through ion discharge across the double-layer capacity* by the same mechanism as when steady current was passing, if a simple discharge step is occurring at a non-ideally polarisable electrode. That is, for an anodic process,

$$(dq/dt)^{o} = -C_{\eta}(d\eta/dt)^{o} = i^{o} = i_{o} \exp \eta^{o}/b \qquad (3)$$

where the superscript ^{o} indicates initial conditions and the negative sign is included since $d\eta/dt$ is negative for an open-circuit anodic process (η positive). If C_{η} has a constant value C, rearrangement of equation (3) gives for any potential

$$\exp[-\eta/b].d\eta = \frac{-i_{o}}{C}\, dt \qquad (4)$$

at any time t. Integration gives

$$-b \exp[-\eta/b] = \frac{-i_{o}t}{C} + I = \frac{-i_{o}}{C}(t + J) \qquad (5)$$

where I and J are integration constants ($J = -IC/i_{o}$). Taking

*However, in cases where a pseudo-capacity associated with adsorption of intermediates is involved, and when the ionic double-layer capacity is much smaller than the pseudo-capacity, the process occurring on open-circuit decay is not simply ion-discharge across the double-layer capacitance as in the treatment of Butler and Armstrong (41). The process occurring in such a case must be the electrochemical removal of the adsorbed film by a process involving mixed anodic and cathodic self-discharge reactions, as discussed previously (59). For example, for removal of an adsorbed species X electrochemically on open-circuit, the steps

$$e + MX \longrightarrow M + X^{-} \qquad \text{(cathodic)}$$

and $MX + X^{-} + e \longrightarrow M + X_{2}$ (anodic) must occur,

or

$$2MX \longrightarrow X_{2} \text{ by a heterogeneous chemical step.}$$

logarithms,

$$-\eta/b = \ln \frac{i_o}{Cb} (t + J) = \ln \frac{i_o}{Cb} + \ln (t + J) \qquad (6)$$

i.e.,

$$-d\eta/d\ln (t + J) = b \qquad (7)$$

so that the e.m.f. decay slope is numerically the same as the Tafel slope assumed in equation (3). When t = o, $\eta = \eta^o$ and $i = i^o$ (the initial current), so that using equation (5),

$$J = Cb/i^o \qquad (8)$$

Except at short times $J \ll t$, so that $d\eta/d \ln t = -b$; evaluation of J for known i^o and b will give C.

If C is an adsorption pseudo-capacity, it may vary limitingly as $C_o \exp -\eta/b'$ or $C_o \exp \eta/b'$ for high and low anodic overpotentials, respectively, where C_o is a constant. Introduction into equation (4) gives

$$\exp [-\eta/b]\, d = \frac{-i_o}{C_o} \exp [\pm \eta/b'].dt \qquad (9)$$

respectively, for the two cases of variation of C with η stated above. Then

$$\exp - [\tfrac{1}{b} \pm \tfrac{1}{b'}] \cdot d\eta = \frac{-i_o}{C_o}\, dt \qquad (10)$$

and $d\eta/d\ln (t + J)$ is given after integration by

$$d\eta/d\ln (t + J) = 1/(\tfrac{1}{b} \pm \tfrac{1}{b'}) \qquad (11)$$

and

$$J = \frac{C}{i_o} /(\tfrac{1}{b} \pm \tfrac{1}{b'}) \qquad (12)$$

The e.m.f. decay slope will hence be greater or less than the Tafel slope depending on the sign of the argument η in the limiting relations of the capacity to potential. For an anodic process, the e.m.f. decay slope will be numerically less than the Tafel slope when C_η is increasing with decreasing potential ($\theta > 0.5$), and vice versa when C_η is decreasing with decreasing potential ($\theta < 0.5$). The e.m.f. decay method is hence valuable in giving the direction of capacity dependence on potential over a range of potentials (4a) and hence in determining indirectly if the coverage by electrochemically active intermediates is small (< 0.5) or large ($\rightarrow 1$).

The actual capacity as a complete function of potential can be calculated by a variation of the above method. Quite generally, at all potentials, (cf. equation 3)

$$C\,(d\eta/dt) = i_o \exp \eta/b = i_\eta \qquad (13)$$

and if the same Tafel parameters i_o and b apply during e.m.f. decay as during polarisation

$$C = i_\eta / (d\eta/dt) \qquad (14)$$

so that C_η can be obtained at all potentials, and integration of C w.r.t. η then can give the change of charge and associated coverage over the range of potentials through which the integration has been carried out. In a number of anodic processes, as in the case of the Kolbe reaction in aqueous

medium, there is a hysteresis between ascending and descending current-potential relations and in the open-circuit decay, the self-discharge current will generally tend to be related to potential in a way analogous to that on the descending current-potential relation taken potentiostatically. In anhydrous systems, the hysteresis is much diminished or eliminated altogether, as will be discussed below, suggesting that it is associated with the formation of oxide films when water is present. The e.m.f. decay method is then less ambiguously related to the current-potential relation.

(c) Galvanostatic Charging Method

The galvanostatic charging method originated in studies of the double-layer capacitance by Bowden and Rideal (50) and was extended by Frumkin and co-workers, particularly for studies of H adsorption (51). It has been developed in specialised ways by various other workers (52,53).

The charge q passed as a function of the electrode potential attained gives the coverage θ as a function of potential since q is proportional to θ through a constant k' where k' is the charge required to produce complete coverage ($\theta = 1$) of the intermediate. If the charging process occurs at potentials above the reversible potential for the overall reaction occurring, then the total current passing is made up

of a non-Faradaic current (i.e., one not involving electron transfer) associated with charging of the double-layer, and a Faradaic current involving two components: (a) the current associated with discharge of ions to form intermediates, the coverage by which is changing with potential (and hence time in the non-steady-state), and (b) the current associated with the rate of the overall process. Usually the latter current is only significant towards the end of the transient at high overpotentials. The equation for the time-dependent potential at constant total current i_T is formally

$$i_T = C_{d.l.}\, d\eta/dt + C_{ads}\, d\eta/dt + i_o \exp [\eta/b] \qquad (15)$$

The middle term (the pseudo-Faradaic current) associated with Faradaic charging is determined by the adsorption capacitance C_{ads} which itself will usually be a function of potential.

In the range of potentials over which adsorption by intermediates is appreciable, $C_{ads} \gg C_{d.l.}$ and if η is not too large ($i_o \exp \eta/b \ll i_T$), i_T is determined largely by $C_{ads}\, d\eta/dt$ and the charge passed is $\int i_T dt$ over the relevant duration of charging. Since $C_{ads} d\eta$ is dq, (the charge associated with changing the coverage by $d\theta$) the capacitance is determined by the slope $(\partial t/\partial \eta)_{iT}$. Since such a slope is graphically difficult to determine with satisfactory precision from oscilloscope photos, a more direct method is desirable and has been recently developed by Kozlowska and Conway (53). It is

described below since it has been used extensively in the present work.

In this method, both the charging curve and its time-differential coefficient are simultaneously recorded by means of a dual beam oscilloscope. The differential curve gives directly a quantity which is the reciprocal of the capacitance as a function of potential. It has the advantage of giving the detailed form of the potential-dependence of the capacitance associated with the charging process and can indicate the presence of two or more intermediates on the surface in more complex reactions, e.g., in the formate oxidation reaction. From the charging curves themselves, which often show only some ill-defined inflections, it is usually difficult to deduce capacitance at all accurately by taking tangents. The differantial method gives greatly improved resolution of the charging region and has theoretical advantages over the potentiodynamic method since steady current kinetics apply.

It has been found (46) that the capacitance values calculated by the galvanostatic charging method sometimes depend on the current density used in the charging transient. Dolin and Ershler (61) and Conway, Gileadi and Kozlowska (46) have discussed this point. The latter authors have developed a non-steady-state kinetic theory of charging, which is

discussed briefly below since the considerations made are relevant to the discussion of the present experimental results.

A galvanostatic charging curve corresponds to a steady-current condition but not to a chemical steady-state condition, since the total charging current i is made up of components i_c, the capacitative true charging current, and any Faradaic current i_F. The situation in hydrogen evolution may be considered but depends on the nature of the consecutive reaction mechanism involved, i.e., whether or not the desorption step (e.g., in hydrogen evolution) proceeds by a chemical atom recombination step or by an electrochemical atom-ion discharge step. In the former case, all the current passes through the reaction resistance of the discharge step since the desorption is non-electrochemical; in the latter case, part of the current is involved in electrochemical removal of the intermediate, e.g., adsorbed H, and part in formation of H. The equivalent circuits are hence somewhat different (Fig. 2a and 2b) and a special symbol is required (see Fig. 2b) for the reaction resistance for the electrochemical atom-ion desorption type of step. The electrons and H^+ ions arising from the metal and solution, respectively, are discharged from the ionic double-layer capacitance while charge corresponding to (the production of) H atoms is withdrawn from the adsorption pseudo-capacitance. No representation alternative to the

Figure 2

(a) Complete equivalent circuit for initial discharge step followed by a non-electrochemical desorption (charging process non-ohmic).

(b) Complete equivalent circuit for initial discharge step followed by an electrochemical (e.g., atom + ion) desorption step.

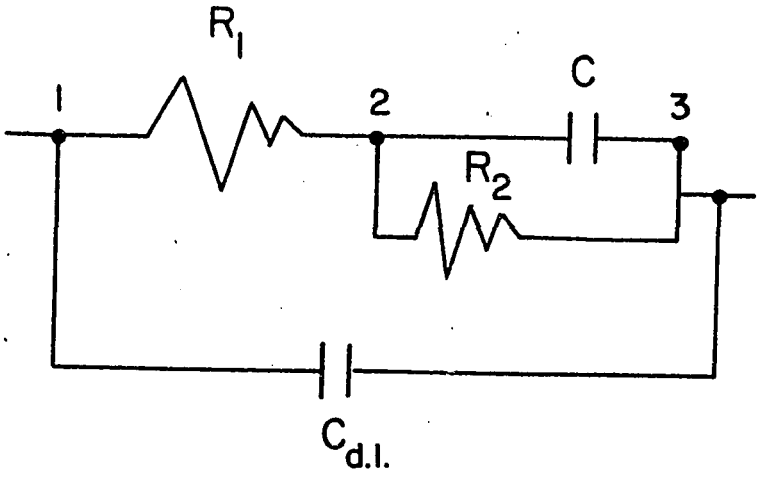
R1
C
1
2
3
R2
Cd.l.

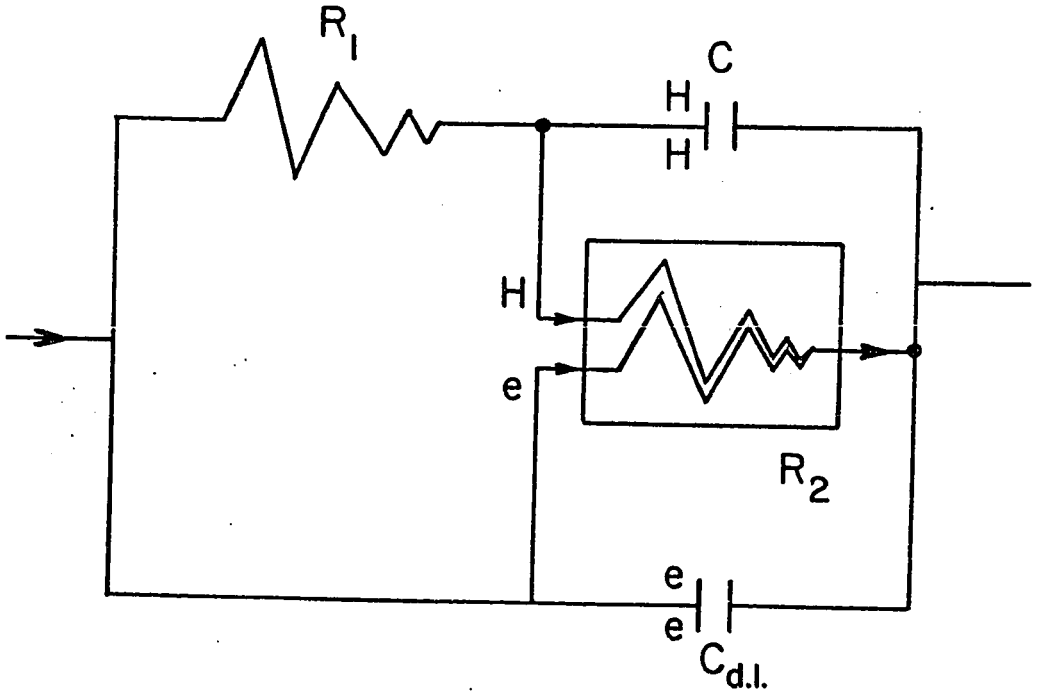
R1
C
H
H
H
e
R2
e
e
Cd.l.

dual channel symbol shown in Fig. 2b is possible for the electrochemical desorption type of process without "short-circuits" being involved. The general electrochemical reaction sequence for, say, an anodic reaction is

$$M + A^- \longrightarrow MA + e \qquad (I)$$

$$MA + A^- \longrightarrow M + A_2 + e \qquad (II)$$

The steady current condition (see Fig. 2b) is

$$i = i_1 + i_2 \qquad (16)$$

and

$$i_1 = \vec{i}_1 - \overleftarrow{i}_1 = i_C + i_2 \qquad (17)$$

where i_C is the net charging current for the pseudo-capacitor C.

In the steady state, $i = 2i_2$ ($i_C \longrightarrow 0$); i_2 is the leakage current from the pseudo-capacity associated with desorption of adsorbed A by step II and is also the electron + ion leakage current across the ionic double-layer capacity $C_{d.l.}$ associated with step II, (in regard to the charge transfer involved).

If θ is the coverage by A at a metal-solution potential difference V, the steady-current condition under Langmuir conditions (cf. 54) gives, in abbreviated form*

*Here the symmetry factor for step I and its reverse, and II are, for convenience, assumed equal to 0.5 so that all the b terms are the same. Also the ionic double-layer charging current $C_{d.l.}(dV/dt)$ has been included in eq. (18). This part of i is generally negligible in potential regions where the adsorption pseudo-capacitance is appreciable, which is the condition considered here.

$$i = k_1 (1-\theta)e^{V/b} - k_{-1}\,\theta\, e^{-V/b} + k_2\theta\, e^{V/b} + C_{d.l.}(dV/dt) \quad (18)$$

which gives θ as

$$\theta = \frac{k_1 e^{V/b} - i}{k_1 e^{V/b} + k_{-1} e^{-V/b} - k_2 e^{V/b}} \quad (19)$$

neglecting the $C_{d.l.}$ terms.

In equations (18) and (19), the k terms are the indicated "rate constants" which include for brevity of representation also the ion concentration terms allowing for double-layer ion distribution effects. For the purpose of the present calculations, it will not be necessary to specify the k terms or the potential quantity V in more detail.

Calculating the pseudo-capacity, we obtain

$$C = k\frac{d\theta}{dV} = \frac{2kk_1k_{-1}/b}{[k_1e^{V/b}+k_{-1}e^{-V/b}-k_2e^{V/b}]^2} - \frac{ki[k_{-1}e^{-V/b}-k_1e^{V/b}+k_2e^{V/b}]/b}{[k_1e^{V/b}+k_{-1}e^{-V/b}-k_2e^{V/b}]^2} \quad (20)$$

The term in rate constants and V is separated from that involving current i since it is seen (cf. 54-56) that the first term becomes the equilibrium pseudo-capacitance for A as a function of V when k_1, $k_{-1} \gg k_2$ (quasi-equilibrium conditions). For the latter condition then, C differs from its equilibrium value (56) by a kinetic term involving the measured rate i of the galvanostatic pulse; (note: this is limitingly only the rate of surface charging when the potential range corresponds to negligible net overall reaction).

Equation (20) can be used for predicting theoretically the behaviour of C w.r.t. V for a range of i values under the usual "quasi-equilibrium" assumption, i.e., k_1, $k_{-1} \gg k_2$. Such behaviour has been predicted and compared with the experimental results for a number of cases by Conway, Gileadi and Kozlowska (46), and the comparison has been found to be satisfactory.

(iii) Characterisation of Kolbe Products

The identity of the gaseous products formed during the Kolbe electrosynthesis was established by means of vapour phase chromatography. Further details are given in Chapter II which follows.

CHAPTER II

EXPERIMENTAL

1. INTRODUCTION

The experimental procedures used in the present work have consisted of:

(i) Steady-state, potentiostatic, current-potential measurements.

(ii) Non-steady state, potentiodynamic, current-potential measurements.

(iii) Studies on the role of intermediates and surface oxides, through the use of direct and differential galvanostatic charging curves.

(iv) Open-circuit decay studies from potentiostatically maintained potentials of polarised electrodes.

(v) Vapour phase chromatographic characterisation of the Kolbe products.

(vi) Exploration of suitable conditions for coulombic-yield studies.

In this chapter, these procedures will be described in detail but a general account of essential experimental technique for solution and gas purification, electrode preparation, cell design etc. will first be given. The experimental methods to be described have been applied to the C_2F_6 Kolbe reaction with trifluoroacetate in (a) anhydrous trifluoroacetic acid (TFA); (b) in TFA containing traces of water and (c) in TFA containing

30% by volume of water. Also acetate solutions in (a) glacial acetic acid and (b) water acidified by acetic acid, have been studied with regard to the C_2H_6 Kolbe reaction.

2. SOLUTIONS

(i) Standard Purification Techniques

(a) Trifluoroacetic Acid

Trifluoroacetic acid (b.p. 70-72°C) was kept over boric anhydride with constant stirring for about two days. The mixture was then refluxed over a quantity of fresh boric anhydride for two to three hours and distilled. The distillation was repeated again over a further fresh quantity of boric anhydride just before the experiment was carried out. Only the fraction distilling at 71.1 ± 0.1°C (760 mm.) was used in the experiments.

(b) Potassium Trifluoroacetate

Potassium trifluoroacetate was prepared by neutralizing previously purified trifluoroacetic acid with potassium hydroxide (analytical grade). The salt was then recrystallised twice from conductivity water. Since the salt is extremely soluble in water, freshly re-distilled, spectroscopically pure dioxane was used to precipitate out the salt from its aqueous solution. The salt was dried under vacuum at about 100°C for 24 hours and then stored in tightly-capped bottles; it was redried under vacuum before use in each experiment.

(c) Acetic Acid

Analytical grade glacial acetic acid was refluxed with 2-5% (by weight) of $KMnO_4$ for 2-6 hours in order to remove traces of acetaldehyde and other oxidizable contaminants and was then distilled. The fraction boiling at 117°-118° (760 mm.) was collected. Traces of water were removed with triacetylborate which reacts with water to form acetic acid and boric acid (insoluble). The reagent was prepared by warming 1 part of boric acid with 5 parts (by weight) of redistilled acetic anhydride to 60°C; on cooling, triacetyl borate separated out and was removed by filtration. The distilled and purified acetic acid was then treated with 2-3 times the amount of triacetyl borate estimated to be required for reaction with the water present, and anhydrous acetic acid was obtained by further distillation. This purification procedure was carried out just before the electrochemical experiment was commenced.

(d) Potassium Acetate

The purest commercially available potassium acetate was crystallised and recrystallised from conductivity water and was dried under vacuum at 100°C for 24 hours.

(e) Trifluoroacetic Anhydride

The purest commercially available trifluoroacetic anhydride was distilled and then redistilled using a semi-micro distillation apparatus with an effective fractionating column, and the middle fraction distilling at 45°C was collected.

This procedure was also carried out, as required, just before the experiment was commenced.

(ii) Preparation of Solutions

Solutions of potassium trifluoroacetate were prepared by drying a weighed amount of salt under vacuum for 24 hours at 100°C. The acid was re-distilled from a fresh quantity of boric anhydride and transferred by pressure of nitrogen, without contact with the atmosphere, to a known weight of the salt to give the concentration desired. This solution was regarded as "pure" but might still have contained microscopic traces of water initially or might have become contaminated with water vapour by diffusion from the atmosphere into the cell and other glass vessels in the first few hours of the experiment (despite the elaborate precautions described below). In order to obtain very anhydrous conditions in certain runs, less than 1% of purified trifluoroacetic anhydride was added to the solution which was stirred by means of a dry purified inert gas, CO_2 (which itself was pre-saturated with solvent vapour by bubbling through a pre-saturator containing the same solvent as the one in the solution under study in the electrolysis cell); this technique was adopted in order to prevent loss of solvent from the test electrode compartment. In several runs, an acidic aqueous medium was desired which was obtained by injecting into the cell 30% by volume of a previously prepared solution of potassium trifluoroacetate in water.

After preparing the very anhydrous solutions, it was necessary to keep them anhydrous for a few hours, i.e., atmospheric moisture had to be prevented from diffusing into the cell during these few hours or in some cases, even a day. This was accomplished as follows.

Direct contact between the electrolytic solution and the atmosphere was prevented by use of drying tubes on the gas outlets from all compartments of the cell. This prevented macroscopic diffusion of moisture into the cell from direct openings but not the microscopic diffusion from the solution-joints, and well-mated "tru-bore" tubings (a modification of the standard joints) which constituted the structure of the cell. Such diffusion could occur since these joints and tubes were not greased in order to avoid obvious contamination of the solution. The prevention of this microscopic diffusion of moisture from the atmosphere into the test electrode compartment of the cell was accomplished by placing the cell in a box which was reasonably air-tight. In this box were placed two large Dewar flasks filled with liquid nitrogen. In the mouth of each of these flasks was suspended a heater (100 watt bulb) which produced a slow but continuous evaporation of liquid nitrogen and this gave an envelope of absolutely dry inert gas around the cell.

Solutions of potassium acetate in acetic acid were prepared in a similar way except that very anhydrous conditions, as were required in several runs, could not be achieved simply

by adding less than 1% acetic anhydride to solutions in pure acetic acid since acetic anhydride reacts only rather slowly with water at the temperature of the experiments (25°C); in contrast, trifluoroacetic anhydride reacts relatively rapidly with traces of water present in TFA. To achieve very anhydrous conditions in the acetic acid system, a somewhat simplified cell (referred to as the "vacuum" cell from here onwards) was designed in which the drying of the salt, purification of acetic acid and preparation of solution were all carried out under vacuum in a closed, continuous system. After the preparation of the solution, dry nitrogen was admitted through a three-way stopcock in the otherwise completely closed cell. The presence of dry nitrogen prevented any possibility of atmospheric moisture leaking into the cell through the development of streaks etc. in the standard joint grease (this simplified cell was designed in such a way as to permit the use of grease on the standard joints) when the cell was held under vacuum (with no continuous evacuation) for an extended length of time. All greased joints and the one stopcock were well outside the region where the solution was distilled and prepared and an internal magnetically controlled dry glass valve was provided for controlling the double distillation and drying procedure (see Fig. 4).

3. GASES

(i) Hydrogen

Hydrogen was rigorously purified before use. The purification train was similar to that previously described (2,6). The train consisted of (a) a dried molecular sieve material (Linde Co., type 13X), (b) calcium chloride (c) magnesium perchlorate, (d) hopcalite, (e) palladised asbestos at 400°C, (f) copper turnings at 450°C, (g) two liquid nitrogen traps and (h) two charcoal traps maintained at liquid nitrogen temperatures.

(ii) Carbon Dioxide

Medical grade carbon dioxide free from hydrogen sulphide, carbon monoxide and sulphur dioxide was passed over molecular sieve (type 13X) material to remove any possible moisture present in it.

(iii) Nitrogen

Nitrogen gas was purified by passing the gas through a train identical with that described previously for the purification of hydrogen.

4. ELECTRODES

Electrodes were prepared by a standardised method to ensure reproducibility of measurements. The electrodes were prepared from spectroscopically pure wires of platinum and gold. The wire was first cleaned by washing for twenty four hours in benzene under reflux. The wire electrode was then heated

for 2-5 minutes in a stream of pure dry hydrogen at temperatures just below the softening temperature of the pyrex glass. It was subsequently sealed under hydrogen in a glass bulb, following the procedure described by Bockris, Conway and Mehl (57). The sealed electrodes were maintained in the cell in the glass bulbs until commencement of each run, when they were successively broken, as required, with the desired potential initially applied before breakage.

5. CELLS

(i) Polarisation Cell

The cell used for all potentiodynamic and potentiostatic polarisation studies, except those under "vacuum", consisted of three all-glass (Pyrex) compartments which were separated from each other by "solution-sealed" stopcocks. The anode and reference electrode compartments were provided with cooling coils, provision being made in each compartment to allow the appropriate gas to be bubbled through the solution. The cell is shown schematically in Fig. 3a) (and in the photograph, Fig. 3b) in which A, C, and R are the anode, cathode and reference compartments, respectively.

(ii) "Vacuum" Cell

This was made of pyrex glass and consisted of a vessel of small volume with three arms connected to it. Each of these arms carried one of the three electrodes, the working,

Figure 3

(a) Schematic diagram of the polarisation cell.

(b) Photograph of the polarisation cell.

Polarisation Cell

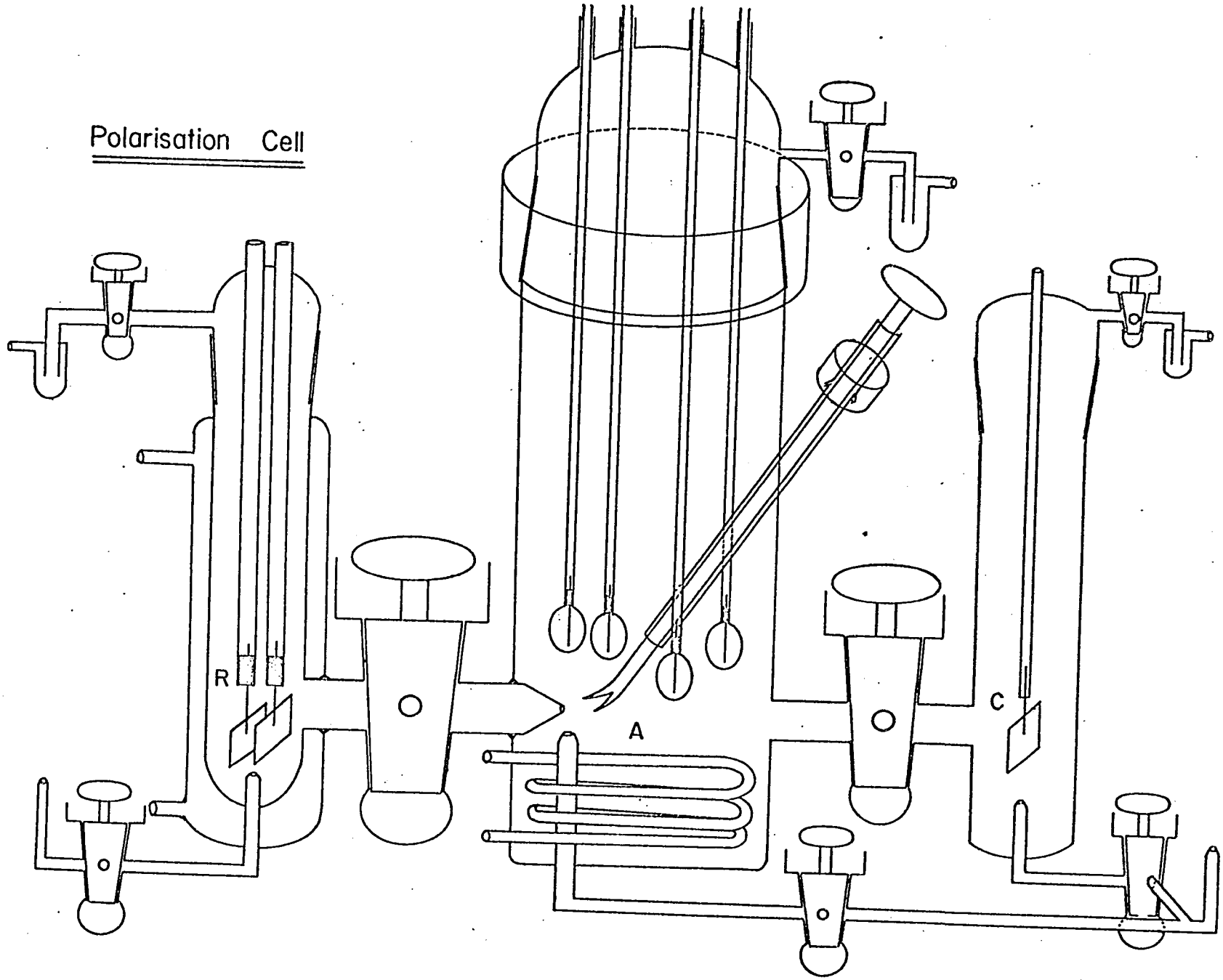

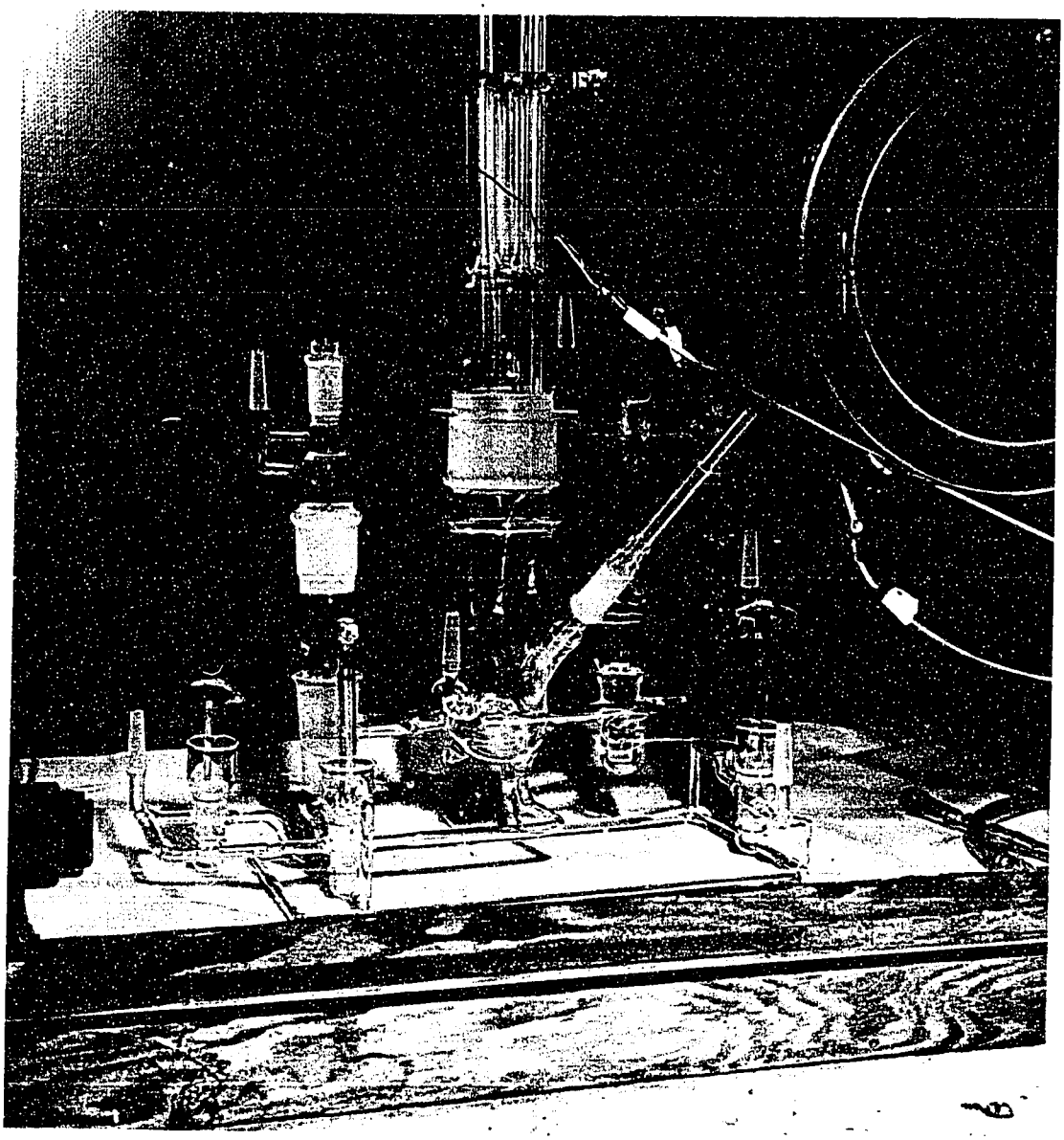

the counter and the reference electrode, all being accommodated on suitable standard joints. This portion, essentially the electrolytic cell, was sealed directly to two distillation flasks in series, and then to a vacuum line and to a source of dry nitrogen by means of a three-way stopcock. After distilling the acid from the first flask to the second, the first flask could be closed off from the system by letting a dry standard-jointed stopper fall in a receptor joint by manipulation of an electromagnet. The cell is shown in Fig. 4.

(iii) Cell for Collection of Kolbe products

This was similar to the polarisation cell described in (i) above except that the dead volume above the solution in the working electrode compartment (i.e. the anode compartment) was very small. Also, the anode compartment carried a special "head" which led a large electrode into the compartment on one side and could be connected to a gas-collecting trap cooled in liquid air on the other side. The cell is shown schematically in Fig. 5.

6. SOLUBILITY APPARATUS (FOR C_2F_6 IN TFA)

This apparatus was fabricated out of four glass bulbs, a burette, a stopcock and some tygon tubing, and is shown in Fig. 6. It was possible, by appropriate manipulation of the

Figure 4

Photograph of the "vacuum" cell.

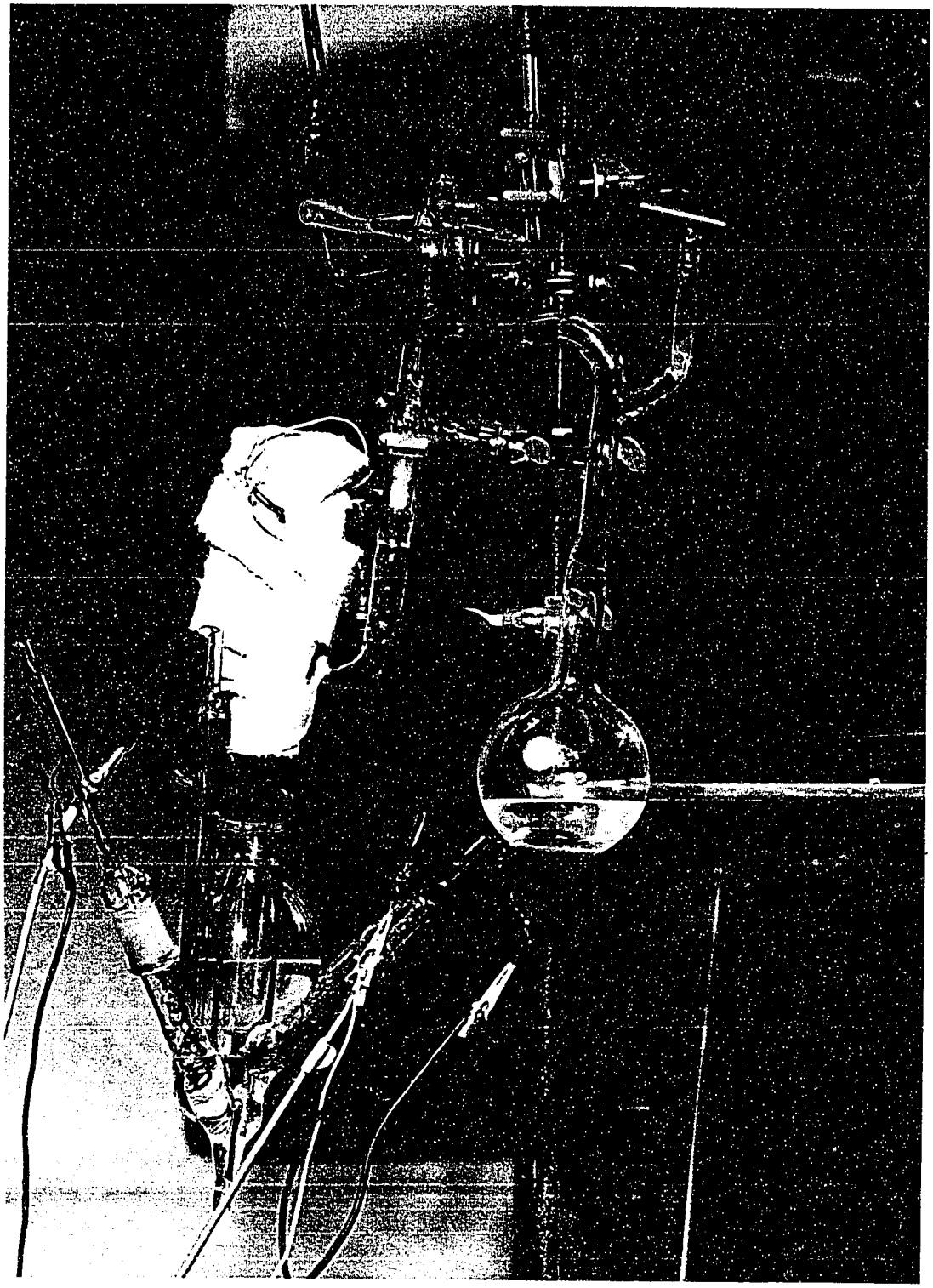

Figure 5

Cell for collection of Kolbe products.

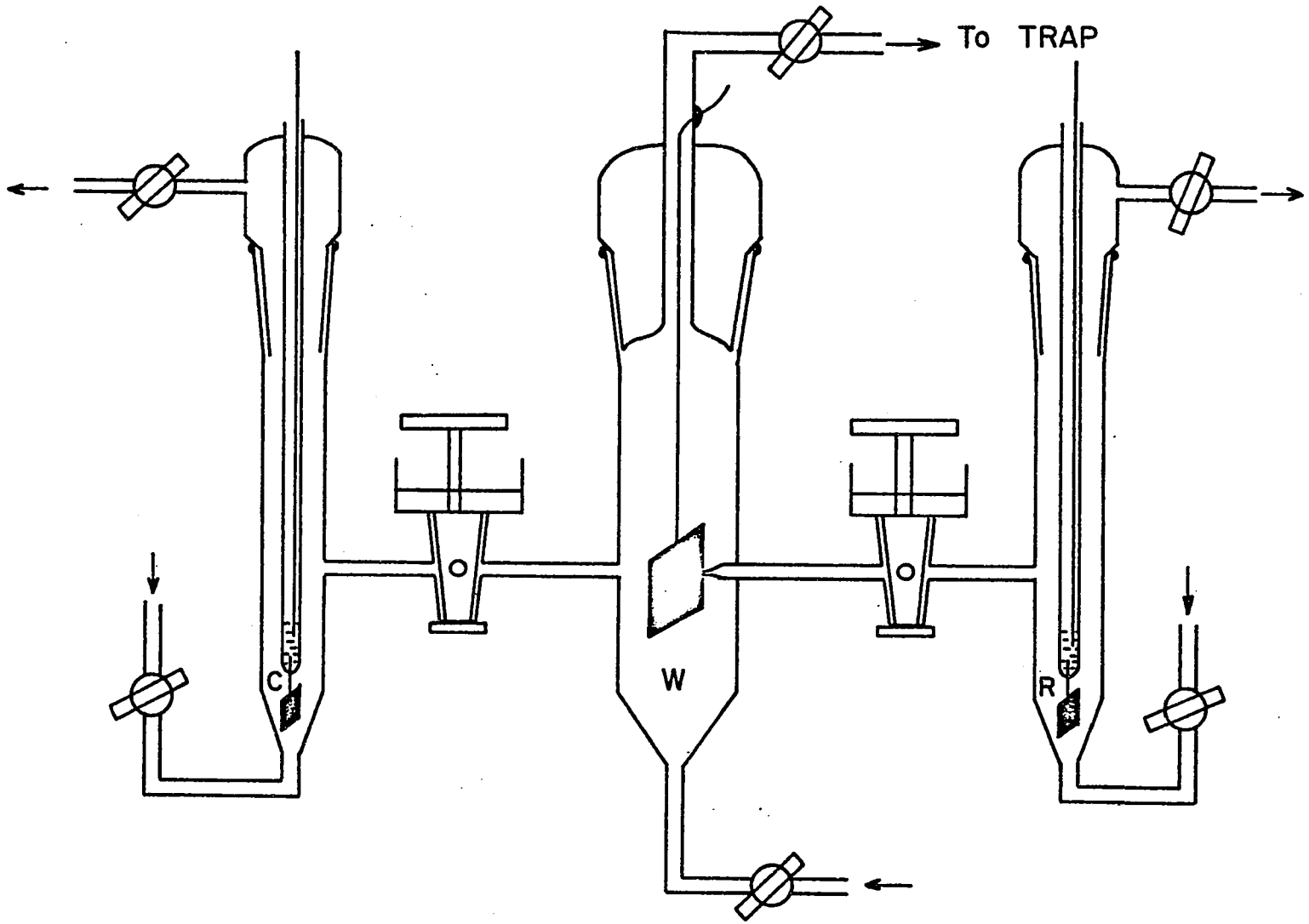
To TRAP
C
W
R

Figure 6

Apparatus for gas solubility measurement.

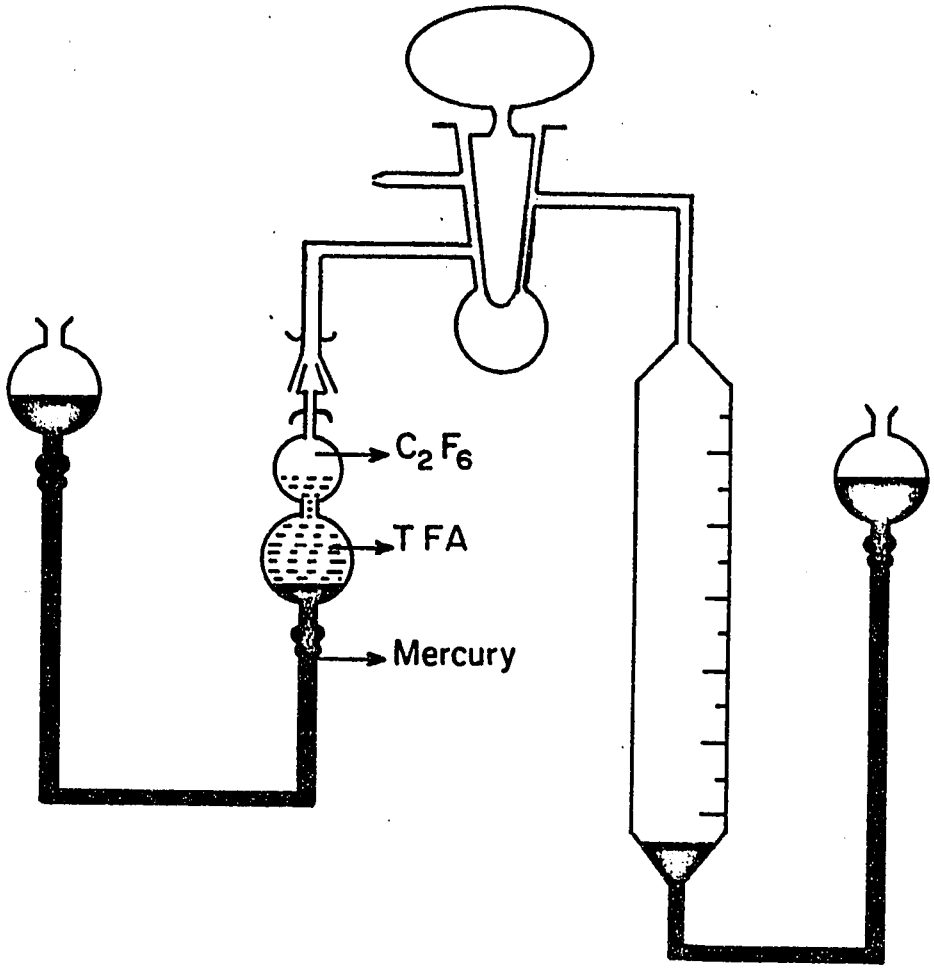
C_2F_6
TFA
Mercury

stopcock and the mercury levels in the two bulbs, to introduce a known volume of TFA and C_2F_6 and determine approximately the equilibrium dissolution of C_2F_6 in TFA at room temperature and under atmospheric pressure.

7. REFERENCE ELECTRODES

(i) Hydrogen Reference Electrodes

(a) Preparation

Hydrogen reference electrodes were prepared by cleaning Pt electrodes in chromic acid solution followed by thorough washing in conductivity water. Two such electrodes were then suspended in a platinizing solution containing three grams of platinic chloride in one hundred millilitres of conductivity water and were connected to a reversing switch and d.c. power supply. The current was adjusted to approximately 5 mA. cm^{-2} so that there was only a moderate evolution of gas (H_2 and Cl_2); the direction of the current was reversed every minute by an automatic switching device. The current was allowed to pass until a moderately thick coating of platinum was obtained. The coating was greyish-black and velvety in appearance. The electrodes were then washed repeatedly with water and kept in distilled water until required for use. When non-aqueous systems were studied, the electrodes were soaked in the appropriate solution for at

least 24 hours, the solution being changed at least three times during this period of time.

(b) Reproducibility and Verification of Reversibility

Before commencement of the measurements, the potential of the hydrogen electrode used was compared with that of another hydrogen electrode; if the potentials were in agreement to within one millivolt, the measurements on the test electrode were carried out. If the comparison was not satisfactory or if the potentials approached the equilibrium value only slowly, the electrodes were removed and a new set of hydrogen electrodes was prepared before any measurements were attempted. Electrodes which are not behaving reversibly rarely give identical potentials nor do they give steady, time-independent values of potential. Hydrogen electrodes are known (58) to behave satisfactorily in non-aqueous solvents of the kind used in the present work and they gave no problems in the systems studied.

(ii) Palladium Reference Electrode

This electrode was specially prepared for the "vacuum" runs where the hydrogen reference electrode could not be used since the cell was a closed system with no inlets or outlets for the gases. A large (4 $cm.^2$), clean palladium foil was saturated with hydrogen by making it a cathode in the electrolysis

of pure glacial acetic acid, through which 2 mA. current was passed for about six days. This was to ensure a slow evolution of hydrogen on the palladium cathode and the ultimate saturation of this cathode by atomic hydrogen absorbed into the interior of the palladium foil. This electrode was then dipped in a solution of the same composition as the solution to be used for the run (1M CH_3COOK in CH_3COOH) in which it showed erratic potentials (against a glass electrode) for about the first twelve hours, after which a stable potential ($\pm$ 4 mV) was obtained for the next twelve hours or so. It was during this period of attainment of a stable potential that the electrode was used in the experiments. After the experiment, the cell was broken open and the potential of the Pd electrode was measured immediately against a standard hydrogen electrode introduced in the same solution for purposes of calibration.

8. ELECTROCHEMICAL MEASUREMENTS AND ELECTRICAL CIRCUITS

(i) Potentiostatic Polarisation Circuit

The polarisation circuit consisted of a Wenking potentiostat for controlled potential polarisations, and the usual measuring instruments, i.e., an ammeter (Sensitive Research micro-milliammeter, Model 5) and a potentiometer (Radiometer Model PHM-4b, input circuit impedance $\div 10^{13}$ ohms). The polarising circuit is shown in Fig. 7.

Figure 7

Potentiostatic polarisation circuit.

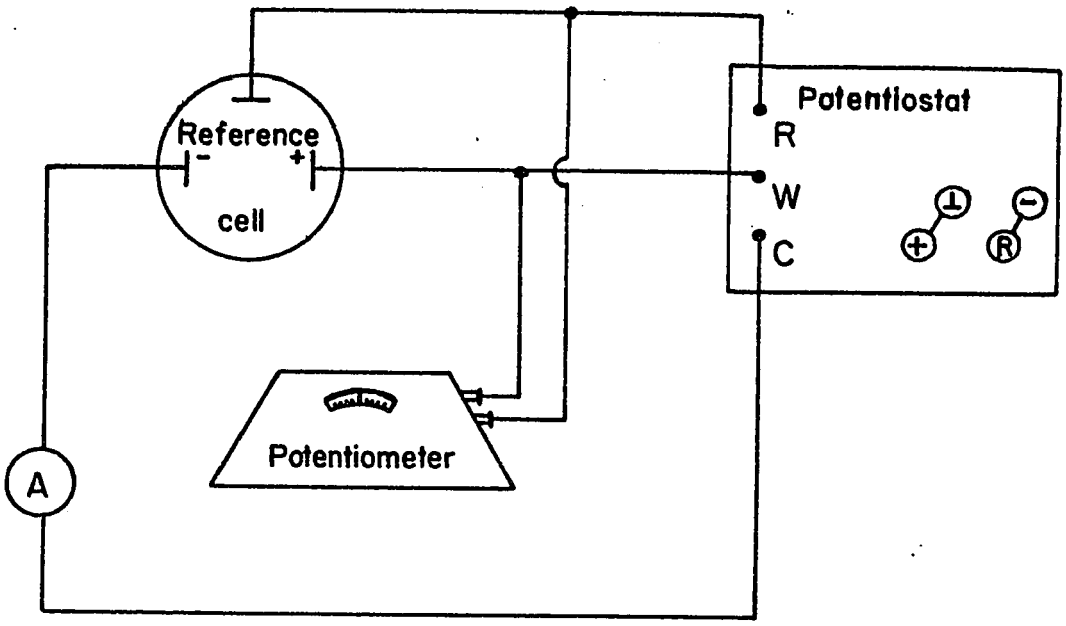
Reference
cell
Potentiostat
R
W
C
Potentiometer
A

(ii) Potentiodynamic circuit

This was a modification of the polarisation circuit described in 8(i) above. Here the reference input to the potentiostat was biased by feeding into it, at appropriate sockets, an output from a triangular sweep generator (Servomex Waveform Generator, Type L.F. 141) which was arranged to generate a constant, pre-determined dV/dt. The magnitude of the sweep signal was checked by measurement on a potentiometer with the generator in a manual ramp configuration. In series in the polarisation circuit was also included a resistance box, the potential across which was used to measure the current in the polarisation circuit and through the cell at a given moment. The voltage drop ΔV across a chosen value R of the resistance gave the current $\Delta V/R$. This current, measured as ΔV, was fed into the vertical axis of an oscilloscope the horizontal axis of which (i.e., the time-base) was driven by the potentiodynamically controlled, continuously varying potential difference between the working electrode and the reference electrode. The circuit is shown in Fig. 8.

(iii) Potential Decay Circuit

The e.m.f. decay circuit was designed so that it could be used both for open-circuit decay studies and for examination of "forced decay" behaviour (i.e., for charging curves taken in a reverse direction to that of the initial polarisation). The circuit consisted of a fast, six-position, mercury-wetted-

Figure 8

Potentiodynamic polarisation circuit.

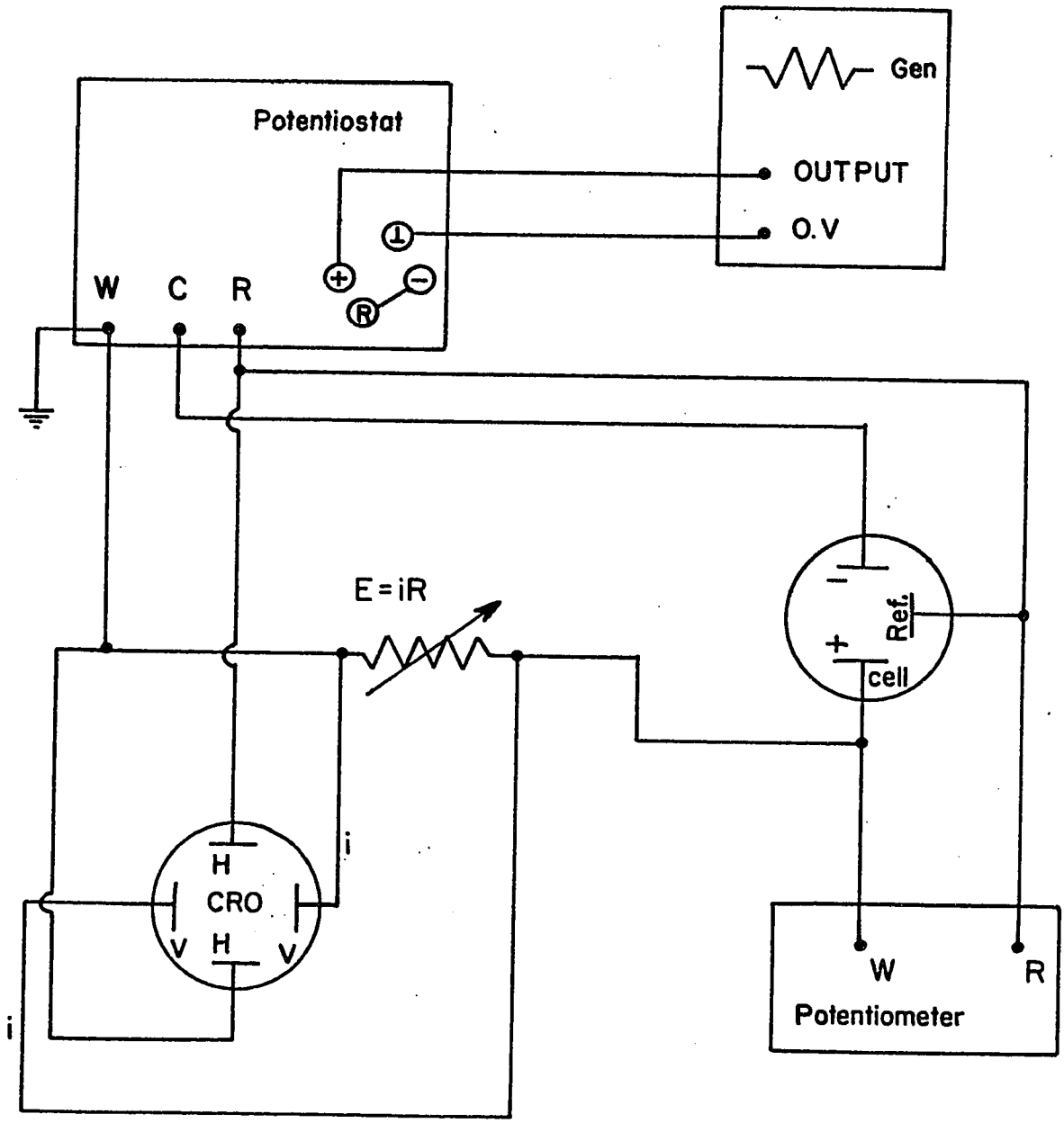
Gen
Potentiostat
OUTPUT
O.V
W
C
R
E = iR
Ref.
cell
H
CRO
V
H
V
i
i
W
R
Potentiometer

contact vacuum relay (C.P. Clare model H G2A-1004), the contacts of which were activated by an internal electromagnet. The circuit is shown in Fig. 9.

For open-circuit decay studies, the potentiostat was connected to positions one and four (Fig. 9b) and the cell was connected to positions two (anode) and five (cathode). This configuration would give controlled potential anodic polarisation which could be interrupted by pressing down a micro-switch which controlled the relay solenoid. The time-potential transient corresponding to the rate of decay of the anode potential could then be recorded on an oscilloscope (Tektronix Type 502A) after passing the signal first through a high input impedance amplifier (Tektronix Type 0 Operational Amplifier Plug-in Unit in unity-gain configuration, rise time ca. 10 μsec.).

For the "forced decay" studies, a constant d.c. current supply (which could be controlled by a series of resistors mounted on a rotary switch) was connected to positions three (negative, to make it cathodic) and six (positive, to make it anodic). In this configuration, normal potentiostatic anodic polarisation of the working electrode (plugged in position two of the relay) could be continued while the micro-switch was closed. On pressing the micro-switch, not only did positions two and five become disconnected from one and four (hence resulting in cessation of anodic polarisation), but instantaneous connection of two and five was made respectively with positions

Figure 9

Decay circuit

(a) Relay configurations for the anodic polarisation stage.

(b) Relay configurations for the open-circuit e.m.f. decay stage.

(c) Relay configurations for the cathodic transient stage.

R.	Relay
M.	Micro-switch
A.	Ammeters
H.I.I.A.	High input impedance amplifier
D.A.	Differentiating amplifier
T.	Trigger terminal
C_1 and C_2.	Two channels of the oscilloscope
W.	Working electrode terminal
C.	Counter electrode terminal
R.	Reference electrode terminal

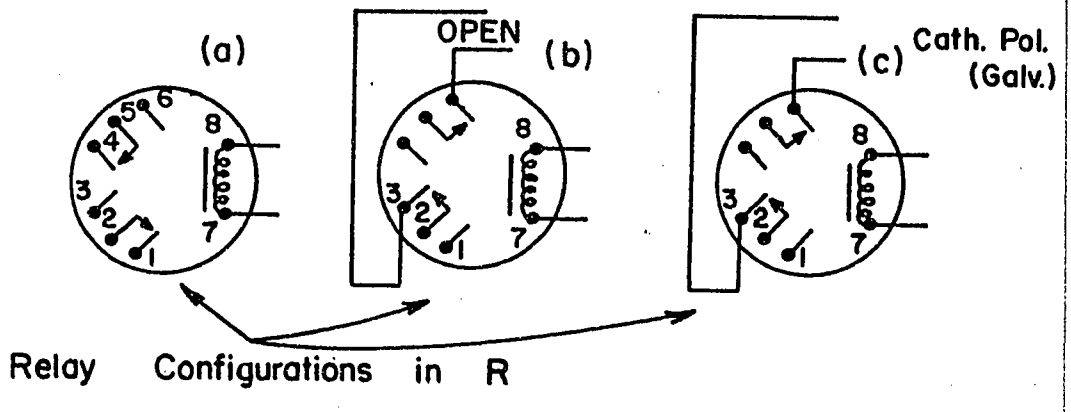
(a)
OPEN
(b)
(c)
Cath. Pol.
(Galv.)
Relay Configurations in R

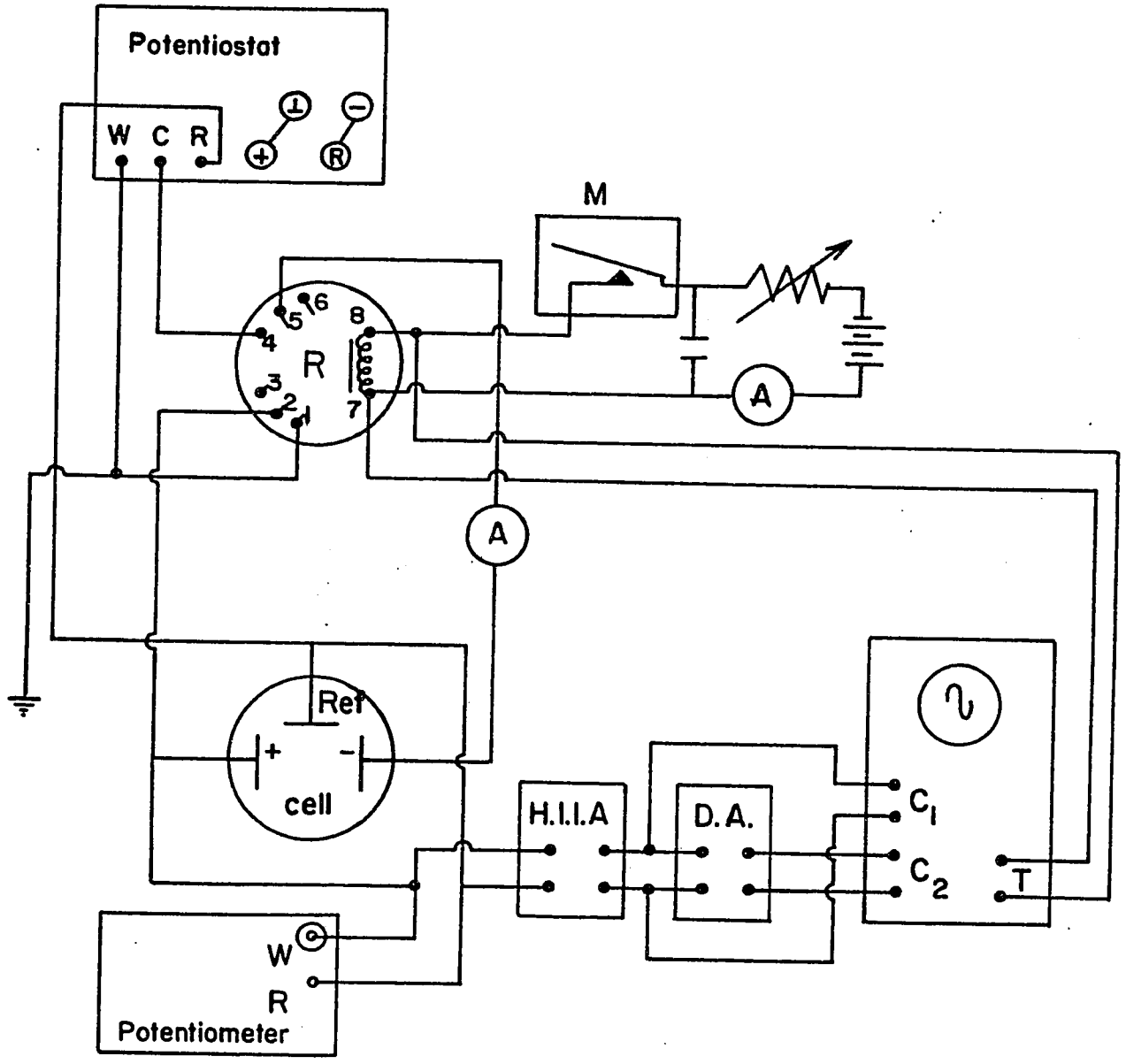
Potentiostat
W C R
M
R
A
A
Ref
cell
H.I.I.A
D.A.
C1
C2
T
W
R
Potentiometer

three and six of the relay (Fig. 9c) (hence commencing the cathodic charging transient). Reversal of polarisation was achieved in a switching time of less than 5×10^{-6} seconds. The potential-time relations at the test electrode (the potential of which was referred to that of the hydrogen electrode in the same solution) were registered by feeding the signal first through a high input impedance amplifier (Tektronix, Type "O" operational Amplifier as mentioned above) and then to one channel of a dual-beam oscilloscope. The signal was also fed into the second channel of the O unit (Tektronix, Type O Operational Amplifier Plug-in Unit) pre-set in a differentiating configuration, the output of which was fed into the second channel of the dual beam oscilloscope. Thus both potential-time relations, as well as the time-differential coefficients of such profiles, were recorded simultaneously on the same oscilloscope photograph. Examples are shown in Figs. 18, 22,29,37,44,49 and 53.

9. EXPERIMENTAL PROCEDURE IN RUNS

(i) Polarisation Measurements

After the solution had been prepared (as described above) and transferred to the cell, the solution was cooled to $5^{\circ}C$ by circulating coolant from a low temperature thermostat through glass coils sealed in the cell. Carbon dioxide was

then bubbled through the solution. Potential measurements were then carried out by lowering one of the encapsulated electrodes under the solution and shattering the glass bulb surrounding the electrode by means of a glass probe*. The electrode was then adjusted carefully against the Luggin capillary and the current measurements were carried out over a potential range of about 0.0V to 3.0V (w.r.t. the reversible hydrogen electrode), which was approximately the limit of effective control by the potentiostat in the solutions studied.

Current measurements were made by waiting for sixty seconds (stop-watch timing) at each given value of potentiostatically controlled anodic potential. This yielded a somewhat arbitrary, though standardised, procedure in which the currents obtained were practically steady, yet the electrodes were not subjected to the possibility of any long-time poisoning effects as sometimes occurs in some solutions, e.g., in the hydrogen evolution reaction.

(ii) Potentiodynamic Measurements

Here the initial setting of the potentiostat and the

*Pre-electrolysis of the solution in the trial runs did not produce any noticeable change in the log[i]-V relations. However, extensive pre-electrolysis for long times was avoided in the subsequent runs since it tended to produce (rather than remove) some impurities by side oxidation of the organic substrates; this could be visually seen in some cases by slight colouration of the solution after prolonged electrolysis.

bias applied to it from a wave-form generator were so arranged that the potential region under study lay within the two extremes of the time-dependent signal. The value of resistance in the resistance box (joined in series in the polarisation circuit) was so chosen that sufficient potential was generated to give a proper display of the charging current peaks (if any) at the appropriate settings of the Y-axis sensitivity of oscilloscope. The minimum series resistance was always used with the maximum oscilloscope Y-axis sensitivity. The current-potential relations thus obtained were recorded on oscilloscopic photographs at several sweep rates. The amplitude of the signal was measured by means of a potentiometer after the sweep runs had been completed, but with the generator now in "ramp" configuration, as mentioned above.

(iii) Potential Decay Measurements

In the studies of open-circuit decay of e.m.f., an electrode was initially polarised to a desired, controlled anodic potential for a standard chosen time (120 sec. in most cases) and the polarisation current was measured. The polarisation current was then interrupted through activation of the mercury relay described above. The potential signal for the test electrode was passed through the high input impedance amplifier and then fed into an oscilloscope where it was recorded photographically as described above.

In the forced decay measurements, i.e., cathodic (dis-) charging curves, the electrode was first polarised to a given controlled anodic potential for a chosen standard time (120 sec.) and the corresponding polarising current was recorded manually by means of an ammeter. The micro-switch was then pressed down which activated the relay, resulting in reversal of the polarisation current. The potential-time transient signal of the test electrode was first fed into the high input impedance amplifier, differentiated and recorded simultaneously in direct and differential forms on the dual-beam oscilloscope as described above. Such transients were recorded for a range of initial anodic potentials; also from a given anodic potential, "forced decay" transients were taken over a range of cathodic current densities.

10. TEMPERATURE CONTROL

The temperature of the TFA solutions in the polarisation cell was maintained constant by circulating a coolant (ethylene glycol-water mixture) through a cooling coil specially sealed in the anode and reference electrode compartments. The coolant was kept at $5^{\circ}C$ by means of two low-temperature thermostats (Wilkins Anderson Company, Model 882). The low-temperature baths were capable of maintaining the temperature constant to within $0.1^{\circ}C$. The cell temperature could be maintained at

$5 \pm 0.2^{\circ}C$. This temperature was used for all the runs in order to minimise the attack on the noble metals, especially gold, under conditions of anodic polarisation, particularly in the non-aqueous solutions studied. However, the runs in the acetate solutions were carried out at room temperature ($25^{\circ}C$) in order to make relevant comparisons with previous work (3,8,11,60) in these solutions.

11. CHARACTERISATION OF GASES EVOLVED

The gases produced in the anode compartment of the special cell used for gas characterisation studies, were condensed into an evacuated trap at liquid air temperatures. After collecting the gases, the temperature of the trap was raised to $-50^{\circ}C$ in an acetone-solid carbon dioxide bath. At this temperature all the Kolbe products were in gaseous form but traces of the acid (i.e., in the electrolyte) which had become co-condensed in the trap were still solid. The gases in the trap were then injected into a vapour phase chromatograph using silica-gel at controlled temperature as the column material. The peaks obtained were characterised by comparison of the retention times with those for known gas mixtures studied under the same column conditions and flow rates and prepared in an attached system of gas burettes. Typical chromatograms are shown in Fig. 10.

Figure 10

Reproduction of V.P.C. recorder tracings for a typical run and a typical calibration.

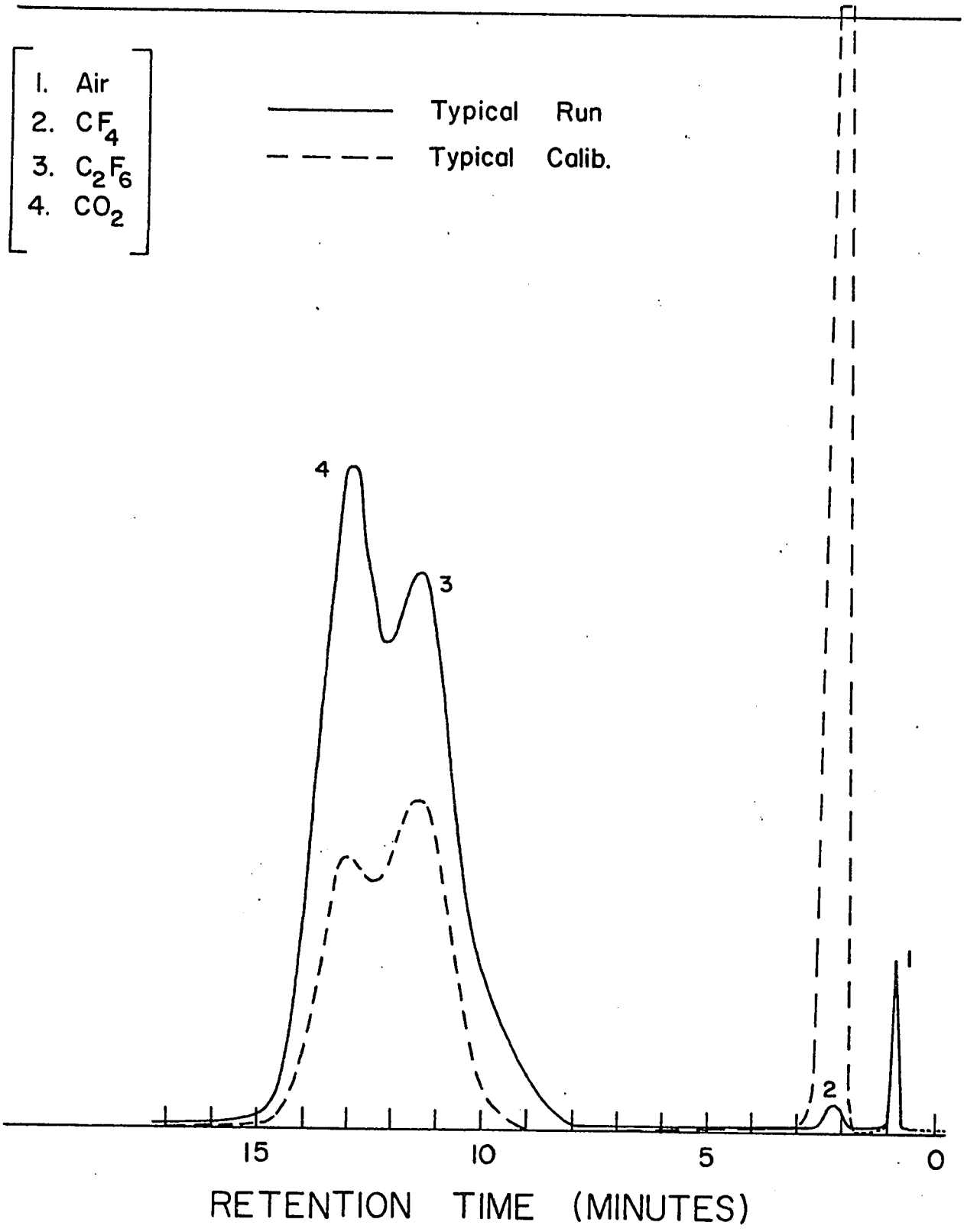
1. Air
2. CF_4
3. C_2F_6
4. CO_2
Typical Run
Typical Calib.
4
3
2
1
15
10
5
0
RETENTION TIME (MINUTES)

12. EXPLORATION OF SUITABLE CONDITIONS FOR COULOMBIC-YIELD STUDIES

When coulombic efficiency studies were contemplated, it was thought necessary to have some estimate of the extent of the solubility of the Kolbe products in the electrolyte being studied. In the simple solubility apparatus described above (see Fig. 6), a known volume (38 ml.) of C_2F_6 was introduced into the dual-bulb compartment containing 100 ml. of pure CF_3COOH under atmospheric pressure. The solution in contact with the gas was agitated at intervals to effect equilibrium dissolution. It was found that about 33 ml. of the gas were dissolved in the acid over a twenty-four hour period. This considerable solubility of the gas in the solvent under study precluded the possibility of exact, quantitative coulombic efficiency studies except at high current densities in pre-saturated solutions, as used in the previous work (2).

Pre-saturation of the solutions by gaseous Kolbe products was considered wrong in principle since it would not be possible to distinguish unambiguously whether the products being characterised were produced during electrolysis or were a result of some de-gassing of the pre-saturated solution.

Also, coulombic efficiency studies were not carrried out in acetic acid solutions since satisfactory and reproducible results had already been published by various authors (3,7,8,14,60)

under comparable conditions. However, the observation that the Kolbe reaction does not proceed with any detectable efficiency on gold (3,7) has been recently contradicted by Sugino and co-workers (60) (see below in Chapter III); hence, it was thought necessary to characterise the anodic products obtained during electrolysis at gold in aqueous acetate solutions.

CHAPTER III

RESULTS

1. POTENTIOSTATIC CURRENT-POTENTIAL RELATIONSHIPS AND CHARACTERISATION OF PRODUCTS

(i) General

As discussed in Chapter I, section 3(i), valuable diagnostic criteria for the assignment of reaction mechanisms can sometimes be given by the Tafel parameters under certain limiting conditions of surface coverage, provided that knowledge of reaction products is available and some plausible kinetic scheme of the consecutive elementary reactions has been formulated.

In the following section, experimental results are first presented for characterisation of products. Current-potential relationships (Tafel plots), obtained under potentiostatic conditions, are then presented for platinum and gold in both completely anhydrous trifluoroacetate-trifluoroacetic acid and acetate-acetic acid solutions, and in these solutions to which small quantities of water had been deliberately added. The Tafel plots are shown in a way which emphasizes the detailed structure of the i-V curve below the Tafel region which is discerned under potentiostatic conditions. Any changes in the structure of this region brought about by addition of traces or excess of water to the anhydrous solution, can easily be detected.

(ii) Characterisation of Products

Characterisation of the products of electrolysis was carried out only in the trifluoroacetate-trifluoroacetic acid system since in the acetate-acetic acid system satisfactory results had already been published by various authors (3,7,8, 14,31,60). However, recently, Sugino and co-workers have reported results (60) on the identity of the gases evolved on gold anodes in aqueous acetate-acetic acid solutions, which contradict some of the observations of earlier workers (3,7). Before Sugino and co-workers reported their results (60), it was believed that (3,7) the Kolbe reaction does not proceed with any detectable efficiency on gold as an anode in aqueous acetate-acetic acid solutions; however, Sugino and co-workers claim (60) to have observed almost quantitative yields of the Kolbe products under these conditions. In the present studies, evolution of oxygen only was detected on gold anodes in aqueous acetate-acetic acid solution, in agreement with the findings of several previous workers (3,7).

In the trifluoroacetate-trifluoroacetic acid system, both under completely non-aqueous conditions and when traces or excess of water were added, CO_2 and C_2F_6 with traces of CF_4 were evolved on electrolysis both at gold and platinum anodes. A typical v.p.c. recorder tracing in an experimental run

together with the calibration curve obtained with the column and other conditions such as flow rate maintained the same, is shown in Fig. 10. In all cases these Kolbe products were found only in the post-transition linear Tafel region corresponding to potentials > ca. 2.3V (E_H) and consequently at high current densities (ca. 10^{-4} a.cm.$^{-2}$). As was pointed out in Chapter II, section 12, the Kolbe products evolved are appreciably soluble in the trifluoroacetate-trifluoroacetic acid solutions used; hence any attempts to establish whether evolution of the Kolbe products occurred at lower potentials (and consequently lower current densities) were rendered unsuccessful by the fact that these products would have to be evolved in quantities well above those necessary to pre-saturate the solutions. Such quantities would be produced only by carrying on the electrolysis at higher potential (and hence higher current densities) or for times too long to be practical.

(iii) Experimental Current-Potential Relationships (Potentiostatic Conditions)

In order to characterise electrochemically the mechanisms of the decarboxylation reactions involved in the present investigations, current-potential measurements were made by measuring the overall rate of the reaction in terms of current at various values of the electrode potential, referred

to the hydrogen electrode in the same solution and maintained constant potentiostatically. The various values of potential chosen were such as would give an even distribution of points on the potential axis. This was accomplished by manual programming of the potentiostat in such a way that the potential was changed in 50 mV steps after being maintained constant for one minute at each particular value of the chosen potential. This method, although arbitrary, established a "practical" steady-state and gave very reproducible results. All measurements in trifluoroacetate-trifluoroacetic acid solutions were carried out at 5°C for reasons discussed in Chapter II. Measurements in acetate-acetic acid solutions were carried out at room temperature (cf. 3,14,31,60) since the oxidation of the substrate metal is not so pronounced in this system.

In the results presented below, the data are based on runs for at least eight electrodes studied in at least two separately prepared solutions.

(a) Platinum in Potassium Trifluoroacetate-Trifluoroacetic Acid Solutions

In this system, potentiostatic current-potential relationships were obtained in completely anhydrous solutions, in solutions which were presumed to contain traces of water, and finally in solutions to which small quantities of an aqueous solution of potassium trifluoroacetate (1M) were

deliberately added. Such solutions were prepared in the following way: firstly a solution of highly purified, anhydrous potassium trifluoroacetate (1M) in anhydrous, scrupulously purified trifluoroacetic acid was prepared. Despite the adoption of extreme precautions (see section 2(ii), Chapter 2) these solutions were believed still to contain minute traces of water (mostly from atmospheric diffusion). Runs were first carried out in this solution on two platinum electrodes and then to this solution was added 1% pure trifluoroacetic-anhydride which reacts rapidly with traces of water and thus renders the solution completely anhydrous without contamination of the solution by any extraneous material of a radically different chemical nature. Runs were carried out in this solution on two fresh platinum electrodes. To this solution was now added 90% by volume of a 1M solution of CF_3COOK in water and then the runs were carried out on two more fresh platinum electrodes. The current-potential plots thus obtained in the completely anhydrous solutions, and in solutions containing traces, or excess, of water have all been plotted together in Fig. 11; also, for the purposes of comparison, the Tafel line obtained at platinum in H_2SO_4 has also been plotted in the same figure. This sequence of runs in solutions containing varying quantities of water, and the corresponding plots on the same graph

Figure 11

Platinum/1MCF_3COOK in CF_3COOH: steady-state current-potential relations:

1. (—·—·—·—·) with anhydride, b = 0.215V;
2. (– – – – – –) without anhydride, b = 0.27V;
3. (————————) with added water, b = 0.25V;

and

4. (—— ——) Pt/1MH_2SO_4, b = 0.12V.

Note: All graphs are based on points measured at 30-50 mV. intervals in the ascending and descending direction of potential change (see also Fig. 14).

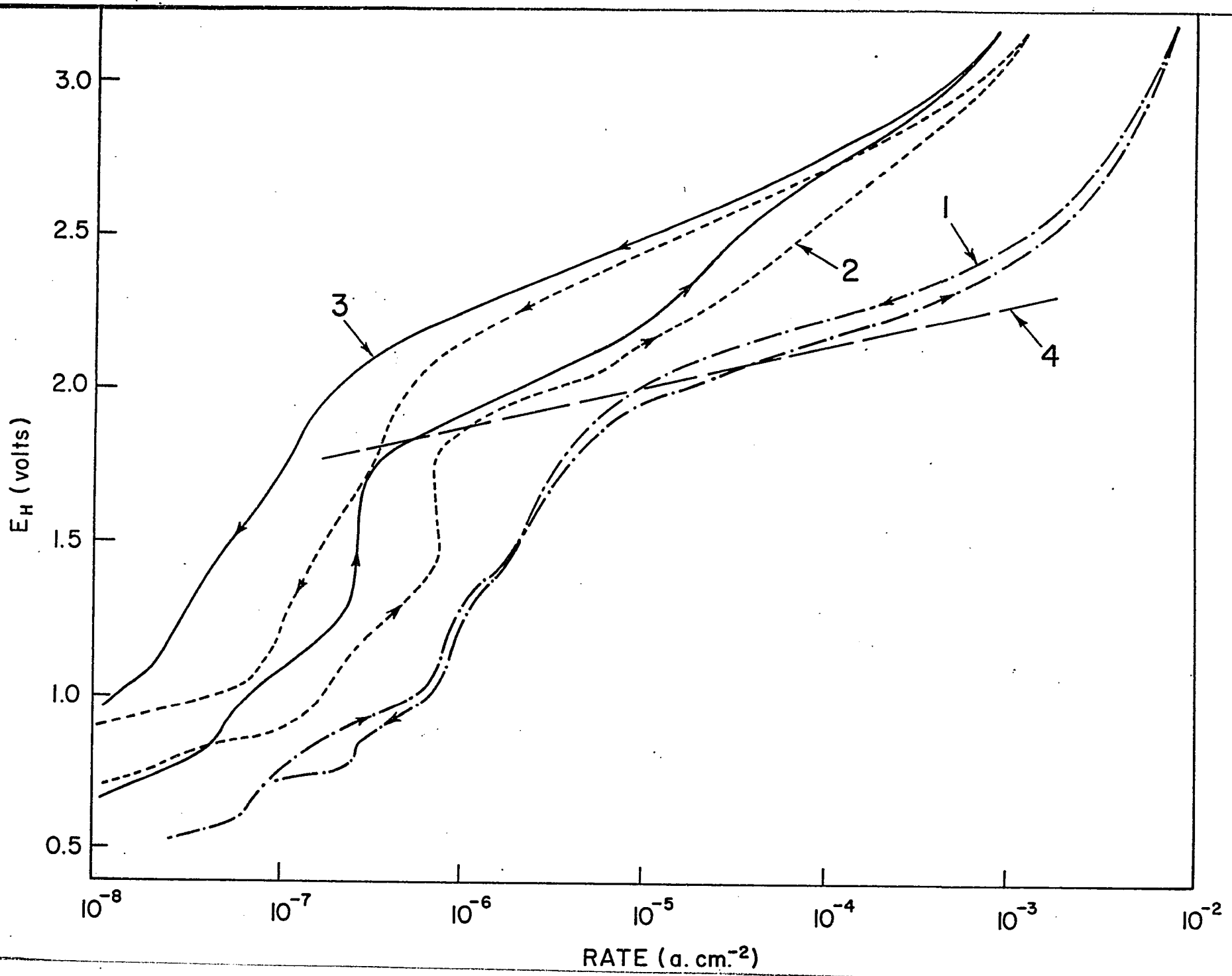
3.0
2.5
2.0
1.5
1.0
0.5
E_H (volts)
10^{-8}
10^{-7}
10^{-6}
10^{-5}
10^{-4}
10^{-3}
10^{-2}
RATE (a. cm.$^{-2}$)
1
2
3
4

(Fig. 11), were purposely selected in order (a) to seek information on the role, in the Kolbe electro-synthesis, of adsorbed oxygenated species arising from water and (b) to emphasize in a comparative way any distinctions which may be observed in the Tafel behaviour for solution compositions altered in a pre-determined manner.

As shown in Fig. 11, the ascending and descending log[i]-V curves show little hysteresis when the solutions are completely anhydrous. In pure TFA (trifluoroacetic acid) solution (which presumably contains some traces of water), a definite hysteresis between the ascending and descending log[rate]-potential curves is observed; also the rates, at a given potential, are smaller in this case in comparison with the ones for the anhydrous system, especially at potentials lower than those corresponding to the commencement of the linear Tafel region. The hysteresis is further augmented, and the rates are correspondingly diminished in the presence of excess water. In all cases, linear Tafel relations are observed in the post-transition region (i.e., post-passivation region) with Tafel slopes $\underline{b}$ on the descending curves equal to 0.215 V (anhydrous solutions), 0.270 V (solutions with traces of water), 0.250 (solutions with excess of water). For comparison, the Tafel line for oxygen evolution on Pt in H_2SO_4 (63) exhibits a slope of 0.12 as also shown in Fig. 11.

The rest potentials* (i.e., the potentials on the descending curve at which the current just tends to become cathodic), are noticeably different in the three types of solutions studied. In the completely anhydrous solutions, the rest potentials were ca. 500 mV; in solutions containing traces of water, the rest potentials were ca. 900 mV; and in solutions containing excess of water, the rest potentials were ca. 950 mV.

(b) Gold in Potassium Trifluoroacetate-Trifluoroacetic Acid Solutions

In this system, the types of solutions studied and the sequence in which they were examined were exactly the same as for the case of platinum in potassium trifluoroacetate-trifluoroacetic acid solutions discussed in (a) above. The results are presented in Fig. 12. Again, under completely anhydrous conditions, little hysteresis is observed in the transition region (i.e., the passivation region) between the ascending and descending log[i]-V curves. The transition region is followed by a linear Tafel relation with a slope b = 0.160 V. In the presence of traces of water, an unusual phenomenon is observed around 1.80 V. The transition region does not extend directly into a normal linear Tafel region as

*The diagnostic significance of the rest potentials observed will be discussed in more detail in Chapter IV, section 2.

Figure 12

Gold/1MCF_3COOK in CF_3COOH: steady-state current potential relations:

——— with anhydride;

----- without anhydride;

—·—·— with added water.

Note: all graphs are based on points measured at 30-50 mV. intervals in the ascending and descending directions of potential change (see also Fig. 14).

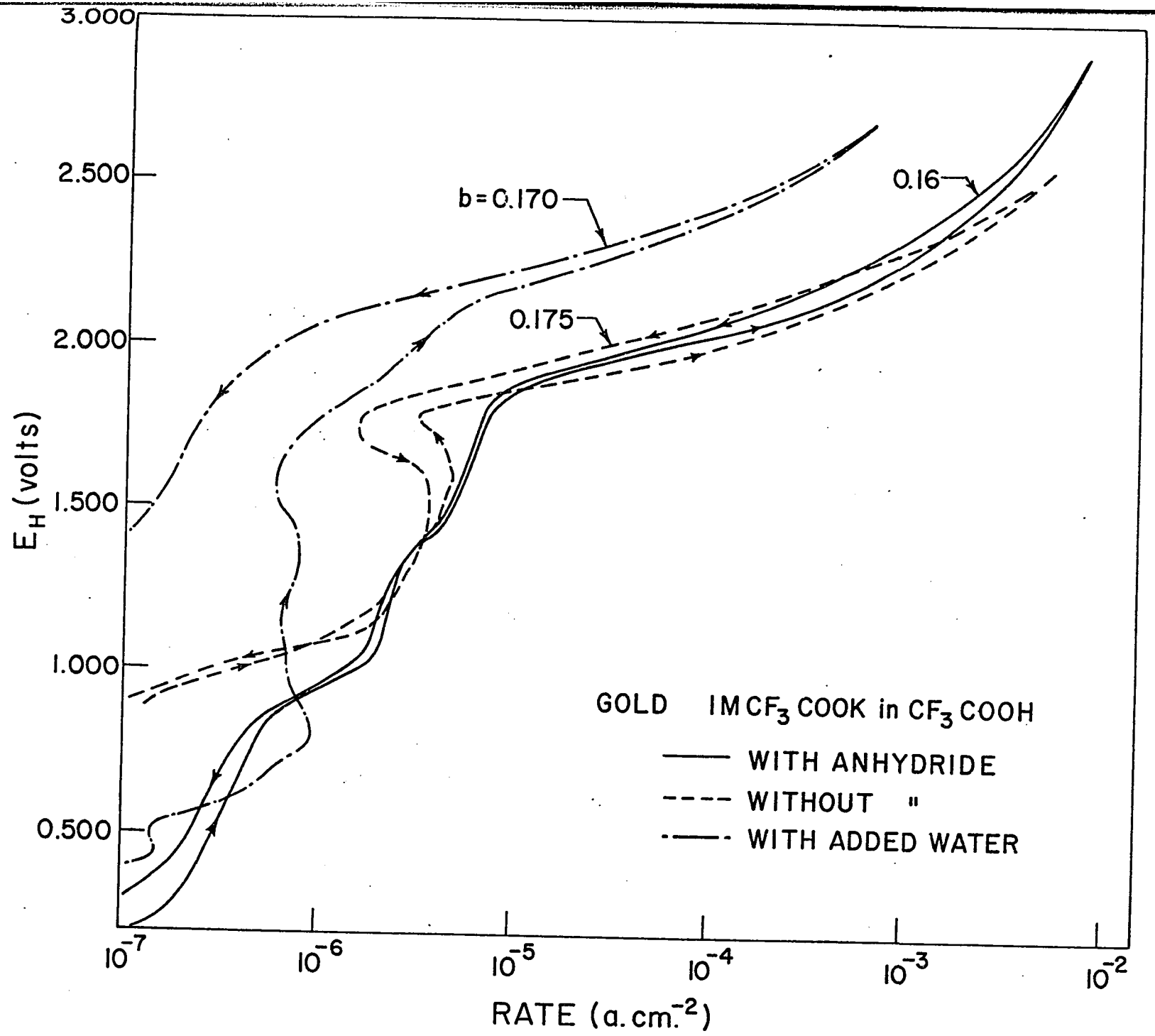
3.000
2.500
2.000
1.500
1.000
0.500
E_H (volts)
b = 0.170
0.16
0.175
GOLD 1M CF_3 COOK in CF_3 COOH
WITH ANHYDRIDE
WITHOUT "
WITH ADDED WATER
10^{-7}
10^{-6}
10^{-5}
10^{-4}
10^{-3}
10^{-2}
RATE (a. $cm.^{-2}$)

in the case of anhydrous solutions; instead, an inversion of rate is observed, i.e., with increased potential, the rate first decreases with increasing potential over a narrow potential range (1.6 - 1.8 V) instead of exhibiting a normal continuous increase with potential. This behaviour manifests itself in the log[i]-V plots in the form of a characteristic inhibition bend of the type discussed recently by Gilroy and Conway (62) in connection with some other electrochemical oxidations. The log[i]-V inversion is followed by a linear Tafel region with a slope b = 0.175 V. In solutions containing excess of water, not only is the rate diminished and the hysteresis between the ascending and descending log[i]-V plots enhanced, but the characteristic inhibition behaviour observed with traces of water also suffers a drastic apparent change in that it is largely obscured. This appears to arise probably because of the fact that the hysteresis is now large enough to encompass the whole range of potentials over which the original inhibition inversion was observed. At sufficiently high potentials, however, a linear Tafel region still arises in the post-transition region with a slope (on the descending curve) of b = 0.170 V.

The rest potential (see p. 71) is also remarkably different in the three cases. In anhydrous solutions, it is ca. 0.25 V; in solutions containing traces of water, it is

ca. 0.90 V; and in solutions containing excess of water it is ca. 1.25 V. Further discussion of these observations will be given in Chapter IV, section 2(ii).

(c) Platinum in Potassium Acetate-Acetic Acid Solutions

The log[current]-potential behaviour was investigated at platinum in anhydrous solutions of potassium acetate (1M) in acetic acid (in the "vacuum" cell) described in Chapter II*; subsequently this solution was made 0.1M in H_2O and current-potential runs were carried out on fresh electrodes. Finally this solution was made 1M in H_2O and the current-potential behaviour was re-examined on fresh platinum electrodes. In a separate aqueous solution, 1M in CH_3COOK and 1M in CH_3COOH, the current-potential relation was also examined independently on fresh platinum electrodes, as a check on the results obtained for successive additions of water. These log[i]-V plots are presented together in Fig. 13 and the linear Tafel relation associated with O_2 evolution at platinum in H_2SO_4 is also shown for comparison on the same graph. This procedure was adopted

*The "vacuum" run in the "vacuum" cell, as described in Chapter II was necessitated by the fact that very anhydrous conditions in the potassium acetate-acetic acid solutions could not be obtained by addition of small quantities of acetic anhydride, as was the case in the TFA solutions discussed above.

Figure 13

Platinum/1MCH_3COOK in CH_3COOH ("vacuum"): steady-state current-potential relations:

2. (—·—·—) completely anhydrous solution, b = 0.14 V;
3. (----------) + 0.1M H_2O, b = 0.14 V;
4. (— — — —) + 1.0 M H_2O, b = 0.135 V;
5. (————) + excess H_2O, b = 0.26 V and b = 0.165 V;

and

7. (—— ——) Pt/1MH_2SO_4, b = 0.12 V.

Note: all graphs are based on points measured at 30-50 mV. intervals in the ascending and descending directions of potential change (see also Fig. 14).

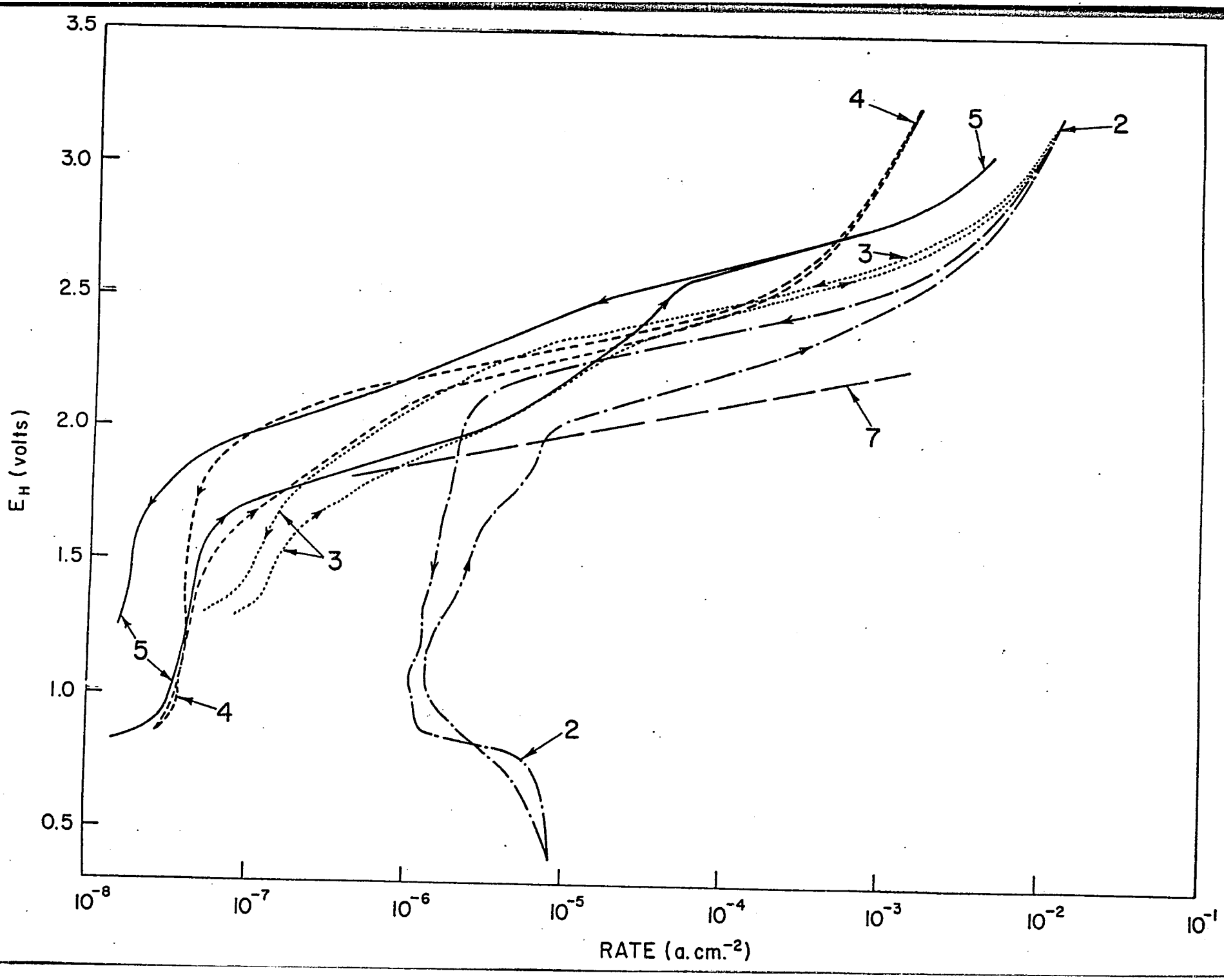
3.5
3.0
2.5
2.0
1.5
1.0
0.5
E_H (volts)
10^{-8}
10^{-7}
10^{-6}
10^{-5}
10^{-4}
10^{-3}
10^{-2}
10^{-1}
RATE (a.cm.$^{-2}$)
4
5
2
3
7
3
5
4
2

in order to emphasize the distinctions between the detailed structures of potentiostatic current-potential profiles corresponding to Kolbe oxidation that may arise on account of the presence of varying amounts of water in the "non-aqueous" system.

It will be noticed that, in general, the greater the amount of water added to the system, the lower is the rate at a given potential and the higher is the rest potential. Significant hysteresis between the ascending and descending curves was observed in all cases. The experimental results obtained in this case are summarised in Table I.

(d) Gold in Potassium Acetate-Acetic Acid Solutions

Current-potential relationships at gold in potassium acetate-acetic acid solutions were examined both in non-aqueous* and aqueous solutions. The results are presented in Fig. 14.

In the non-aqueous system, a small hysteresis is observed in the transition region (i.e., passivation region) between the ascending and descending log[i]-V curves. The transition region is followed by a linear Tafel relation with a slope b = 0.11 V. The rest potential is ca. 1.30 V.

---

*Non-aqueous solutions were prepared by a systematic and scrupulous purification procedure described in Chapter II. Runs were not carried out under high vacuum conditions in the case of gold since it was thought that the use of that procedure in the case of platinum was sufficient to demonstrate the role of water.

Table I

Current-potential behaviour at Pt in potassium acetate-acetic acid solutions etc. (Fig. 13).

Table I. Current-Potential Behaviour at Pt in Potassium Acetate-Acetic Acid Solutions etc. (Fig. 13)

Solution	Tafel Slopes (b)	Rest Potential
1M CH_3COOK in CH_3COOH (anhydrous)	b = 0.14 V (ca. 2.0 V⟶)	0.2 V
1M CH_3COOK + 0.1M H_2O in CH_3COOH	b = 0.135 V (ca. 2.0 V⟶)	0.8 V
1M CH_3COOK + 1M H_2O in CH_3COOH	)b = 0.14 V (ca. 2.0 V⟶))b = 0.31 V (ca. 1.6 V⟶ 2.0 V)	1.1 V
1M CH_3COOK + 1M CH_3COOH in water	)b = 0.165 V (ca. 2.5 V⟶))b = 0.26 V (ca. 2.2 V⟶2.5 V))b = 0.20 V (ca. 1.8 V⟶2.2 V)	1.1 V
1M H_2SO_4	b = 0.17 V	1.1 V

Figure 14

Gold/1M CH_3COOK in CH_3COOH: steady-state current-potential relations, also showing population of experimental points on a typical curve:

● nominally anhydrous solution;

○ aqueous solution.

Note: Curve for nominally anhydrous solution is curved at high i due to significant resistance p.d. (potential drop) in the non-aqueous solution.

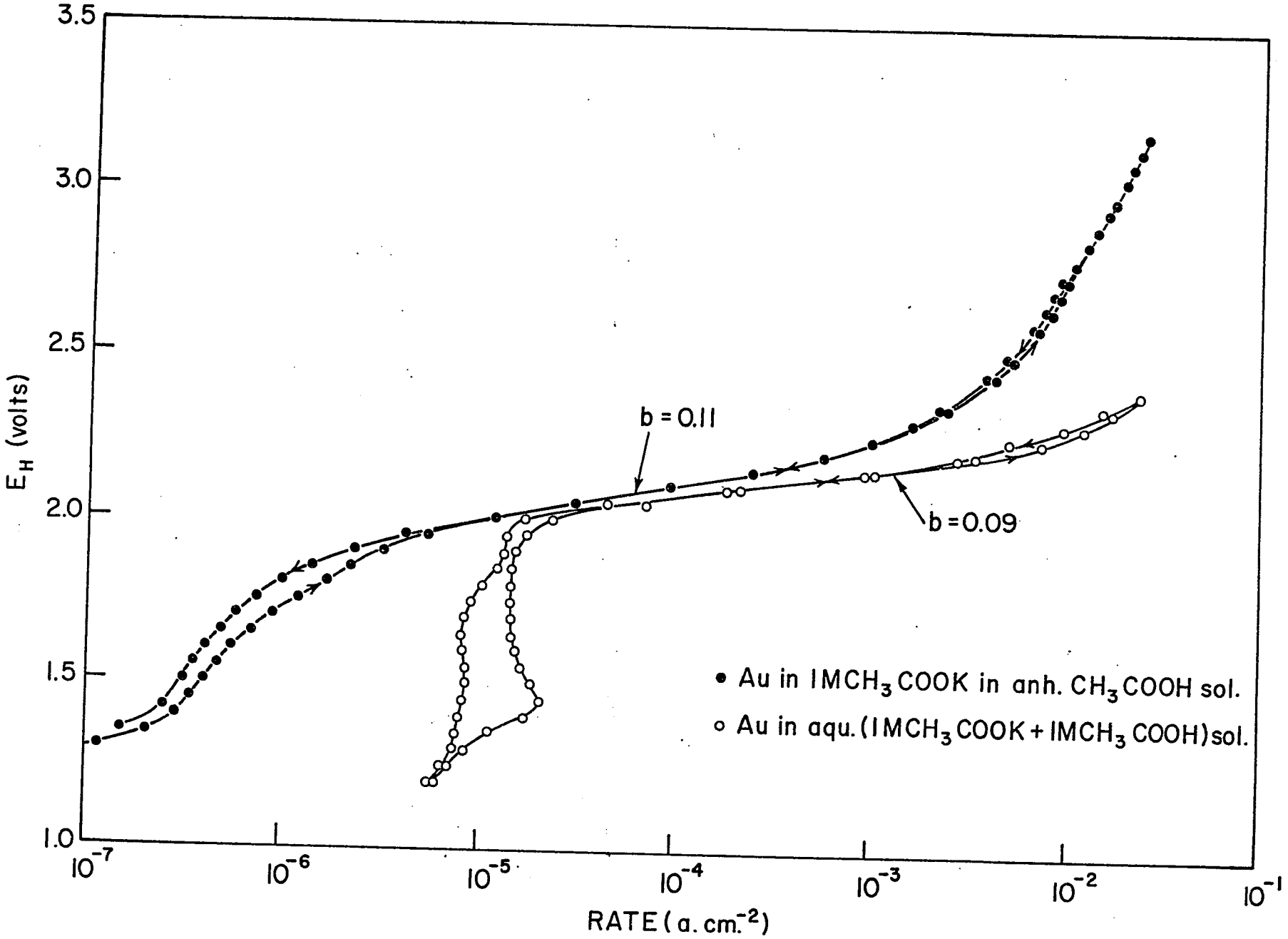
3.5
3.0
2.5
2.0
1.5
1.0
E_H (volts)
b = 0.11
b = 0.09
• Au in $IMCH_3COOK$ in anh. CH_3COOH sol.
○ Au in aqu. ($IMCH_3COOK$ + $IMCH_3COOH$) sol.
10^{-7}
10^{-6}
10^{-5}
10^{-4}
10^{-3}
10^{-2}
10^{-1}
RATE (a. $cm.^{-2}$)

In the aqueous solution, a larger hysteresis than in the non-aqueous case is observed in the transition region and a slight inhibition bend arises both in the ascending and descending curves. This behaviour is similar to that observed in the case of gold in the TFA solutions containing traces of water [see (b) above]. The transition region is followed by a linear Tafel relation with a slope $b = 0.09$ V. The rest potential is ca. 1.25 V.

An unusual feature is noticed in this system in that the rate is higher in the aqueous system than in the non-aqueous system.

2. SELF-DISCHARGE AND DRIVEN-DECAY BEHAVIOUR FROM POTENTIOSTATICALLY-MAINTAINED ANODE POTENTIALS

(i) General

As discussed in Chapter I, section 3(ii), complementary information on the pseudo-capacity of the electrode and the related extent of surface coverage of the electrode by adsorbed intermediates can be deduced from the decay of electrode potential either on open-circuit or on cathodic charging from anodic potentials initially maintained potentiostatically at various values (59,51,52,53). Usually the presence of adsorbed intermediates is indicated by "arrests"

(i.e. maxima and minima in the constantly changing slope dV/dt) in the decay profiles*.

In some cases, on self-decay of the initial polarisation potential, a "residual" potential** was observed. This residual potential is associated with the presence of some adsorbed intermediates on the electrode which are difficult to remove by a self discharge reaction; in certain cases, these intermediates can be subsequently removed from the electrode by driven decay (cathodic discharge) from the residual potential.

In addition to the open-circuit decay measurements, cathodic charging was employed to effect the decay of the initial anodic potentials of the electrodes. These charging curves yield additional information on the pseudo-capacity and coverage behaviour associated with the adsorbed intermediates formed on the electrode during anodic polarisation. This approach is particularly valuable in cases where the adsorbed intermediates are not so easily reducible and hence

---

*This is strictly true only if the adsorbed intermediates are "electro-active", i.e., if they are susceptible to reduction (and hence removal from the anode) either by the self-discharge or by the cathodic charging process.

**The term "residual" potential refers to the potential attained by the electrode after rapid self-decay of part of its initial polarisation potential. The residual potential will thus be the quasi-steady potential that the electrode attains after a few minutes of cessation of polarisation.

are not spontaneously removed during open-circuit decay.

(ii) Experimental Relationships for Decay of Potential

Experimental measurements aimed at the study of potential-time relations observed on self-discharge and forced decay of anodic potentials were carried out as described in Chapter II, section 9(iii). The results obtained are described below.

(a) Platinum in Potassium-Trifluoroacetate-Trifluoroacetic Acid Solutions

Potential decay behaviour was examined in: (α) completely anhydrous solutions; (β) solutions containing, presumably, traces of water, i.e., nominally anhydrous solutions; (γ) solutions to which excess of aqueous 1M CF_3COOK solution (30% by volume) was deliberately added. The results obtained in the three types of solutions are summarised and compared in Table II, sections 2 and 3.

Open-Circuit decay behaviour: In the completely anhydrous solutions, no arrests are observed in the open-circuit potential-time relations and the capacity values are of the order of the d.l. capacity (ca. 100 μF. cm.$^{-2}$). The residual potential is ca. 0.6 V. Similar comments apply to solutions containing presumably traces of water except that the residual potential in this case attains a somewhat higher value of 0.9 V. The C-V profiles calculated from open-circuit decay from various

Table II

Behaviour at Platinum: potassium trifluoroacetate-trifluoroacetic acid solutions.

TABLE II. BEHAVIOUR AT PLATINUM

EXPERIMENTAL EVIDENCE	SOLUTION: 1M CF_3COOH IN CF_3COOH + 1M $CF_3CO.O.COCF_3$	SOLUTION: 1M CF_3COOK IN CF_3COOH	SOLUTION: 1M CF_3COOK IN CF_3COOH + 1M CF_3COOK IN H_2O	REMARKS (GENERAL)
1. CURRENT-POTENTIAL RELATIONS				
(i) TAFEL SLOPES.	(i) 0.215 V	(i) 0.22 V	(i) 0.25 V	
(ii) HYSTERESIS?	(ii) NO HYSTERESIS	(ii) HYSTERESIS	(ii) LARGE HYSTERESIS.	
(iii) REST POTENTIAL.	(iii) 0.5 V	(iii) 0.9 V	(iii) 0.950 V	WITH INCREASING AMOUNTS OF H_2O IN THE SOLUTION, HYSTERESIS BECOMES LARGER, RATE BECOMES LOWER, AND THE REST POTENTIAL BECOMES HIGHER.
(iv) ADDITIONAL FEATURES OR COMMENTS				
2. OPEN-CIRCUIT DECAYS				
(i) ARREST?	(i) NO ARRESTS.	(i) NO ARRESTS.	(i) NO ARREST.	
(ii) MAGNITUDE OF C	(ii) d.l. CAPACITY ($<100\ \mu F\ cm^{-2}$).	(ii) d.l. CAPACITY ($<100\ \mu F\ cm^{-2}$).	(ii) $C_{max.} = 468\ \mu F\ cm^{-2}$ AT 1.405 V.	
(iii) RESIDUAL POTENTIAL.	(iii) 0.6 V	(iii) 0.9 V	(iii) 1.175 V.	
(iv) FORCED DECAY FROM RESIDUAL POTENTIAL? (a) VALUES OF $C_{max.}$ AND $V_{C_{max.}}$. (b) VALUES OF Q AND POTENTIALS OF ARRESTS CORRESPONDING TO Q.			(iv) FORCED DECAY OF RESIDUAL POTENTIAL GIVES ARRESTS. (a) $C_{max.} = 2684\ \mu F\ cm^{-2}$; $V_{C_{max.}} = 0.59$ V. (b) $Q_1 = 0.537\ mCcm^{-2}$ (0.58 V). $Q_2 = 0.392\ mCcm^{-2}$ (0.15 V).	PSEUDO-CAPACITY ON OPEN-CIRCUIT DECAY OBSERVED ONLY IN THE AQUEOUS CASE. RESIDUAL POTENTIAL INCREASES WITH THE INCREASE IN THE AMOUNT OF H_2O PRESENT IN THE SOLUTION.
(v) ADDITIONAL FEATURES OR COMMENTS.				

....CONTINUED....

3. FORCED DECAYS				
(i) ARREST?	(i) NO ARRESTS	(i) NO ARRESTS OBSERVED IN VERY FRESH SOLUTIONS; AFTER 72 HOURS SOME ARRESTS OBSERVED.	(i) ARRESTS OBSERVED.	
(ii) $C_{max.}$ AND $V_{C_{max.}}$ VALUES.	(ii) $C_{max.} \simeq 10\,\mu F\ cm^{-2}$; $V_{C_{max.}} = 75$ mV.	(ii) $C_{max.} \simeq 250$ TO $450\,\mu F\ cm^{-2}$ (DEPENDING ON $i_{cath.}$)	(ii) $C_{max.} \simeq 1650\,\mu F\ cm^{-2}$; $V_{C_{max.}}$ 0.6 V - 0.7 V.	
(iii) EFFECT OF $i_{cath.}$ ON $C_{max.}$ AND $V_{C_{max.}}$	(iii) NOT STUDIED SINCE C VALUES d.l.	(iii) DETAILED C vs. V PROFILE (AT VARIOUS $i_{cath.}$ VALUES) NOT STUDIED SINCE IT HAS NO QUANTITATIVE SIGNIFICANCE DUE TO INDETERMINATE TRACES OF H_2O PRESENT.	(iii) INCREASING $i_{cath.}$ TENDS TO DEPRESS $V_{C_{max.}}$ TO MORE CATHODIC VALUES; EFFECT OF $i_{cath.}$ ON $C_{max.}$ SHOWS NO REGULAR TREND.	
(iv) PLOT OF $i_{cath.}$ vs. $1/C$, AT A GIVEN V_1; Q FROM THIS PLOT.	(iv) THIS PLOT COULD NOT BE MADE SINCE THERE WERE NO ARRESTS.	(iv) STRAIGHT LINE; 0.106 $mCcm^{-2}$.	(iv) STRAIGHT LINE; 1.05 $mCcm^{-2}$.	ARRESTS AND APPRECIABLE PSEUDO-CAPACITY AND CHARGE ASSOCIATED WITH ARRESTS INCREASE WITH INCREASING AMOUNTS OF H_2O PRESENT.
(v) PLOT OF Q vs. V_1.	(v) NO Q CALCULATED SINCE THERE WERE NO ARRESTS.	(v) Q INCREASES WITH V_1.	(v) Q IS INDEPENDENT OF V_1 IN THE RANGE 2.2 V TO 2.9 V.	
(vi) ADDITIONAL FEATURES OR COMMENTS.	(vi) ABOVE FEATURES INDICATE EITHER ABSENCE OR ADSORBED INTERMEDIATES OR PRESENCE OF IRREVERSIBLY ADSORBED (i.e., IRREDUCIBLE OR "ELECTRO-INACTIVE") INTERMEDIATES.	(vi) ARRESTS AND Q AND PSEUDO-CAPACITANCE ASSOCIATED WITH THESE ARRESTS, APPEAR ONLY AFTER 72 HOURS OF SOLUTION PREPARATION - PRESUMABLY SOME MOISTURE ENTERS THE SOLUTION FROM THE ATMOSPHERE BY DIFFUSION DURING THIS TIME AND IS RESPONSIBLE FOR THE ORIGIN OF SPECIES ADSORBED ON THE ELECTRODE AS INDICATED BY FORCED DISCHARGE BEHAVIOUR	(vi) IN THIS AQUEOUS CASE, APPRECIABLE PSEUDO-CAPACITANCE IS OBSERVED AND Q IS TEN TIMES MORE THAN THE CASE WHEN TRACES OF WATER ARE PRESENT. THIS INDICATES THAT IN THIS CASE, THERE IS APPRECIABLE COVERAGE OF THE ELECTRODE BY SPECIES WHICH ORIGINATE FROM H_2O.	
4. SWEEP RUNS				
(i) PLOT OF PEAK CURRENT vs. $(dV/dt)^{\frac{1}{2}}$.	(i) NO PEAKS OBSERVED; JUST HYSTERESIS.	(i) NO STRAIGHT LINE OBTAINED; HENCE PEAK CURRENTS NOT DIFFUSION-CONTROLLED.	(i) STRAIGHT LINE FOR CATHODIC PEAK; HENCE CATHODIC PEAK IS DIFFUSION-CONTROLLED.	
(ii) DEPENDENCE OF Q ON (dV/dt)		(ii) WHEN (dV/dt) IS INCREASED TEN TIMES, Q DECREASES APPROX. TO 25% OF ITS ORIGINAL VALUE.	(ii) FOR ANODIC PEAK, WHEN dV/dt IS INCREASED TEN TIMES, Q DECREASES APPROX. TO 30% OF ITS ORIGINAL VALUE.	
(iii) IF CHARGING PEAKS, Q VALUES FOR THE PEAKS		(iii) PEAKS ARE NOT CHARGING PEAKS SINCE Q DEPENDS APPRECIABLY ON dV/dt	(iii) PEAKS ARE NOT CHARGING PEAKS SINCE CATHODIC PEAK IS DIFFUSION CONTROLLED AND ANODIC PEAK SHOWS COMPOSITE CURRENTS SINCE Q DEPENDS APPRECIABLY ON dV/dt.	
(iv) $C_{max.}$ AND $V_{C_{max.}}$	(iv) CAPACITY ASSOCIATED WITH THE HYSTERESIS IS d.l. CAPACITY ($\simeq 20\,\mu F\ cm^{-2}$).			IN EVERY CASE WHERE A PEAK WAS OBSERVED, CURRENTS ASSOCIATED WITH THE PEAK WERE FOUND TO BE COMPOSITE CURRENTS, e.g., CHARGING CURRENTS, FARADAIC CURRENTS, AND DIFFUSION CURRENTS.
(v) EFFECT OF dV/dt ON $C_{max.}$ AND $V_{C_{max.}}$				
(vi) ADDITIONAL FEATURES OR COMMENTS.		(vi) C, Q AND $V_{C_{max.}}$ ETC. NOT CALCULATED SINCE PEAK CURRENTS ARE COMPOSITE CURRENTS.	(vi) C, Q AND $V_{C_{max.}}$ ETC. NOT CALCULATED SINCE PEAK CURRENTS ARE COMPOSITE CURRENTS.	
5. PRODUCTS OF ELECTROLYSIS; REMARKS				
	C_2F_4, CO_2 AND A SMALL AMOUNT OF CF_4 OBSERVED AT c.d.'s $> 2\times10^{-3}$ a.cm.$^{-2}$ APPROX. (i.e. $E_a > 2.3$ V)	C_2F_4, CO_2 AND A SMALL AMOUNT OF CF_4 OBSERVED AT c.d.'s $> 2\times10^{-3}$ a.cm^{-2} APPROX. (i.e., $E_a > 2.3$ V)	C_2F_4, CO_2 AND A SMALL AMOUNT OF CF_4 OBSERVED AT c.d.'s $> 2\times10^{-3}$ a.cm.$^{-2}$ APPROX. (i.e., $E_a > 2.3$ V)	FORCED ELECTROLYSIS PROCEEDS AT HIGHER POTENTIALS ($E_a > 2.5$ V) IN ALL THE THREE CASES.

values of initial anodic potentials in both of these solutions are shown in Fig. 15.

In solutions containing excess of water, the open-circuit decay profiles show no arrests, yet the values of capacity calculated from these decays (400 to 500 μF. cm.$^{-2}$) are higher than the d.l. capacity; also, the rsidual potential in this case has a high value of ca. 1.175 V. However, on forced decay from this residual potential, arrests are observed. The $C_{max.}$ associated with the main arrest has a value equal to 2680 μF. cm.$^{-2}$ and $V_{C_{max.}}$ = 0.58 V. The value of charge Q_1 for this arrest, is 0.537 mC. cm.$^{-2}$. Another arrest is observed around 0.15 V and the value of charge for the arrest is Q_2 = 0.392 mC. cm.$^{-2}$. The C-V profiles calculated from the open-circuit decay profiles and also from forced decay from the residual potential in this solution are shown in Fig. 16 for two values of initial polarisation potential, V_i (or E_i).

Forced decay behaviour: When a cathodic charging transient is applied to the electrode immediately after the cessation of anodic polarisation (i.e., forced decay conditions), no arrests are observed in completely anhydrous solutions. Values of $C_{max.}$ are of the order of $C_{d.l.}$ and $V_{C_{max.}}$ = 0.075 V. Since there are no arrests, no Q values could be calculated.

Figure 15

Platinum/1M CF_3COOK in CF_3COOH (+ 1% trifluoroacetic anhydride): C-V plots calculated from open-circuit e.m.f. decay profiles obtained from various initial anodic potentials, V_i:

□ V_i = 3.2 V;

△ V_i = 2.2 V;

▲ V_i = 2.0 V;

○ V_i = 1.8 V (+ anhydride);

× V_i = 2.2 V (+ anhydride);

● V_i = 1.6 V (+ anhydride).

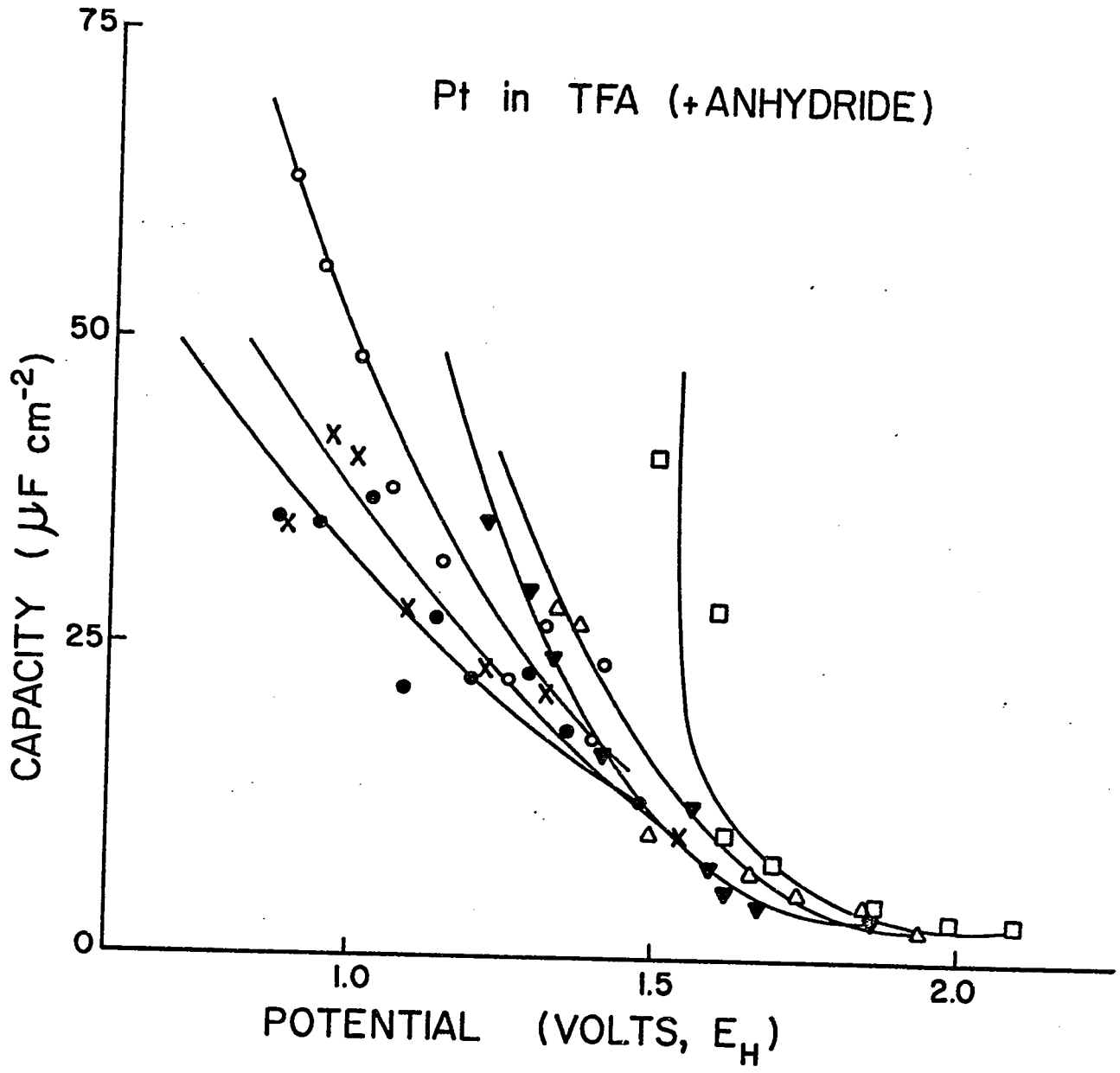
Pt in TFA (+ANHYDRIDE)
75
50
25
0
CAPACITY (μF cm-2)
1.0
1.5
2.0
POTENTIAL (VOLTS, EH)

Figure 16

Platinum/1M CF_3COOK in CF_3COOH (+ water): C-V profiles calculated from open-circuit e.m.f. decay curves and from curves obtained on forced decay from the residual potential:

- ○ (V_1 = 2.3 V) — C-V relations above 1.5 V are from open-circuit curves;
- △ (V_1 = 2.2 V) — C-V relations below 1.5 V are from forced decay curves.

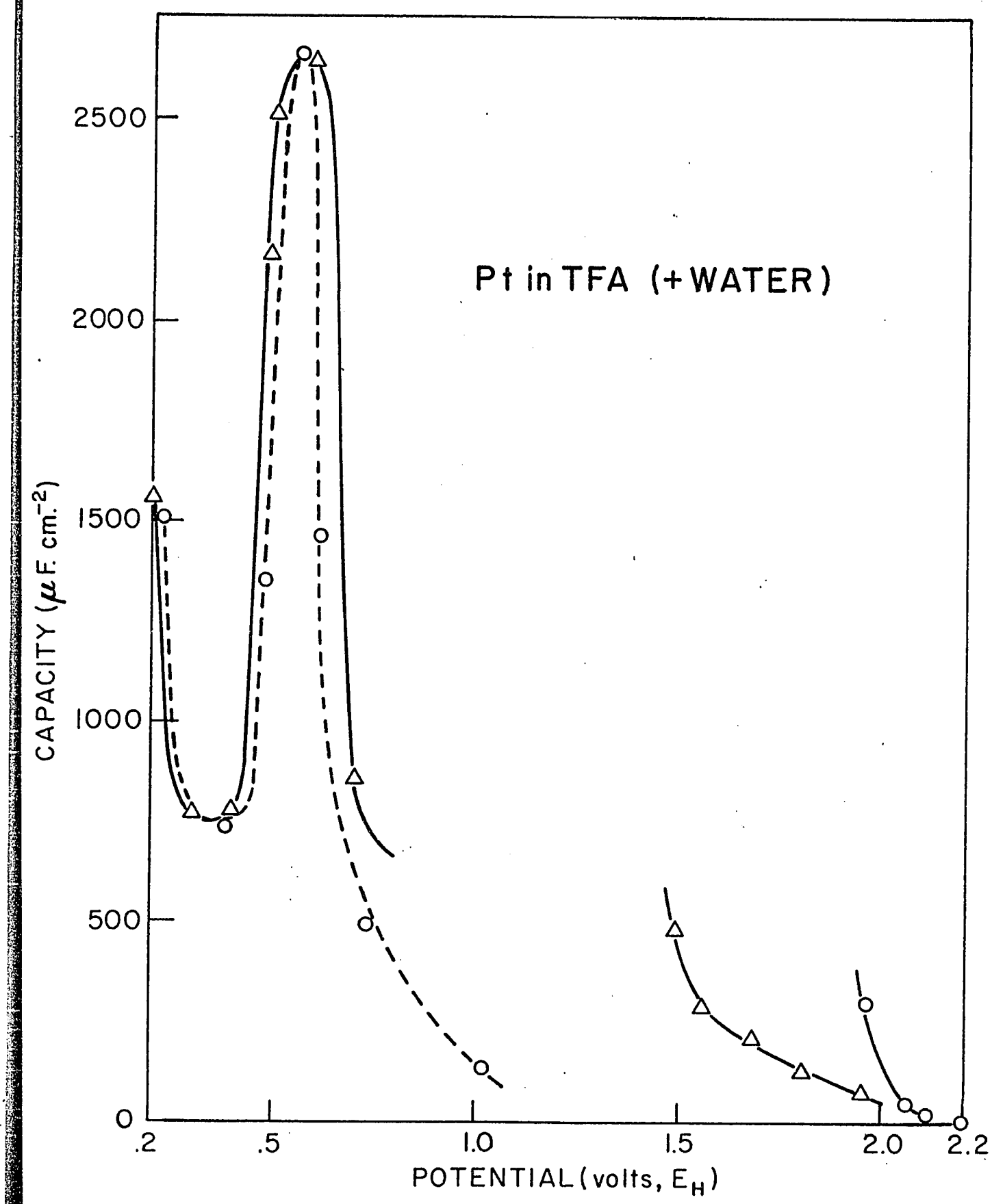
Pt in TFA (+WATER)
CAPACITY (μF. cm.⁻²)
2500
2000
1500
1000
500
0
.2
.5
1.0
1.5
2.0
2.2
POTENTIAL (volts, E_H)

The forced decay behaviour in solutions of fresh 1M CF_3COOK in CF_3COOH [no $(CF_3CO)_2O$ added] is also not associated with any arrests. However, after about 72 hours from the commencement of the run, slight arrests were observed in the potential-time profiles obtained by forced decay of the potential of the anodically polarised electrode. This behaviour is presumably due to the fact that very small, though indeterminate, amounts of atmospheric moisture diffuse into the solution despite the elaborate precautions which have been discussed in Chapter II, section 2, (ii). Moisture seems to be the source of adsorbed intermediates, which manifest themselves by the arrests in the potential-time profiles; this is suggested by the fact that these arrests appear only after significant times after the commencement of the run. The values of $C_{max.}$ calculated from the forced decay profiles range between 250 to 450 μF. cm.$^{-2}$ depending on the $i_{cath.}$ (i.e., cathodic current density) used in the forced discharge and also on the amounts of moisture present in the solution. The plot* of $i_{cath.}$ vs. $1/\tau$ gives a straight line and the charge Q_{total} is given by the slope of

*τ is the time in seconds, at a given $i_{cath.}$, required to reduce completely a particular adsorbed species present so that $i_{cath.} \times \tau = Q$, the charge used in reducing completely and quantitatively a particular adsorbed species. On the differentiated potential-time profiles, it is the time in seconds between two C_{minima}.

this line as 0.108 mC. cm.$^{-2}$ (Fig. 17). The straight line obtained in the $i_{cath.}$ vs. $1/\tau$ plot signifies that $i_{cath.}$ has been utilised entirely for "peeling" off (i.e., discharging) the adsorbed intermediate and that Q is independent of the the value of $i_{cath.}$ used, and, is given by slope of this line. The values of capacity C and charge Q obtained for the electrode in this solution, it must be noted, have no precise quantitative significance because of indeterminate traces of water present in the solution. These C and Q values, nevertheless, have a semi-quantitative significance which has a most important bearing on the comparative discussion of results for completely non-aqueous solutions, for solutions containing traces of water and for solutions to which excess water has been deliberately added (see Chapter IV).

After establishing that Q is independent of $i_{cath.}$ (Fig. 17), a plot of Q vs. V_i, the initial polarisation potential, was examined. It is found that Q increases with increasing V_i (Fig. 18). In Fig. 18, two polaroid photographs are also shown which are actual oscillographic records of the experimental forced decay curves together with the corresponding differentiated profiles obtained in completely anhydrous solutions and in solutions containing, presumably, traces of water. It is important to note that no "peak"

Figure 17

Platinum in nominally anhydrous 1M KTFA/TFA solution: a plot of $i_{cath.}$ vs. $1/T$.

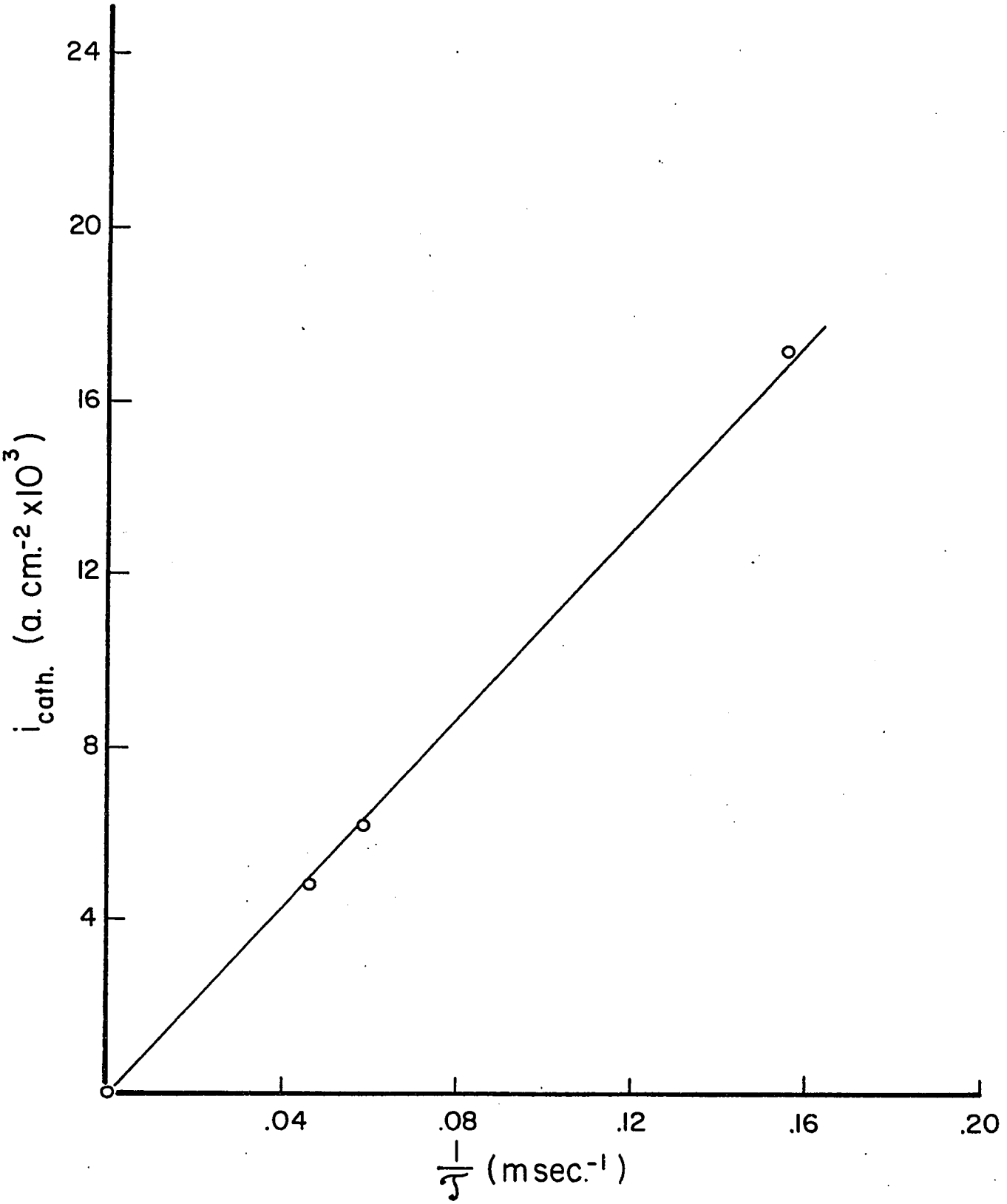
24
20
16
12
8
4
$i_{cath.}$ (a. cm.$^{-2}$ x10^{3})
.04
.08
.12
.16
.20
$\frac{1}{\tau}$ (m sec.$^{-1}$)

Figure 18

Platinum in nominally anhydrous 1M KTFA/TFA solution: a plot of Q vs. E_1.

Pt / TFA + Anh.

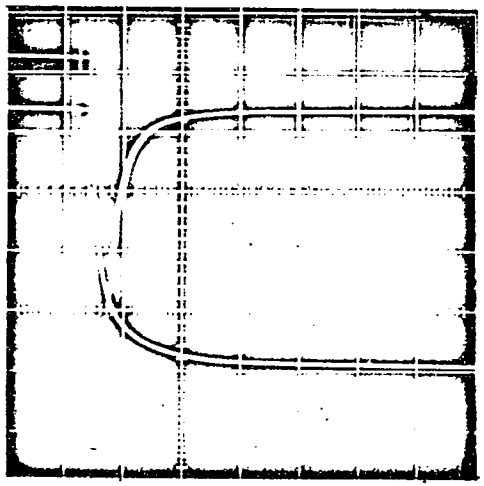

2 m sec. cm.$^{-1}$

3.24 x 10^{-2} a. cm^{-2}

Pt / TFA

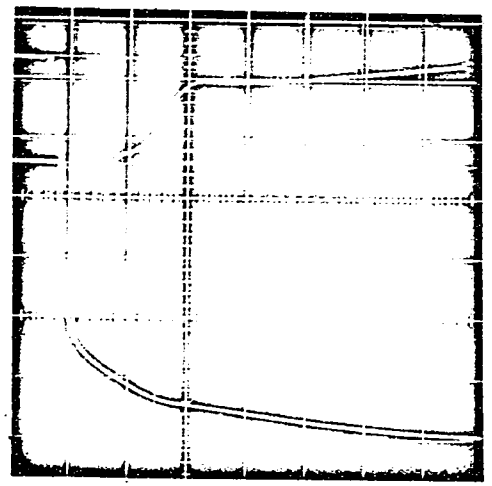

2 m sec. cm^{-1}

5.52 x 10^{-2} a. cm.$^{-2}$

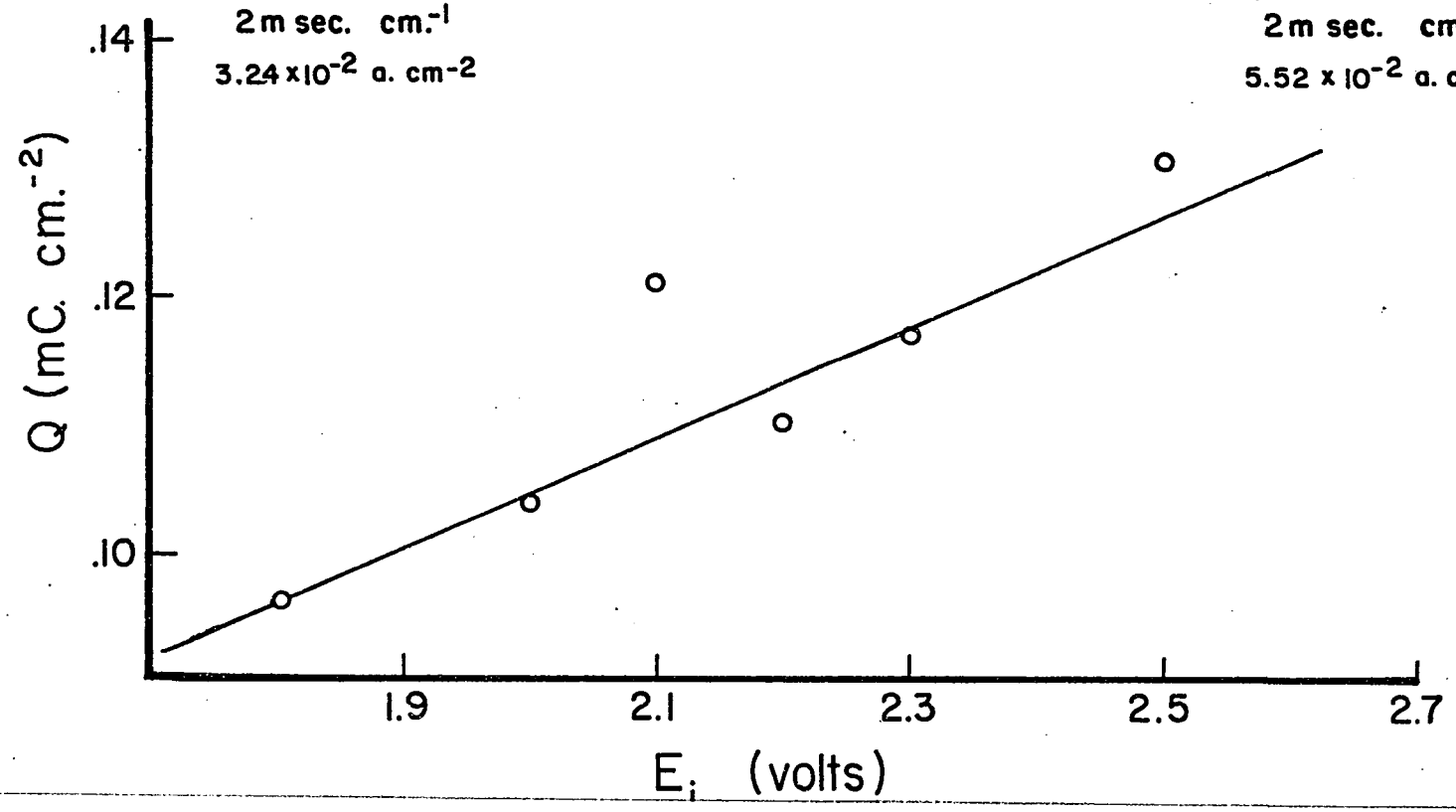

(i.e., $C_{min.}$, which is actually a differentiated arrest) is observed in completely anhydrous solution while a slight arrest is observed in solutions believed to contain traces of water.

In solutions containing excess of water, appreciable arrests are observed which appear as minima on the differentiated potential-time profiles. These arrests are associated with significant coverage of the electrode by adsorbed intermediates and are not observed in the case of electrodes in anhydrous solutions. Such arrests are manifested only slightly in solutions containing traces of water. Appreciable pseudo-capacity C, as calculated from the differentiated potential-time profiles, is observed. The value of $C_{max.}$ is equal to 1650 μF. cm.$^{-2}$ and the value of $V_{C_{max.}}$ ranges between 0.6 V to 0.2 V depending on the $i_{cath.}$ used in the forced decay transient. Increasing $i_{cath.}$ tends to shift $V_{C_{max.}}$ to more cathodic potentials though the effect of $i_{cath.}$ on values of $C_{max.}$ itself does not show a regular trend (Fig. 19). The C-V profiles at four values of $i_{cath.}$ are shown in Fig. 20.

A plot of $i_{cath.}$ vs. $1/\tau$ at a given value of initial polarisation potential V_i or E_i, gives a straight line (see Fig. 21). In Fig. 21, a plot of $i_{cath.}$ vs. $1/\tau^{\frac{1}{2}}$

Figure 19

Platinum/1M CF_3COOK in CF_3COOH (+ water):

- ● Plot of $C_{max.}$ vs. $i_{cath.}$;
- ○ Plot of $V_{C_{max.}}$ vs. $i_{cath.}$.

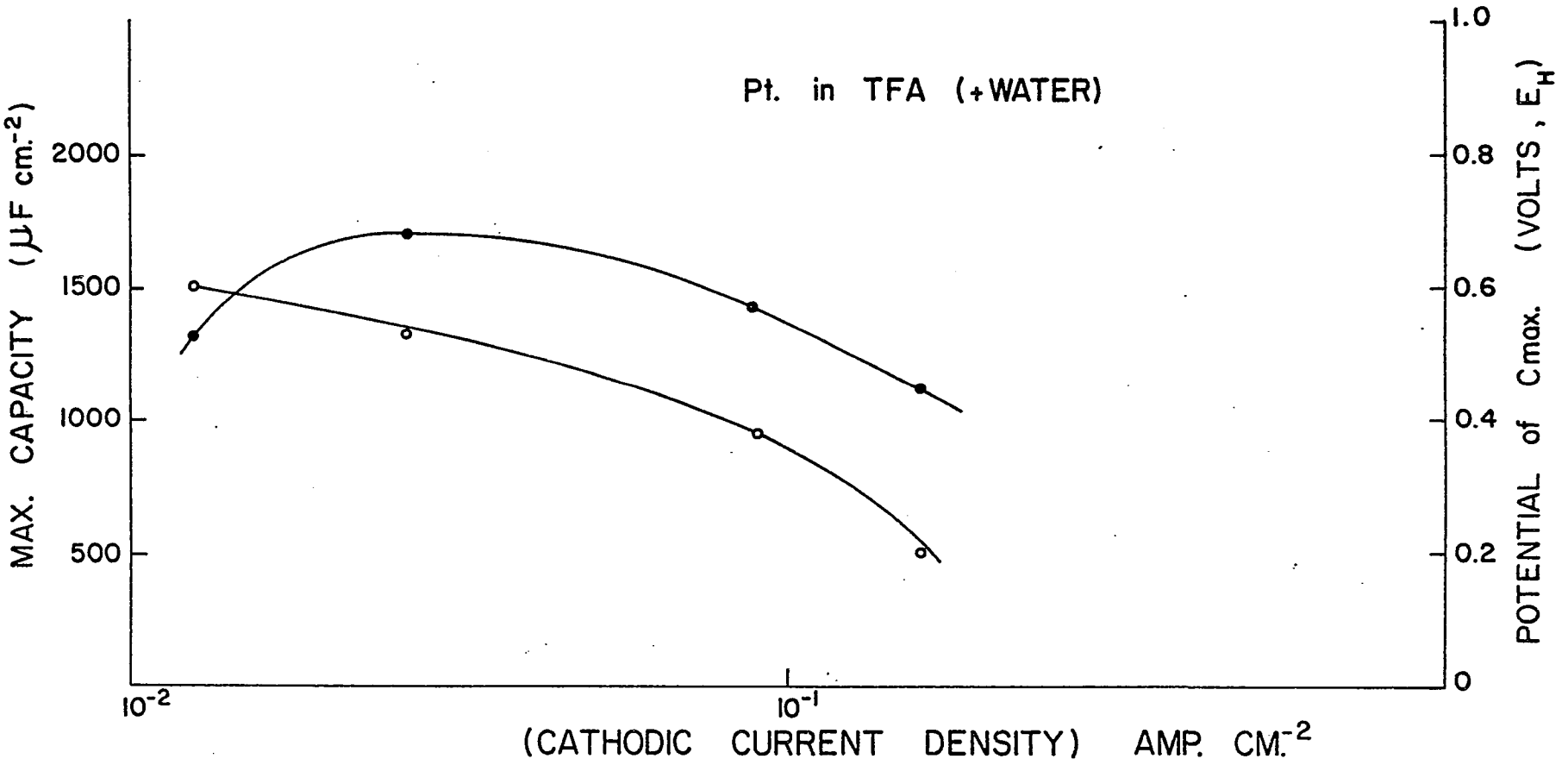
Pt. in TFA (+WATER)
MAX. CAPACITY (μF cm.-2)
2000
1500
1000
500
1.0
0.8
0.6
0.4
0.2
0
POTENTIAL of Cmax. (VOLTS, EH)
10-2
10-1
(CATHODIC CURRENT DENSITY) AMP. CM.-2

Figure 20

Platinum/1M CF_3COOK in CF_3COOH (+ water): C-V profiles as a function of charging cathodic current density, $i_{cath.}$, for the adsorbed species in the Kolbe oxidation: $i_{cath.}$ (in a. $cm.^{-2}$):

▲ 1.25×10^{-2}

△ 2.65×10^{-2};

o 8.82×10^{-2};

● 16.18×10^{-2};

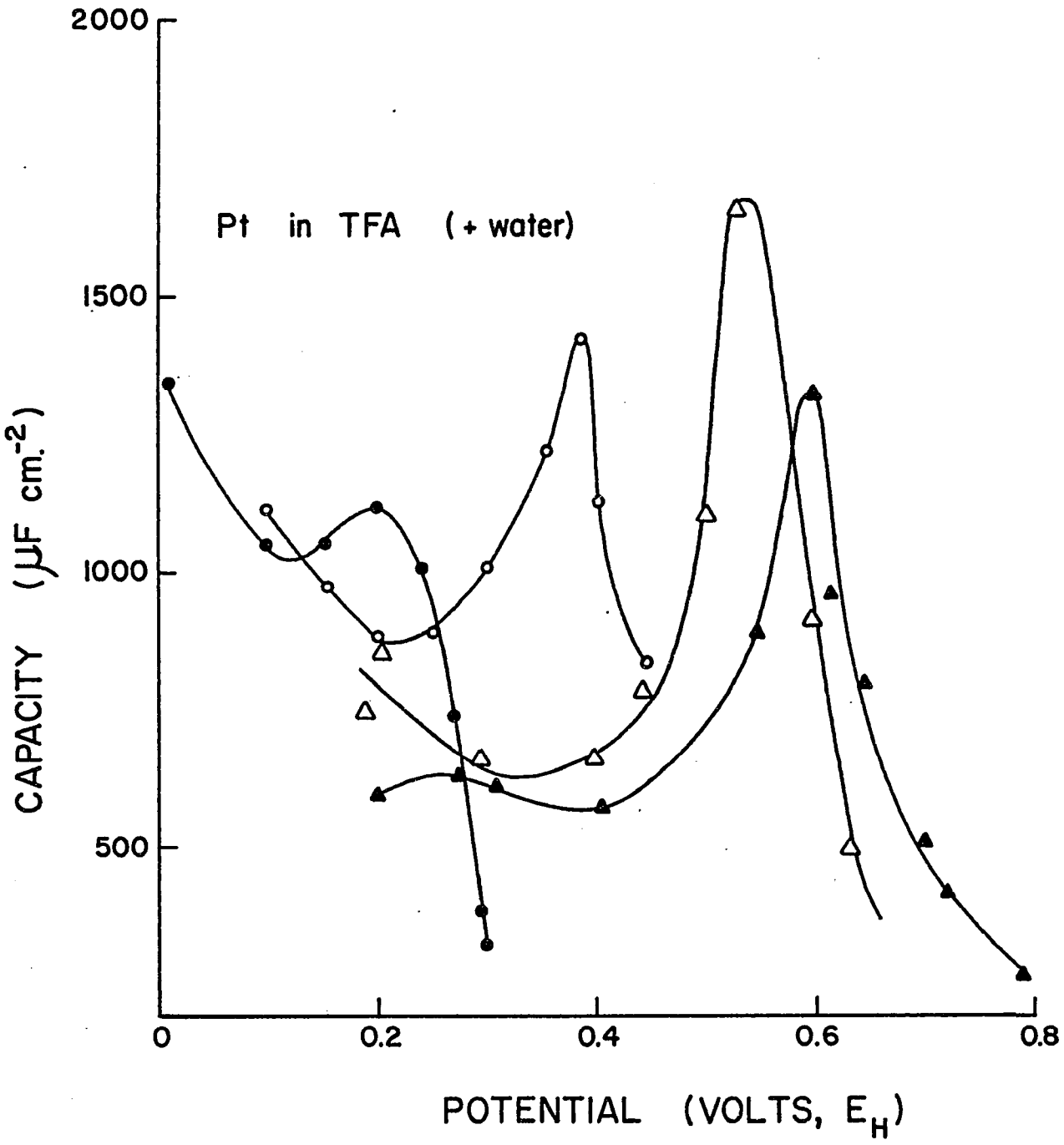
Pt in TFA (+ water)
2000
1500
1000
500
CAPACITY (μF cm.-2)
0
0.2
0.4
0.6
0.8
POTENTIAL (VOLTS, E_H)

Figure 21

Platinum in 1M KTFA/TFA (+ water) solution: plots of $i_{cath.}$ vs. $1/\tau$ (Δ) and $i_{cath.}$ vs. $1/\tau^{\frac{1}{2}}$ (o)

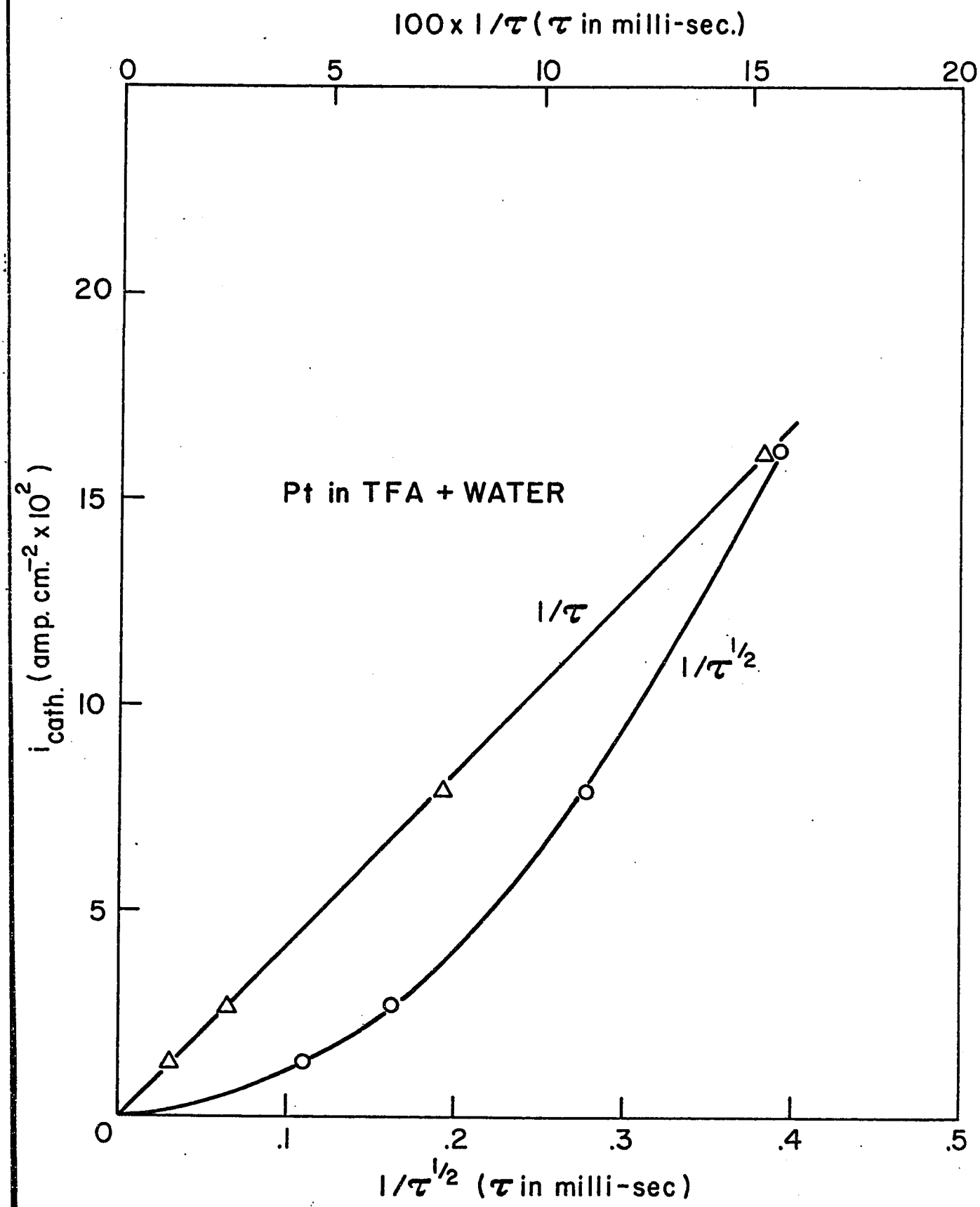
100 x 1/τ (τ in milli-sec.)
0
5
10
15
20
Pt in TFA + WATER
1/τ
1/τ^1/2
i_cath. (amp. cm^-2 x 10^2)
0
5
10
15
20
.1
.2
.3
.4
.5
1/τ^1/2 (τ in milli-sec)

is also shown, and is clearly not a straight line. This fact emphasizes in a complementary way an important conclusion from the $i_{cath.}$ vs. $1/\tau$ plot, namely, that $i_{cath.}$ is not utilised for a diffusion controlled process and is entirely used for the (dis-) charging process of "peeling" off the adsorbed intermediates from the electrode. The value of total charge Q given by the slope of $i_{cath.}$ vs. $1/\tau$ plot (Fig. 21) is equal to 1.05 mC. cm.$^{-2}$; this value, it must be noted, is about ten times greater than the value of charge, Q_{total}, obtained for electrodes in solutions which contained only traces of water.

After establishing that Q is independent of $i_{cath.}$ (Fig. 21), Q was plotted as a function of initial polarisation potential V_i. It is found that for either of the two C_{minima} observed in the differentiated potential-time profile, the charge Q is independent of V_i (Fig. 22). In Fig. 22, an actual experimental forced decay curve together with its differentiated profile is also shown. It is clear that the differentiated potential-time profiles clarify any uncertainty in the arrests or inflections in the potential-time curves into sharp peaks (i.e, the appropriate C_{maxima} and C_{minima}) and hence permit more precise calculations of the quantities C and Q deduced from these profiles, and the observation of the potentials at which the inflections occur.

Figure 22

Platinum in 1M KTFA/TFA (+ water) solution: plots of Q [for each of the two peaks (see photograph)] vs. E_i.

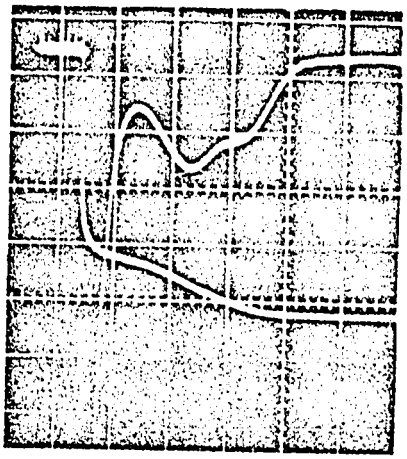

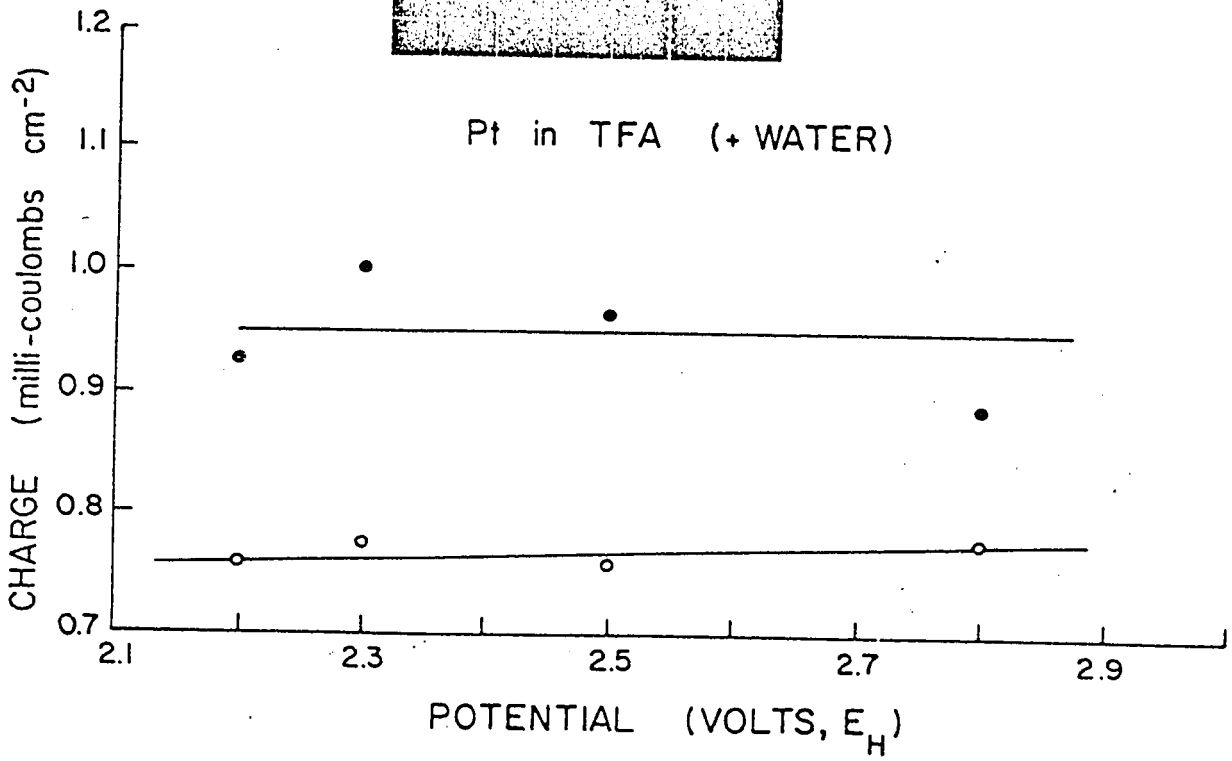
Pt in TFA (+ WATER)
CHARGE (milli-coulombs cm^{-2})
1.2
1.1
1.0
0.9
0.8
0.7
2.1
2.3
2.5
2.7
2.9
POTENTIAL (VOLTS, E_H)

(b) Gold in Potassium Trifluoroacetate-Trifluoroacetic Acid Solutions

Potential-time relationships, observed on open-circuit and forced decay from anodic potentials, were investigated as above in: (α) completely anhydrous solutions; (β) solutions presumably containing traces of water; (γ) solutions to which excess of aqueous 1M CF_3COOK solution (30% by volume) was deliberately added. The results obtained in the three types of solutions are summarised in Table III, sections 2 and 3.

Open-circuit decay behaviour: In completely anhydrous solutions, a slight arrest was observed on self-decay of the anodic potential. The value of $C_{max.}$ is of the order of 90-140 μF. cm.$^{-2}$, depending on V_1 (Fig. 23). The residual potential is 0.4 V.

In solutions containing traces of water, an arrest is observed on self-discharge of potential of the gold anode. The values of $C_{max.}$ and $V_{C_{max.}}$ seem to depend on initial polarisation potential, V_1, and are as follows:

$C_{max.}$ = 60 μF. cm.$^{-2}$; $V_{C_{max.}}$ = 1.62 V; V_1 = 2.5 V

$C_{max.}$ = 225 μF. cm.$^{-2}$; $V_{C_{max.}}$ = 1.37 V; V_1 = 1.8 V

The rest potential in this case is ca. 0.9 V, which is higher than that observed under completely anhydrous conditions.

Table III

Behaviour at gold: potassium trifluoroacetate-trifluoroacetic acid solutions.

TABLE III. BEHAVIOUR AT GOLD

EXPERIMENTAL EVIDENCE	SOLUTION: 1M CF_3COOK IN CF_3COOH + 1% $CF_3CO.O.COCF_3$	SOLUTION: 1M CF_3COOK IN CF_3COOH	SOLUTION: 1M CF_3COOK IN CF_3COOH + 1M CF_3COOK IN H_2O	REMARKS (GENERAL)
1. CURRENT-POTENTIAL RELATIONS				
(i) TAFEL SLOPES	(i) 0.160 V	(i) 0.175 V	(i) 0.170 V	
(ii) HYSTERESIS?	(ii) NO HYSTERESIS	(ii) HYSTERESIS; "INHIBITION BEND" OBSERVED.	(ii) LARGE HYSTERESIS	WITH INCREASING AMOUNTS OF H_2O IN THE SOLUTION, HYSTERESIS BECOMES LARGER, RATE BECOMES LOWER, AND THE REST POTENTIAL BECOMES HIGHER
(iii) REST POTENTIAL.	(iii) 0.25 V	(iii) 0.9 V	(iii) 1.25 V	
(iv) ADDITIONAL FEATURES OR COMMENTS.				
2. OPEN-CIRCUIT DECAYS				
(i) ARREST?	(i) VERY SLIGHT ARREST.	(i) ARREST OBSERVED; V_1 = 2.5 V.		
(ii) MAGNITUDE OF C	(ii) $C_{max.}$ = 90-140 μF cm^{-2} DEPENDING ON V_1.	(ii) $C_{max.}$ = 60 μF cm^{-2} ($V_{C_{max.}}$ = 1.62 V; V_1=2.5V) $C_{max.}$ = 225 μF cm^{-2} ($V_{C_{max.}}$ = 1.37 V; V_1=1.8 V)	(ii) 2500 μF cm^{-2}	
(iii) RESIDUAL POTENTIAL.	(iii) 0.4 V.	(iii) 0.9 V.	(iii) 1.3 V	BOTH PSEUDO-CAPACITY AND RESIDUAL POTENTIAL TEND TOWARDS HIGHER VALUES WITH INCREASING AMOUNTS OF H_2O PRESENT IN THE SOLUTION.
(iv) FORCED DECAY FROM RESIDUAL POTENTIAL? (a) VALUES OF $C_{max.}$ AND $V_{C_{max.}}$ (b) VALUES OF Q AND POTENTIALS OF ARRESTS CORRESPONDING TO Q.				
(v) ADDITIONAL FEATURES OR COMMENTS.				

....CONTINUED....

3. FORCED DECAYS				
(i) ARREST?	(i) ARREST OBSERVED.	(i) LONG ARREST.	(i) AN ARREST IS OBSERVED.	
(ii) $C_{max.}$ AND $V_{C_{max.}}$ VALUES.	(ii) $C_{max.} = 100\ \mu F\ cm^{-2}$; $V_{C_{max.}} = 0.15$ TO 0.68 V DEPENDING ON $i_{cath.}$	(ii) $C_{max.} \simeq 500$ TO $1580\ \mu F\ cm^{-2}$ DEPENDING ON $i_{cath.}$; $V_{C_{max.}} \simeq -0.35$ V TO 0.85 V DEPENDING ON $i_{cath.}$	(ii) $C_{max.} = 2250$ TO $3500\ \mu F\ cm^{-2}$ DEPENDING ON $i_{cath.}$; $V_{C_{max.}} \simeq 0.89$ V TO 1.05 V DEPENDING ON $i_{cath.}$	
(iii) EFFECT OF $i_{cath.}$ ON $C_{max.}$ AND $V_{C_{max.}}$	(iii) INCREASING $i_{cath.}$ SHIFTS $C_{max.}$ TO HIGHER VALUES AND $V_{C_{max.}}$ TO LESS ANODIC VALUES	(iii) WITH INCREASING $i_{cath.}$, $V_{C_{max.}}$ SHIFTS TO LESS ANODIC VALUES BUT TREND IN THE SHIFT OF $C_{max.}$ IS DIFFICULT TO ESTABLISH.	(iii) WITH INCREASING $i_{cath.}$, $V_{C_{max.}}$ GETS SHIFTED TO LESS ANODIC VALUES BUT THE TREND IN THE SHIFT OF $C_{max.}$ IS DIFFICULT TO ESTABLISH.	
(iv) PLOT OF $i_{cath.}$ vs. $1/t$, AT A GIVEN V_1; Q FROM THIS PLOT.	(iv) STRAIGHT LINE; $Q = 0.084\ mCcm^{-2}$	(iv) STRAIGHT LINE; $Q = 0.175\ mCcm^{-2}$	(iv) STRAIGHT LINE; $Q = 1.09\ mCcm^{-2}$.	
(v) PLOT OF Q vs. V_1.	(v) Q INCREASES WITH V_1.	(v) Q INCREASES WITH INCREASING V_1.	(v) Q INCREASES WITH INCREASING V_1.	
(vi) ADDITIONAL FEATURES OR COMMENTS.				BOTH C AND Q VALUES INCREASE WITH INCREASING AMOUNTS OF H_2O PRESENT IN THE SOLUTION; ALSO, WITH INCREASING V_1, Q SHOWS A MORE RAPID INCREASE WITH INCREASING AMOUNTS OF H_2O PRESENT IN THE SOLUTION.
4. SWEEP RUNS				
(i) PLOT OF PEAK CURRENT vs. $(dV/dt)^{\frac{1}{2}}$.	(i) STRAIGHT LINE BOTH FOR ANODIC AND CATHODIC PEAKS.	(i) STRAIGHT LINE FOR ANODIC PEAK; CATHODIC PEAK NOT WELL-DEFINED.	(i) STRAIGHT LINE BOTH FOR ANODIC AND CATHODIC PEAKS.	
(ii) DEPENDENCE OF Q ON (dV/dt)				
(iii) IF CHARGING PEAKS, Q VALUES FOR THE PEAKS.				
(iv) $C_{max.}$ AND $V_{C_{max.}}$				DIFFUSION-CONTROLLED PEAKS OBSERVED IN ALL THE THREE CASES DUE, PRESUMABLY, TO ANODIC DISSOLUTION OF GOLD.
(v) EFFECT OF (dV/dt) ON $C_{max.}$ AND $V_{C_{max.}}$				
(vi) ADDITIONAL FEATURES OR COMMENTS.				
5. PRODUCTS OF ELECTROLYSIS; REMARKS	C_2F_6, CO_2 AND A SMALL AMOUNT OF CF_4 OBSERVED AT c.d.'s $> 5\times10^{-3}$ $a.cm^{-2}$ APPROX. (i.e., $E_H > 2.2$ V).	C_2F_6 AND CO_2 OBSERVED AT c.d.'s $> 5\times10^{-3}$ $a.cm^{-2}$ APPROX. (i.e., $E_H > 2.2$ V).	C_2F_6 AND CO_2 OBSERVED AT c.d.'s $> 5\times10^{-3}$ $a.cm^{-2}$ APPROX. (i.e., $E_H > 2.2$ V).	KOLBE REACTION PROCEEDS AT HIGHER POTENTIALS ($E_H > 2.2$ V) IN ALL THE THREE CASES.

Figure 23

Gold/1M CF_3COOK in CF_3COOH (+ 1% anhydride): C-V profiles calculated from open-circuit e.m.f. decay curves obtained from various values of initial anodic potential V_i:

× V_i = 1.7 V;

o V_i = 1.9 V;

● V_i = 2.1 V.

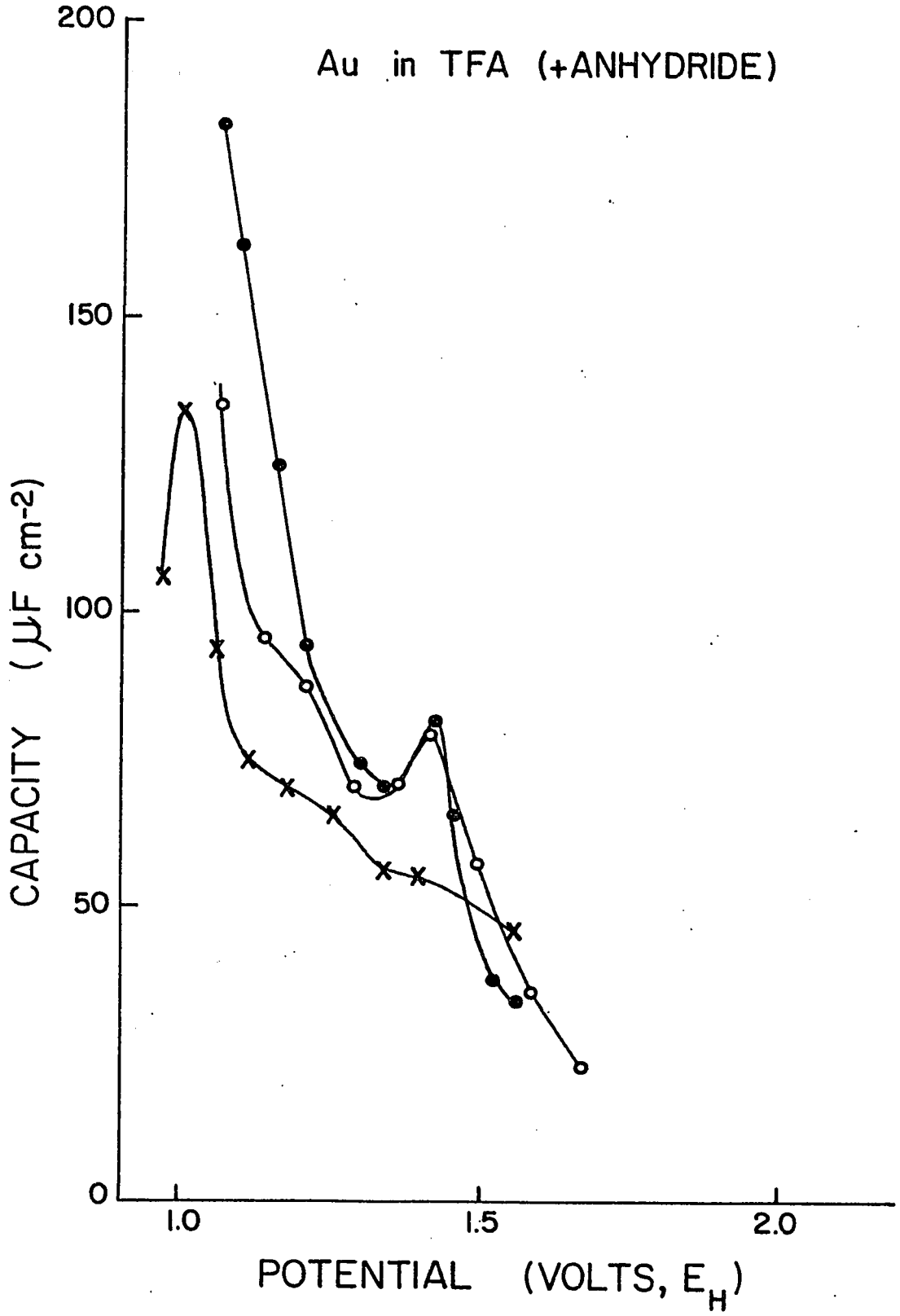

The C-V relations calculated from open-circuit decay profiles for this case are shown in Fig. 24.

In solutions containing excess of water, no arrests are observed in profiles of the decay of the anodic potential though the values of pseudo-capacity calculated from the self-discharge profiles are very high (ca. 2500 μF. cm.$^{-2}$ This is indicative of the presence of some adsorbed intermediates.). The rest potential observed is quite high (1.3 V). [Again, this suggests that some adsorbed intermediates which are not easily reduced by a spontaneous self-discharge reaction are present on the electrode.]. The C-V relations calculated from open-circuit decay curves obtained from a variety of initial polarisation potentials are shown in Fig. 25.

Forced decay behaviour: When an anodically polarised gold electrode is subjected to a cathodic charging transient immediately after the cessation of initial anodic polarisation in completely anhydrous solutions, an arrest is observed (contrast the case of Pt). The $C_{max.}$ value calculated from a differentiated profile of this arrest is equal to 100 μF. cm.$^{-2}$ approximately and $V_{C_{max.}}$ ranges between 0.15 V to 0.68 V. Both $C_{max.}$ and $V_{C_{max.}}$ values depend on $i_{cath.}$ used in the cathodic charging transients. Increasing $i_{cath.}$ shifts $C_{max.}$ to higher values and $V_{C_{max.}}$ to more cathodic potentials (Fig. 26). The C-V profiles at four different values of $i_{cath.}$,

Figure 24

Gold/1M CF_3COOK in CF_3COOH: C-V profiles calculated from open-circuit e.m.f. decay curves obtained from various values of initial anodic potential, V_i:

o	V_i = 1.4 V;
•	V_i = 1.8 V;
x	V_i = 2.5 V.

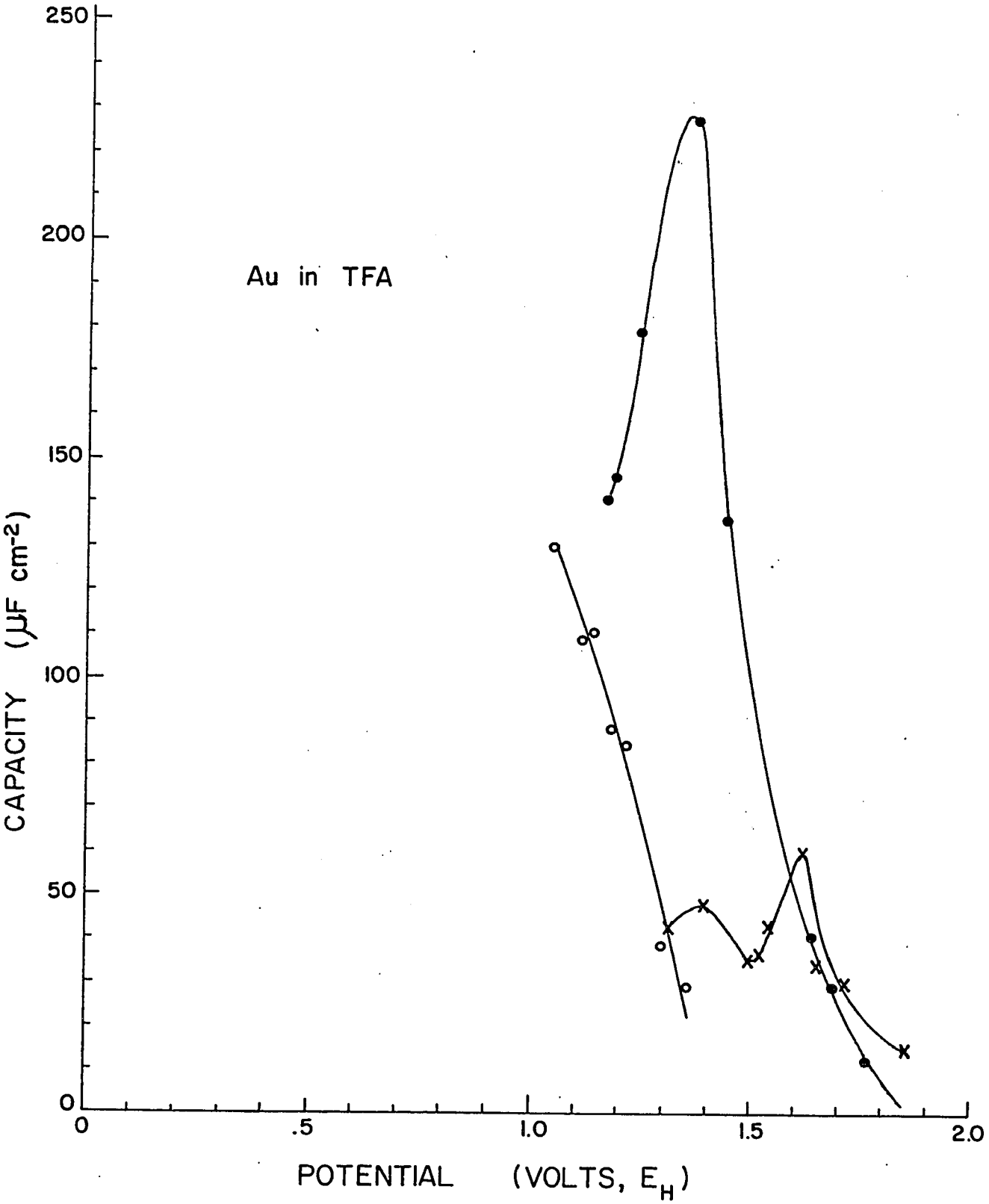
Au in TFA
250
200
150
100
50
0
CAPACITY (μF cm-2)
0
.5
1.0
1.5
2.0
POTENTIAL (VOLTS, E_H)

Figure 25

Gold/1M CF_3COOK in CF_3COOH (+ water): C-V profiles calculated from open-circuit e.m.f. decay curves obtained from various values of initial anodic potential, V_i (or E_i):

o $V_i = 2.1$ V;

Δ $V_i = 2.3$ V;

□ $V_i = 2.4$ V.

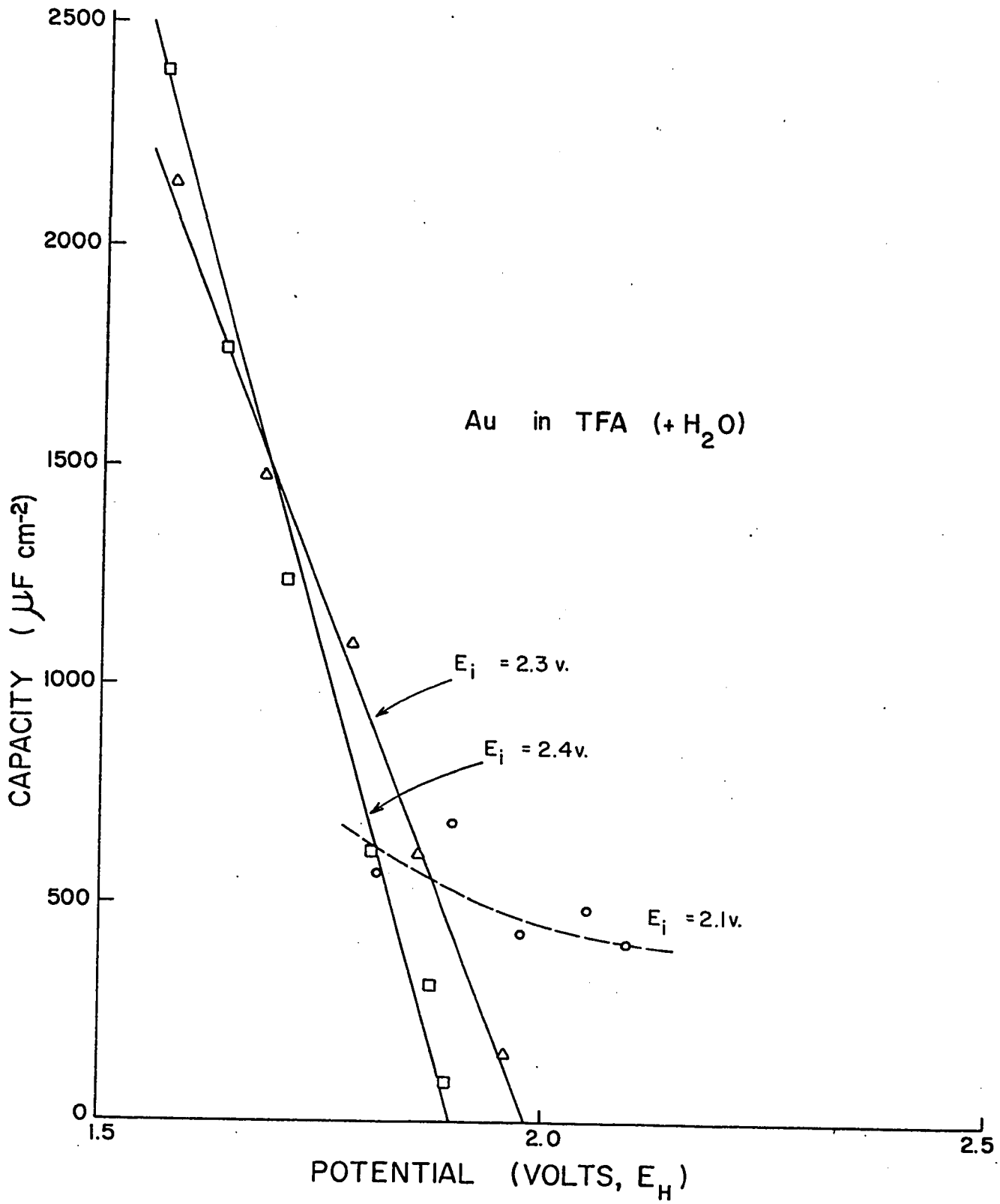
2500
2000
1500
1000
500
0
CAPACITY (μF cm-2)
Au in TFA (+ H2O)
Ei = 2.3 v.
Ei = 2.4v.
Ei = 2.1v.
1.5
2.0
2.5
POTENTIAL (VOLTS, EH)

Figure 26

Gold/1N CF_3COOK in CF_3COOH (+ 1% anhydride):

× plot of $C_{max.}$ vs. $i_{cath.}$;

o plot of $V_{C_{max.}}$ vs. $i_{cath.}$.

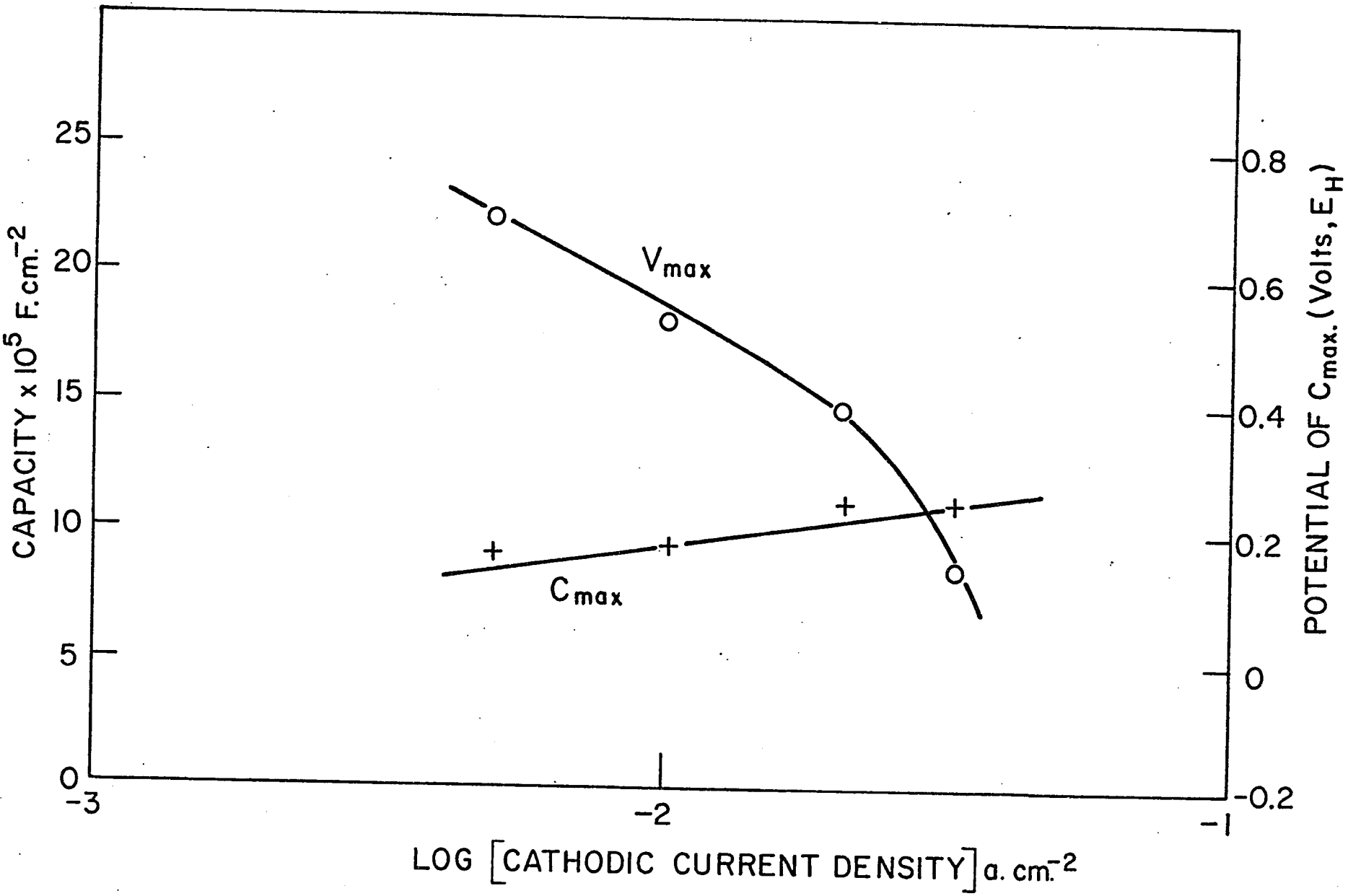
CAPACITY x 10^5 F.cm.^-2
25
20
15
10
5
0
-3
-2
-1
V max
C max
0.8
0.6
0.4
0.2
0
-0.2
POTENTIAL OF C max. (Volts, E_H)
LOG [CATHODIC CURRENT DENSITY] a. cm.^-2

computed from differentiated potential-time relations obtained on driven decay, are shown in Fig. 27.

A plot of $i_{cath.}$ vs. $1/\tau$ gives a straight line (Fig. 28) and the value of charge, Q_{total}, obtained from the slope of this line = 0.084 mC. cm.$^{-2}$. In Fig. 28, a plot of $i_{cath.}$ vs. $1/\tau^{\frac{1}{2}}$ is also shown in order to emphasize the inferences to be drawn from the $i_{cath.}$ vs. $1/\tau$ relations. After establishing that Q was independent of $i_{cath.}$ (Fig. 28), a plot of Q vs. V_i (or E_i), the initial polarisation potential, was studied. It is found that Q increases with increasing V_i (Fig. 29).

Forced decay of anodic potential in nominally anhydrous solutions, but presumably containing traces of water, shows a long arrest in the potential-time curve. The values of $C_{max.}$ range from ca. 500 to 1580 μF. cm.$^{-2}$ and those of $V_{C_{max.}}$ range from -0.35 V to 0.85 V, both values being dependent on the magnitude of $i_{cath.}$ used in the driven decay. With increasing $i_{cath.}$, $V_{C_{max.}}$ shifts to more cathodic values, while the trend in the shift of $C_{max.}$ with varying $i_{cath.}$ is difficult to establish (Fig. 30). The C-V profiles for a series of $i_{cath.}$ values are shown in Fig. 31.

On plotting $i_{cath.}$ vs. $1/\tau$, a straight line is obtained (Fig. 32) and the charge Q, given by the slope of

Figure 27

Gold/1M CF_3COOK in CF_3COOH (+ 1% anhydride): C-V profiles as a function of charging cathodic current density, $i_{cath.}$, for the adsorbed species in the Kolbe oxidation: $i_{cath.}$ (in a. $cm.^{-2}$):

o 5.02×10^{-3};

□ 10.03×10^{-3};

Δ 21.0×10^{-3};

+ 32.8×10^{-3}.

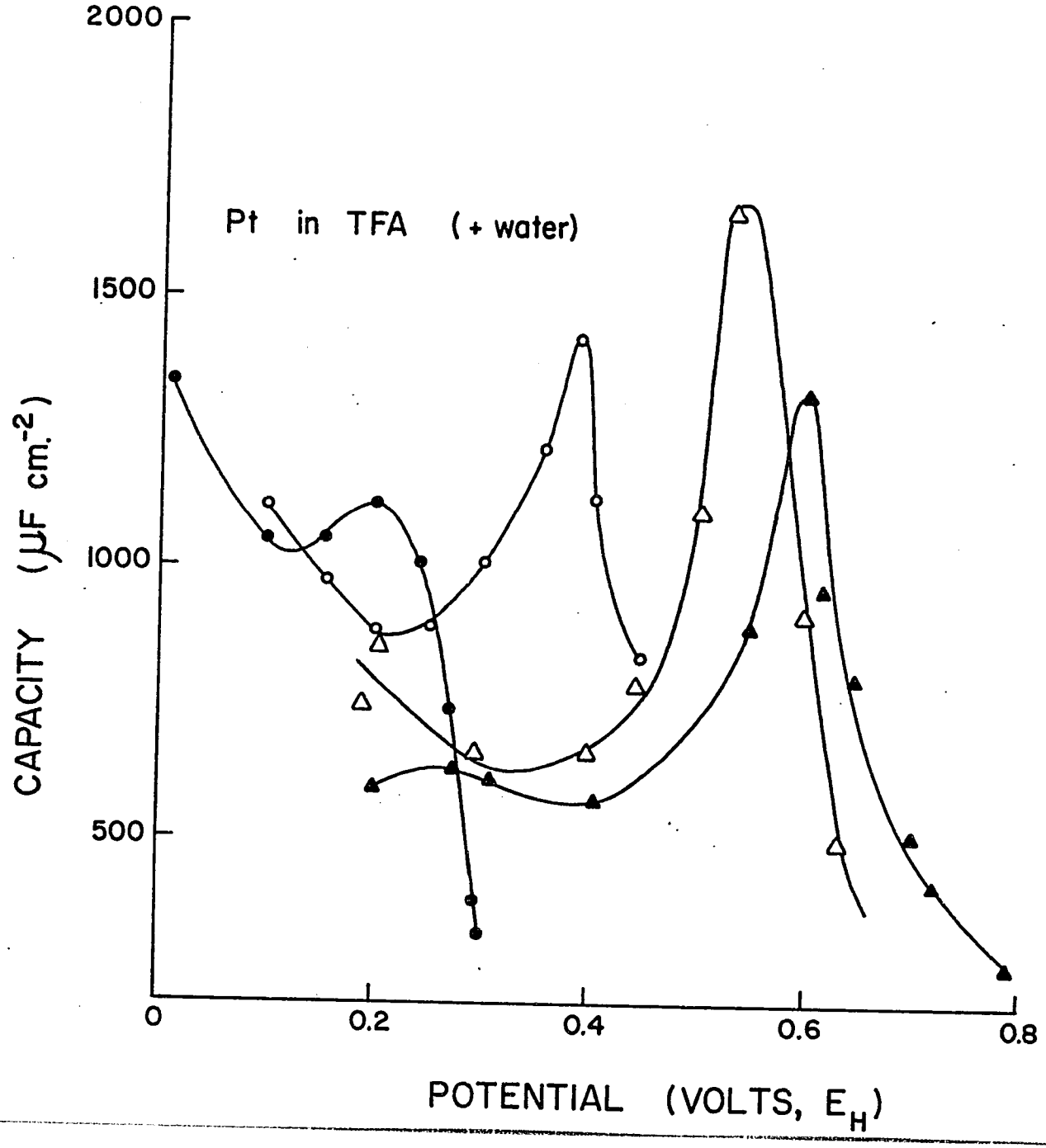
Pt in TFA (+ water)
2000
1500
1000
500
0
0.2
0.4
0.6
0.8
CAPACITY (μF cm.-2)
POTENTIAL (VOLTS, E_H)

Figure 28

Gold in very anhydrous 1M KTFA/TFA solution: plots of $i_{cath.}$ vs. $1/\tau$ (Δ) and $i_{cath.}$ vs. $1/\tau^{\frac{1}{2}}$ (o).

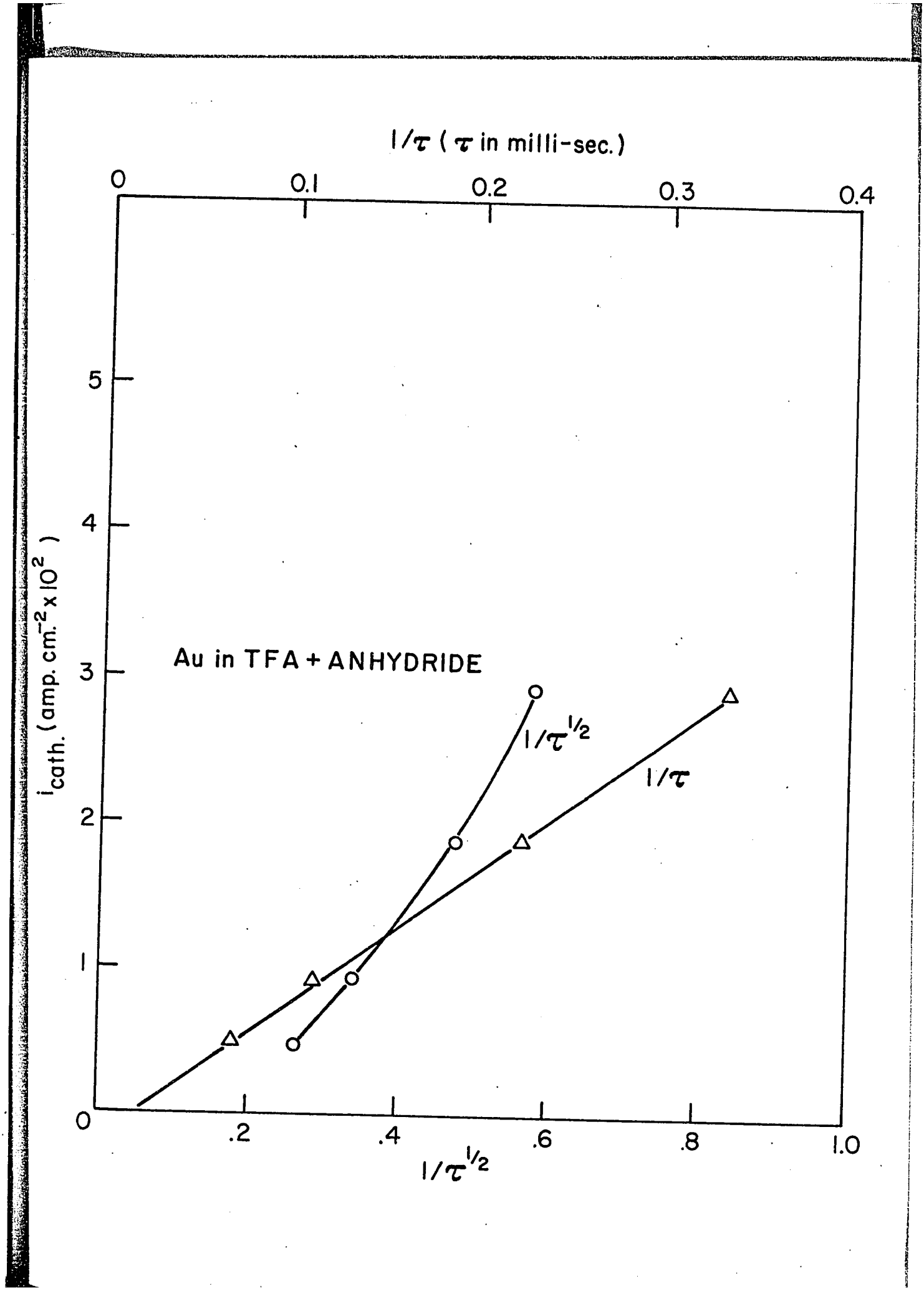
1/τ (τ in milli-sec.)
0
0.1
0.2
0.3
0.4
5
4
3
2
1
0
i cath. (amp. cm.⁻² x 10²)
Au in TFA + ANHYDRIDE
1/τ^1/2
1/τ
.2
.4
.6
.8
1.0
1/τ^1/2

Figure 29

Plot of Q vs. E_1: 1M KTFA/TFA solutions:

⊡ gold in very anhydrous solution;

● gold in nominally anhydrous solution;

▲ gold in aqueous solution.

Au/TFA - Anh.

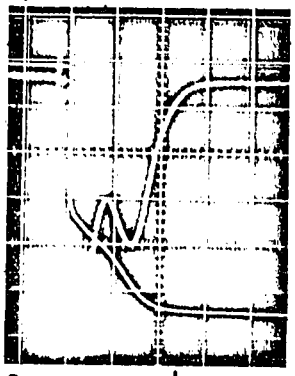

2 m sec. $cm.^{-1}$

3.28×10^{-2} a. $cm.^{-2}$

Au/TFA

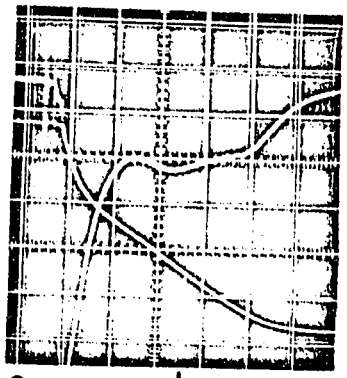

2 m sec. $cm.^{-1}$

2.29×10^{-2} a. $cm.^{-2}$

Au/TFA-H_2O

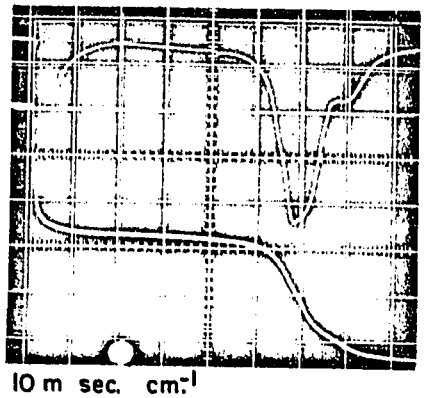

10 m sec. $cm.^{-1}$

5.79×10^{-2} a. $cm.^{-2}$

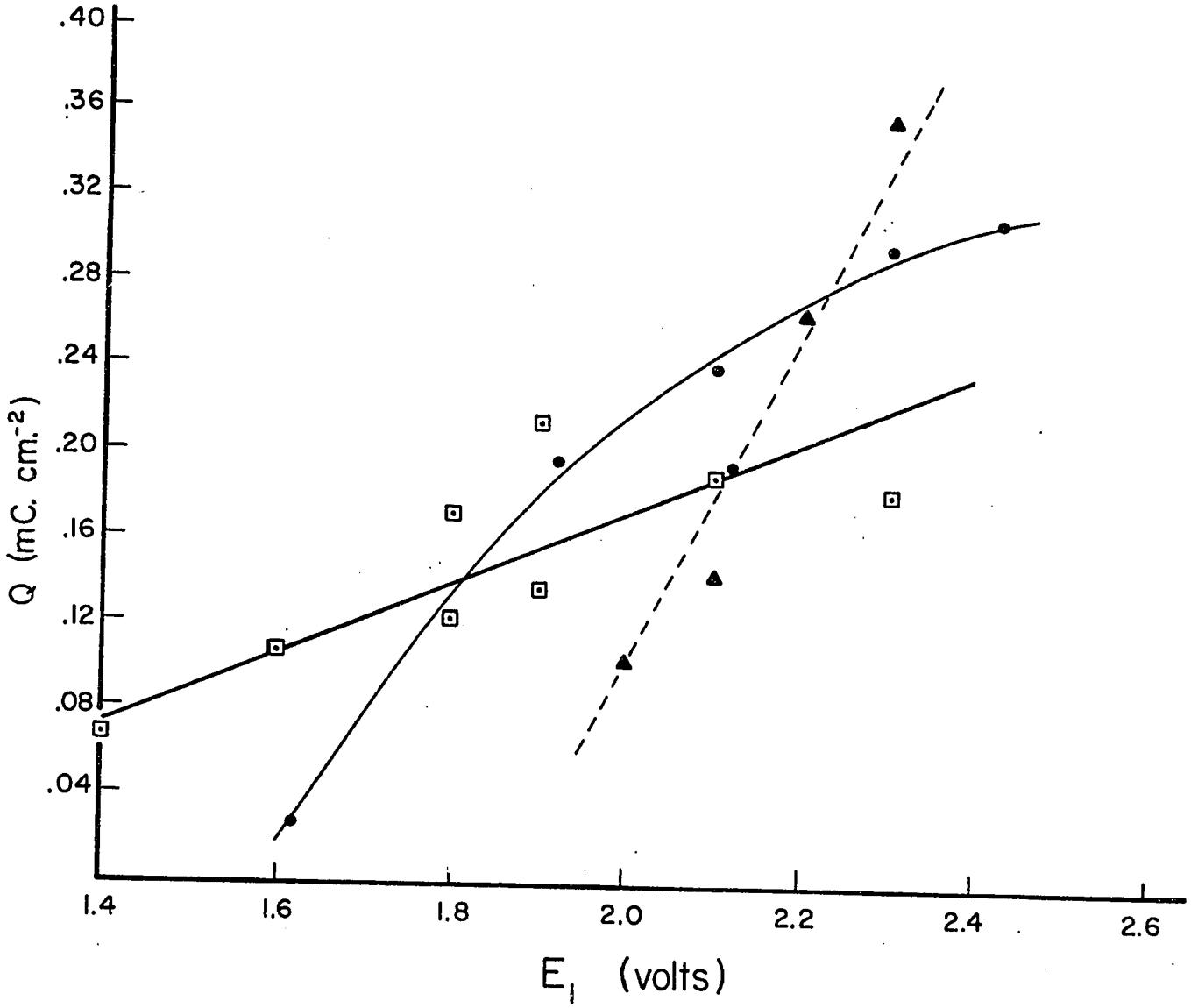

Figure 30

Gold/1M CF_3COOK in CF_3COOH:

o plot of $C_{max.}$ vs. $i_{cath.}$;

• plot of $VC_{max.}$ vs. $i_{cath.}$.

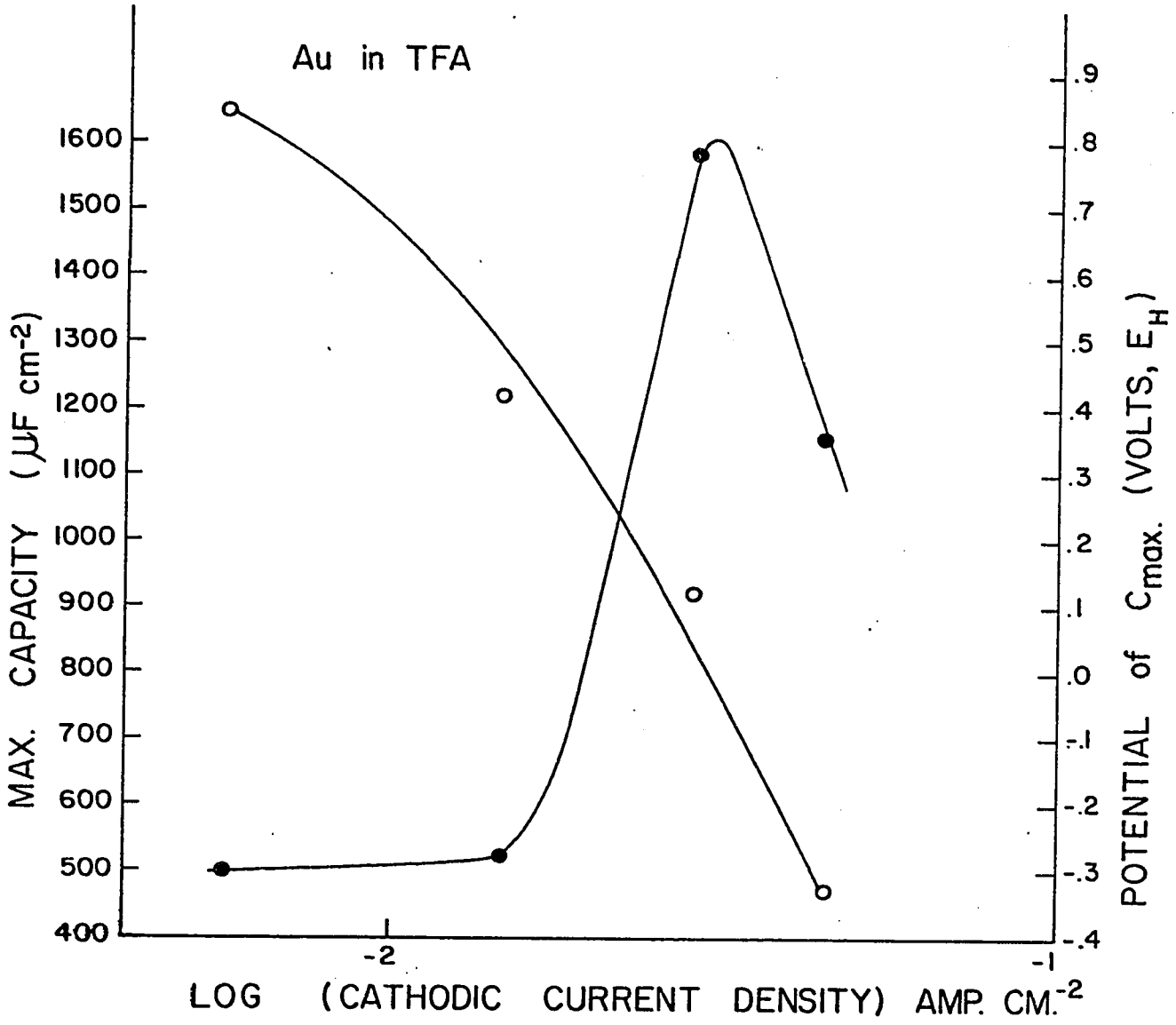
Au in TFA
MAX. CAPACITY (μF cm-2)
1600
1500
1400
1300
1200
1100
1000
900
800
700
600
500
400
-2
-1
LOG (CATHODIC CURRENT DENSITY) AMP. CM.-2
.9
.8
.7
.6
.5
.4
.3
.2
.1
.0
-.1
-.2
-.3
-.4
POTENTIAL of Cmax. (VOLTS, EH)

Figure 31

Gold/1M CF_3COOK in CF_3COOH: C-V profiles as a function of charging cathodic current density, $i_{cath.}$, for the adsorbed species in the Kolbe oxidation: $i_{cath.}$ (in a. $cm.^{-2}$):

Δ	5.65×10^{-3};
x	14.66×10^{-3};
o	28.6×10^{-3};
●	44.2×10^{-3}.

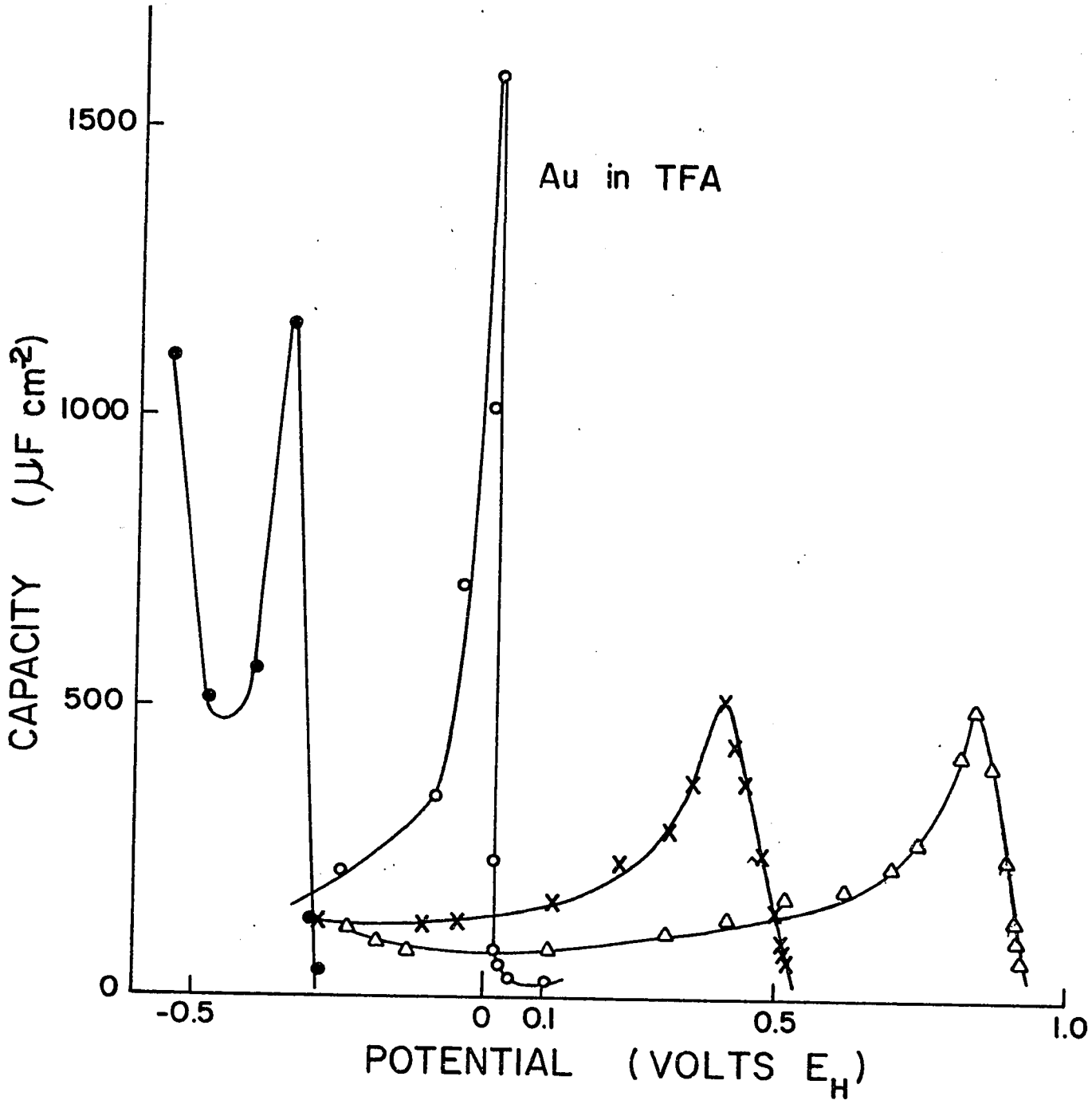
Au in TFA
1500
1000
500
0
CAPACITY (μF cm⁻²)
-0.5
0
0.1
0.5
1.0
POTENTIAL (VOLTS E_H)

Figure 32

Gold in nominally anhydrous 1M KTFA/TFA solution: plots of $i_{cath.}$ vs. $1/\tau$ (Δ) and $i_{cath.}$ vs. $1/\tau^{\frac{1}{2}}$ (o).

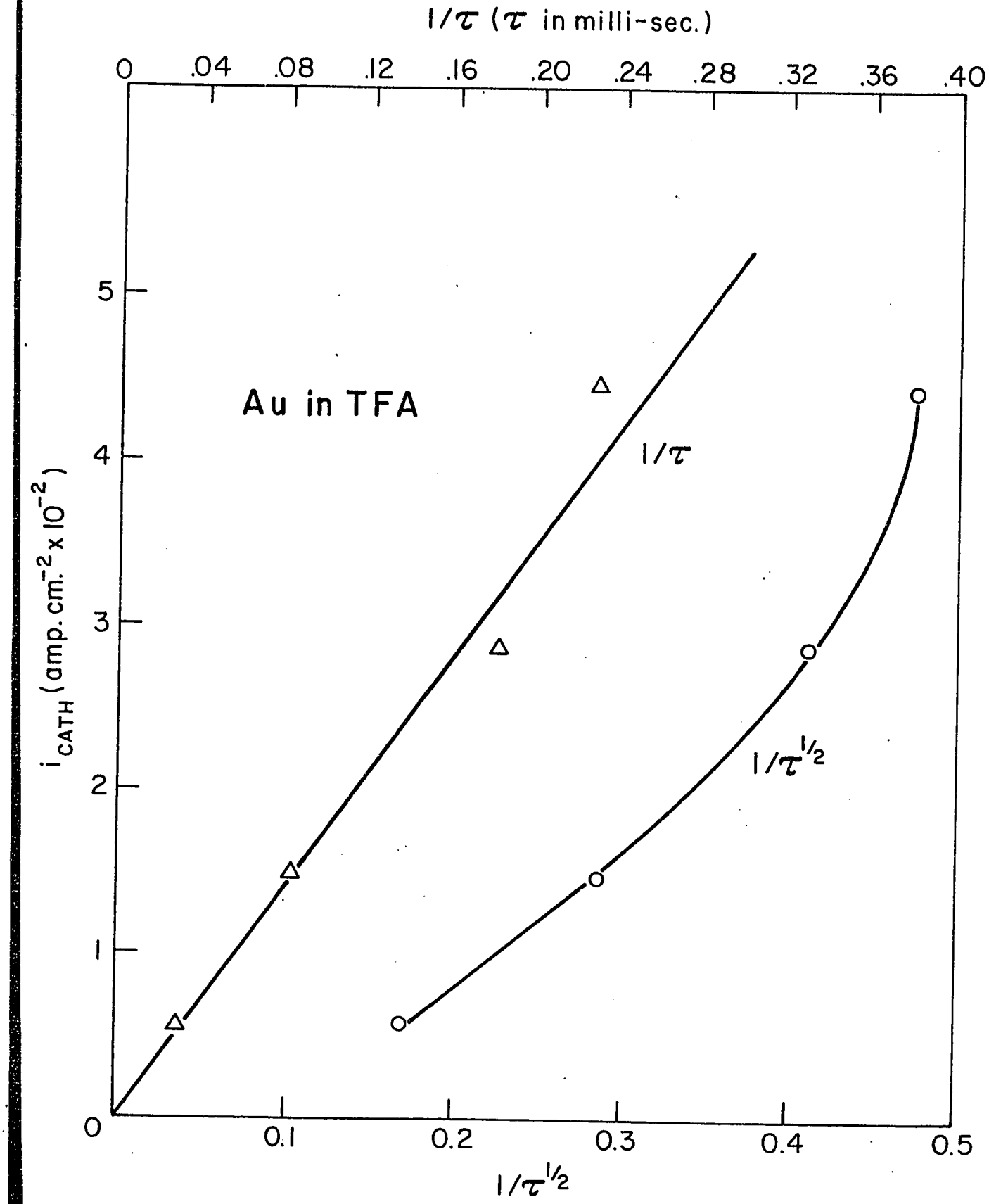
1/τ (τ in milli-sec.)
0
.04
.08
.12
.16
.20
.24
.28
.32
.36
.40
Au in TFA
1/τ
1/τ^1/2
i_CATH (amp. cm.^-2 x 10^-2)
5
4
3
2
1
0
0.1
0.2
0.3
0.4
0.5
1/τ^1/2

this line is 0.175 mC. cm.$^{-2}$. The significance of the $i_{cath.}$ *vs.* $1/\tau$ plot is further emphasized, as above, by the absence of a straight line when $i_{cath.}$ is plotted *vs.* $1/\tau^{\frac{1}{2}}$ (Fig. 32). It should be noted that Q is about twice as great in magnitude as the Q obtained in very anhydrous solutions.

After establishing in this case that Q was independent of $i_{cath.}$ (Fig. 32), the dependence of Q on initial polarisation potential V_i was examined. It was found that Q increased with increasing V_i (Fig. 29).

In solutions containing excess of water, a long arrest in the potential-time curve obtained by forced decay of V_i is observed. The pseudo-capacity in this case attains much higher values than those found for the electrodes in anhydrous solutions or in solutions with traces of water. The $C_{max.}$ values range from *ca.* 2500 μF. cm.$^{-2}$ to 7500 μF. cm.$^{-2}$ and $V_{C_{max.}}$ values from 0.89 V to 1.05 V. Both $C_{max.}$ and $V_{C_{max.}}$ values depend on the magnitude of $i_{cath.}$ used in the driven decay. With increasing $i_{cath.}$ values, shifts in both $V_{C_{max.}}$ and $C_{max.}$ show irregular trends (Fig. 33). The C-V relations, computed from differentiated forced decay curves, at various $i_{cath.}$ values are shown in Fig. 34. The arrest in the forced discharge profile is almost horizontal so that a surface species with almost bulk reduction behaviour is indicated.

Figure 33

Gold/1M CF_3COOK in CF_3COOH (+ water):

- O plot of $C_{max.}$ vs. $i_{cath.}$;
- ● plot of $V_{C_{max.}}$ vs. $i_{cath.}$.

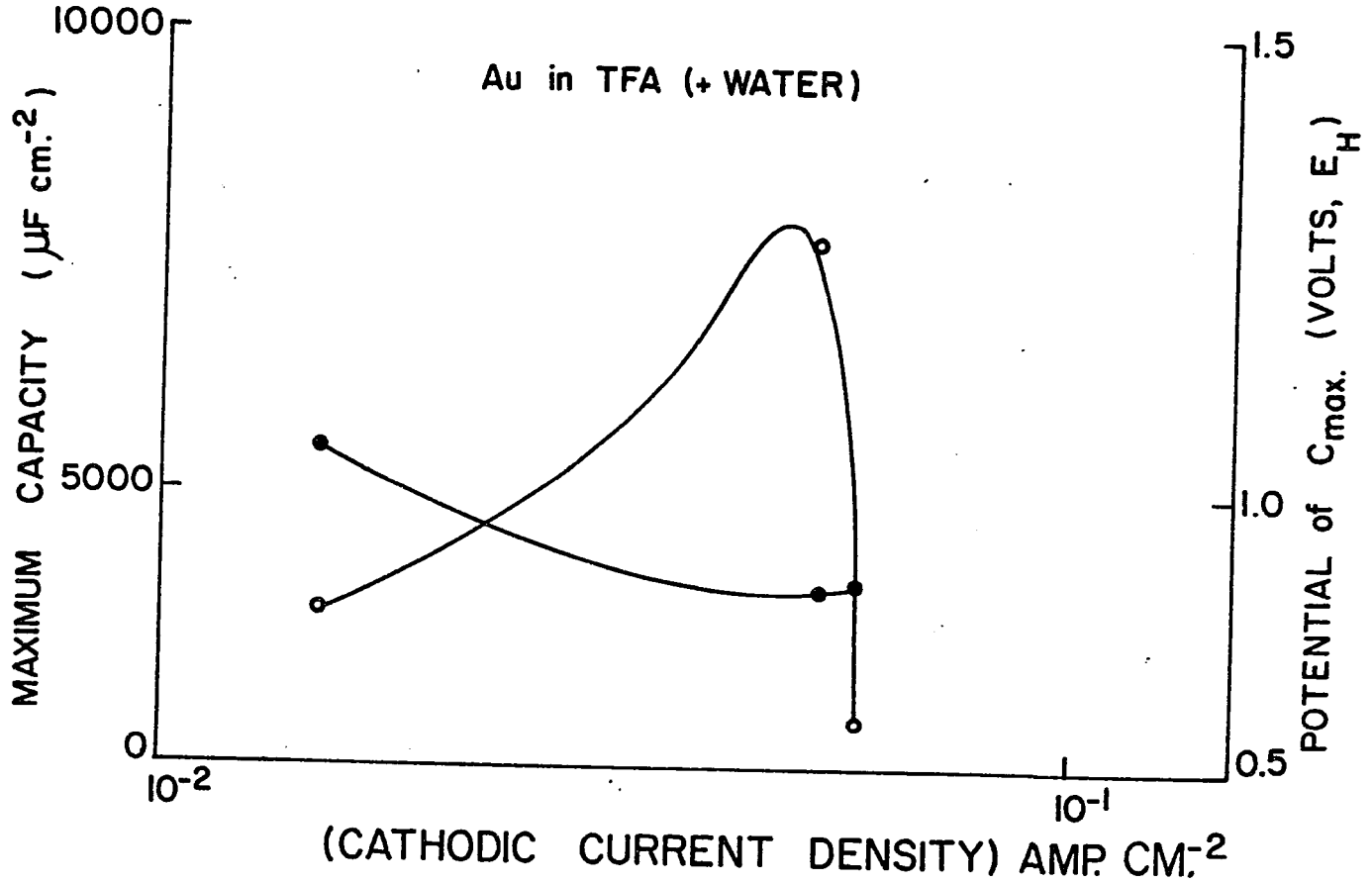
Au in TFA (+ WATER)
10000
5000
0
MAXIMUM CAPACITY (μF cm.-2)
1.5
1.0
0.5
POTENTIAL of Cmax. (VOLTS, EH)
10-2
10-1
(CATHODIC CURRENT DENSITY) AMP. CM.-2

Figure 34

Gold/1M CF_3COOK in CF_3COOH (+ water): C-V profiles as a function of charging cathodic current density, $i_{cath.}$, for the adsorbed species in the Kolbe oxidation: $i_{cath.}$ (in a. $cm.^{-2}$):

o	1.5×10^{-2};
•	5.29×10^{-2};
x	5.82×10^{-2}.

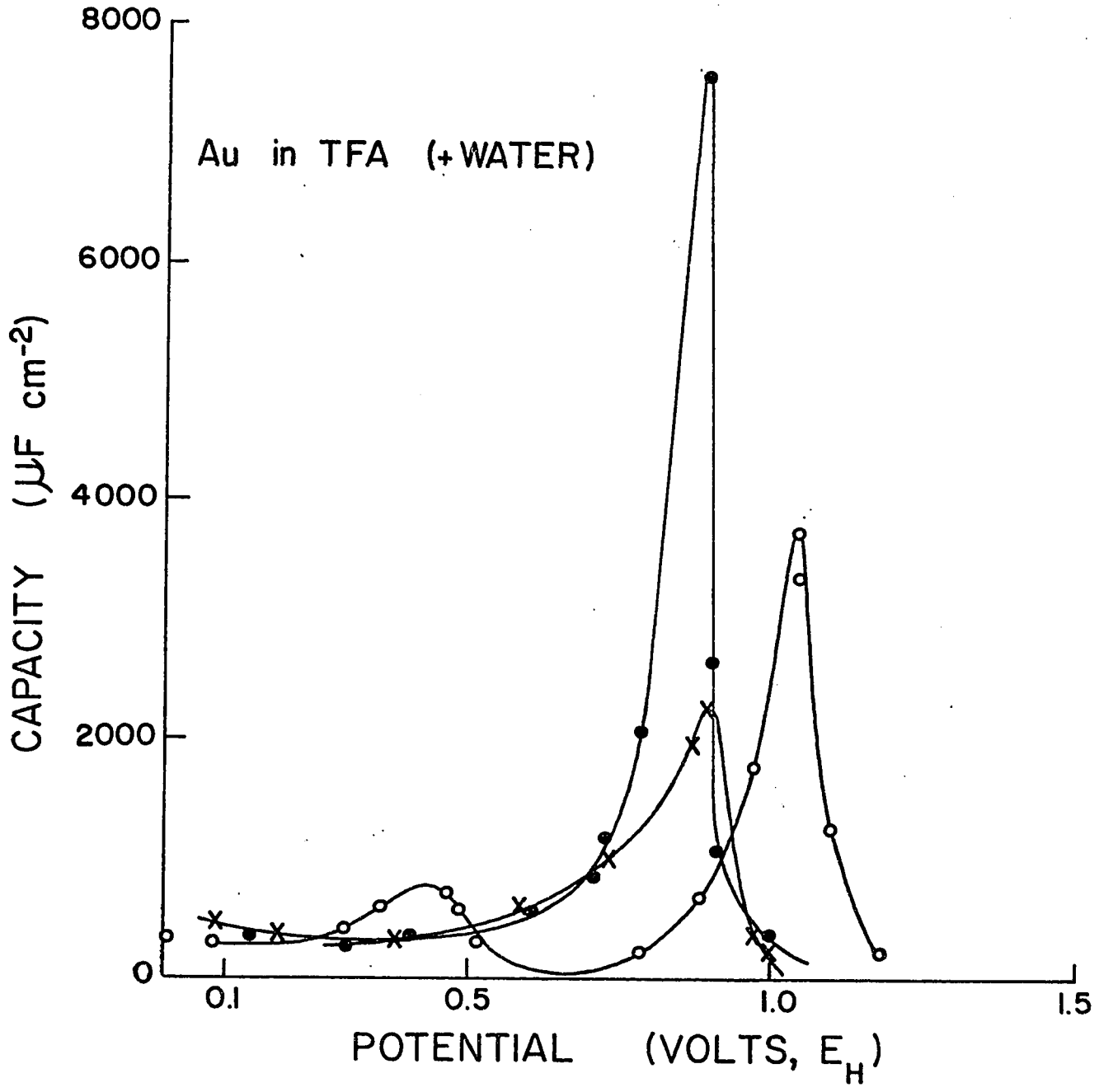
8000
6000
4000
2000
0
Au in TFA (+WATER)
CAPACITY (μF cm-2)
0.1
0.5
1.0
1.5
POTENTIAL (VOLTS, EH)

On plotting $i_{cath.}$ against $1/\tau$, a straight line is obtained (Fig. 35) and the value of charge Q given by the slope of this line is 1.09 mC. cm.$^{-2}$. This value of Q is several times greater than that obtained either in anhydrous solutions or in solutions containing traces of water. The conclusions to be drawn from the linearity of the $i_{cath.}$ vs. $1/\tau$ plot (viz., that only a discharging process of ad-species is involved) is further emphasized, as above, by the absence of a straight line in the plot of $i_{cath.}$ vs. $1/\tau^{\frac{1}{2}}$, also shown in Fig. 35.

After thus establishing that Q was independent of $i_{cath.}$, a plot of Q against V_i, the initial polarisation potential, was examined. It is found that Q increases with increasing V_i (Fig. 29).

In Fig. 29 are also shown three polaroid photographs on which the actual experimental forced decay transients and corresponding differentiated profiles were recorded for the indicated conditions of water content.

(c) Platinum in Potassium Acetate-Acetic Acid Solutions

Potential-time relationships obtained on open-circuit and forced decay of potentials of anodically polarised platinum electrodes were examined in: (a) completely anhydrous conditions achieved in the "vacuum run" described

Figure 35

Gold in 1M KTFA/TFA + water solution: plots of $i_{cath.}$ vs. $1/\tau$ (Δ) and $i_{cath.}$ vs. $1/\tau^{\frac{1}{2}}$ (o).

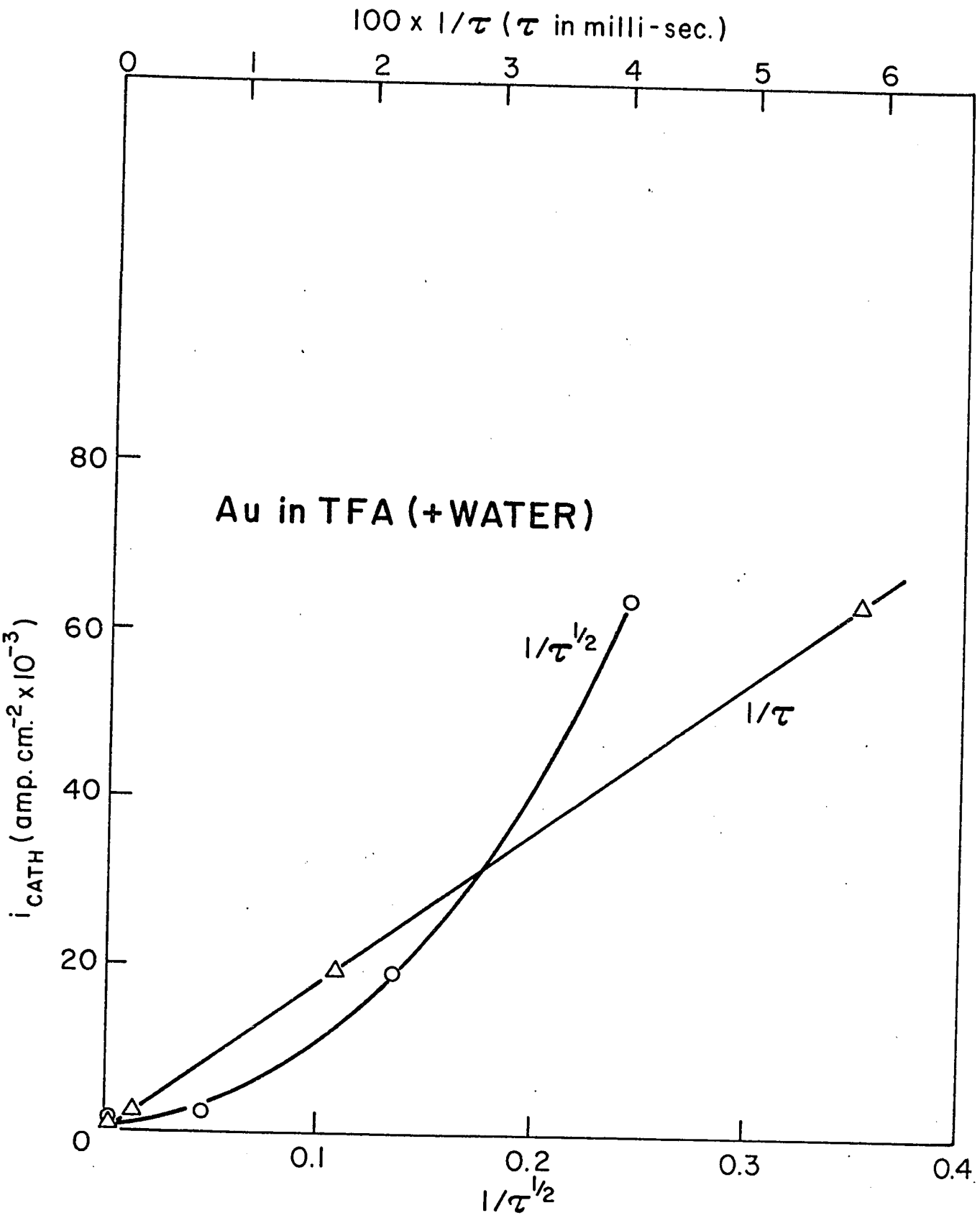
100 x 1/τ (τ in milli-sec.)
0
1
2
3
4
5
6
80
60
40
20
0
Au in TFA (+WATER)
1/τ^1/2
1/τ
i_CATH (amp. cm.^-2 x 10^-3)
0.1
0.2
0.3
0.4
1/τ^1/2

Table IV

Behaviour at platinum: potassium acetate-acetic acid solutions.

TABLE IV. BEHAVIOUR AT PLATINUM

EXPERIMENTAL EVIDENCE	SOLUTION: 1M CH_3COOK in CH_3COOH (VACUUM)	SOLUTION: 1M CH_3COOK + 1M CH_3COOH IN WATER	REMARKS (GENERAL)
1. CURRENT-POTENTIAL RELATIONS			
(i) TAFEL SLOPES	(i) 0.14 V	(i) 0.165 V (2.5 V ⟶); 0.260 V (2.2 V ⟶ 2.5 V); 0.20 V (1.8 V ⟶ 2.2 V).	GRADUAL ADDITION OF PREDETERMINED AMOUNTS OF H_2O SHOWS THAT REST POTENTIALS BECOME HIGHER, RATES BECOME LOWER AND HYSTERESIS BECOMES LARGER WITH INCREASING AMOUNTS OF H_2O. (Fig. 13).
(ii) HYSTERESIS?	(ii) HYSTERESIS	(ii) HYSTERESIS	
(iii) REST POTENTIAL	(iii) $\cong$ 0.2 V	(iii) $\cong$ 1.25 V	
(iv) ADDITIONAL FEATURES OR COMMENTS			
2. OPEN-CIRCUIT DECAYS			
(i) ARREST?	(i) ARREST OBSERVED	(i) NO ARREST	RESIDUAL POTENTIAL, AND HIGH C AND Q VALUES OBSERVED ONLY IN AQUEOUS SOLUTION
(ii) MAGNITUDE OF C	(ii) d.l. CAPACITY ($< 100\ \mu F\ cm^{-2}$)	(ii) d.l. CAPACITY	
(iii) RESIDUAL POTENTIAL	(iii) NO RESIDUAL POTENTIAL OBSERVED	(iii) 0.70 V	
(iv) FORCED DECAY FROM RESIDUAL POTENTIAL? (a) VALUES OF $C_{max.}$ AND $V_{C_{max.}}$ (b) VALUES OF Q AND POTENTIALS OF ARRESTS CORRESPONDING TO Q.		(iv) ARRESTS OBSERVED ON FORCED DECAY (a) $C_{max.} = 6500\ \mu F\ cm^{-2}$ ($V_1 = 1.9$ V; $V_{C_{max.}} = 0.63$ V); $C_{max.} = 9000\ \mu F\ cm^{-2}$ ($V_1 = 2.5$ V; $V_{C_{max.}} = 0.59$ V) (b) $Q_1 = 1.024\ mCom^{-2}$ ($V_{C_{max.}} = 0.60$ V), $Q_2 = 0.692\ mCom^{-2}$ ($V_{C_{max.}} = 0.25$ V) $\left\{ V_1 = 2.5 \text{ V} \right\}$	
(v) ADDITIONAL FEATURES OR COMMENTS			

....CONTINUED....

3. FORCED DECAYS			
(i) ARRESTS?	(i) ARRESTS OBSERVED.	(i) ARRESTS OBSERVED	
(ii) $C_{max.}$ AND $V_{C_{max.}}$ AND Q VALUES.	(ii) 4.1. CAPACITY ($< 100 \mu F\ cm^{-2}$) OBSERVED.	(ii) (a) $1250 \mu F\ cm^{-2}$ to $1500 \mu F\ cm^{-2}$ DEPENDING ON $i_{cath.}$ ($V_1 = 1.0$ V) - TWO LARGE AND ONE SMALL $C_{max.}$'s OBSERVED WITH $V_{C_{max.}} = 0.5$ V, 0.225 V, 0.025 V RESPECTIVELY. (b) $4500 \mu F\ cm^{-2}$ to $5000 \mu F\ cm^{-2}$ ($V_1 = 2.5$ V). TWO $C_{max.}$'s OBSERVED ($V_{C_{max.}} = 0.5$ V AND 0.2 V). (c) $Q_1 = 0.15\ mCcm^{-2}$; $Q_2 = 0.22\ mCcm^{-2}$; $Q_3 = 0.17\ mCcm^{-2}$ ($V_1 = 1.0$ V) (d) $Q_1 = 1.17\ mCcm^{-2}$; $Q_2 = 0.63\ mCcm^{-2}$; $(Q_1/Q_2 = 1.86)$ ($V_1 = 2.5$ V)	
(iii) EFFECT OF $i_{cath.}$ ON $C_{max.}$ AND $V_{C_{max.}}$	(iii) NOT STUDIED SINCE NO APPRECIABLE C VALUES OBTAINED IN (ii) ABOVE.	(iii) (a) $V_1 = 1.0$ V: IN THIS CASE TWO MAIN $C_{max.}$'s AND ONE SMALL $C_{max.}$ OBSERVED: INCREASED $i_{cath.}$ SHIFTS ONE MAIN $C_{max.}$ TO HIGHER VALUES WHILE EFFECT OF $i_{cath.}$ ON OTHER $C_{max.}$'s AND ALL $V_{C_{max.}}$ SHOWS NO REGULAR TREND. (b) $V_1 = 2.5$ V; IN THIS CASE INCREASED $i_{cath.}$ SHIFTS BOTH $V_{C_{max.}}$ TO MORE CATHODIC POTENTIALS AND ONE $C_{max.}$ ($V_{C_{max.}} = 0.2$ V) TO HIGHER VALUES.	ARRESTS, AND HIGH C AND Q VALUES ASSOCIATED WITH THE ARRESTS, OBSERVED ONLY IN AQUEOUS CASE.
(iv) PLOT OF $i_{cath.}$ vs. $1/\varphi$, AT A GIVEN V_1; Q FROM THIS PLOT.	(iv) STRAIGHT LINE; $Q = 15.8 \mu Ccm^{-2}$.	(iv) (a) STRAIGHT LINE; $Q_{total} = 0.54\ mCcm^{-2}$ ($V_1 = 1.0$ V) (b) STRAIGHT LINE; $Q_{total} = 1.8\ mCcm^{-2}$ ($V_1 = 2.5$ V).	
(v) PLOT OF Q vs. V_1.	(v) SINCE Q IS NEGLIGIBLE, NO PLOT CAN BE MADE.	(v) Q INCREASES WITH INCREASING V_1 UP TO 2.0 V; AT 2.0 V, Q BECOMES INDIFFERENT TO A FURTHER RISE IN V_1. (THIS IS TRUE FOR ALL THE THREE PEAKS, WITH $V_{C_{max.}}$ 0.5 V, 0.2 V, 0.02 V).	
(vi) ADDITIONAL FEATURES OR COMMENTS.			
4. SWEEP RUNS			
(i) PLOT OF PEAK CURRENT vs. $(dV/dt)^{\frac{1}{2}}$	(i) NO PEAK OBSERVED; ONLY HYSTERESIS OBTAINED; "PEAK" CURRENT (FROM THE CENTRE OF THE HYSTERESIS) vs. $(dV/dt)^{\frac{1}{2}}$ PLOT IS A STRAIGHT LINE.	(i) NO STRAIGHT LINE IS OBTAINED	
(ii) DEPENDENCE OF Q ON (dV/dt).		(ii) DEPENDENCE OF Q ON (dV/dt) IS VERY SLIGHT.	
(iii) IF CHARGING PEAKS, Q VALUES FOR THE PEAKS.		(iii) $Q_A = 0.84\ mCcm^{-2}$ (0.55 V) RATIO $= \frac{Q_A}{Q_B} = 1.556$ (RANGE SCANNED = 0-1.8 V) $Q_B = 0.54\ mCcm^{-2}$ (0.10 V) WHEN KOLBE REGION IS ALSO SCANNED, RATIO $= \frac{Q_A}{Q_B} = 1.514$ (SAME $dV/dt = 3.78$ V $sec.^{-1}$) (RANGE SCANNED = 0-2.6 V) $\frac{Q_O}{Q_H}$ (FOR Pt IN H_2SO_4; $dV/dt = 3.6$ V $sec.^{-1}$) = 2.428 (RANGE SCANNED = 0-1.8 V)	CHARGING PEAKS OBSERVED ONLY IN THE AQUEOUS CASE. VALUES OF Q AND $V_{C_{max.}}$ SHOW THAT THESE PEAKS CORRESPOND TO THE CHARGING PROCESSES OF OXIDE AND HYDROGEN FORMATION AND IONIZATION.
(iv) $C_{max.}$ AND $V_{C_{max.}}$	(iv) d.l. CAPACITY OBTAINED AT ALL SWEEP RATES AS CALCULATED FROM THE "PEAK" CURRENT FROM THE CENTRE OF THE HYSTERESIS.	(iv) $C_{max.}$ $2536 \mu F\ cm^{-2}$ ($V_{C_{max.}} \simeq 0.55$ V) LIMITS: $[(dV/dt) = 3.78$ V $sec.^{-1}$; $(0-1.8$ V$)]$	
(v) EFFECT OF (dV/dt) ON $C_{max.}$ AND $V_{C_{max.}}$		(v) (a) WITH INCREASING dV/dt, $V_{C_{max.}}$ AT 0.55 V SHIFTS VERY SLIGHTLY TO LESS ANODIC VALUES, FOR THE OXIDE REDUCTION PEAK. (b) WITH INCREASING dV/dt, $C_{max.}$ DECREASES SLIGHTLY WHEN RANGE SCANNED IS (0-1.8 V); IT DECREASES APPRECIABLY WHEN RANGE SCANNED IS (0-2.6 V).	
(vi) ADDITIONAL FEATURES OR COMMENTS.			

in Chapter II, section 2(ii); (β) aqueous solution of (1M CH_3COOK + 1M CH_3COOH). The results obtained, both in aqueous and non-aqueous solutions, are summarised in Table IV, sections 2 and 3.

Open-circuit decay behaviour: In the non-aqueous solution, an arrest is observed on open-circuit decay but the value of $C_{max.}$ (60 μF. $cm.^{-2}$) is of the order of $C_{d.l.}$. No residual potential is observed.

In the aqueous solution, no arrest is observed and $C_{max.}$ has a value of the order of $C_{d.l.}$. The residual potential in this case is 0.79 V. On forced decay from this residual potential, two further arrests are, however, observed. The values of $C_{max.}$ and $V_{C_{max.}}$ for the main arrest seem to depend on the initial polarisation potential, V_i, and are as follows (Fig. 36);

$C_{max.}$ = 6500 μF. $cm.^{-2}$; $V_{C_{max.}}$ = 0.63 V; V_i = 1.9 V

$C_{max.}$ = 9000 μF. $cm.^{-2}$; $V_{C_{max.}}$ = 0.59 V; V_i = 2.5 V.

The values of charges calculated for both of these arrests are

Q_1 = 1.024 mC. $cm.^{-2}$ ($V_{C_{max.}}$ = 0.60 V) $\left\{ V_i = 2.5 \text{ V} \right\}$

Q_2 = 0.692 mC. $cm.^{-2}$ ($V_{C_{max.}}$ = 0.25 V) $\left\{ V_i = 2.5 \text{ V} \right\}$

Q_{total} = 1.716 mC. $cm.^{-2}$.

$\frac{Q_1}{Q_2}$ = 1.48

Figure 36

Platinum in aqueous (1M CH_3COOK + 1M CH_3COOH) solution: C-V profiles calculated from curves obtained on forced decay from the residual potential:

- ● V_1 = 1.9 V; $V_{res.}$ = 1.06 V;
- o V_1 = 2.5 V; $V_{res.}$ = 0.9 V.

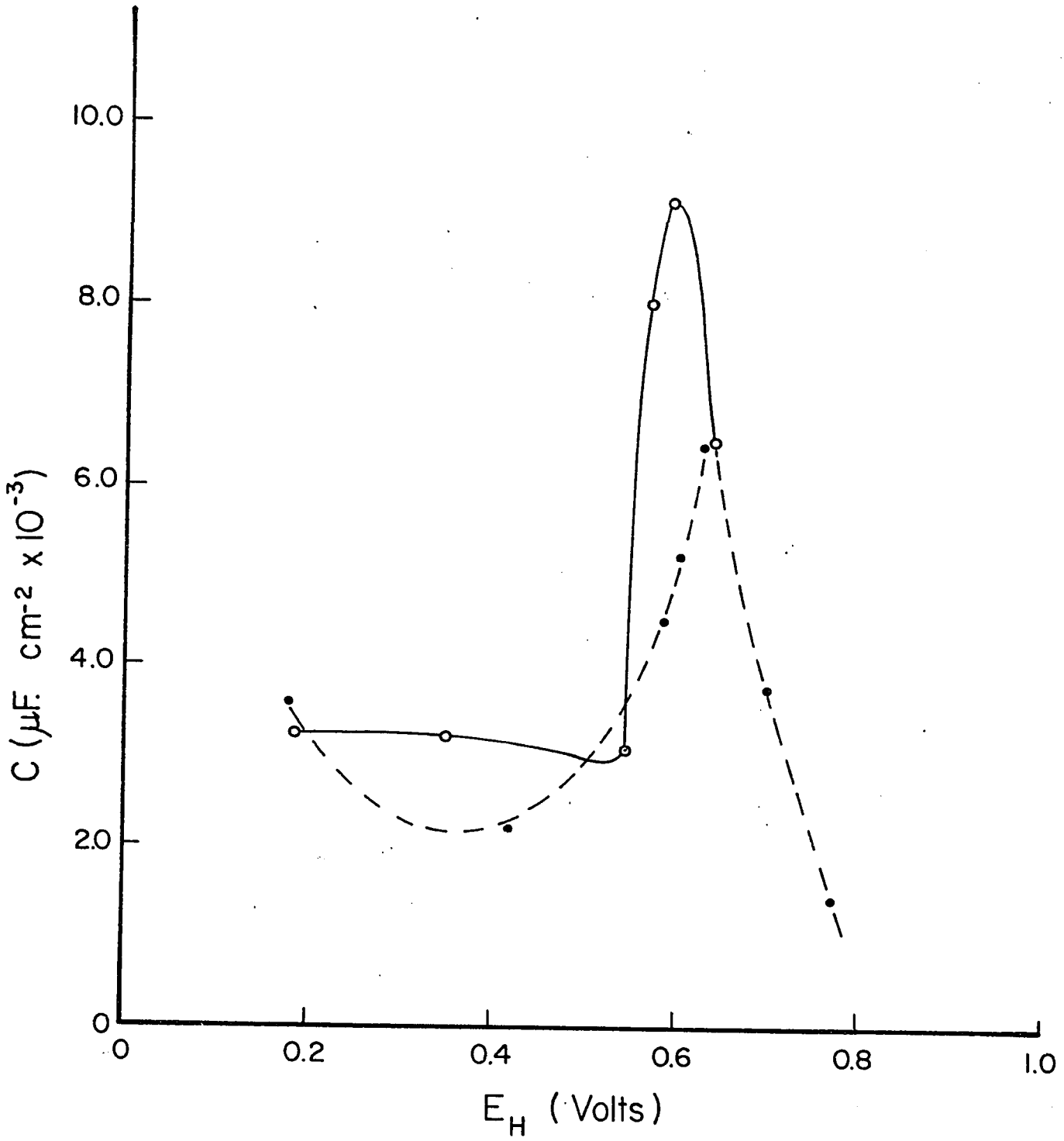
10.0
8.0
6.0
4.0
2.0
0
C (μF. cm-2 x 10-3)
0
0.2
0.4
0.6
0.8
1.0
EH (Volts)

Forced decay behaviour: In non-aqueous solutions, on driven decay from anodic potentials arrests are observed but the values of $C_{max.}$ (60 μF. cm.$^{-2}$) are found to be of the order of $C_{d.l.}$. On plotting $i_{cath.}$ vs. $1/\tau$, a straight line is obtained the slope of which gives Q, the charge. The Q has a value = 15 μC. cm.$^{-2}$ (Fig. 37). Thus, in non-aqueous solutions, very small values of C and Q are observed.

In Fig. 37, a plot of $i_{cath.}$ vs. $1/\tau^{\frac{1}{2}}$ is also shown, as previously, to emphasize the non-diffusion controlled nature of the transition time. Corresponding photographs of the transients are also given.

In aqueous solutions, however, when a cathodic charging transient is applied to the electrode immediately after the cessation of anodic polarisation, appreciable arrests are observed. In these solutions, cathodic charging curves were studied by polarising the electrode to two initial anodic potentials, (α) = 1.0 V, (β) = 2.5 V, in order to distinguish charging processes associated with oxygenated species and with Kolbe species in the presence of oxygenated species.

Figure 37

Platinum in very anhydrous ("vacuum run") 1M CH_3COOK/CH_3COOH solution: plots of $i_{cath.}$ vs. $1/\tau$ (o) and $i_{cath.}$ vs. $1/\tau^{\frac{1}{2}}$ (•).

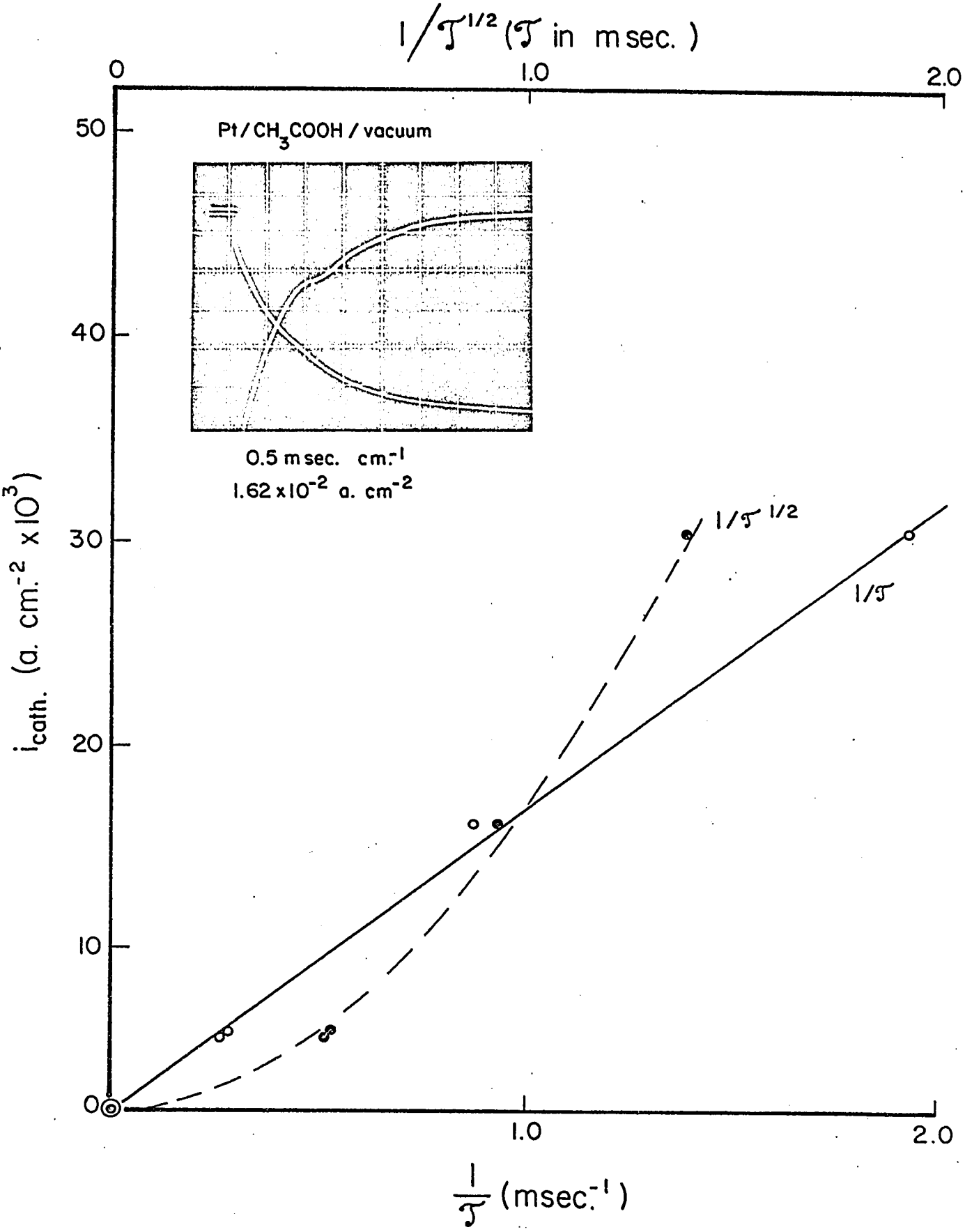
$1/\tau^{1/2}$ (τ in msec.)
0
1.0
2.0
50
40
30
20
10
0
Pt / CH_3COOH / vacuum
0.5 msec. cm.$^{-1}$
1.62 x 10^{-2} a. cm^{-2}
$i_{cath.}$ (a. cm.$^{-2}$ x 10^3)
$1/\tau^{1/2}$
$1/\tau$
1.0
2.0
$\frac{1}{\tau}$ (msec.$^{-1}$)

(α) Initial anodic polarisation potential, V_i = 1.0 V

In this case, several significant arrests were observed. Two large and one small $C_{max.}$ are present in the C-V profiles (Fig. 38) computed from forced discharge curves. The $C_{max.}$ values for large capacity maxima range between 1250 μF. cm.$^{-2}$ and 1500 μF. cm.$^{-2}$ depending on $i_{cath.}$ used in the forced decay. The $V_{C_{max.}}$ values for the three capacity maxima are 0.5 V, 0.225 V and 0.025 V respectively. An increase of $i_{cath.}$ has the effect of shifting one of the main capacity maxima to somewhat higher values (Fig. 39) while shifts in other $C_{max.}$ and all $V_{C_{max.}}$ with increased $i_{cath.}$ show no regular trend. On plotting $i_{cath.}$ against $1/\tau$ (τ here refers to total time in seconds for all the observed arrests*), a straight line is obtained (Fig. 40) and Q_{total}, as given by the slope of this straight line is 0.54 mC. cm.$^{-2}$. This Q_{total} corresponds to three arrests and hence to three sub-values which are

$$Q_1 = 0.15 \text{ mC. cm.}^{-2} \quad (V_{C_{max.}} = 0.5 \text{ V})$$
$$Q_2 = 0.22 \text{ mC. cm.}^{-2} \quad (V_{C_{max.}} = 0.225 \text{ V})$$
$$Q_3 = 0.17 \text{ mC. cm.}^{-2} \quad (V_{C_{max.}} = 0.025 \text{ V})$$
$$Q_{total} = 0.54 \text{ mC. cm.}^{-2}$$

* τ here refers to all the arrests because at higher values of $i_{cath.}$, all these arrests tend to merge to give a single arrest. This suggests that at lower $i_{cath.}$ multiple arrests are observed for the same (or closely related) adsorbed species, e.g., two arrests for oxide on Pt are well known if the potentials are sufficiently anodic.

Figure 38

Platinum in aqueous (1M CH_3COOK + 1M CH_3COOH) solution: C-V profiles as a function of charging cathodic current density, $i_{cath.}$, for the adsorbed species:
V_1 = 1.0 V: $i_{cath.}$ (a. $cm.^{-2}$):

o 1.02×10^{-2};

● 2.56×10^{-2};

▲ 4.15×10^{-2};

□ 5.88×10^{-2}.

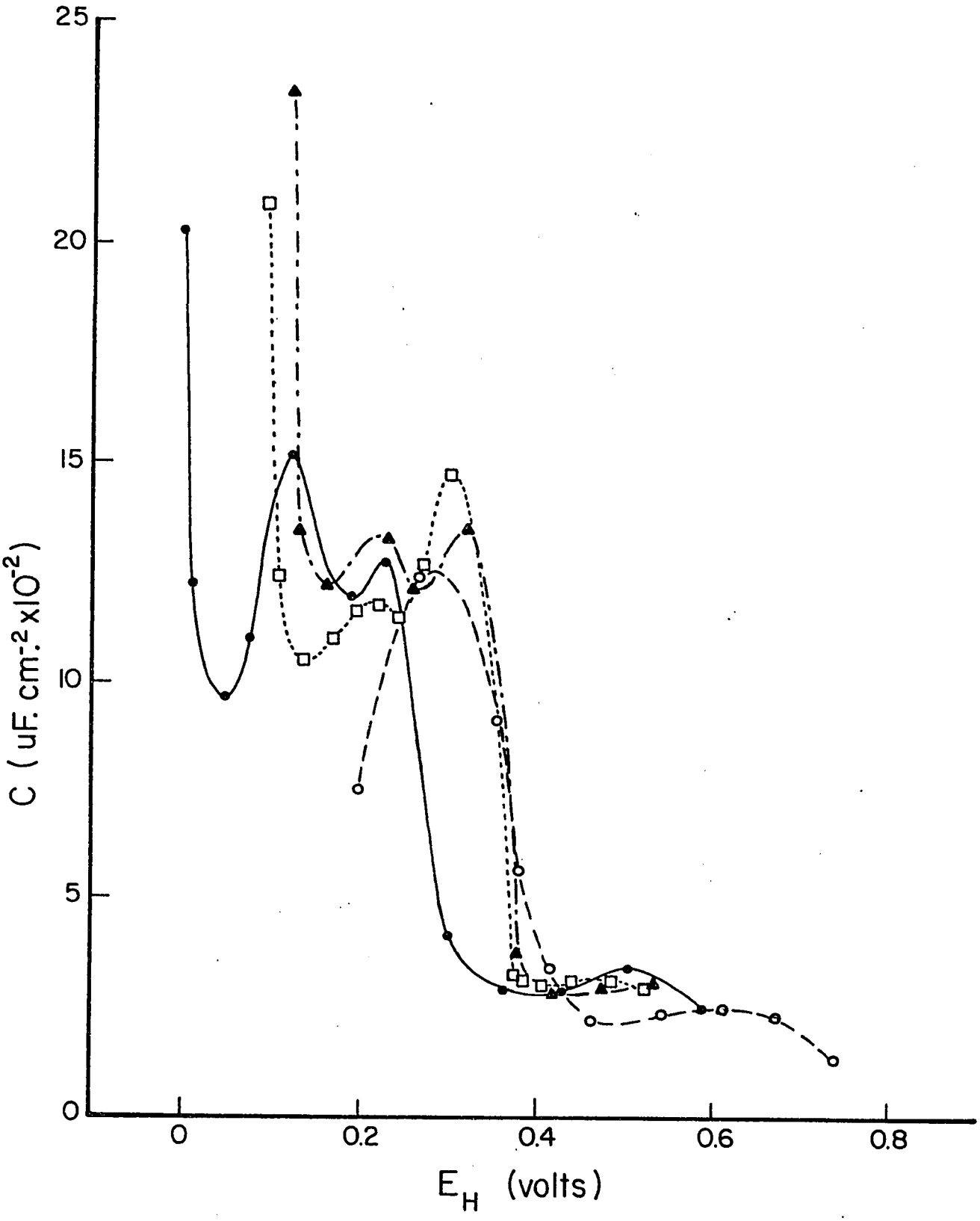
25
20
15
10
5
0
0
0.2
0.4
0.6
0.8
C (uF. cm.-2 x10-2)
EH (volts)

Figure 39

Platinum in aqueous (1M CH_3COOK + CH_3COOH) solution: plot of $C_{max.}$ vs. $i_{cath.}$ (V_1 = 1.0 V).

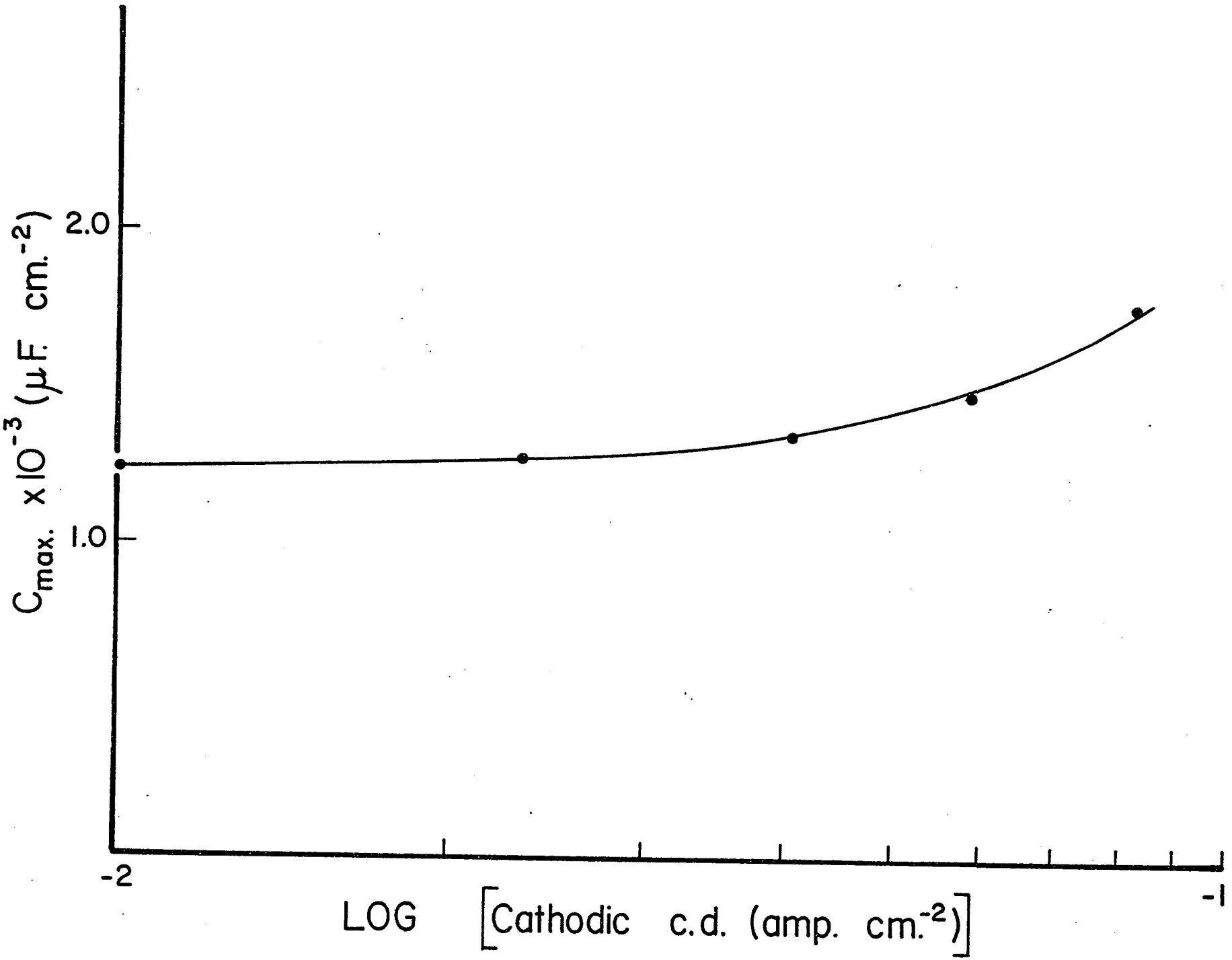
2.0
1.0
$C_{max.} \times 10^{-3}$ (μF. cm.$^{-2}$)
-2
-1
LOG [Cathodic c.d. (amp. cm.$^{-2}$)]

Figure 40

Platinum in aqueous (1M CH_3COOK + 1M CH_3COOH) solution: a plot of $i_{cath.}$ vs. $1/\tau$ (V_1 = 1.0 V).

The Q_1, Q_2 and Q_3 however merge at high $i_{cath.}$ as mentioned previously.

(β) Initial anodic polarisation potential, V_i = 2.5 V

In this case, the arrests observed are more pronounced than those in the case when V_i = 1.0 V. Correspondingly higher values of pseudo-capacity and charge are found to be associated with these arrests.

Two capacity maxima are observed with $V_{C_{max.}}$ = 0.5 V and 0.2 V. The values of $C_{max.}$ for the major arrest ($V_{C_{max.}}$ = 0.5 V) range between 4500 μF. cm.$^{-2}$ to 5000 μF. cm.$^{-2}$, depending on the $i_{cath.}$ used. On plotting $i_{cath.}$ against $1/\tau$ (where τ is the total time in seconds for all the arrests), a straight line is observed and Q_{total}, as given by the slope of this line, is 1.8 mC. cm.$^{-2}$ (Fig. 41). This Q consists of two contributions Q_1 and Q_2 corresponding to the two $C_{max.}$ observed. Values of the component Q's are

Q_1 = 1.17 mC. cm.$^{-2}$ ($V_{C_{max.}}$ = 0.5 V)

Q_2 = 0.63 mC. cm.$^{-2}$ ($V_{C_{max.}}$ = 0.2 V)

Q_{total} = 1.8 mC. cm.$^{-2}$ and Q_1/Q_2 = 1.86

The C-V profiles, computed from the forced decay curves, for a range of $i_{cath.}$ values are shown in Fig. 42.

Figure 41

Platinum in aqueous (1M CH_3COOK + 1M CH_3COOH) solution: a plot of $i_{cath.}$ vs. $1/\tau$ (V_i = 2.5 V).

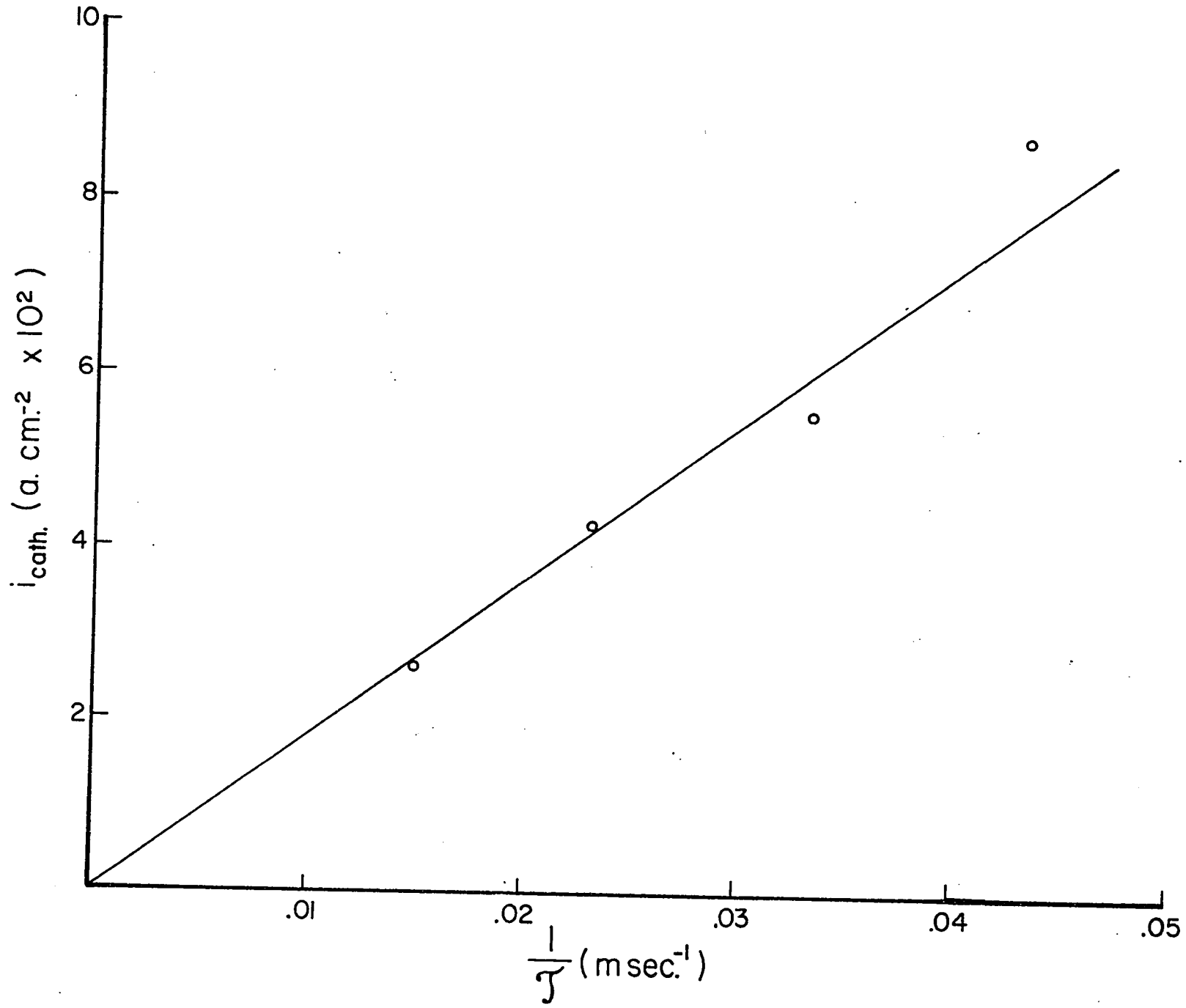
10
8
6
4
2
$i_{cath.}$ (a. cm.$^{-2}$ x 10^2)
.01
.02
.03
.04
.05
$\frac{1}{\tau}$ (m sec.$^{-1}$)

Figure 42

Platinum in aqueous (1M CH_3COOK + 1M CH_3COOH) solution: C-V profiles as a function of charging cathodic current density, $i_{cath.}$, for the adsorbed species in the Kolbe oxidation: V_1 = 2.5 V: $i_{cath.}$ (in a. $cm.^{-2}$):

o	2.62×10^{-2};
•	4.25×10^{-2};
▲	6.04×10^{-2};
□	8.628×10^{-2}.

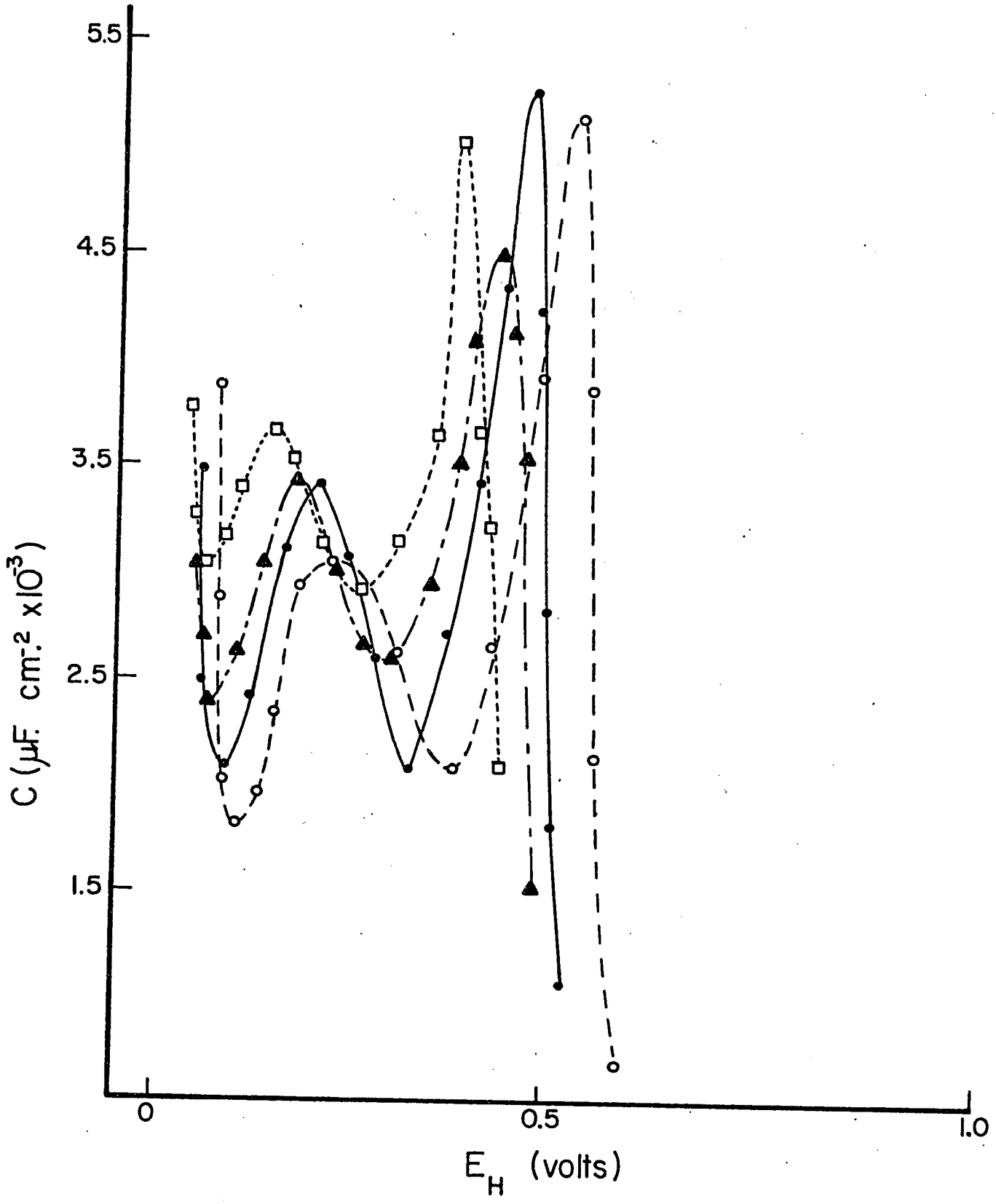
5.5
4.5
3.5
2.5
1.5
C (μF. cm.-2 x10-3)
0
0.5
1.0
EH (volts)

Increase of $i_{cath.}$ tends to shift both $V_{C_{max.}}$ values to more cathodic values; one of the capacity maxima ($V_{C_{max.}}$ = 0.2 V) attains higher values with increasing $i_{cath.}$, while the trend in the shift of the second capacity maximum ($V_{C_{max.}}$ = 0.5 V) is difficult to establish (Fig. 43).

After establishing as in the previous cases that Q_{total} is independent of $i_{cath.}$ (Figs. 40 and 41), the relation between Q and V_i was examined. It was found that for both the arrests, Q increases with increasing V_i up to 2.0 V but above 2.0 V, Q becomes insensitive to any further increase in V_i (Fig. 44). In Fig. 44 a typical photograph of the transient is also shown. The arrests can be easily identified as well-defined peaks on the differentiated forced decay curves.

(d) Gold in Potassium Acetate-Acetic Acid Solutions

The behaviour of gold in: (α) non-aqueous (CH_3COOK in CH_3COOH) solutions; (β) aqueous (CH_3COOK + CH_3COOH) solutions, on open-circuit and forced decay was examined. The results obtained are summarised in Table V, section 2 and 3.

Open-circuit decay behaviour: In non-aqueous solutions, an arrest is observed on self-discharge of an anodically polarised gold electrode but capacity values, computed from

Figure 43

Platinum in aqueous (1M CH_3COOK + 1M CH_3COOH) solution: V_i = 2.5 V:

▲ plot of $V_{C_{max.}}$ vs. $i_{cath.}$ (first large $C_{max.}$);

● plot of $C_{max.}$ vs. $i_{cath.}$ (first large $C_{max.}$);

△ plot of $V_{C_{max.}}$ vs. $i_{cath.}$ (second small $C_{max.}$);

⊙ plot of $C_{max.}$ vs. $i_{cath.}$ (second small $C_{max.}$).

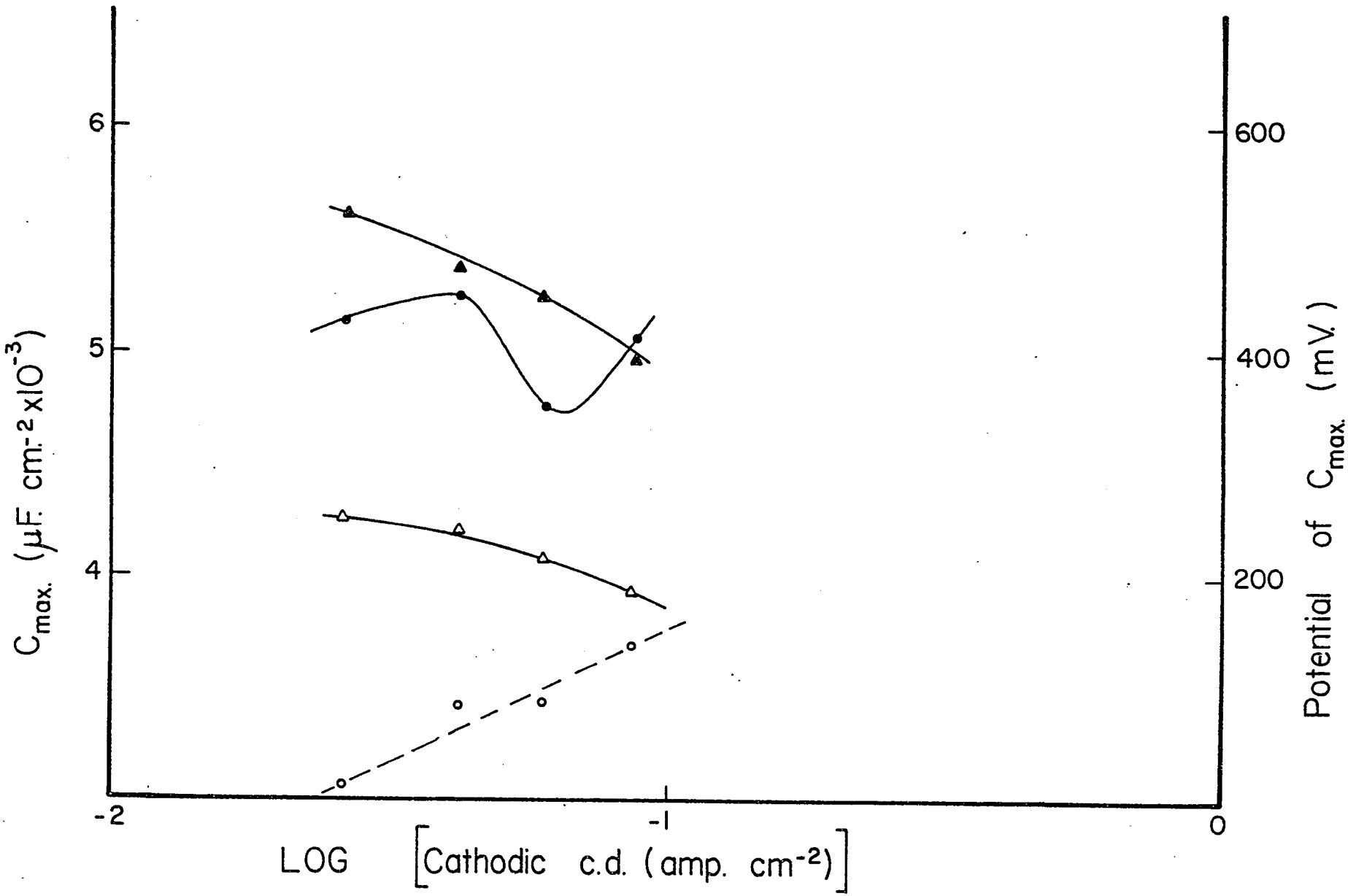
6
5
4
-2
-1
0
600
400
200
$C_{max.}$ (μF. cm.$^{-2}$ x10^{-3})
Potential of $C_{max.}$ (mV.)
LOG [Cathodic c.d. (amp. cm^{-2})]

Figure 44

Platinum in aqueous (1M CH_3COOK + 1M CH_3COOH) solution: plots of Q [for each of the two peaks (see photograph)] vs. E_i.

o	for total charge
•	for charge associated with the smaller peak
×	point for third peak seen at the lowest current density.

Pt. in aqu. (1M CH_3COOK + 1M CH_3COOH) sol.

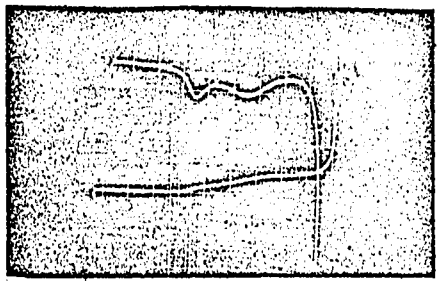

5 m sec. cm.$^{-1}$

5.5 x 10^{-2} a. cm.$^{-2}$

Table V

Behaviour at gold: potassium acetate-acetic acid solutions.

TABLE V. BEHAVIOUR AT GOLD

EXPERIMENTAL EVIDENCE	SOLUTION: 1M CH_3COOK IN CH_3COOH	SOLUTION: 1M CH_3COOK + 1M CH_3COOH IN WATER	REMARKS (GENERAL)
1. CURRENT-POTENTIAL RELATIONS			
(i) TAFEL SLOPES.	(i) 0.11 V	(i) 0.09 V	
(ii) HYSTERESIS?	(ii) VERY SMALL HYSTERESIS	(ii) HYSTERESIS; SLIGHT INHIBITION BEND OBSERVED.	RATE AT A GIVEN POTENTIAL IS HIGHER IN AQUEOUS CASE THAN IN THE NON-AQUEOUS CASE (Fig. 14). REST POTENTIAL IS THE SAME IN BOTH THE CASES WHICH INDICATES THAT NON-AQUEOUS SOLUTION STILL CONTAINS TRACES OF H_2O.
(iii) REST POTENTIAL.	(iii) 1.3 V	(iii) 1.25 V	
(iv) ADDITIONAL FEATURES OR COMMENTS			
2. OPEN-CIRCUIT DECAYS			
(i) ARREST?	(i) ARREST OBSERVED.		
(ii) MAGNITUDE OF C	(ii) d.l. CAPACITY.		
(iii) RESIDUAL POTENTIAL.	(iii) 1.28 V		IN THE NON-AQUEOUS CASE, THE RESIDUAL POTENTIAL IS 1.28 WHICH INDICATES THAT THE SOLUTION STILL CONTAINS TRACES OF H_2O AND THAT THE VALUES OF Q ARE DUE TO A SPECIES ADSORBED ON THE ELECTRODE WHICH ORIGINATES IN WATER - AN INFERENCE SUPPORTED BY THE FACT THAT Q VALUES INCREASE APPRECIABLY IN THE AQUEOUS SYSTEM (AS SHOWN BY THE FORCED DECAYS IN 3 BELOW).
(iv) FORCED DECAY FROM RESIDUAL POTENTIAL? (a) VALUES OF $C_{max.}$ AND $V_{C_{max.}}$ (b) VALUES OF Q AND POTENTIALS OF ARRESTS CORRESPONDING TO Q.	(iv) ARRESTS OBSERVED ON FORCED DECAY OF THE RESIDUAL POTENTIAL. (a) $(C_{max.})_1 = 1150 \mu F\ cm^{-2}$ ($V_{C_{max.}} = 0.78$ V) $(C_{max.})_2 = 2050 \mu F\ cm^{-2}$ ($V_{C_{max.}} = 0.44$ V) (b) $Q_{total} = 0.839\ mCcm^{-2}$		
(v) ADDITIONAL FEATURES OR COMMENTS.		(v) OPEN CIRCUIT DECAYS WERE TOO NOISY (PERHAPS DUE TO THICK OXIDE FILM - A BROWNISH DEPOSIT ON THE ELECTRODE COULD EASILY BE SEEN VISUALLY) AND HENCE WERE NOT RECORDED.	

....CONTINUED....

3. FORCED DECAYS			
(i) ARRESTS?	(i) ARRESTS OBSERVED.	(i) ARRESTS OBSERVED.	
(ii) $C_{max.}$ AND $V_{C_{max.}}$ VALUES.	(ii) $C_{max.} \simeq$ 4000 TO 8000 μF cm^{-2} AND $V_{C_{max.}} \simeq$ 0.18 TO 0.88 V DEPENDING ON $i_{cath.}$ USED.	(ii) AT LEAST TWO $C_{max.}$'s OBSERVED WITH VALUES OF CAPACITY RANGING BETWEEN 1950 - 4100 μF cm^{-2} DEPENDING ON i_{cath}; $V_{C_{max.}}$ 1.08 V TO 1.85 V DEPENDING ON $i_{cath.}$	
(iii) EFFECT OF $i_{cath.}$ ON $C_{max.}$ AND $V_{C_{max.}}$	(iii) INCREASING $i_{cath.}$ PUSHES $V_{C_{max.}}$ TO MORE CATHODIC VALUES BUT EFFECT OF $i_{cath.}$ ON $C_{max.}$ ITSELF SHOWS NO REGULAR TREND.	(iii) $V_{C_{max.}}$ - SHIFTS TO MORE CATHODIC VALUES WITH INCREASING $i_{cath.}$ $C_{max.}$ - INCREASES WITH INCREASING $i_{cath.}$	
(iv) PLOT OF $i_{cath.}$ vs. $1/t$, AT A GIVEN V_i; Q FROM THIS PLOT.	(iv) STRAIGHT LINE; $Q_{total} \simeq$ 0.687 mCcm^{-2} UP TO THE MAIN PEAK ($V_{C_{max.}}$ = .180 TO .88 DEPENDING ON $i_{cath.}$ Q_1 = 0.61 mCcm^{-2}; $V_{C_{max.}} \simeq$ 0.88 V; $i_{cath.}$ = 1.197 x 10^{-2} a.cm^{-2} Q_2 = 0.09 mCcm^{-2}; $V_{C_{max.}} \simeq$ 0.30 V	(iv) STRAIGHT LINE; AVERAGE Q_{total} UP TO THE MAIN ARREST IS = 2.5 mCcm^{-2} Q_1 = 1.04 mCcm^{-2} (1.4 V) Q_2 = 1.62 mCcm^{-2} (0.43 V) Q_3 = 0.41 mCcm^{-2} (0.004 V)	Q VALUES INCREASE APPRECIABLY IN AQUEOUS SOLUTION AS COMPARED TO THE NON-AQUEOUS ONE. IT INDICATES THAT THE SPECIES ADSORBED ON THE ELECTRODE ORIGINATE FROM WATER.
(v) PLOT OF Q vs. V_i.	(v) Q INCREASES WITH V_i INITIALLY BUT AT 1.9 V, Q STARTS DECREASING WITH INCREASING V_i.	(v) INITIAL Q INCREASES WITH INCREASING V_i BUT IT DECREASES AT 1.65 V AND STARTS INCREASING AGAIN AT 1.95 V TO VERY HIGH VALUES (e.g., 10 mCcm^{-2} AT 2.55 V; 27 mCcm^{-2} at 2.75 V).	
(vi) ADDITIONAL FEATURES OR COMMENTS.			
4. SWEEP RUNS			
(i) PLOT OF PEAK CURRENT vs. $(dV/dt)^{\frac{1}{2}}$.	ANODIC DISSOLUTION OF GOLD WOULD GIVE DIFFUSION-CONTROLLED CURRENTS; HENCE SWEEP RUNS WERE NOT CARRIED OUT IN THIS SYSTEM.	ANODIC DISSOLUTION OF GOLD WOULD GIVE DIFFUSION-CONTROLLED CURRENTS; HENCE SWEEP RUNS WERE NOT CARRIED OUT IN THIS SYSTEM.	
(ii) DEPENDENCE OF Q ON (dV/dt).			
(iii) IF CHARGING PEAKS, Q VALUES FOR THE PEAKS.			
(iv) $C_{max.}$ AND $V_{C_{max.}}$			
(v) EFFECT OF (dV/dt) ON $C_{max.}$ AND $V_{C_{max.}}$			
(vi) ADDITIONAL FEATURES OR COMMENTS			

these self-discharge curves, are of the order of $C_{d.l.}$. The residual potential is 1.28 V. On cathodic discharge from this residual potential, two arrests are observed which manifest themselves as two capacity maxima in the C-V profiles calculated from these forced decay curves (Fig. 45). The values of $C_{max.}$ and corresponding $V_{C_{max.}}$ are:

$(C_{max.})_1$ = 1150 μF. cm.$^{-2}$; $V_{C_{max.}}$ = 0.78 V

$(C_{max.})_2$ = 2050 μF. cm.$^{-2}$; $V_{C_{max.}}$ = 0.44 V

The value of Q_{total} = 0.84 mC. cm.$^{-2}$.

In the aqueous solutions, open-circuit decay transients were very "noisy", (perhaps due to an oxide film of high resistance; a brownish layer on the electrode could easily be seen visually), and hence were not recorded. Normally the noise level on the transients was $\simeq$ 1 mV.

Forced decay behaviour: In non-aqueous solutions, on driven decay of the potential of an anodically polarised electrode, significant arrests were observed. Very high values of pseudo-capacity were obtained as shown by the C-V profiles for a range of values of $i_{cath.}$ (Fig. 46). The $C_{max.}$ values range between 4000 μF. cm.$^{-2}$ and 8000 μF. cm.$^{-2}$ and $V_{C_{max.}}$ values between 0.18 V and 0.88 V, depending on the magnitude of $i_{cath.}$ used in the cathodic discharge. Increasing $i_{cath.}$ shifts $V_{C_{max.}}$ to more cathodic potentials but the changes

Figure 45

Gold in nominally anhydrous (1M CH_3COOK + 1M CH_3COOH) solution: C *vs.* V plot calculated from the profile obtained on forced discharge from the residual potential.

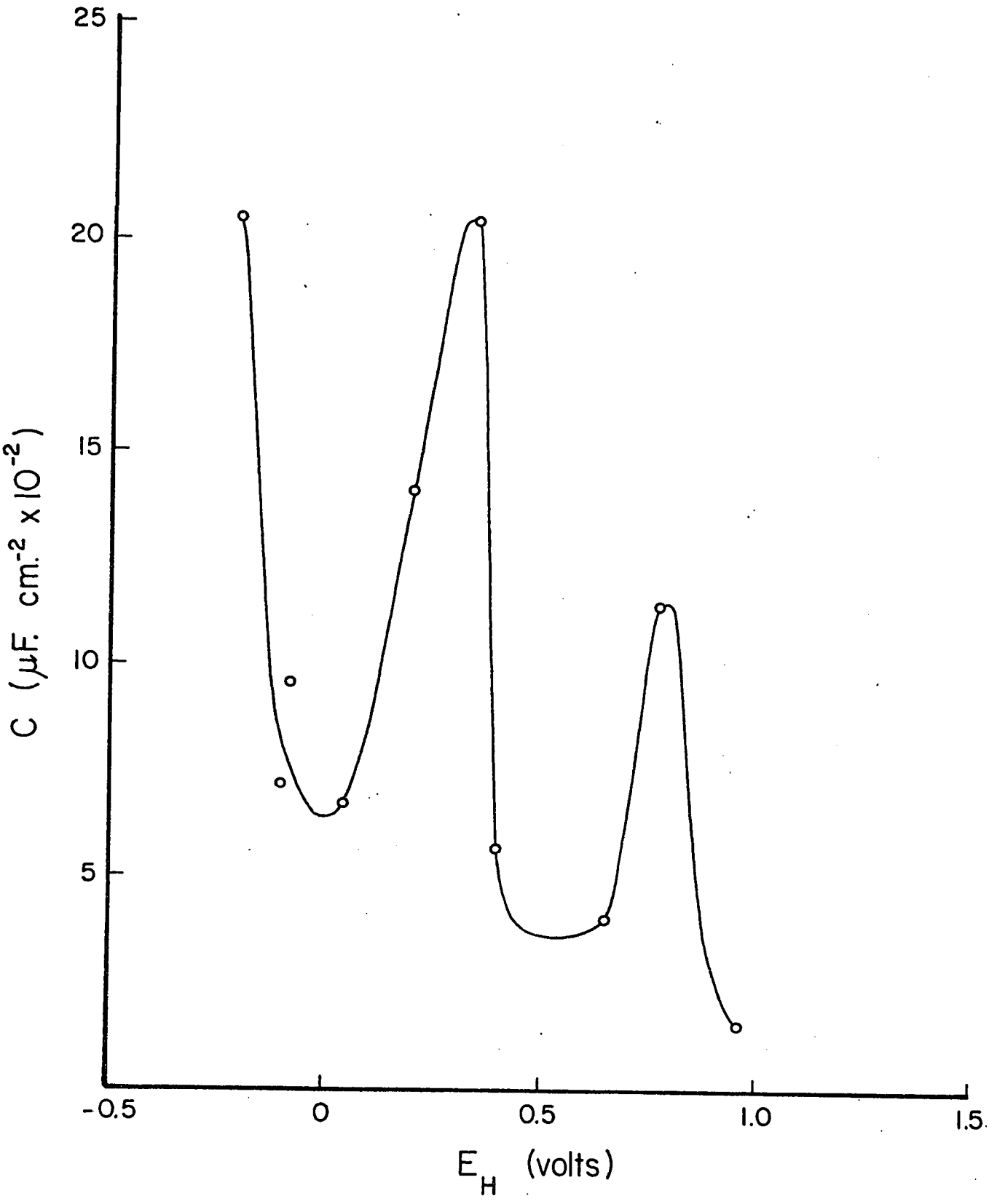
25
20
15
10
5
C (μF. cm.$^{-2}$ x 10^{-2})
-0.5
0
0.5
1.0
1.5
E_H (volts)

Figure 46

Gold/1M CH_3COOK in CH_3COOH: C-V profiles as a function of charging cathodic current density, $i_{cath.}$, for the adsorbed species in the Kolbe oxidation: $i_{cath.}$ (in a. $cm.^{-2}$):

○	1.20×10^{-2};
●	2.32×10^{-2};
▲	3.86×10^{-2};
□	5.41×10^{-2}.

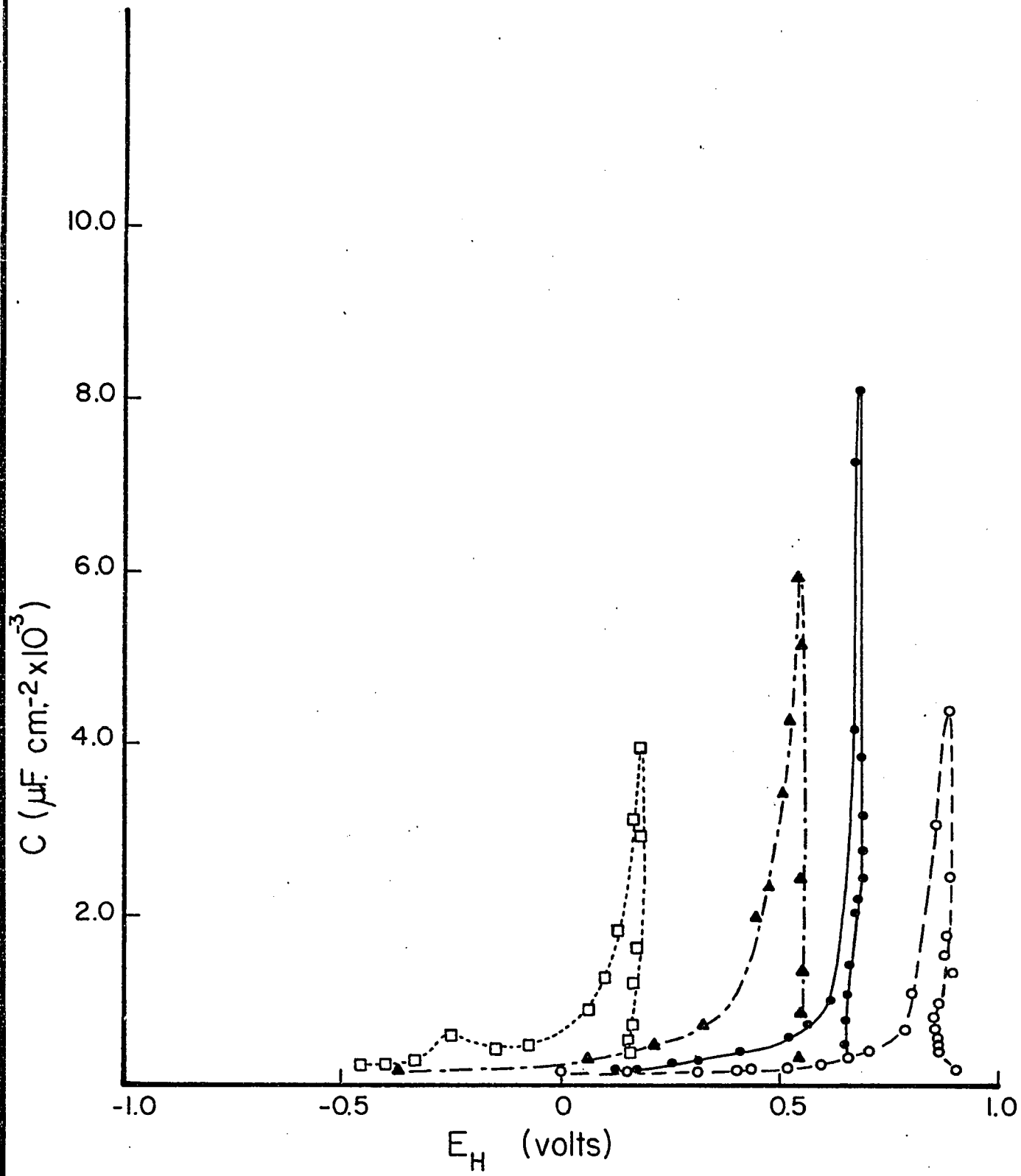
10.0
8.0
6.0
4.0
2.0
C (μF cm-2 x10-3)
-1.0
-0.5
0
0.5
1.0
E_H (volts)

in the $C_{max.}$ values show no regular pattern (Fig. 47).

A plot of $i_{cath.}$ vs. $1/\tau$ (where τ here is the transition time in seconds up to the main $C_{min.}$) gives a straight line and Q_{total} obtained from the slope of this line is 0.687 mC. cm.$^{-2}$ (Fig. 48).

Again the Q_{total} is compound and the individual component arrests correspond to the following charges:

Q_1 = 0.61 mC. cm.$^{-2}$; $V_{C_{max.}}$ = 0.88 V

Q_2 = 0.09 mC. cm.$^{-2}$; $V_{C_{max.}}$ = 0.3 V

Q_{total} = 0.7 mC. cm.$^{-2}$

After establishing, as usual, that Q_{total} was independent of $i_{cath.}$, the dependence of Q on V_i was investigated. It was found that Q increased with increasing V_i initially but at 1.9 V, Q began to decrease with increasing V_i (Fig. 49). In Fig. 49, a photograph of a typical transient is also shown.

In the aqueous solutions, the cathodic transients exhibited very large arrests. In the C-V profiles, computed from the differentiated forced decay curves, at least two capacity maxima can be detected with values ranging from 1950 μF. cm.$^{-2}$ to 4100 μF. cm.$^{-2}$, depending on the magnitude of $i_{cath.}$ used in the transient (Fig. 50). Values of $V_{C_{max.}}$

Figure 47

Gold/1M CH_3COOK in CH_3COOH:

- ● plot of $C_{max.}$ vs. $i_{cath.}$;
- ○ plot of $V_{C_{max.}}$ vs. $i_{cath.}$.

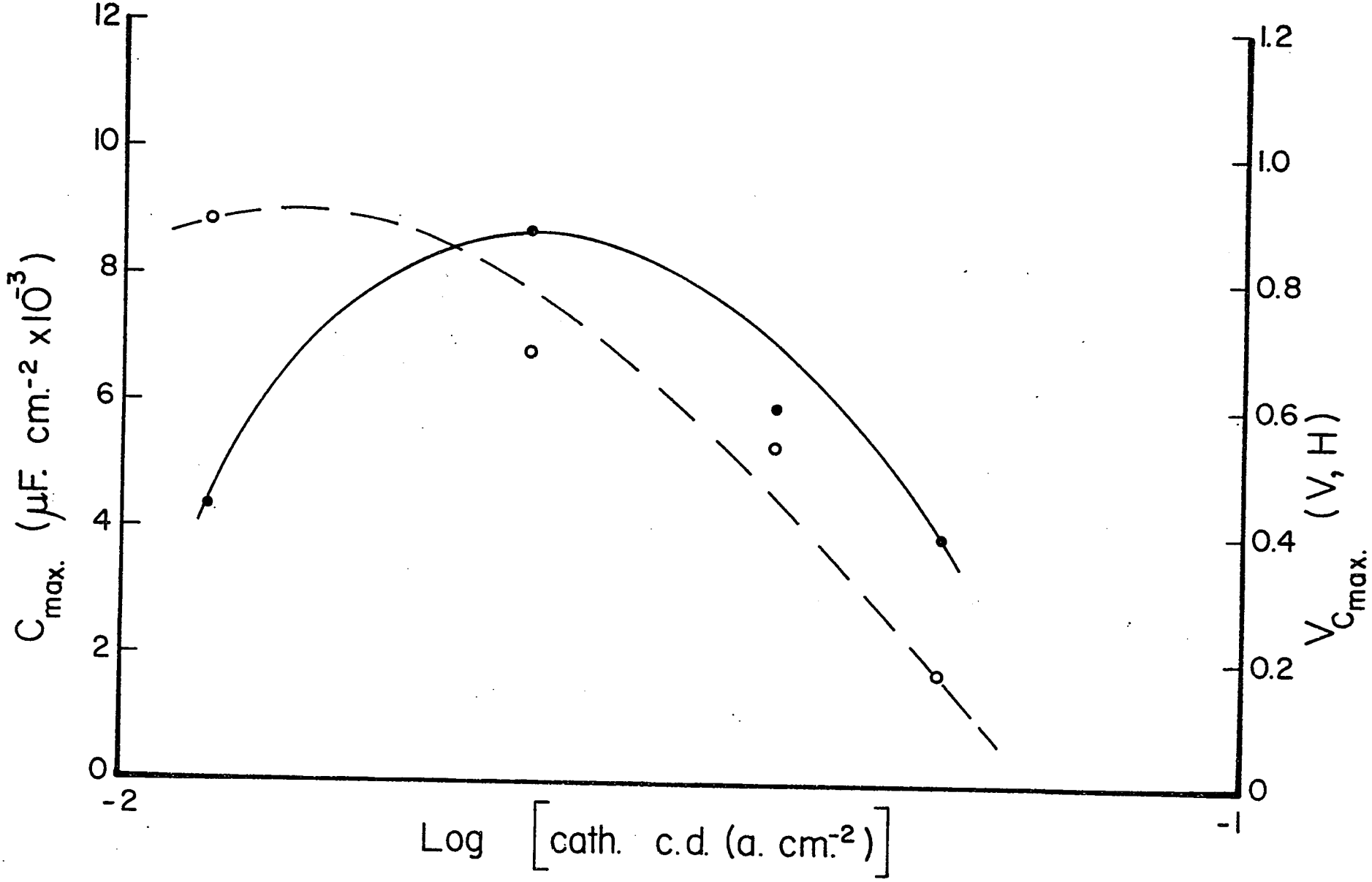
12
10
8
6
4
2
0
-2
-1
1.2
1.0
0.8
0.6
0.4
0.2
0
$C_{max.}$ (μF. cm.$^{-2}$ x10^{-3})
$V_{C_{max.}}$ (V, H)
Log [cath. c.d. (a. cm.$^{-2}$)]

Figure 48

Gold in nominally anhydrous 1M CH_3COOK in CH_3COOH solution: a plot of $i_{cath.}$ vs. $1/\tau$.

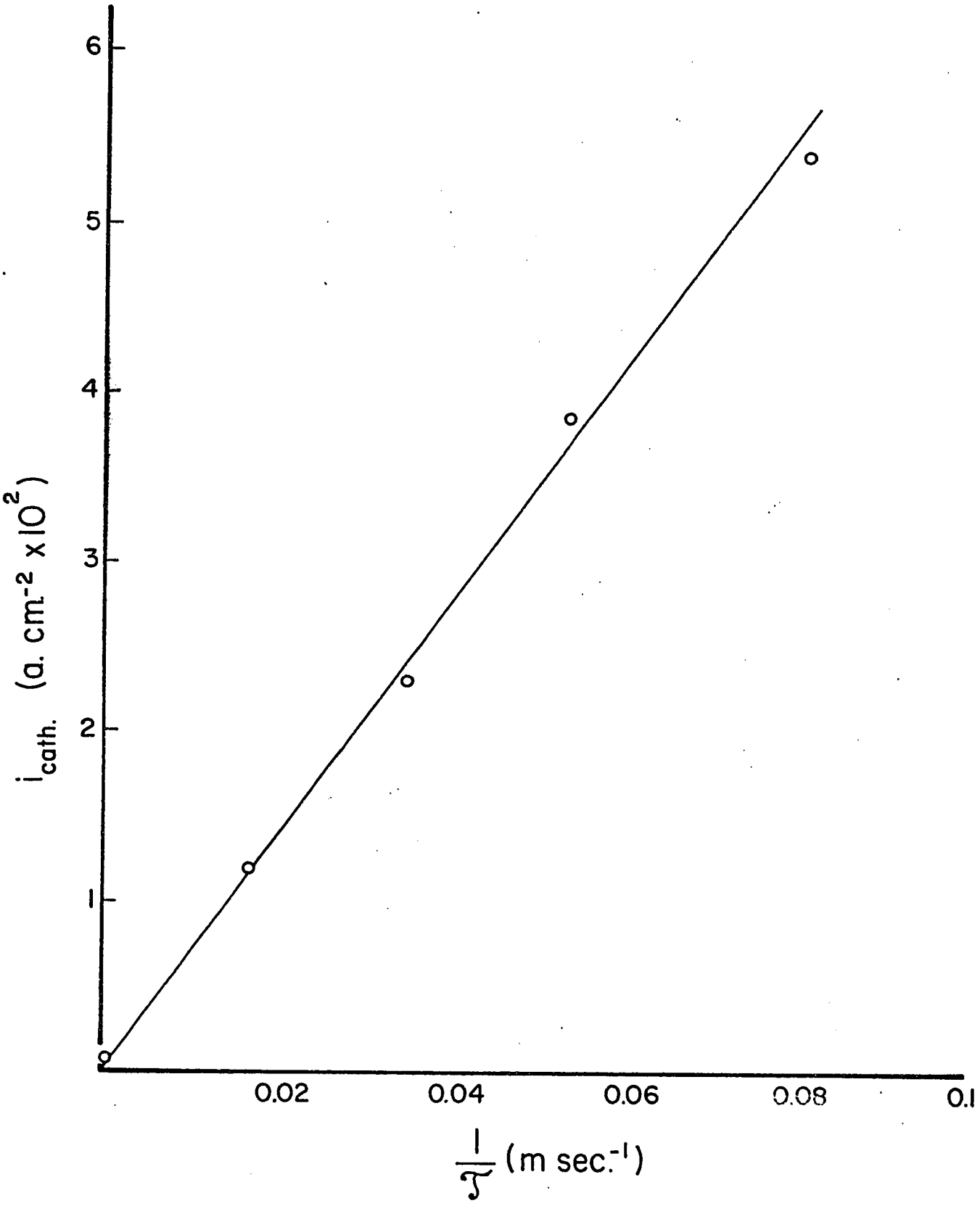
6
5
4
3
2
1
$i_{cath.}$ (a. $cm^{-2} \times 10^2$)
0.02
0.04
0.06
0.08
0.1
$\frac{1}{\tau}$ (m $sec.^{-1}$)

Figure 49

Gold in nominally anhydrous (1M CH_3COOK in CH_3COOH) solution: a plot of Q vs. E_1.

Au in (1M CH_3COOK in CH_3COOH)

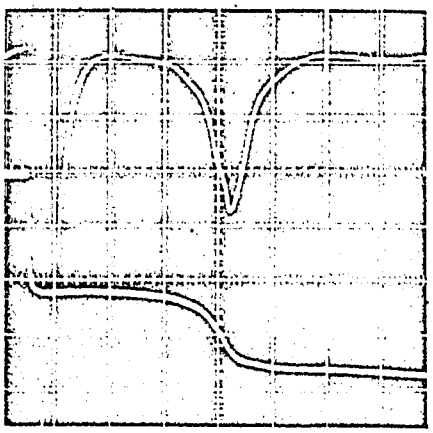

5 msec. $cm.^{-1}$
3.86×10^{-2} a. $cm.^{-2}$

Figure 50

Gold in aqueous (1M CH_3COOK + CH_3COOH) solution: C-V profiles as a function of charging cathodic current density, $i_{cath.}$, for the adsorbed species in the Kolbe oxidation: $i_{cath.}$ (in a. $cm.^{-2}$):

- o 3.82×10^{-2};
- ● 10.70×10^{-2};
- ▲ 21.65×10^{-2};
- □ 46.69×10^{-2}.

Note: merging of peaks at higher c.d.'s.

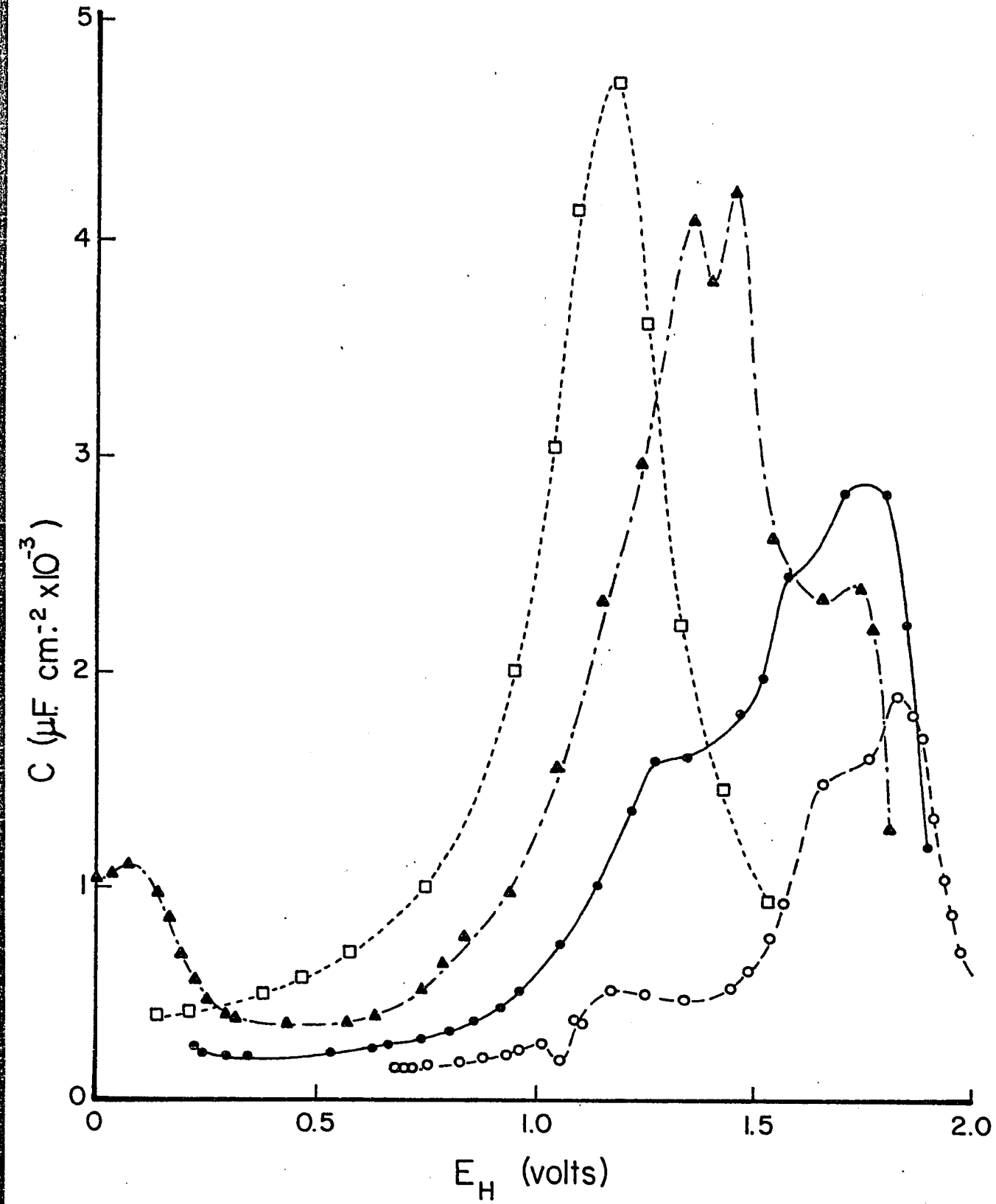
5
4
3
2
1
0
0
0.5
1.0
1.5
2.0
C (μF cm.-2 x10-3)
EH (volts)

also depend on $i_{cath.}$ and range between 1.08 V to 1.85 V. Increasing $i_{cath.}$ shifts $C_{max.}$ to higher values and $V_{C_{max.}}$ to more cathodic potentials (Fig. 51). On plotting $i_{cath.}$ vs. $1/\tau$ (τ here is the time in seconds to the end of the main arrest), a straight line is obtained, the slope of which gives an average value of $Q_{total} = 2.5$ mC. cm.$^{-2}$ corresponding to the τ used in the plot (Fig. 52).

The Q_{total} is again compound and the two component values are as follows:

$$Q_1 = 1.04 \text{ mC. cm.}^{-2}; \quad V_{C_{max.}} = 1.4 \text{ V.}$$

$$Q_2 = 1.52 \text{ mC. cm.}^{-2}; \quad V_{C_{max.}} = 0.43 \text{ V.}$$

$$Q_{total} = 2.64 \text{ mC. cm.}^{-2},$$

which is fairly close to the average value of Q_{total} (2.5 mC. cm.$^{-2}$) found from the plot of $i_{cath.}$ vs. $1/\tau$.

At certain values of $i_{cath.}$ used, a third small arrest can be observed around 0.004 V and Q_3 for this arrest is equal to 0.41 mC. cm.$^{-2}$.

After concluding, as above, that Q_{total} was independent of $i_{cath.}$ (Fig. 52), the dependence of Q_{total} on the initial polarisation potential, V_i, was examined. It was found that at low V_i values Q increases with increasing V_i; at 1.65 V, Q decreases with increasing V_i but it begins to increase again at 1.95 V and continues increasing to very high values with

Figure 51

Gold in aqueous (1M CH_3COOK + 1M CH_3COOH) solution:

- ● plot of $C_{max.}$ vs. $i_{cath.}$;
- o plot of $V_{C_{max.}}$ vs. $i_{cath.}$.

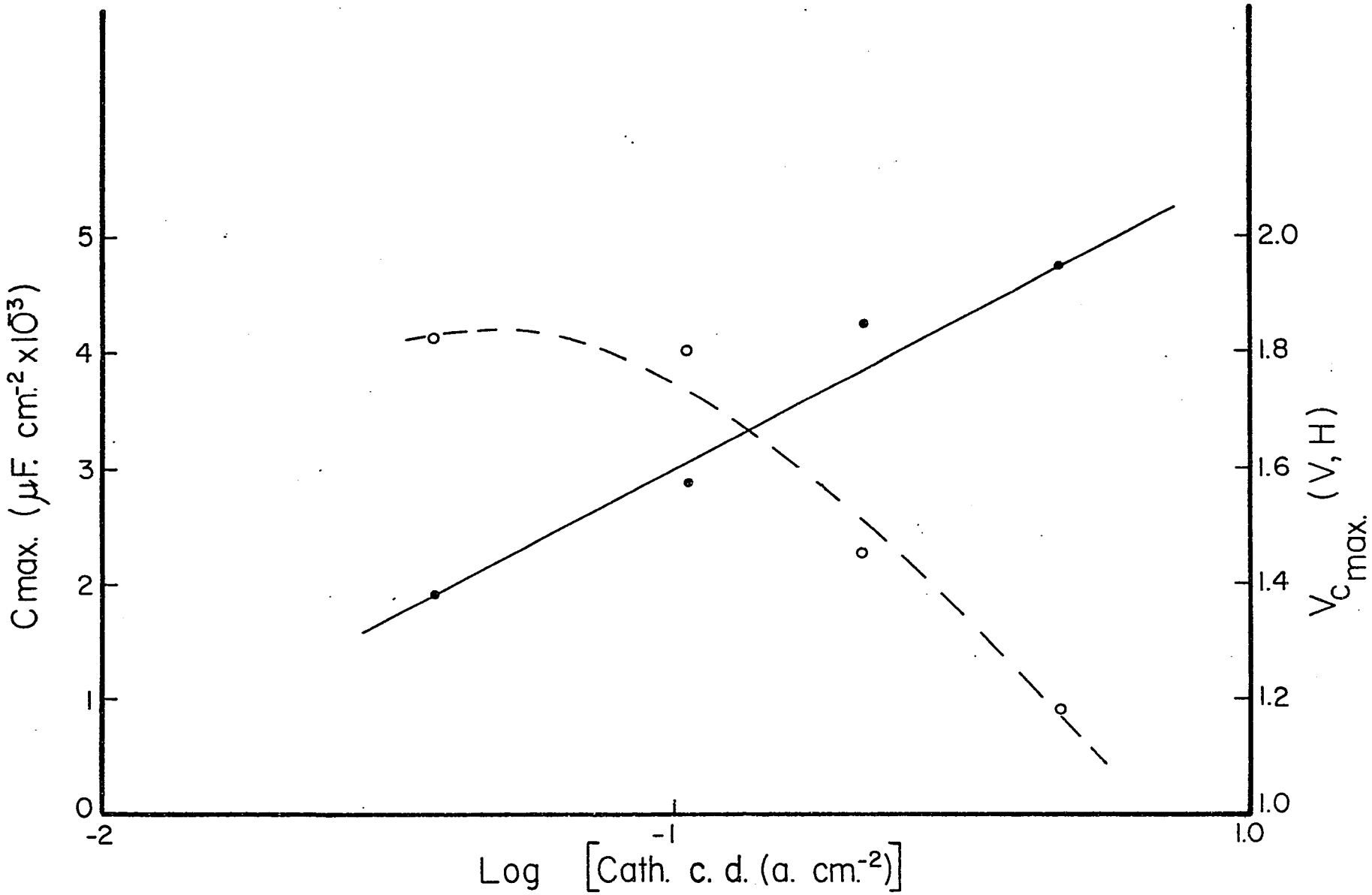
Cmax. (μF. cm.$^{-2}$ x10^{3})
0
1
2
3
4
5
-2
-1
1.0
Log [Cath. c. d. (a. cm.$^{-2}$)]
1.0
1.2
1.4
1.6
1.8
2.0
$V_{C\,max.}$ (V, H)

Figure 52

Gold in aqueous (1M CH_3COOK + 1M CH_3COOH) solution: plots of $i_{cath.}$ vs. $1/\tau$ (o) and $i_{cath.}$ vs. $1/\tau^{\frac{1}{2}}$ (•).

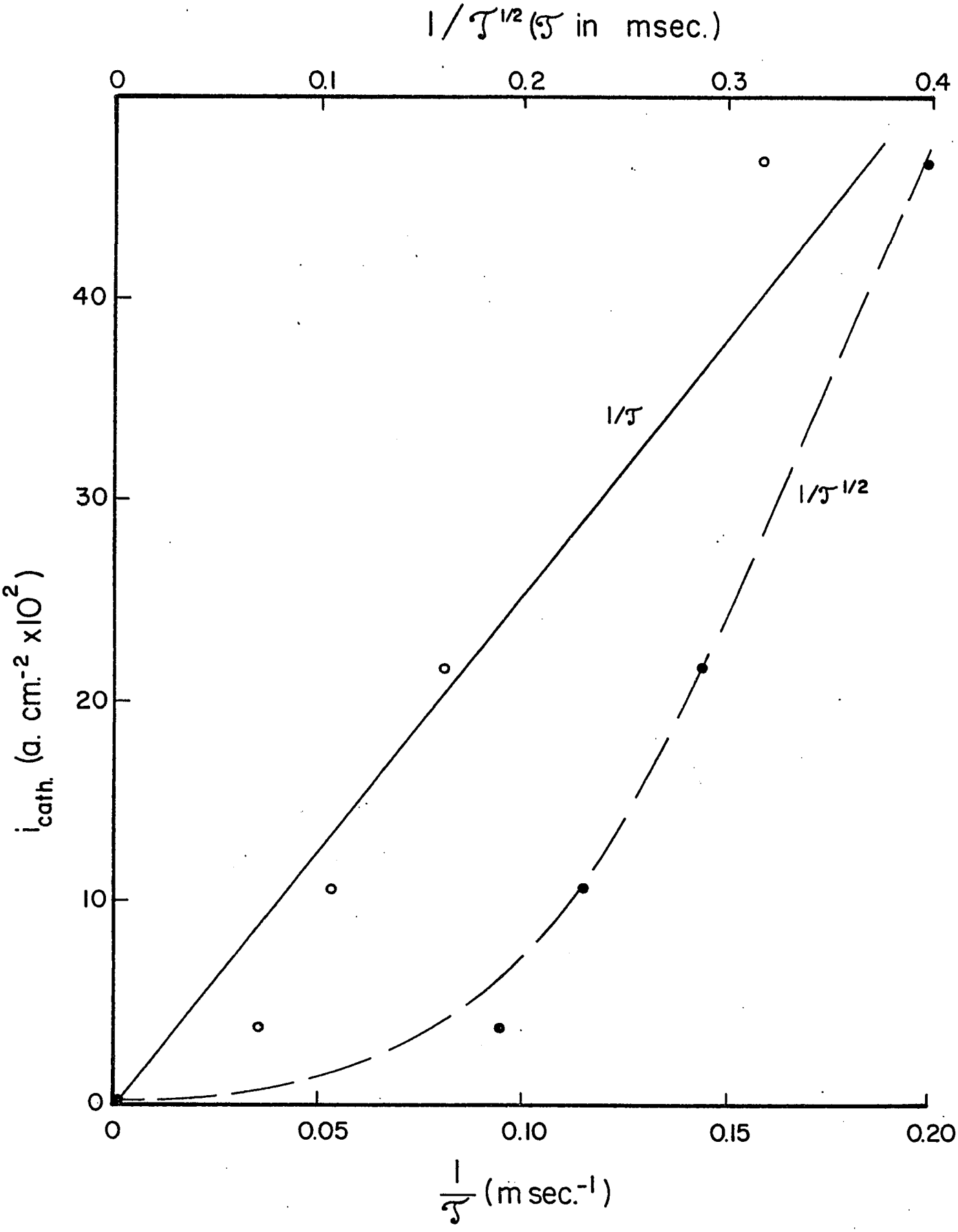
$1/\tau^{1/2}$ (τ in msec.)
0
0.1
0.2
0.3
0.4
40
30
20
10
0
$1/\tau$
$1/\tau^{1/2}$
$i_{cath.}$ (a. cm.$^{-2}$ x10^{2})
0
0.05
0.10
0.15
0.20
$\frac{1}{\tau}$ (m sec.$^{-1}$)

increasing V_1, e.g., 8.4 mC. cm.$^{-2}$ at 2.55 V (Fig. 53), indicating probably the build up of a substantially thick oxide film having more or less "bulk" properties (cf. section 2(ii) b in this Chapter). In Fig. 53, a photograph of a typical transient is also shown.

3. POTENTIODYNAMIC CURRENT-POTENTIAL PROFILES

(i) General

Potentiodynamic measurements (or "sweep" runs) were carried out in order to obtain machine-programmed curves analogous to manually-obtained current-potential relations. The important distinction between the two types of measurements, it may be recalled, is that potentiodynamic i-V relations are obtained under conditions where neither a steady-state nor a steady current exists, whereas the manual i-V relations usually correspond to a "practical" steady-state. Hence potentiodynamic measurements yield experimental results which require more complex kinetic analysis and are only complementary to the steady-state i-V relations obtained manually.

(ii) Experimental Difficulties - An Analysis

In a potentiodynamic run, the aim is to obtain a i-V relation in which charging peaks associated with adsorption and desorption of intermediates on the electrode can be observed in a well-resolved and reproducible manner. In several cases, these peaks are not true charging peaks, i.e., the peak currents are not true charging currents. In these

Figure 53

Gold in aqueous (1M CH_3COOK + 1M CH_3COOH) solution: a plot of Q *vs.* E_1.

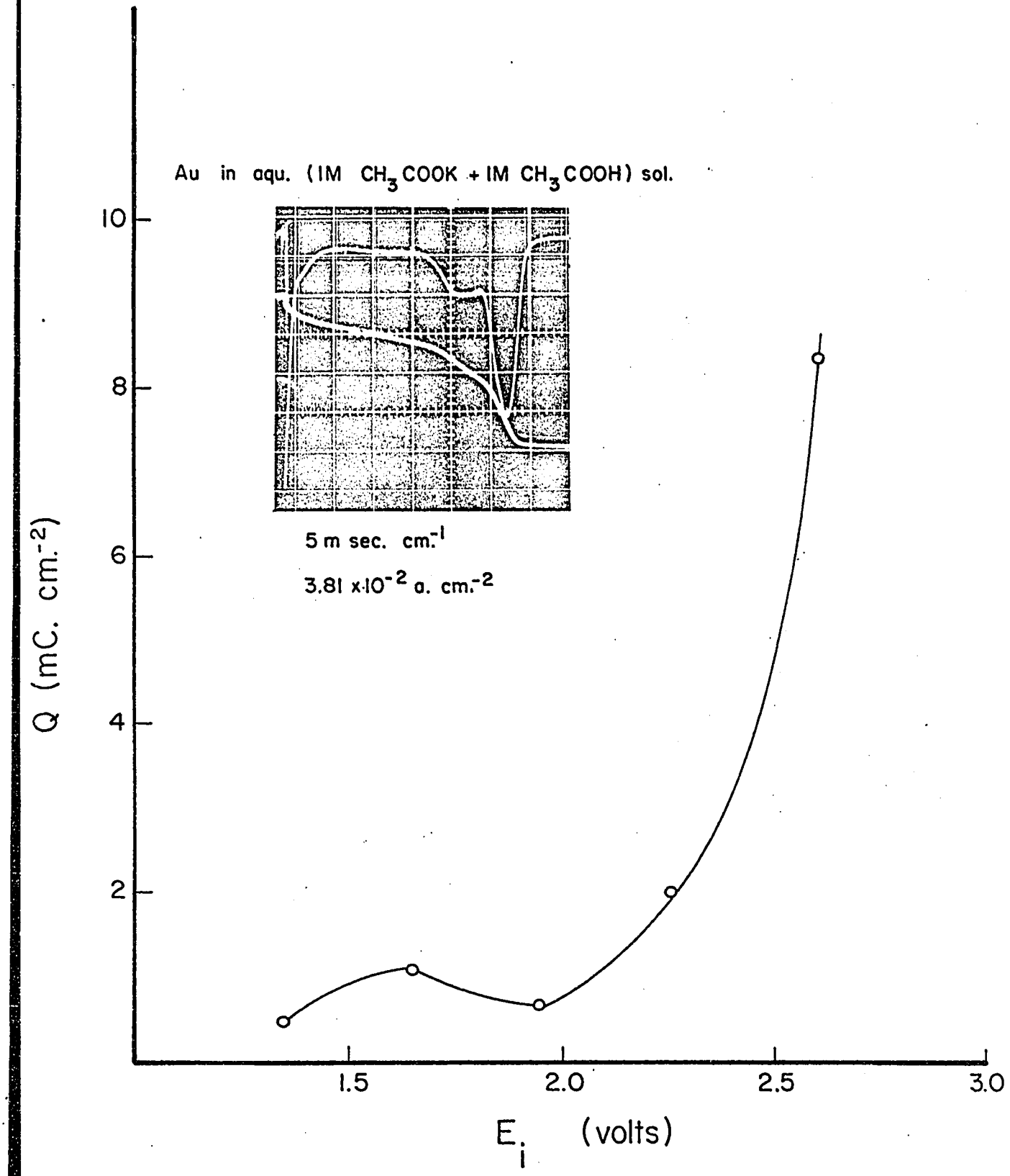
Au in aqu. (1M CH3COOK + 1M CH3COOH) sol.
5 m sec. cm.-1
3.81 x10-2 a. cm.-2
Q (mC. cm.-2)
10
8
6
4
2
1.5
2.0
2.5
3.0
Ei (volts)

cases, the peak currents are composite and arise from contributions from Faradaic processes for the overall reaction and a pseudo-Faradaic process of surface oxidation (cf. p16).

In certain other cases, charging peaks corresponding to two different pseudo-Faradaic processes can merge into each other, completely or partially, and create difficulties in the interpretation of the peaks. This is particularly important at high values of dV/dt where potentials of $C_{max.}$ of the peaks can become drastically displaced.

In the presentation of results in this section, special care has been taken in identifying true charging peaks and separating them from any Faradaic reaction peaks. This has been accomplished by making certain test plots which are discussed at appropriate places in this section.

(iii) Experimental Potentiodynamic Current-Potential Profiles

An experimental current-potential profile under ideal conditions (i.e., when well-defined true charging peaks appear) tends to resemble the schematic profile shown in Fig. 1. Potentiodynamic profiles were examined in all types of solutions studied in the present investigation, both on gold and platinum. True charging peaks were observed only in the case of platinum in aqueous (1M CH_3COOK + 1M CH_3COOH) solution. In all other

cases, the peaks were associated with composite currents. Gold electrodes in the three types of solutions investigated gave peaks which were due to diffusion-controlled currents associated, perhaps, with anodic dissolution of gold.

(a) Platinum in Potassium Trifluoroacetate-Trifluoroacetic Acid Solutions

The results obtained in this case are summarised in Table II, section 4. In completely anhydrous solutions, no peaks are observed. A hysteresis is obtained and capacities associated with this hysteresis are of the order of $C_{d.l.}$.

In nominally anhydrous solutions containing, presumably, traces of water, significant peaks are observed. When a plot of peak current density vs. $(dV/dt)^{\frac{1}{2}}$ is examined, a straight line is not obtained indicating that the peaks are not associated with diffusion controlled currents (Fig. 54). This conclusion is emphasised by the fact that a straight line is obtained when log (dV/dt) is plotted against peak current density (Fig. 54). These results are thus also consistent with the transition times discussed above for this case. A further test was applied to ascertain whether the peaks observed were true charging peaks. The charge Q for the main peak was calculated as a function of dV/dt. The results obtained are summarised below.

Figure 54

Platinum in nominally anhydrous 1M KTFA in TFA solution; plots of peak current vs. $(dV/dt)^{\frac{1}{2}}$ (o) and peak current vs. log (dV/dt) (□), for anodic peak only.

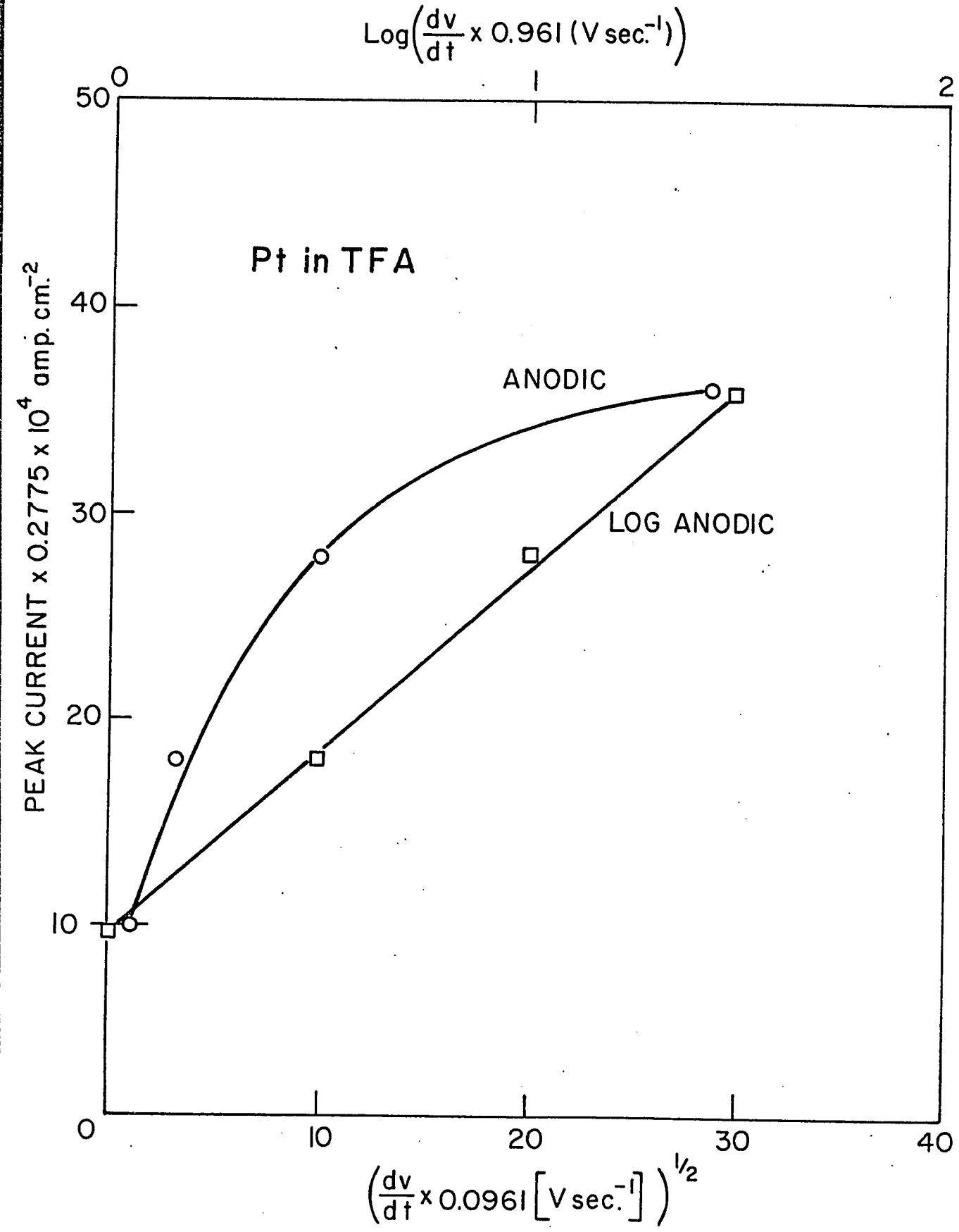
Log(dv/dt x 0.961 (V sec.⁻¹))
0
1
2
50
40
30
20
10
0
Pt in TFA
ANODIC
LOG ANODIC
PEAK CURRENT x 0.2775 x 10⁴ amp. cm.⁻²
10
20
30
40
(dv/dt x 0.0961 [V sec.⁻¹])^1/2

dV/dt (V sec.$^{-1}$)	Q (mC. cm.$^{-2}$)
1.04	1.92
10.4	0.50
104.0	0.152

It is seen that Q depends significantly on dV/dt thus showing that the peaks are associated with composite currents and are not in fact simple charging peaks. Hence the Q and C values obtained from these peaks are difficult to use for interpretation of the charging processes that may be involved in the Kolbe electrosynthesis.

In solutions to which an excess of water (30% by volume, 1M CF_3COOK solution in water) was deliberately added, both anodic and cathodic peaks can be observed. A plot of peak current density vs. $(dV/dt)^{\frac{1}{2}}$ (Fig. 55) shows that the cathodic peak is clearly diffusion controlled but no conclusions can be drawn about the anodic peak from this plot. When the apparent charge Q under the anodic peak is calculated as a function of dV/dt, the following results are obtained.

dV/dt (V sec.$^{-1}$)	Q (mC. cm.$^{-2}$)
0.155	1.67
0.618	1.12
1.545	0.56

It is seen that Q depends appreciably on dV/dt thus showing that the currents associated with the anodic peak are

Figure 55

Platinum in 1M KTFA in TFA (+water) solution: plots of peak current vs. $(dV/dt)^{\frac{1}{2}}$, both for anodic (o) and cathodic peaks (Δ).

Note: The fact that the cathodic line indicates diffusion control is anomalous; however, this behaviour may arise from a diffusion controlled reduction of a trace by-product formed in the anodic cycles of the repetitive sweep.

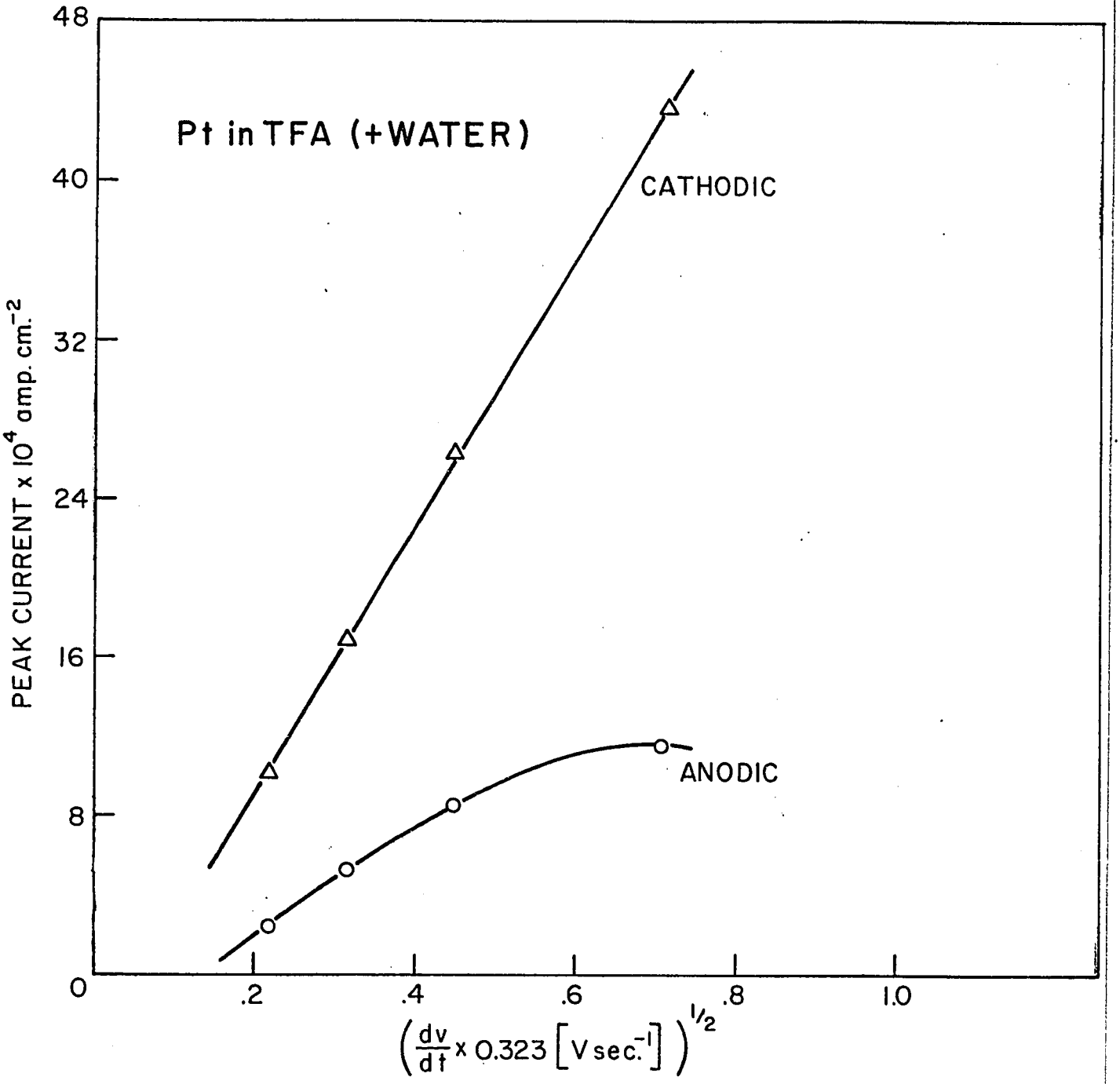
Pt in TFA (+WATER)
CATHODIC
ANODIC
PEAK CURRENT x 10^4 amp. cm.^-2
48
40
32
24
16
8
0
.2
.4
.6
.8
1.0
(dv/dt x 0.323 [V sec.^-1])^1/2

not simply charging currents and hence C and Q values calculated from this peak have no quantitative significance for interpretations in terms of intermediates adsorbed on the electrode.

(b) Gold in Potassium Trifluoroacetate-Trifluoroacetic Acid Solutions

Experimental results for this case are summarised in Table III, section 4.

In completely anhydrous solutions, both anodic and cathodic peaks are found to be diffusion controlled as shown by the straight lines obtained when the peak current density is plotted vs. $(dV/dt)^{\frac{1}{2}}$ for each of the two peaks (Fig. 56).

In nominally anhydrous solutions containing, presumably traces of water, only an anodic peak is observed while the cathodic peak is not well-defined. On plotting the peak current density against $(dV/dt)^{\frac{1}{2}}$ for this peak, a straight line is obtained thus indicating that the peak currents are diffusion controlled (Fig. 57).

In solutions containing excess of water, both anodic and cathodic peaks are found to be diffusion controlled (Fig. 58). These effects are believed to be due to dissolution and redeposition of Au ions under the cycling conditions where a protective oxide film does not have an opportunity to be formed under steady d.c. field growth conditions.

Figure 56

Gold in very anhydrous 1M KTFA in TFA solution: plots of peak current vs. $(dV/dt)^{\frac{1}{2}}$, both for anodic (o) and cathodic peaks (Δ).

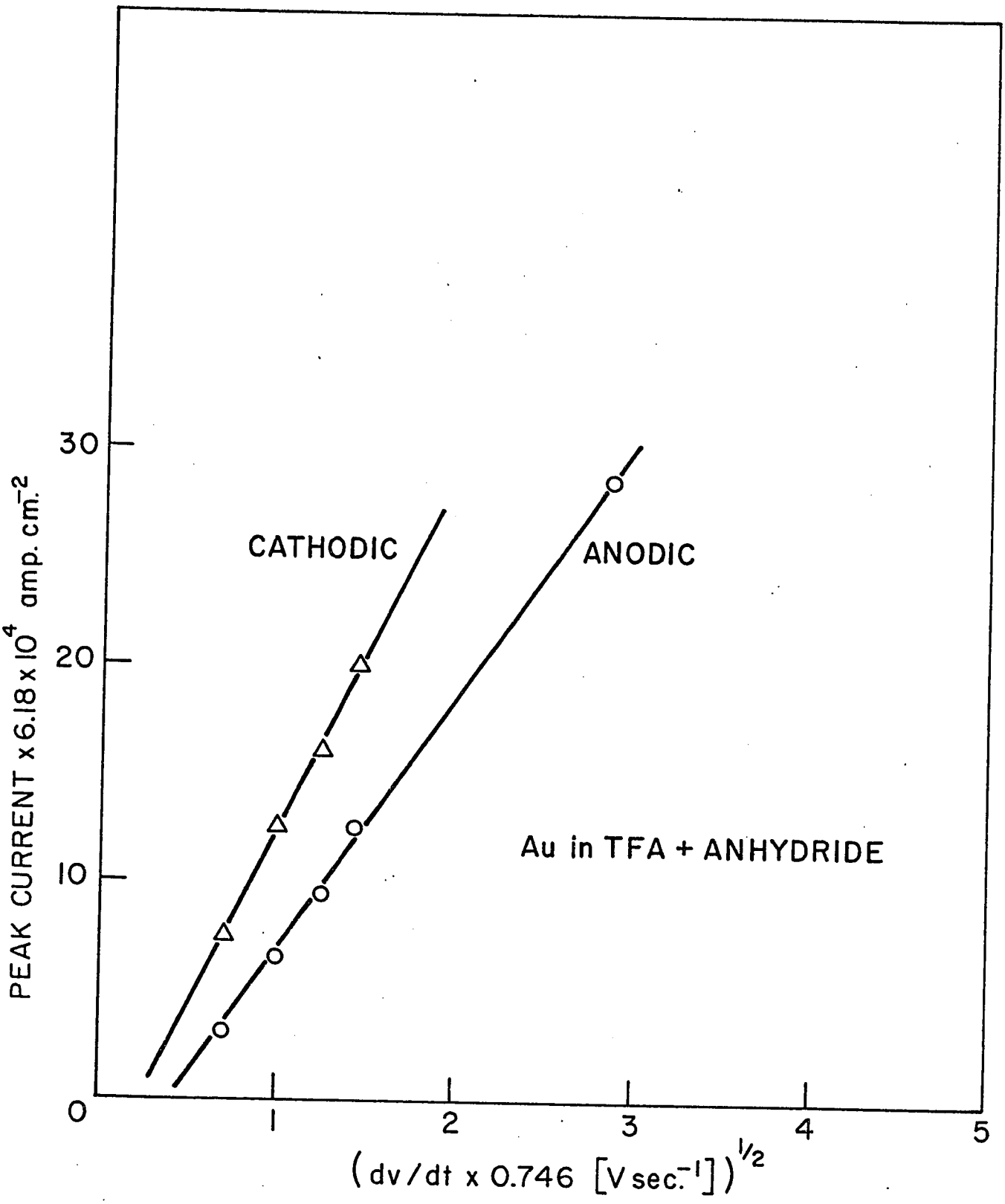
PEAK CURRENT x 6.18 x 10^4 amp. cm^-2
30
20
10
0
CATHODIC
ANODIC
Au in TFA + ANHYDRIDE
1
2
3
4
5
(dv/dt x 0.746 [V sec.^-1])^1/2

Figure 57

Gold in nominally anhydrous 1M KTFA in TFA solution: a plot of peak current vs. $(dV/dt)^{\frac{1}{2}}$ for the anodic peak.

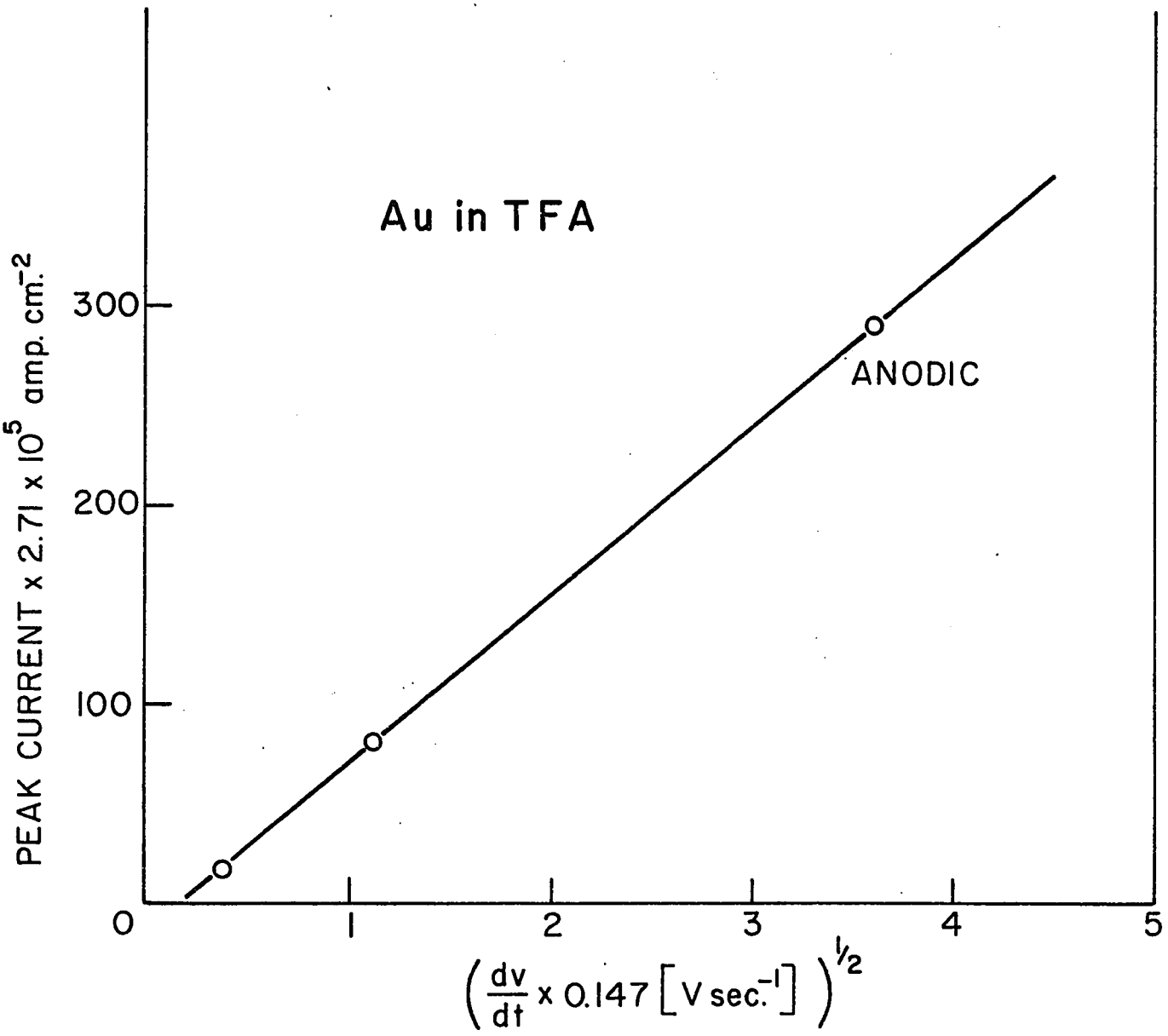
Au in TFA
ANODIC
PEAK CURRENT x 2.71 x 10^5 amp. cm.^-2
300
200
100
0
1
2
3
4
5
(dv/dt x 0.147 [V sec.^-1])^1/2

Figure 58

Gold in 1M KTFA in TFA (+ water) solution: peak current vs. $(dV/dt)^{\frac{1}{2}}$ plots, both for anodic (o) and cathodic (Δ) peaks.

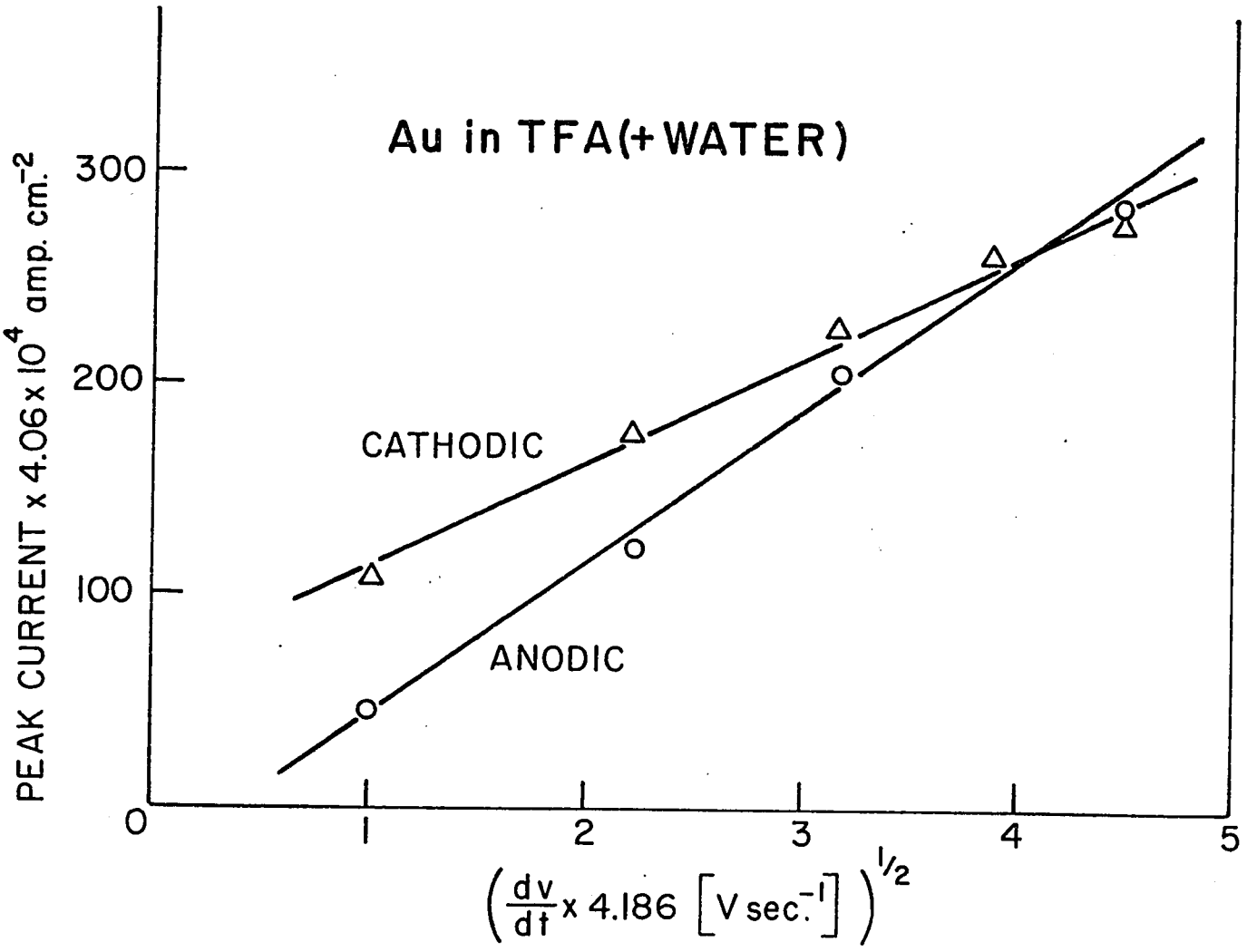
Au in TFA(+WATER)
PEAK CURRENT x 4.06 x 10^4 amp. cm.^-2
300
200
100
0
CATHODIC
ANODIC
1
2
3
4
5
(dv/dt x 4.186 [V sec.^-1])^1/2

(c) Platinum in Potassium Acetate-Acetic Acid Solutions

Potentiodynamic i-V relations were examined both in completely non-aqueous (under "vacuum") solutions and in aqueous solutions. The results obtained are summarised in Table IV, section 4.

In the non-aqueous solutions, no peaks are observed; only hysteresis is exhibited. The plot of "peak" current (measured at the centre of the hysteresis region) vs. $(dV/dt)^{\frac{1}{2}}$ gives a straight line (Fig. 59). Capacity values, calculated at the point of maximum hysteresis, are of the order of $C_{d.l.}$ at all sweep rates.

In the aqueous solutions, well defined anodic and cathodic peaks are observed. When peak current density is plotted against $(dV/dt)^{\frac{1}{2}}$, no straight line is obtained thus indicating that the peaks are not due to diffusion-controlled currents. A plot of peak current density vs. $(dV/dt)^{\frac{1}{2}}$ for the largest peak is shown in Fig. 60. The charge Q under a particular peak was calculated as a function of dV/dt and it was found that Q depended only slightly on dV/dt for each one of the peaks observed. This shows that for all practical purposes, the peaks obtained in this case can be treated as true charging peaks.

Figure 59

Platinum in very anhydrous ("vacuum") 1M CH_3COOK in CH_3COOH solution: a plot of "peak" current (calculated at the point of maximum hysteresis) against $(dV/dt)^{\frac{1}{2}}$.

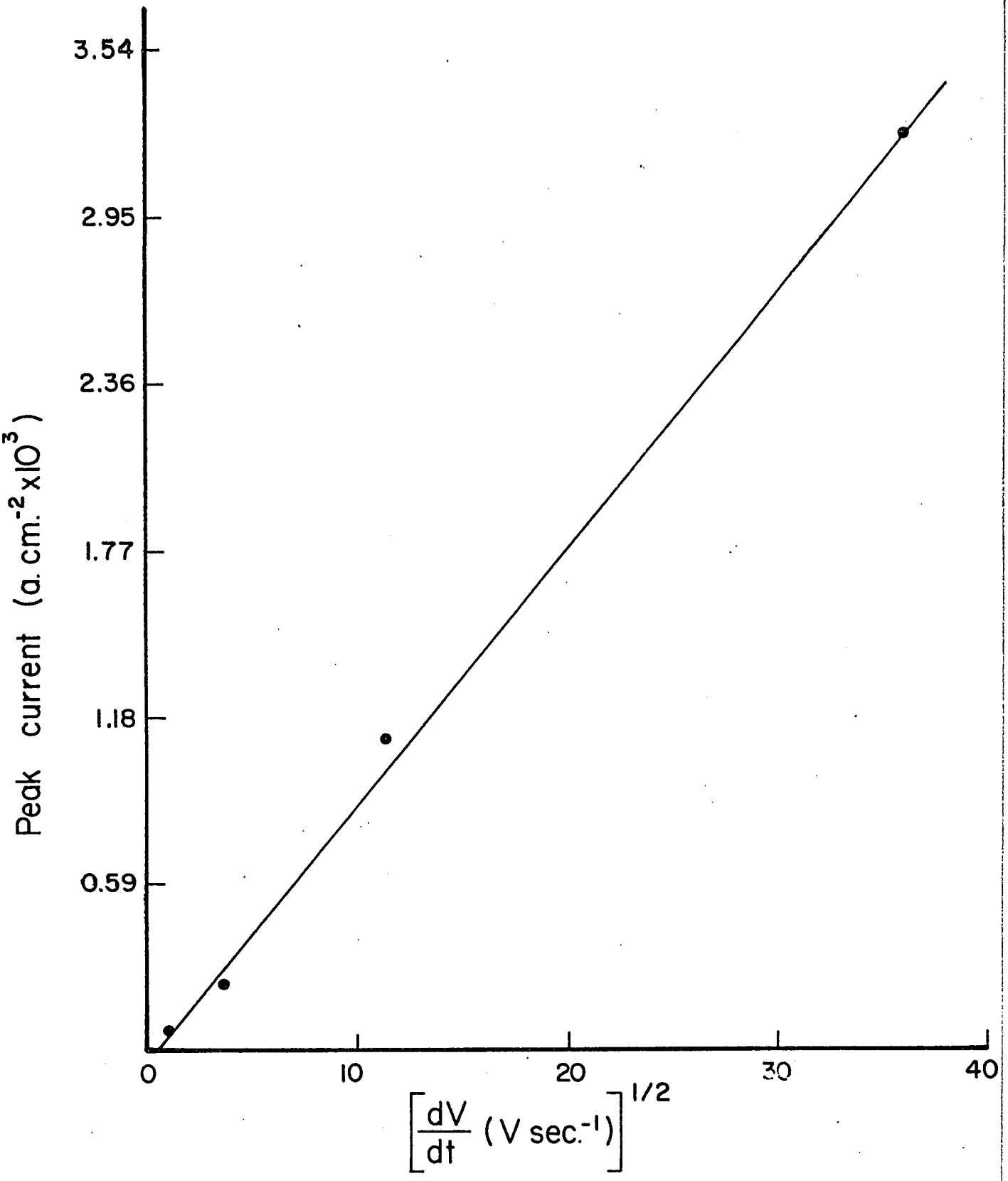
3.54
2.95
2.36
1.77
1.18
0.59
Peak current (a.cm.$^{-2}$x10^{3})
0
10
20
30
40
$\left[\frac{dV}{dt}\ (V\ sec.^{-1})\right]^{1/2}$

Figure 60

Platinum in aqueous (1M CH_3COOK + 1M CH_3COOH) solution: a plot of peak current against $(dV/dt)^{\frac{1}{2}}$.

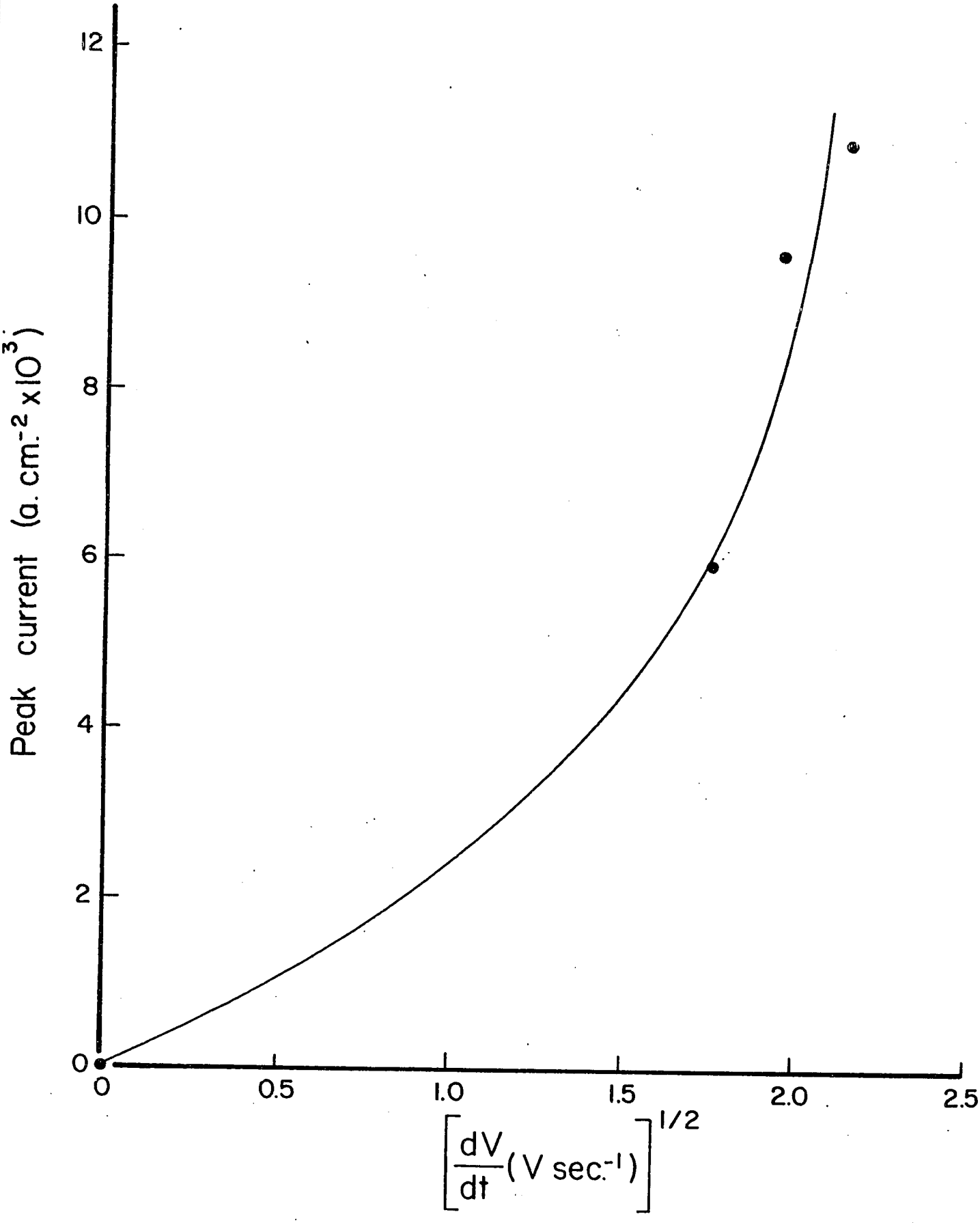
12
10
8
6
4
2
0
Peak current (a. cm.$^{-2}$ x10^{3})
0
0.5
1.0
1.5
2.0
2.5
$\left[\frac{dV}{dt}(V\ sec.^{-1})\right]^{1/2}$

The general shape of the profile is similar to that shown schematically in Fig. 1 for Pt in H_2SO_4 solutions. The peaks obtained, and the potentials at which the peaks appear, are similar to those observed at Pt in H_2SO_4. In Fig. 61, potentiodynamic i-V profiles obtained on Pt in aqueous acetate solutions at three sweep rates are shown; also for the purpose of comparison, a potentiodynamic i-V profile for Pt in H_2SO_4 (63) at a comparable value of (dV/dt) is also shown in this figure. The i-V profiles in Fig. 61 are the ones obtained by scanning the electrode potentiodynamically between -0.03 V and +1.86 V; it is to be noted that the potential region in which a Faradaic Kolbe reaction occurs ($>$ ca. 2.1 V) has purposely not been scanned. Potentiodynamic profiles for the potential range -0.06 V to +2.6 V, i.e., a range which also covers the potentials over which the Kolbe reaction is known to occur, are shown in Fig. 62 for several sweep rates. The peaks, and the potentials at which the peaks appear, are identical in Fig. 61 and Fig. 62. The only difference between the curves in the two figures is that the ones in Fig. 62 are over a potential range in which overall Faradaic processes occur and exhibit kinetic hysteresis in the potential region 2.0 V to 2.6 V.

The behaviour in Fig. 61, in which peaks for Pt in potassium acetate and sulphuric acid solutions are compared,

Figure 61

Potentiodynamic profiles: "Kolbe region"
(> 2.1 V) not scanned:

(———) Pt/aq. (1M CH_3COOK + 1M CH_3COOH) solution: 4.54 V sec^{-1};

(------) Pt/aq. (1M CH_3COOK + 1M CH_3COOH) solution: 3.78 V $sec.^{-1}$;

(—·—·—) Pt/aq. (1M CH_3COOK + 1M CH_3COOH) solution: 3.02 V $sec.^{-1}$;

(—··—··—) Pt/1M H_2SO_4: 3.6 V $sec.^{-1}$.

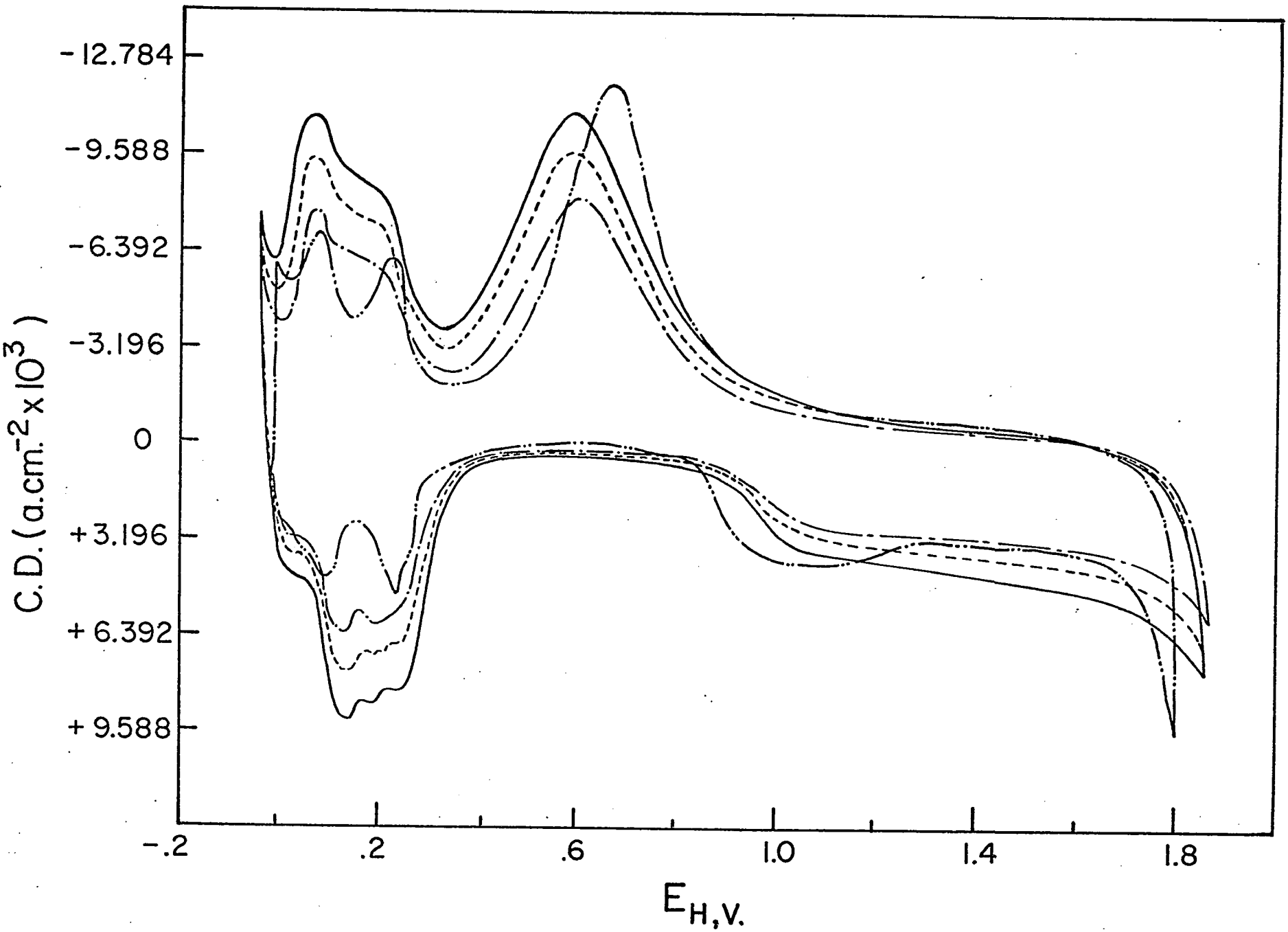
-12.784
-9.588
-6.392
-3.196
0
+3.196
+6.392
+9.588
C.D. (a.cm.$^{-2}$ x 10^{3})
-.2
.2
.6
1.0
1.4
1.8
$E_{H,V.}$

Figure 62

Potentiodynamic profiles: "Kolbe region" (> 2.1 V) scanned: Pt/aq. (1M CH_3COOK + 1M CH_3COOH), solution:

(———) 1.06 V $sec.^{-1}$;

(- - - -) 0.80 V $sec.^{-1}$;

(—.—.) 0.53 V $sec.^{-1}$.

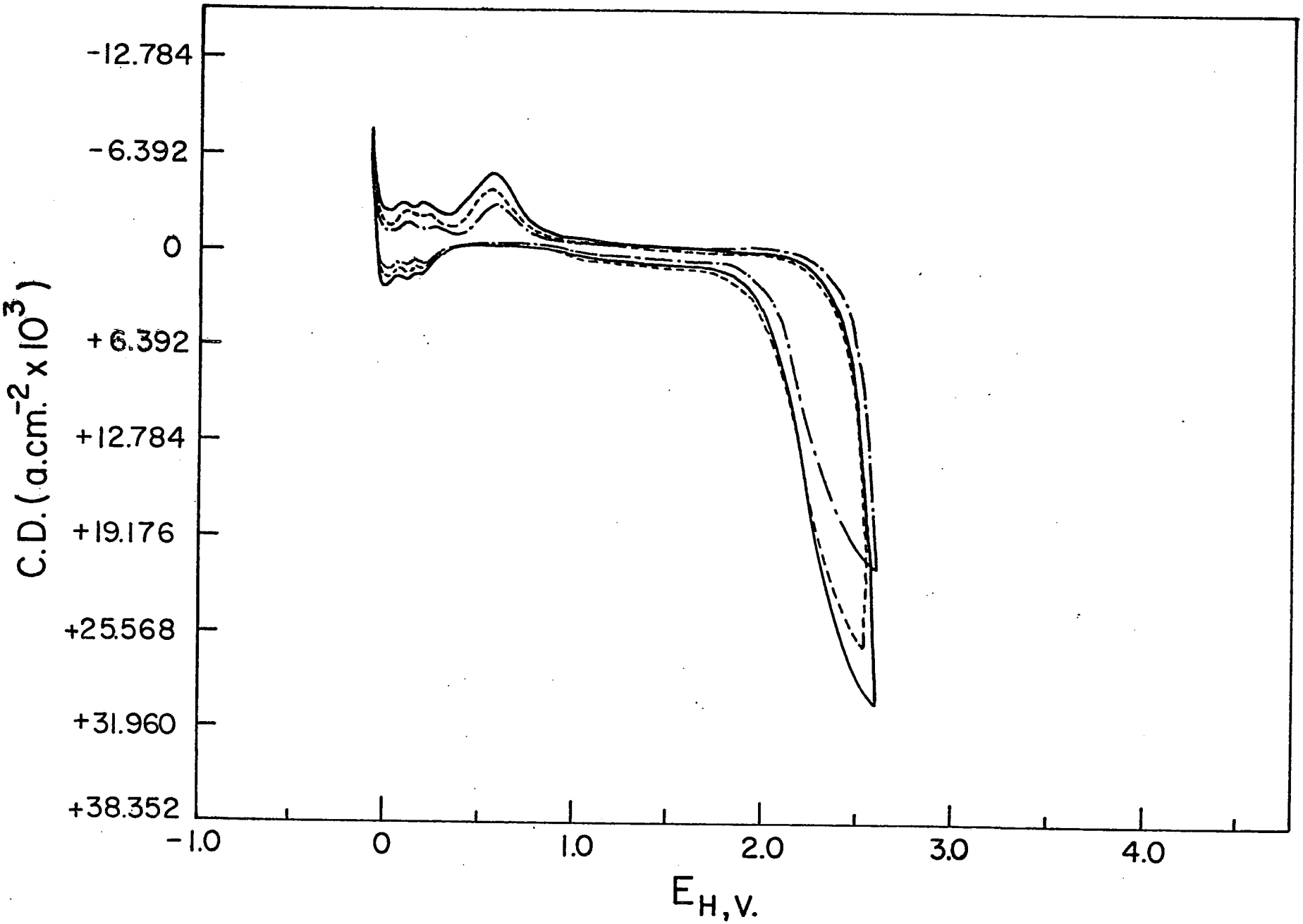
-12.784
-6.392
0
+6.392
+12.784
+19.176
+25.568
+31.960
+38.352
C.D. (a.cm.$^{-2}$ x 10^{3})
-1.0
0
1.0
2.0
3.0
4.0
$E_{H,V.}$

strongly suggests that the peaks for Pt in acetate solutions are "modified" peaks for oxygen and hydrogen deposition and desorption processes.

The ratios $\frac{\text{oxide reduction charge, } (Q_A)}{\text{hydrogen deposition charge, } (Q_B)}$ for the various cases studied are as follows:

Table VI

Case	Potential range	dV/dt (V sec.$^{-1}$)	$\frac{Q_A}{Q_B}$
Pt in aq. CH_3COOK	-0.03 V to 1.86 V	3.78	1.566
Pt in aq. CH_3COOK	-0.06 to 2.6 V	3.78	1.514
Pt in H_2SO_4	0.0 to 1.8 V	3.60	2.428

It is seen that the ratio of Q_A/Q_B for platinum in aqueous CH_3COOK solution is the same for the same value of dV/dt and is independent of whether the Faradaic Kolbe region is scanned or not. However, the ratio Q_A/Q_B for platinum in H_2SO_4 solution is substantially higher (by 58%) than that for Pt in acetate solutions.

The ratio Q_A/Q_B for potassium acetate solution as obtained from cathodic transients is 1.85 (V_1 = 2.5 V). It is gratifying that this value of Q_A/Q_B is identical with the value obtained potentiodynamically in potassium acetate solution at a sweep rate of dV/dt = 0.73 V sec.$^{-1}$.

The values of the pseudo-capacity maxima are summarised in Table VII.

The value of $C_{max.}$ for the oxide reduction peak in the case of Pt in H_2SO_4 is 4802 μF. cm.$^{-2}$ which is almost twice the value of $C_{max.}$ for the oxide reduction peak obtained for Pt in CH_3COOK solution at comparable dV/dt values (ca. 3.6 V sec.$^{-1}$). The $C_{max.}$ value for hydrogen deposition peaks is 2933 μF. cm.$^{-2}$ for Pt in H_2SO_4 as compared with 2494 μF. cm.$^{-2}$ for Pt in aq. CH_3COOK solution for a comparable value of dV/dt (ca. 3.6 V sec.$^{-1}$). These data show that the $C_{max.}$ value for the oxide reduction peak at Pt in H_2SO_4 is almost twice the value for Pt in aq. CH_3COOK solution. However, the $C_{max.}$ value for hydrogen deposition peaks in the two cases are of comparable magnitude for the same range of potentials scanned and for similar sweep rates.

It is interesting to examine the dependence of $C_{max.}$ and $V_{C_{max.}}$ for the peaks on dV/dt. It is found that with increasing dV/dt values, the cathodic peaks are shifted somewhat to more cathodic potentials and anodic peaks to slightly more anodic potentials (Fig. 61). When a potential range of only -0.03 V to 1.86 V is scanned, an increase of dV/dt shifts $C_{max.}$ to slightly lower values (Table VII). However, for the potential range -0.06 V to 2.6 V an increase of dV/dt shifts $C_{max.}$ to appreciably lower values.

In Fig. 63, photographs of some of the experimentally-obtained potentiodynamic profiles are presented.

Table VII

Values of $C_{max.}$ and Q calculated for various peaks observed in potentiodynamic profiles:

(A) platinum in (1M CH_3COOK + 1M CH_3COOH) in water;

(B) platinum in 1M H_2SO_4 solution.

Table VII

(A) Platinum in (1M CH_3COOK + 1M CH_3COOH) in Water

V range scanned	dV/dt ($V\ sec.^{-1}$)	$C_{max.}$ ($\mu F.\ cm.^{-2}$)		Q ($mC.\ cm.^{-2}$)		
		Oxide reduction peak	H deposition peak	Oxide reduction	H deposition	$\frac{Q_{oxide\ reduction}}{Q_{H\ deposition}}$
-0.03 V to 1.86 V	3.024	2647	2536	0.94	0.55	1.69
"	3.78	2537	2494	0.84	0.54	1.57
"	4.536	2400	2378	0.80	0.52	1.54
-0.06 V to 2.6 V	0.532	5406	3304	1.53	0.86	1.79
"	0.798	4806	2803	1.26	0.74	1.71
"	1.064	3003	2928	1.3	0.79	1.67

(B) Platinum in 1M H_2SO_4 solution

0.0 V to 1.8 V	3.6	4802	2933	1.59	0.65	2.42

Figure 63

Some experimentally-obtained potentiodynamic profiles:

(i) $dV/dt = 3.6$ V sec.$^{-1}$;

(ii) $dV/dt = 3.78$ V sec.$^{-1}$;

(iii) $dV/dt = 0.80$ V sec.$^{-1}$.

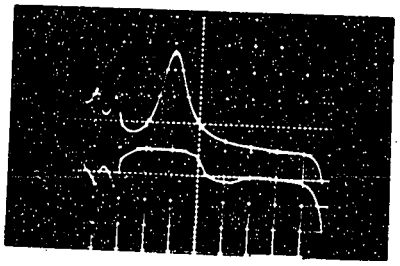

(i) Pt in IM H_2SO_4 (0.0V — 1.8V)

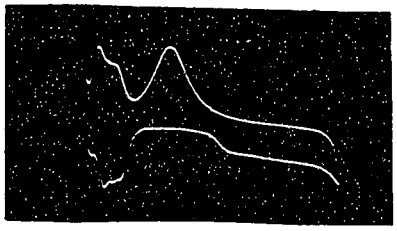

(ii) Pt in aqu. (IM CH_3COOK + IM CH_3COOH) (-0.03V — 1.86V)

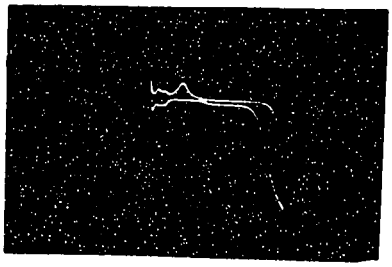

(iii) Pt in aqu. (IM CH_3COOK + IM CH_3COOH) (-0.06V — 2.6V)

(d) Gold in Potassium Acetate-Acetic Acid Solutions

Anodic dissolution of gold could be visually observed both in aqueous as well as in non-aqueous solutions. Potentiodynamic studies were not carried out in this case since anodic dissolution of gold would lead to complex currents as in the case of gold in potassium trifluoroacetate-trifluoroacetic acid solutions (Table III, Section 4) discussed previously. Again the cyclic treatment presumably prevents the onset of passivation which requires a steady anodic current for anodic barrier-layer film formation.

CHAPTER IV

DISCUSSION

1. GENERAL

(1) Introduction

The aims of the present investigation have been to provide new information which may assist elucidation of the mechanism(s) of the Kolbe reaction by treating it from the point of view of a heterogeneous catalysed electrochemical reaction. The emphasis in the present work has been to examine quantitatively schemes of consecutive elementary processes that might be involved in the overall two-electron Kolbe reaction. This approach necessarily requires a thorough study of the behaviour of intermediates that might be adsorbed on the electrode, and involves examination of the electrode coverage and potential-dependence of the coverage of the electrode by such intermediates.

Earlier attempts at elucidation of the mechanism of this reaction involved rather empirical conclusions based on the techniques and principles of organic chemistry supplemented by an analysis of the products of electrolysis (7-10, 12, 13, 17, 19-27). However, some studies on the Kolbe reaction from the point of view of relating the above types of observation to the basic electrochemical kinetics of the reaction have been reported only recently (2,3). However, both these

investigations (2,3) were carried out under conditions of controlled-current polarisation. In the present investigation, controlled-potential techniques (both potentiostatic and potentiodynamic) have been employed and are to be preferred to galvanostatic techniques for reasons discussed in Chapter I, section 3. Also, the role of surface oxides that might be co-adsorbed on the electrode with the Kolbe ad-species when traces or excess of water are present in the solutions, has been examined systematically in the present work in relation to the kinetics of the overall Kolbe process. In short, modern electrochemical approaches and quantitative ideas of electrode kinetics have been brought to bear on the problem of the mechanism of the Kolbe reaction.

In the second part of this section 1, some elementary thermodynamic aspects of this reaction have been examined. In section 2 of this chapter, a discussion of some interpretations of the various quantities and plots presented in Chapter III is presented and some correlations between the predictions of electrode-kinetic theory and the relevant experimentally-accessible parameters are proposed.

In section 3 of this chapter, mechanisms for the Kolbe reaction both at Pt and Au in various solutions, are proposed. These mechanistic proposals are based on the ideas to be developed in section 2 of this chapter.

(ii) Thermodynamic Considerations and the Kinetic Behaviour at the Reversible Potentials

Before examining the detailed kinetics of an electrode process, it is useful to know something about its thermodynamic behaviour. More specifically, it is important to establish, when possible, if the standard reversible potential E^{o} for the overall reaction of interest lies within the range of potentials usually accessible in the laboratory. Thus, the E^{o} has been calculated for the Kolbe reaction in potassium acetate solutions; relevant thermodynamic data for evaluation of E^{o} for the Kolbe reaction in potassium trifluoroacetate solutions is, unfortunately, not available in the literature.

The standard reversible potential (on the hydrogen scale) for the overall Kolbe reaction in aqueous potassium acetate solutions may be calculated as follows:

The overall reaction is:

$$2\,CH_3COO^- + 2H^+ \rightleftharpoons C_2H_6 + 2CO_2 + H_2 \qquad (a)$$

and may be regarded as consisting of the two elementary reactions:

$$2CH_3COOH \rightleftharpoons C_2H_6 + 2CO_2 + H_2 \qquad (b)$$

and

$$2CH_3COO^- + 2H^+ \rightleftharpoons 2CH_3COOH \qquad (c)$$

$$\overline{2CH_3COO^- + 2H^+ \rightleftharpoons C_2H_6 + 2CO_2 + H_2} \qquad (a)$$

From Tables (64), the following data may be obtained for the standard free energies of formation ΔG_f° of the species involved:

ΔG_f° $(2CO_2)$ = -94.25 x 2 = -188.50 kcals.

ΔG_f° (C_2H_6) = -7.8 kcals.

ΔG_f° $(2CH_3COOH)$ = -187.6* kcals.

Also the pK_A for the reaction $CH_3COOH \overset{K_A}{\rightleftharpoons} H^+ + CH_3COO^-$ is equal to 4.756 and writing

$$\Delta G_A^\circ = -RT\ln K_A$$

$$= 1.98 \times 298 \times 2.303 \times 4.756$$

$$= 6.46 \text{ kcal. mole}^{-1}.$$

From the above data, the following quantities may then be obtained:

ΔG° for reaction (b) = -8.72 kcals.

ΔG° for reaction (c) = -12.92 kcals.

so that

ΔG° for reaction (a) = -21.64 kcals.

---

*The figure used here actually refers to the ΔG_f° for formation of $2CH_3COOH$ liq., no figure being given for the standard state aqueous solution. However, from the known heat of formation (64) in aqueous solution (undissociated state), we conclude that the ΔG_f° for formation in aqueous solution would not differ from the value quoted by more than ca. 0.3 kcal. mole^{-1}.

With the well known relation

$$\Delta G^{\circ} = -zFE_H^{\circ} \quad \text{or} \quad E_H^{\circ} = -\Delta G^{\circ}/zF$$

and calculating the E_H° for the half-cell reaction $2e + CO_2 + C_2H_6 \rightleftharpoons 2CH_3COO^-$ on the hydrogen scale, we then obtain

$$E_H^{\circ} \doteq \frac{-21,644 \times 4,182 \times 1000}{2 \times 96487} = \underline{-0,469 \text{ V}}$$

so that the standard reversible potential for the Kolbe reaction in aqueous potassium acetate solutions = $\underline{-0,469 \text{ V}}$ (Stockholm Convention).

This value of E_H° shows that the Kolbe reaction in acetate solutions should tend to proceed within the range of potentials easily attainable in the laboratory. However, in practice the Kolbe reaction does not begin to proceed at an appreciable rate (ca. 5×10^{-4} a.cm.$^{-2}$) until potentials of ca. 2.2 V are attained, so that a large overpotential is normally involved. Even though the relevant data for calculation of the reversible potential for the Kolbe reaction in potassium trifluoroacetate solutions are not available, it seems reasonable to assume that E_H° for the reaction in this solution is not very different from the E_H° for the analogous reaction in potassium acetate solution. Thus, the potential at which the Kolbe reaction in potassium trifluoroacetate solutions begins to proceed at appreciable rates is found to be quite

close to that for the reaction in potassium acetate solutions. Also, on general chemical grounds, the standard free energy for the reaction of type (a) but with CF_3COO^-, would not tend to be very different from that for CH_3COO^- since only C-C bonds are broken and re-formed in the reaction. The presence of the 3F atoms will have, however, secondary inductive effects, particularly in the pK_A value so that ΔG° for reaction (c) will tend to be sevenal kcal. $mole^{-1}$ less negative.

It is important to emphasize that the E_H° for the overall reaction:

$$2CH_3COO^- + 2H^+ \rightleftharpoons C_2H_6 + 2CO_2 + H_2,$$

is the same at all anodes. However, the values of the exchange current density, i_o, may differ substantially at various types of anode for normal kinetic reasons. For a series of metal anodes, this i_o value may be different because it is indirectly related to the work function, ϕ, for a given metal. The dependence of energy of adsorption of a particular adsorbed intermediate on the work function ϕ for the adsorbent metal can give rise to different i_o values for a series of different metals [cf. the case for hydrogen evolution and adsorption]. Thus, coverage effects determine, in part [65,66], the rates of electrode processes at the reversible potential. The same considerations also apply to the rates

of electrode processes at potentials further removed from the reversible potential. This concept is one of importance in considering the different rates of the Kolbe reaction (or any other electrode reaction for that matter) at a given over-potential for a series of metal electrodes studied under otherwise identical conditions. In previous studies of organic electrode processes, the relevance of these rather fundamental factors in determining the influence of anode material on the rate of the reaction has not usually been considered.

The E_H^o value for reaction (a) in non-aqueous medium (pure CH_3COOH as solvent) will differ from that calculated through the difference of ionization constant of acetic acid in water and in itself as solvent, but the actual value of the reversible potential against the hydrogen electrode in the same solution, where a_{H^+} is determined by the ionization equilibrium, is identical with the value in aqueous solution.

2. SIGNIFICANCE OF THE EXPERIMENTAL DATA IN RELATION TO THEORIES OF ELECTRODE PROCESSES

In this section, some of the main principles of interpretation of the experimental data (presented in Chapter III) are first discussed.

(i) Kinetic Analysis of the Steady-State Current-Potential Relations

The Tafel slopes, b, obtained from the current-potential relations have been used as diagnostic criteria for mechanisms of electrode reactions for many years. In some of the earlier studies on the Kolbe reaction (7-10, 12, 13, 17, 19-27) and even in more recent ones (11, 14, 60), current-potential relations were reported without discussion of their kinetic significance. Dickinson and Wynne-Jones (3) were the first authors to discuss current-potential relations in terms of electrochemical kinetic parameters, e.g. the b values, and in terms of coverage effects in the Kolbe reaction. However, these authors did not discuss the diagnostic significance of b values in proposing a mechanism. Such an attempt was made by Conway and Dzieciuch (2).

Before presenting a sequence of elementary processes that might be involved in the overall Kolbe reaction, certain other features of the steady-state current-potential plots must be noted.

When a current-potential relation is obtained potentiostatically as in the present investigation, a steep rise of potential at a given value of current (i.e., a "transition region") can correspond to either a range of

potentials over which the electrode is being covered by some adsorbed species, or a region of potential where some alternative reactions are proceeding. If a Tafel line is obtained in the post-transition region, it can often be assumed that (cf. 67) an overall Faradaic process which this Tafel line represents is proceeding on an electrode covered by adsorbed intermediates. An hysteresis between the ascending and descending curves of a (potentiostatic) current-potential relation suggests the presence of an irreversibly adsorbed electroactive species. If any rest potential (defined in Chapter III, section 2) is observed, this again can indicate involvement of some adsorbed intermediates.

In general, most electrochemical reactions, except perhaps one-electron ionic redox processes, proceed by at least two consecutive steps. It is unlikely that the Kolbe reaction which involves two ions, decarboxylation, coupling and transfer of two electrons for one act of the overall reaction takes place in one step; it must proceed through a sequence of consecutive elementary processes. A discussion of such a scheme together with its kinetic consequences based on the considerations developed by Conway and Dzieciuch (2,6), is presented below.

In the overall Kolbe reaction

$$2RCOO^- \longrightarrow R\text{-}R + 2CO_2 + 2e, \qquad (A)$$

a sequence of the following consecutive elementary steps* may be envisaged:

$$RCOO^- \rightleftharpoons RCOO\,(M) + e \qquad (B)$$

$$RCOO^{\bullet}\,(M) \longrightarrow R^{\bullet}\,(M) + CO_2 \qquad (C)$$

$$R^{\bullet}(M) + R^{\bullet}\,(M) \longrightarrow R\text{-}R \qquad (D)$$

or $$RCOO^{\bullet}(M) + RCOO^{\bullet}\,(M) \longrightarrow R\text{-}R + 2CO_2 \qquad (D')$$

or $$RCOO^{\bullet}\,(M) + R^{\bullet}\,(M) \longrightarrow R\text{-}R + CO_2 \qquad (D'')$$

and alternatively

$$RCOO^{\bullet}\,(M) + RCOO^- \longrightarrow R\text{-}R + 2CO_2 + e \qquad (E)$$

or

$$R^{\bullet}\,(M) + RCOO^- \longrightarrow R\text{-}R + CO_2 + e \qquad (E')$$

Step B in the above scheme represents the initial discharge of the carboxylate ion on the electrode to give an adsorbed** $RCOO^{\bullet}$ radical; this step is usually referred to

---

* A number of other side-reactions such as formation of RH by atom abstraction or formation of esters by reaction of R with $RCOO^{\bullet}$ may also occur (25). However, in most of the present work conditions have been chosen to minimize such processes (cf. 2).

**This factor of adsorption of the intermediate species is one that has not always been appreciated by organic chemists who have studied the Kolbe reaction. Thus the reactivity of such species when adsorbed must not be confused with the supposed high reactivity of such species in homogeneous solution (68).

as the "discharge step". Step C is a heterogeneous catalysed "chemical step" of production of R• from RCOO• on the electrode surface; this step is chemical because no charge transfer across the metal-solution interface is involved. Steps D, D', D" are kinetically (but not chemically) equivalent since each one is a "recombination step", i.e., it involves recombination of two radicals, the identity of which it is desirable to establish from other evidence. Steps E and E' are again kinetically equivalent; E or E' will be referred to as "electrochemical desorption step" (or "radical-ion reaction" in the terminology of Parsons).

In the overall Kolbe reaction, carboxylate radicals must be produced in a "discharge step" and perhaps decompose in a subsequent "chemical step" to give R•. For the production of the Kolbe products, i.e., R-R + CO_2, the radicals thus formed on the electrode must be removed from the electrode by coupling through either a "recombination step" (D or D', or D") or an "electrochemical desorption step" (E or E').

For simplicity of discussion, the kinetically indistinguishable steps in the above scheme will be ignored for the time being. The above scheme is then reduced to:

$$RCOO^- \rightleftharpoons RCOO^\bullet\ (M) + e \qquad B$$

$$RCOO^\bullet\ (M) \longrightarrow R^\bullet\ (M) + CO_2 \qquad C$$

$$R^\bullet\ (M) + R^\bullet\ (M) \longrightarrow R\text{-}R \qquad D$$

$$R^\bullet\ (M) + RCOO^- \longrightarrow R\text{-}R + CO_2 + e \qquad E$$

The problem now is to examine the kinetic consequences in terms of Tafel slopes and coverage effects for the possibility of each one of the above steps being the rate-determining step (r.d.s) in the above sequence of consecutive processes constituting the overall Kolbe reaction.

The derivation of Tafel slopes for this scheme has been discussed previously (2,6) and the procedures for derivation of Tafel slopes for any general case have already been reviewed (34,40). The theoretically-deduced values (2,6) for the present scheme are summarised in Table VIII.

Table VIII

r.d.s.	Tafel slope	Limiting Conditions
B	2RT/F	Rate constants for the following steps relatively large so that $\theta_{RCOO^{\bullet}} \longrightarrow 0$
C	(a) RT/F	(a) $\theta_{RCOO^{\bullet}} = f(V)$
	(b) Limiting current	(b) $\theta_{RCOO^{\bullet}} \longrightarrow 1$ and potential-independent.
D	(a) RT/F	(a) B and C in quasi-equilibrium and coverage by $R^{\bullet}$ potential-dependent.
	(b) Limiting current	(b) $\theta_{R^{\bullet}} \longrightarrow 1$ and potential-independent.
E	(a) 2RT/F	(a) B and C in quasi-equilibrium and $\theta_{R^{\bullet}} \longrightarrow 1$ and potential independent.
	(b) 2RT/3F	(b) $\theta_{R^{\bullet}}$ potential-dependent.

The Tafel slopes given in Table VIII are the limiting values derived by assuming Langmuir conditions (69,70). The corresponding Tafel slopes under conditions where coverage-dependence of activation energies (69,70) must be included in the kinetic equations have not been included in the table; the reason being that the values of Tafel slopes obtained in the present investigation are in general $> 2RT/F$ and are hence beyond the range of application of the treatment for Temkin conditions which always gives b values less than 2RT/F.

The Tafel equation for an anodic reaction (eqn. 2) is

$$\eta = a + b \ln i \qquad (2)$$

where $a = (RT/\alpha F) \ln [i_o' (1-\theta)]$,

$b = RT/\alpha F$

and α is the transfer coefficient depending on the symmetry factor β and the reaction mechanism (71); β may be defined (71)* as the fraction of the total metal-solution potential difference through which change must formally pass before the transition state is attained (work done in the reaction <u>after</u> the reacting particles have passed the transition state does not affect the velocity of the reaction). For an elementary

*Other definitions of β have been considered elsewhere in terms of potential energy diagrams, and are equivalent under certain conditions (40) (see below).

reaction involving transfer of one electron, the Tafel slope b can be written as

$$b = RT/\beta F$$

and β is usually near 0.5 (but see special cases discussed below).

The definition of β given above (68) is due to Bockris and Potter. The more generally accepted (40) significance of β is that β is simply a charge-transfer symmetry factor and has a value = 0.5, assuming a <u>symmetrical</u> barrier at the metal-solution interface. The quantity defined as β by Bockris and Potter may be referred to as an "effective" symmetry factor (referred to the total metal-solution potential difference). This "effective" symmetry factor is identical with the simple charge transfer symmetry factor β only for a simple discharge step, and each β has a numerical value close to 0.5 in the absence of any adsorbed barrier layers across which a part of the total metal-solution potential difference may operate. If thin and moderately conducting barrier-layer films are involved at the interface, part of the total metal-solution potential drop falls across this film (72,74) and part across the ionic double-layer, through which the ion discharge takes place. This latter process then occurs with an effective symmetry factor (referred

to the total metal-solution potential difference) which can be less than 0.5 and may be as low as 0.25 - 0.2 depending on the properties of the electrode metal and the barrier film (73). This matter is of importance in explaining Tafel slopes which are higher than 2RT/F.

Thus, values of the effective symmetry factor less than 0.5 can arise and lead to an explanation of slopes greater than 2RT/F which often arise in anodic processes. Tafel slopes greater than 2RT/F have been observed in the present investigation and suggest the presence of some adsorbed barrier-layer films on the electrode. These high Tafel slopes for the Kolbe reaction were also observed by Conway and Dzieciuch (2,6) in their galvanostatic studies on this reaction. At the "valve" metals (Ta. Zr, Ti, Al), much thicker barrier films of oxides can be formed and most of the total metal-solution potential drop occurs across these films giving rise to extremely high Tafel slopes (74,75).

Returning to the discussion of the scheme of elementary steps on p.174, it is to be noted that an important consequence of the above scheme in terms of coverage effects is as follows: if the discharge step B is rate-determining (i.e., if it has the smallest rate constant), all the subsequent steps (i.e., the steps involved in the removal of the discharged $RCOO^{\bullet}$) will tend to have appreciably higher rate constants with

coverage of the electrode by RCOO* consequently approaching zero. However, this does not imply that the electrode may not be covered by some species adsorbed by the electrode from the ambient solution by a chemical catalytic process. If any step other than the discharge step B is rate-determining, partial or complete electrode coverage should usually be observed in the complementary transient studies, assuming that the adsorbed species is electro-active, i.e., if it can undergo a more or less reversible electron transfer reaction.

(ii) Evidence used in the Identification of Adsorbed Intermediates

For complete elucidation of the mechanism of an electrode process, the kinetic analysis given in (i) above must be supported by knowledge of the identity and nature of any adsorbed intermediates. However, in electrochemical measurements the identity of the adsorbed species must be deduced indirectly from the data obtained in various non-steady-state measurements (presented in Chapter III). For example, the types of ad-species involved in hydrocarbon electro-oxidation have recently been deduced by this approach using the potentiodynamic method (76). Here a brief discussion of some of the general principles involved in the elucidation of the identity of the adsorbed species is presented. Any

considerations of a special nature that may arise in the course of discussion of actual reaction mechanisms (section 3 of this Chapter) will be developed at the appropriate places.

It must be stressed, however, that identification of adsorbed species by purely electrochemical charging studies can never be chemically certain. Only by using several complementary electrochemical approaches for a given reaction, can such methods be of some value. This approach has been used in the present work. Further elucidation of the identity of adsorbed species may be obtained in favourable cases by use of C^{14} - labelled reactants. Work of this kind has recently been initiated in this laboratory. However, even this method is not entirely unambiguous since ions specifically adsorbed in the double-layer cannot be distinguished from chemisorbed species which may arise from discharge of the ions. Alternatively, substitution or addition reactions which the adsorbed species can undergo with an added substrate molecule, e.g., trinitrotoluene in the case of the acetate Kolbe reaction may be indicative of the nature of the species involved. Such information cannot, however, give an indication of relative coverage by the species, only of the relative reactivity of the ad-species in the overall consecutive series of reactions with respect to the reactivity with the added substrate.

The following, then, are some of the general approaches used in identifying the ad-species in the present investigation.

(a) Potential of Commencement of the Tafel Region

In a potentiostatic steady-state current-potential curve, the potential at which the Tafel region commences in relation to the behaviour of the Tafel line for a known process may enable some preliminary conclusions to be made.

The Tafel line for the Kolbe reaction on Pt in aqueous solution of KTFA + TFA commences above 2.1 V suggesting that in the part of transition region from 1.7 V (which is approximately the potential at which the Tafel region for oxygen evolution in acid solutions normally arises at c.d.'s of ca. 10^{-6} a.cm.$^{-2}$) to 2.1 V, formation of some adsorbed intermediates (possibly $CF_3COO^{\bullet}$ or $CF_3^{\bullet}$) has perhaps taken place. However, the possibility of oxidation of trace impurities or the occurrence of alternative (side) reactions in this potential range must not be ignored. The current densities involved here are, however, too small to allow coulombic analyses to be made.

(b) Rest Potential

This is a qualitative guide to the identity of the species that might be irreversibly adsorbed on the electrode (cf.91), e.g., if a surface oxide is the only species adsorbed on the electrode, then the rest potential usually approximates to

the reversible potential for the oxygen evolution reaction, i.e., 1.23 V or some related mixed potential. This is found experimentally, e.g., for the case of oxygen evolution at anodes of Pt or Au when the electrodes are left on open-circuit even in N_2 containing solutions. If oxide were covering only part of the electrode surface, and the remainder of the surface was either bare or partially covered by a species formed in a reaction with a much lower reversible potential, the experimentally observed rest potential could be a mixed potential and could arise roughly between 0.8 V and 1.3 V, depending on the proportion of the electrode surface covered by the oxide. In the present work, this rest potential, it must be noted, has been treated in a purely empirical manner.

(c) Residual Potential

The residual potential observed on open-circuit e.m.f. decay has a significance similar to that of the rest potential.

(d) Inhibition Inflection

In certain organic oxidations, a characteristic inhibition inflection is observed in the current-potential relation (62). If a linear log[current]-potential relation beyond this passivation bend is observed, it can indicate that either (α) discharge can occur onto the layer of

inhibiting species after that layer has been formed in the steady-state to an appreciable extent of coverage, or (β) a new mechanism can arise as the potential is made more anodic (62). In the present investigation, this inhibition inflection has been observed in the current-potential relations for gold in nominally anhydrous solutions of KTFA in TFA (Fig. 12). When coupled with other evidence (see below), this inhibition bend can be useful in indicating whether an inhibiting species is co-adsorbed or not.

(e) Magnitudes of Q and C

The magnitudes of Q and C calculated from discharge transients or potentiodynamic profiles, can, in some cases, be a useful guide to the identity of the adsorbed species. Experimentally determined Q values may be compared with theoretically estimated values of Q (38,39,41,51,71) corresponding, for example, to a monolayer of R°, RCOO° and/or oxide. It is not difficult to estimate to within an uncertainty of 20% (or better in some cases) the values of Q corresponding to a monolayer of R°, RCOO°, oxide etc. by assuming a simple model of closed-packed spheres and a plausible roughness factor for the electrode surface, which can often be supported by determinations of the electrochemical H accommodation on the same electrode. The most probable orientations of these radicals on the electrode surface

should also be taken into account.

(f) Relation Between Solution Composition and Magnitudes of C and Q

Experimental determinations of Q and C in very anhydrous solutions and then in solutions containing varying amounts of water may lead to some estimate of the Q and C values attributable to oxide only in those solutions where (α) water is present and (β) co-adsorption of oxygenated species is suggested by other evidence.

(g) Potentials of Arrests in Cathodic Discharge Profiles

In the C-V profiles, the values of $V_{C_{max.}}$ (e.g., Fig. 27) observed correspond to the potentials of arrests in the respective cathodic discharge profiles. Thus $V_{C_{max.}}$ values can be helpful in the identification of the adsorbed species; e.g., if $V_{C_{max.}}$ lies in the range 0.5 V - 1.0 V, the presence of an oxide would seem to be indicated.

(h) Effect of $i_{cath.}$ on the C-V Profiles

The effect of $i_{cath.}$ on $C_{max.}$ and $V_{C_{max.}}$ may also be of value in the identification of an adsorbed species. Thus, it can be shown theoretically (46) that for an irreversibly-adsorbed electroactive species, increase in $i_{cath.}$ used in the cathodic transient should shift $C_{max.}$ to higher values and $V_{C_{max.}}$ to more cathodic potentials. This effect arises

because the capacity measured in a constant current charging process is not necessarily the "equilibrium capacity", i.e., it is not the value of capacity that would correspond to the value extrapolated to zero a.c. frequency if the capacity measurements were made by an a.c. method. In d.c. measurements of capacity, as used in the present investigation, a concept of "equivalent frequency" is applicable, as discussed by Conway, Gileadi and Kozlowska (46), and a theoretical treatment predicts the shifts in $C_{max.}$ and $V_{C_{max.}}$ values with varying $i_{cath.}$*. This effect has been to some extent experimentally confirmed by the small amount of data which, at present, exists in the literature on irreversibly adsorbed species (46). In the present investigation, shifts in the values of $C_{max.}$ and $V_{C_{max.}}$ agree with the theoretically predicted trend only in those cases where presence of one adsorbed species is unambiguously indicated. An example is the case of gold in very anhydrous solutions of 1M CF_3COOK in CF_3COOH where the only adsorbed species is believed to be $CF_3COO^{\bullet}$ (Fig.26,27); again, in the case of gold in aqueous solution of 1M CH_3COOK + 1M CH_3COOH, oxygen evolution is the only Faradaic process so that the only adsorbed species is believed to be the oxide. In all other cases studied, the effect of $i_{cath.}$ on $C_{max.}$ shows no regular trend which suggests empirically that in all these cases, more than one species may be adsorbed

*This variation of $V_{C_{max.}}$ with $i_{cath.}$ can in fact be another characteristic of the type of ad-species involved (see p.216).

on the electrode and hence causes more complex behaviour to arise. This empirical conclusion is of some value, when used in conjunction with other types of evidence, in indicating the identity of the species adsorbed on the electrode.

(i) Potential of Peaks in the Potentiodynamic Profiles

The potentials at which the peaks appear in the potentiodynamic profiles can be indicative of the identity of the adsorbed species, especially if the profiles have been obtained at slow sweep rates. For instance, the peak for the reduction of the adsorbed oxide on Pt appears around 0.6 V and the two peaks for hydrogen deposition between +0.3 V and 0.0 V. The significance of potentials at which the peaks appear in the potentiodynamic profiles is, in principle, the same as that of $V_{C_{max.}}$ in the C-V profiles calculated from the cathodic transients. In the potentiodynamic method, this argument will only apply to peaks that can be justified as being associated with charging processes (see p. 16).

(j) Q vs. Rate Relations

The principles involved in interpretation of such plots are briefly as follows: (α) If increased Q values correspond to decreased rates, Q is probably associated with an inhibiting, co-adsorbed species. (β) If this Q is associated with an inhibiting species and is observed only when some water is present in the solutions, the inhibiting species must

originate, directly or indirectly, from water. (γ) If the magnitude of Q increases with increase in the amount of water present in the solution, then it may be assumed once again that Q is associated with an inhibiting (surface oxide) species, originating from water.

The actual details of experimental plots of these kinds will be discussed in section 3 of this chapter, where mechanisms for the Kolbe reaction are proposed and examined.

(k) Q vs. V_i Relations

The significance of this type of plot must be considered in relation to the other evidence for the mechanism of a given reaction and may best be illustrated by taking a particular example. In Fig. 49, a plot of Q vs. V_i is shown for gold in 1M CH_3COOK in "anhydrous" CH_3COOH solution (presumably containing traces of water). It can be seen that for this particular case, Q increases initially with increasing V_i but at 1.9 V the value of Q begins to decrease with increasing V_i. This is because, at lower potentials with increase in V_i, Q corresponding to the adsorbed oxide (arising from the traces of water) tends to increase; at 1.9 V, however, the relatively large $CH_3COO^{\bullet}$ radicals may be regarded as being discharged at certain sites previously occupied by the oxide with a consequent decrease in Q values with increasing polarising potential above 1.9 V. This point will be elaborated

further in relation to other evidence to be presented in section 3 (iv) of this chapter.

3. PROPOSED MECHANISMS FOR THE KOLBE REACTION

For each of the systems studied, a variety of related data and derived quantities has been obtained. In this section, it will be necessary to make a detailed analysis of this data (in terms of the approaches summarised in the previous section, p.170) and introduce closely argued proposals concerning reaction mechanisms and adsorbed intermediates. In such a treatment, numerous cross references unfortunately cannot be avoided.

(i) Platinum in Potassium Trifluoroacetate-Trifluoroacetic Acid Solutions

Reaction in Completely Anhydrous Solutions (with TFA-Anhydride)

(a) A Tafel slope of 0.215 V is observed in the post-transition region (Fig. 11). This suggests that the reaction is proceeding on a covered electrode and the high Tafel slope indicates the presence of a barrier film across which a part of the total metal-solution potential drop operates. The following experimental facts (summarised in Table II), however, indicate clearly and complementarily the absence of significant quantities of electrochemically detectable adsorbed intermediates on the electrode in this case.

(b) Low values of the rest potential (0.5 V); absence of hysteresis between the ascending and the descending current potential relations (Fig. 11); absence of arrests in open-circuit and forced decay profiles (see photograph in Fig. 18); low values of residual potential obtained on open-circuit decay of the anodic potential; small values ($< 100\ \mu F.\ cm.^{-2}$) of $C_{max.}$ calculated from open-circuit and forced decay profiles; absence of peaks in the potentiodynamic sweep runs.

In order to reconcile the apparently contradictory experimental evidence of (a) and (b) above, [since (a) indicates some barrier layer of ad-species] it is suggested that an appreciable coverage by electrochemically inactive radicals is involved. An electro-inactive radical is one which is adsorbed in a highly irreversible manner on the electrode surface and is not susceptible to facile reduction in a cathodic transient. However, its presence is indicated from the fact that the Kolbe reaction is proceeding in the post-transition region and hence probably on a covered electrode; also, the high values of Tafel slopes ($>2RT/F$) can be reasonably explained only on the assumption that a barrier-layer of some kind is present on the electrode.

There is an important assumption involved here and in the argument to be presented below, that, in the absence of any barrier layer, the symmetry factor β must have a value near to 0.5 ($\pm$ 10%). This is borne out by the fact that for many qualitatively quite different ion discharge reactions, β is close to 0.5 when other evidence indicates that a barrier layer is not present or could not under any circumstances be involved. Also, theoretically, a value of β close to 0.5 is expected for most reactions, as may be deduced by consideration of potential energy barriers for discharge processes (78,79). A further point is the fact that for widely different types of

acids and bases, Bronsted's "α" or "β" coefficients, which have a significance closely analogous to that of β, are often near to 0.5 and hence support this argument*.

Finally, it cannot be argued that a low value of β arises for some intrinsic geometrical or other special reason for the discharge of $RCOO^-$ ($R = CH_3$) since a more normal value of β is actually observed in the Tafel line for the acetate Kolbe reaction in strictly anhydrous solutions (in vacuo preparation of solutions - see Chapter III). On the basis of the above evidence and discussion, the following mechanism is therefore suggested for the Kolbe reaction on Pt in anhydrous solutions of 1M CF_3COOK in CF_3COOH.

The overall reaction is

$$2CF_3COO^- \longrightarrow C_2F_6 + 2CO_2 + 2e \qquad (A)$$

and the following elementary steps may be envisaged:

Step	Derived Tafel Slope (from Table VIII)
$CF_3COO^- \rightleftharpoons CF_3COO^{\bullet}(M) + e$	$2RT/F$, $\theta_{CF_3COO^{\bullet}} = 0$ (B)

*Some exceptions do arise in base-catalysed reactions but it seems that anomalies only arise for bases with high pK's, as expected.

$$CF_3COO^{\bullet}(M) \longrightarrow CF_3(M)+CO_2 \qquad \begin{cases} RT/F,\ \theta_{CF_3COO^{\bullet}} = f(v) \\ \text{Limiting, current } \theta_{CF_3COO^{\bullet}} \longrightarrow 1 \end{cases} \qquad (C)$$

$$CF_3^{\bullet}(M)+CF_3^{\bullet}(M) \longrightarrow C_2F_6 \qquad \begin{cases} RT/F,\ \theta_{CF_3^{\bullet}} = f(v) \\ \text{Limiting, current } \theta_{CF_3^{\bullet}} \longrightarrow 1 \end{cases} \qquad (D)$$

Alternatively to (D) the following steps may occur:

$$CF_3COO^{\bullet}(M)+CF_3COO^{\bullet}(M) \longrightarrow C_2F_6+2CO_2 \qquad \begin{cases} RT/F,\ \theta_{CF_3COO^{\bullet}} = f(v) \\ \text{Limiting, current } \theta_{CF_3COO^{\bullet}} \longrightarrow 1 \end{cases} \qquad (D')$$

or

$$CF_3COO^{\bullet}(M) + CF_3^{\bullet}(M) \longrightarrow C_2F_6+CO_2 \qquad \begin{cases} RT/F,\ \theta_{CF_3COO^{\bullet}/CF_3^{\bullet}} = f(v) \\ \text{Limiting, current } \theta_{CF_3COO^{\bullet}/CF_3^{\bullet}} \longrightarrow 1 \end{cases} \qquad (D'')$$

or

$$CF_3COO^{\bullet}(M)+CF_3COO^{-} \longrightarrow C_2F_6+2CO_2+e \qquad \begin{cases} 2RT/F,\ \theta_{CF_3COO^{\bullet}} \longrightarrow 1 \\ 2RT/3F,\ \theta_{CF_3COO^{\bullet}} = f(v) \end{cases} \qquad (E)$$

or

$$CF_3^{\bullet}(M)+CF_3COO^{-} \longrightarrow C_2F_6+CO_2+e \qquad \begin{cases} 2RT/F,\ \theta_{CF_3^{\bullet}} \longrightarrow 1 \\ 2RT/3F,\ \theta_{CF_3^{\bullet}} = f(v) \end{cases} \qquad (E')$$

First of all, it is necessary to elaborate upon the nature of the possible electro-inactive species adsorbed on the electrode. The adsorbed "barrier layer" on the electrode must consist of either $CF_3^{\bullet}$ or $CF_3COO^{\bullet}$ radicals or both. If $CF_3COO^{\bullet}$ were present on the electrode, it would be expected to have its oxygen atoms, which have a partial negative charge due to resonance and induction effects 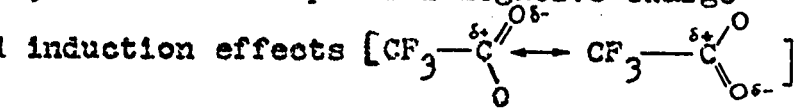 oriented towards the positively charged electrode. This would result in the adsorbed $CF_3COO^{\bullet}$ being bound to the Pt metal through "Pt - O" bonds as follows (note that the carboxyl carbon is sp^2 hybridised so that the two O atoms and the two C atoms are co-planar).

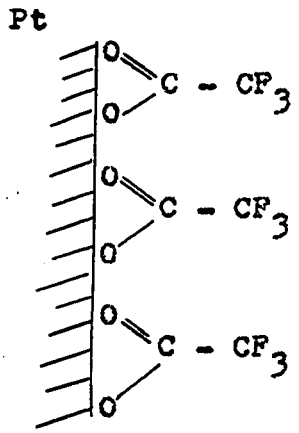

In terms of its possible reduction in cathodic transients, $CF_3COO^{\bullet}$ thus adsorbed on the Pt metal would be expected to behave like a "substituted" oxide (Fig. 64), i.e., adsorbed $CF_3COO^{\bullet}$ would be expected to be reducible (and hence

Figure 64

A schematic representation of the "substituted oxide" layer adsorbed on the substrate platinum metal.

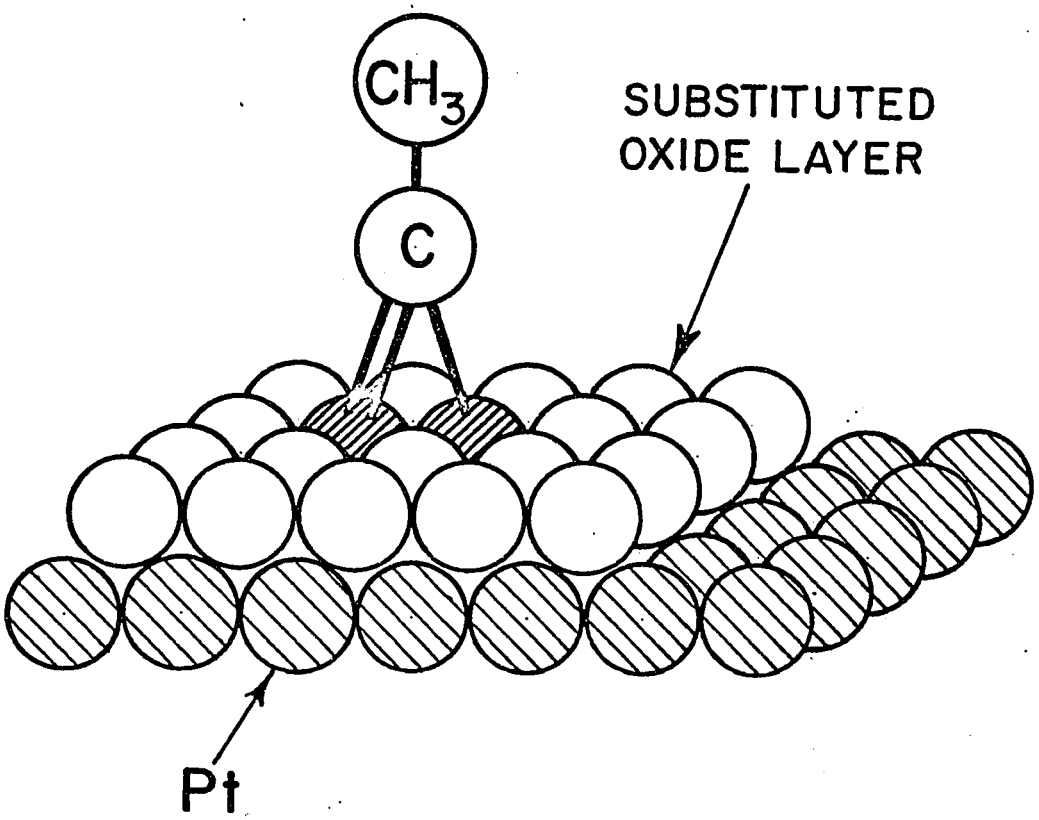
CH3
C
SUBSTITUTED
OXIDE LAYER
Pt

"electro-active") like any other oxygenated species adsorbed through the formation "Pt-O" bonds, e.g., OH• adsorbed on Pt. On the basis of these considerations, it is believed that the electro-inactive species adsorbed on the electrode is <u>not</u> $CF_3COO^{\bullet}$; it must, hence, be $CF_3^{\bullet}$. This eliminates steps D', D", and E from further discussion of this scheme of consecutive processes.

Since the high Tafel slopes indicate the presence of a barrier layer, it may be concluded that $\theta_{CF_3^{\bullet}} \longrightarrow 1$. Step B cannot be rate-determining since such a condition would imply $\theta_{CF_3^{\bullet}} \longrightarrow 0$. Again, step C would not be rate-determining since it would involve the existence of the electro-active species $CF_3COO^{\bullet}$ as the adsorbed intermediate against which we have argued above; also, even if it is assumed for the sake of argument that the adsorbed intermediate is $CF_3COO^{\bullet}$, a limiting current would then tend to be observed at high coverages (see Table VIII); neither of these possibilities is in agreement with the experimental slope of <u>ca.</u> 7RT/2F. Step D, if rate-determining, would give rise to a limiting current at high coverage and a Tafel slope of RT/F at low coverages; experimentally, <u>no</u> limiting current is observed, although appreciable coverage due to a barrier-layer film is indicated by the high Tafel slopes. Hence, on the basis of this argument, D must be rejected as a possible r.d.s. The only step left to be

considered as the possible rate-determining process in the above scheme is therefore E'; low coverage conditions when E' is the r.d.s. must be rejected because neither low coverages are indicated by the experimental log[i]-V relation nor are the experimental Tafel slopes (7RT/2F) at all close in magnitude to the one (2RT/3F) which may be deduced for low coverage conditions with E' as the r.d.s. Thus the only possibility remaining to be considered is that of E' being the r.d.s. in the above scheme under conditions when $\theta_{CF_3\cdot} \longrightarrow 1$. The predicted Tafel slope (2RT/F with a <u>normal</u> value of $\beta = 0.5$) in this case also does not agree with the experimental value (7RT/2F); however, it is no further removed from the experimental value than are any of the other values in the above scheme. It also satisfies the experimentally-indicated condition that the electrode is highly covered by an electro-inactive species. If, however, it is assumed that a part of the total metal-solution potential drop operates across the barrier layer of irreversibly-adsorbed $CF_3^{\cdot}$, (and is hence not available for the potential dependent activation controlled charge transfer process at the barrier-solution interface involved in step E') the <u>effective</u> value of the symmetry factor β can then become (<u>cf.</u> 72,73,74) less than 0.5* with a corresponding <u>increase</u>

*β is of course still 0.5 with respect to the <u>local</u> p.d. operating between the initial and final states of the discharge step. The situation is hence no exception to the general argument given on page 189.

in the value of the Tafel slope deduced, RT/βF. For example, if half of the total metal-solution potential drop operates across the $CF_3^\bullet$ barrier, the effective value of β becomes 0.25 and that of the Naperian Tafel slope 0.24 (viz. 2.3 4RT/F). The value of Tafel slope thus deduced can hence be shown to be consistent with the experimental one on the basis of this effect and a rational argument concerning the coverage conditions.

The mechanism proposed on the basis of the above discussion is therefore:

$$CF_3COO^- \rightleftharpoons CF_3COO^\bullet(M)+e \qquad (B)$$

$$CF_3COO^\bullet(M) \longrightarrow\!\!\!\!\!\rightarrow CF_3^\bullet(M)+CO_2 \ (\theta_{CF_3^\bullet} \longrightarrow 1) \qquad (C)$$

$$CF_3^\bullet(M)+CF_3COO^- \longrightarrow C_2F_6+CO_2+e \qquad (E')$$

$CF_3COO^\bullet$ radicals are produced by the discharge step B having a relatively high rate constant and are decarboxylated rapidly in the step C; $CF_3^\bullet$ radicals formed in C are electrochemically desorbed by the rate-determining step E'. Desorption by step D is eliminated as a possibility since this would give a Tafel slope of RT/2F rather unambiguously.

In order to have an effective barrier-layer of the electro-<u>inactive</u> $CF_3^\bullet$ radicals <u>only</u>, as is required by the high experimental Tafel slopes and absence of arrests in the cathodic transients, it is necessary to assume that in the step C the

equilibrium lies mostly to the right principally because the back reaction rate constant is very small. This has been indicated by a double arrow in the reaction C on page 196. Such an assumption satisfies the requirement that in the steady-state, the species present on the electrode must principally be $CF_3^{\bullet}$; if some $CF_3COO^{\bullet}$ were also present, as would be expected if step C were at equilibrium and $\overleftarrow{k}_c$ were comparable with $\vec{k}_c$, arrests would tend to be observed in the cathodic transients. Experimentally, no such arrests are indicated (Table II).

Reaction in Nominally Anhydrous Solutions

These solutions presumably contained very small traces of water since treatment with the anhydride was not employed in this case. As indicated in the Summary of experimental results (Table II) high Tafel slopes (= 9RT/2F) are observed in the post-transition region (Fig. 11). This again indicates the presence of a barrier layer on the electrode. The rest potential now has a value ca. 0.9 V (cf. the value of 0.5 V for the anhydride treated solution) which suggests partial coverage of the electrode by an oxide. The appearance of hysteresis between the ascending and descending i-V relations (Fig. 11) in this solution is also a strong indication (since this behaviour occurs in virtually all anodic oxidations where oxide is present) that the surface is covered by some species

which is irreversibly formed but in this case is electro-active*. Since the only additional constituent in this solution is water (present in traces), this/these species must arise directly or indirectly from the traces of water. In nominally anhydrous solution, it is to be noted that the rate at a given potential is lower than the corresponding rate in completely anhydrous solutions (Fig. 11). This indicates that the presence of traces of water tends to inhibit the Kolbe reaction, perhaps due to co-adsorption of oxide. Again, the residual potential attained on open-circuit decay from the initial anodic polarising potential is ca. 1.0 V which is suggestive of the presence of some oxide on the surface. In the forced decay profiles, arrests appear only several hours after the preparation of solutions (see photograph in Fig. 18); this indicates, rather directly, that these arrests, and hence the corresponding adsorbed intermediates they represent, originate directly or indirectly from the

*If the species were irreversibly adsorbed and electro-inactive as in the case of the completely anhydrous solutions, the barrier/solution interface would behave like a metal-solution interface in the i-V relations with a consequent absence of hysteresis in the ascending and the descending i-V curves (Fig. 11). The hysteresis appears because of irreversibility of the formation and reduction of the species produced in the ascending curve. The presence of some electro-inactive species on the electrode, it must be emphasized, does not imply, of course, that the electrode surface becomes inactive for the overall Faradaic process.

microscopic traces of water that diffuse into the solution through the stopcocks and seals of the cell.

It has been observed (Table II) that values of Q_{total} ($\approx$ 0.108 mC. cm.$^{-2}$) and $C_{max.}$ ($\approx$ 250-450 μF. cm.$^{-2}$) arise for the reaction under the nominally anhydrous conditions. These small values of charge and pseudo-capacity suggest that <u>either</u> the electrode is partially covered and the adsorbed species is not very bulky, e.g., an oxide is involved, <u>or</u> the electrode is substantially covered in a geometrical sense but a high proportion of the coverage is associated with a bulky radical, e.g., $CF_3COO^{\bullet}$. High Tafel slopes in the post-transition region suggest again the presence of a barrier layer; hence it is to be concluded that the electrode may be appreciably covered by a barrier-layer film of electro-active $CF_3COO^{\bullet}$ with small amounts of co-adsorbed oxide.

The supposition that Q_{total} is associated here with $Q_{CF_3COO^{\bullet}} + Q_{Ox.}$ is corroborated by the following facts; (a) In Fig. 65, for a given type of solution, a curve is shown passing through a family of points where each point represents the value of Q at a particular potential (calculated from the forced decay profiles) and the corresponding value of rate at that potential (determined from the steady-state i-V plot). Such a curve is represented by the solid line in

Figure 65

Platinum/1M KTFA in TFA: a plot of Q vs. rate (———) and a plot of Q vs. rate "normalised" to 2.1 V (– – – –).

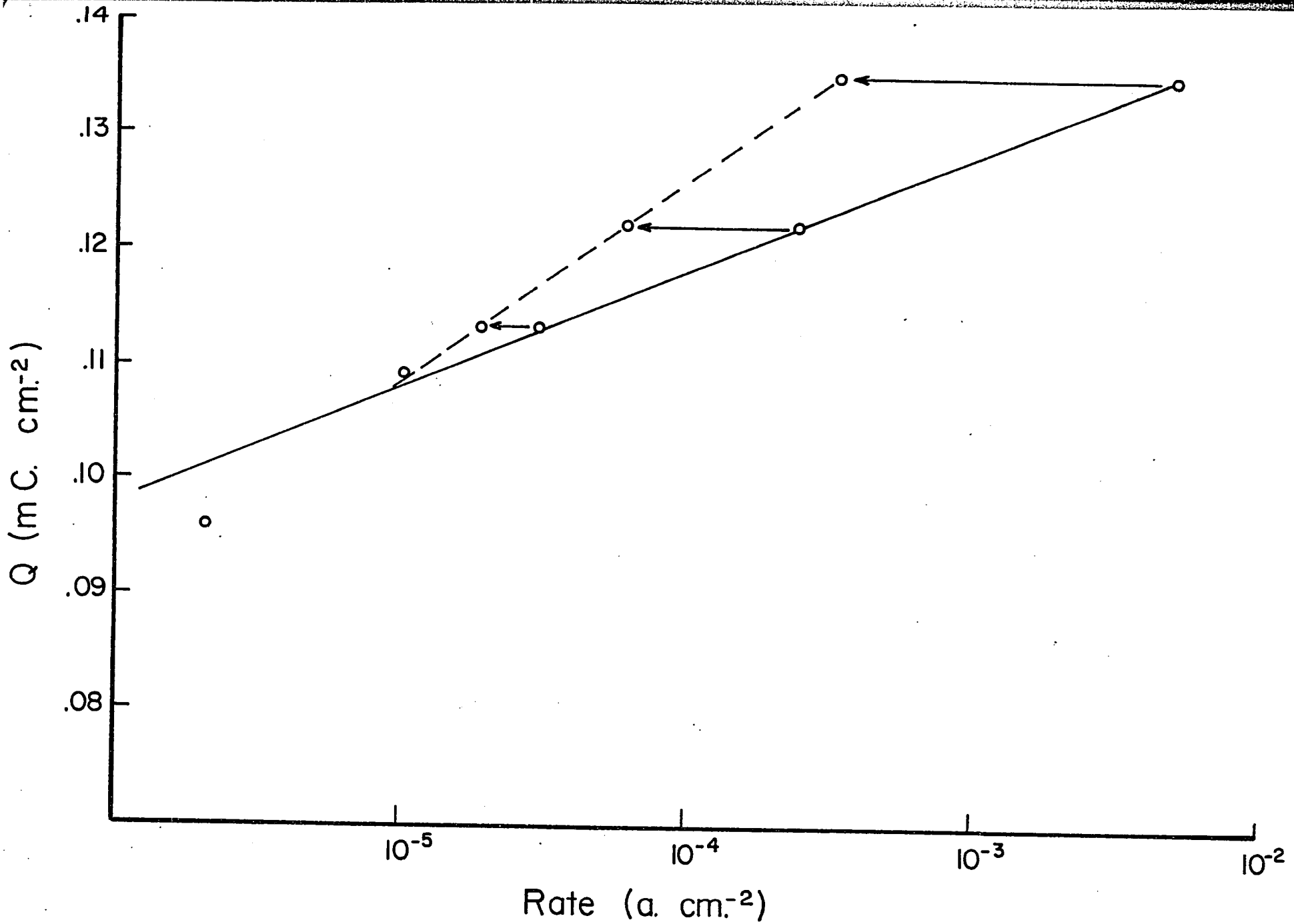
.14
.13
.12
.11
.10
.09
.08
Q (m C. cm.-2)
10-5
10-4
10-3
10-2
Rate (a. cm.-2)

Fig. 65, and indicates that the rate increases with increasing Q. However, the increase in rate and in Q may arise independently of each other; part of the increase in rate will be due to the increasing potential implicitly represented by the ascending direction of points on the Q axis. In order to explore this matter further, a plot of Q *vs.* rate was examined in which the rate at each potential V higher than 2.1 V (i.e., at the beginning of the Tafel region) was arbitrarily normalised to this potential of 2.1 V in order to determine the effect on rate of increasing Q alone. The normalisation was made by multiplying each rate by $\exp(2.1-V)/b$ where b is the observed Tafel slope. The results of this procedure are shown by the dotted line in Fig. 65. The rate is still found to increase with increasing Q and indicates that a significant part of the Q is due to an adsorbed species which is involved directly in the Kolbe reaction, i.e., either $CF_3COO^\bullet$ or $CF_3^\bullet$, rather than oxide which would be expected to inhibit the reaction. The species must presumably be $CF_3COO^\bullet$ since $CF_3^\bullet$ is believed to be electro-inactive (see p. 189) and hence incapable of being observed in the forced decay profiles.

(b) The possibility that Q_{total} may also correspond to some co-adsorbed oxide associated with a charge $Q_{ox.}$ is deduced as follows: when excess water is added to the solution, Q_{total}

increases but the rate (and hence $Q_{CF_3COO\cdot}$) decreases (Table II; Fig. 11). It seems reasonable to regard this increase in Q_{total} as arising from an increased contribution by $Q_{Ox.}$ when water is present in increasing amounts up to excess. Thus, an increased contribution to Q_{total} by $Q_{Ox.}$ will decrease the rate, as indeed is experimentally observed, since co-adsorption of oxide we suppose inhibits the Kolbe reaction. Increased inhibition of the Kolbe reaction with increased amounts of water added to the non-aqueous solution was also observed qualitatively by Fairweather and Walker (8) in terms of product yields.

The suggestion that Q_{total} is associated with contributions $Q_{CF_3COO\cdot} + Q_{Ox.}$ and not with $Q_{CF_3\cdot} + Q_{Ox.}$ is also to be expected on the basis of general considerations such as have been discussed in the previous section. The presence of small amounts of co-adsorbed surface oxide will tend to change the electro-catalytic properties of the substrate platinum metal and its adsorption behaviour for other species would be expected to be radically different from that of the bare Pt metal. On these grounds, it is not surprising that the radicals principally adsorbed in completely anhydrous and in nominally anhydrous solutions do not appear to be identical. Also, the presence of small amounts of surface oxide would, perhaps, facilitate the co-adsorption of $CF_3COO\cdot$

as a "substituted" oxide in preference to the adsorption of $CF_3^{\bullet}$ radicals (see Fig. 64).

It is found that Q increases with increasing V_i (Fig. 18). At higher potentials, an increase in Q is due either to an increasing coverage by discharged $CF_3COO^{\bullet}$ or to oxidation of adsorbed "OH" formed at lower potentials to a higher surface oxide, or to both effects. Thus, increasing values of Q at increasing V_i strictly may or may not correspond to increasing geometrical coverage θ of the electrode. In this particular case, it is therefore seen that the plot shown in Fig. 18 is not of much value in establishing the identity of the species adsorbed on the electrode.

In the corresponding potentiodynamic sweep runs, composite peaks are observed which again do not help in the identification of the adsorbed species.

From the foregoing discussion, it may be concluded that on Pt in nominally anhydrous solutions, the Kolbe reaction proceeds on an electrode covered by a barrier-layer film containing a significant proportion of $CF_3COO^{\bullet}$ species together with some co-adsorbed oxide which plays an inhibitory role. The following sequence of consecutive steps may then be envisaged:

Step	Derived b values	
$CF_3COO^- \rightleftharpoons CF_3COO^{\bullet}(M)+e$	2RT/F	(B)

together with

$H_2O+M \longrightarrow$ "MOH" (or "MO")* $+H^+ +e$

$CF_3COO^{\bullet}(M)+CF_3{}^{\bullet}COO(M) \longrightarrow C_2F_6+2CO_2$	RT/F Limiting current	(D')
$CF_3COO^{\bullet}(M)+CF_3COO^- \longrightarrow C_2F_6+2CO_2+e$	2RT/F 2RT/3F	(E)

In the above scheme, (B) cannot be the r.d.s. since that would imply $\theta_{CF_3COO^{\bullet}} \longrightarrow 0$, which does not seem to be compatible with the experimentally-observed high Tafel slopes which would, it may be recalled, be strongly indicative of the presence of a barrier-layer. Step (D') must be rejected as the possible r.d.s. since it predicts a limiting current under experimentally-indicated conditions of high coverage, and not a Tafel slope of 9RT/2F. The only other possible r.d.s. is (E) under conditions where $\theta_{CF_3COO^{\bullet}} \longrightarrow 1$. The predicted slope is 2RT/F. However, if about half of the total metal-solution potential drop is assumed to operate across a barrier-layer

*This representation of the surface "oxide" species does not imply any exact stoichiometry in the surface phase.

of adsorbed $CF_3COO^{\bullet}$, as in the case of the adsorbed $CF_3^{\bullet}$ barrier-layer at Pt in completely anhydrous solutions, the value of predicted slope becomes 4RT/F, which is consistent with the experimental value of 9RT/2F.

The role of small amounts of co-adsorbed oxide is only inhibitory as discussed above (i.e., rates in solutions containing water are lower); some of the electrode surface sites may be occupied by such oxide species and be rendered unavailable for catalytic steps in the Kolbe reaction.

Hence, the mechanism for the overall Kolbe reaction

$$2CF_3COO^- \longrightarrow C_2F_6 + 2CO_2 + 2e \qquad (A)$$

under the conditions considered in this section may be written as:

$$CF_3COO^- \rightleftharpoons CF_3COO^{\bullet}(M) + e \qquad (B)$$

$$CF_3COO^{\bullet}(M) + CF_3COO^- \longrightarrow C_2F_6 + 2CO_2 + e \qquad (E)$$

In this scheme, an initial discharge step (B) having a relatively large rate constant is envisaged and is followed by the rate-determining step of electrochemical desorption (E) resulting in the Kolbe products; the charge transfer process in the r.d.s. has to negotiate a potential barrier across a film of adsorbed $CF_3COO^{\bullet}$ (in <u>addition</u> to the usual energy barrier for the process at the metal-solution interface); hence high Tafel slopes can arise.

Reaction in Aqueous Solutions

The experimental observations (Table II) on the Kolbe reaction at Pt in 1M CF_3COOK in (CF_3COOH + 30% H_2O) as solvent indicate that the mechanism of the reaction is the same as that in nominally anhydrous solutions. However, there is an increased contribution of $Q_{Ox.}$ and $C_{Ox.}$ to the total Q and C values, with a consequently increased inhibition of the Kolbe reaction. All the experimental evidence (Table II and Figures referred to below) points to the fact that there is an increased coverage by oxide on the electrode in aqueous solutions. The hysteresis between ascending and descending i-V relations is enhanced (compared with results in the more non-aqueous solutions) and the rates are correspondingly diminished (Fig. 11). In the forced decay profiles, large arrests are observed (see photograph in Fig. 22). The values of Q_{total} and $C_{max.}$ are 1.05 mC. $cm.^{-2}$ and 1650μF. $cm.^{-2}$, respectively (Table II) indicating that the electrode is highly covered by electroactive species; that the electrode tends to be completely covered is also shown by the fact that Q becomes independent of V_i at high potentials (Fig. 22). In the plot of C vs. V (Fig. 20), $V_{C_{max.}}$ lies between 0.6 V and 0.2 V depending on the value of $i_{cath.}$ used in the cathodic transient. This is roughly the potential range where $V_{C_{max.}}$ for the oxide reduction peak would be expected (C_a 0.6 V)

(63). No regular trend is exhibited in the dependence of $C_{max.}$ on $i_{cath.}$ (Fig. 20) which suggests that more than one species may be adsorbed; the situation is thus far more complex than that expected for one species. However, the effect of $i_{cath.}$ on $V_{C_{max.}}$ agrees qualitatively with the trend predicted for reduction of irreversibly adsorbed intermediates, i.e., increased $i_{cath.}$ tends to push $V_{C_{max.}}$ to more cathodic potentials (Fig. 19), due to "overpotential" or irreversibility effects in the charging. This effect is seen (cf. Fig. 67) to be much larger than in the case of oxide capacitance alone, and thus supports the conclusion that other species than oxide are involved in this case (see below). On open-circuit decay from the initial anodic potentials, substantial values of pseudo-capacity indicative of coverage by the adsorbed intermediates are observed (Table II). A residual potential of 1.175 V, suggesting the presence of an oxide is also observed; forced discharge from this potential gives arrests which correspond to $C_{max.}$ in C-V profiles (Fig. 16). The values of $V_{C_{max.}}$ are 0.58 V and 0.15 V for the two arrests; the corresponding values of charges are Q_1 = 0.537 mC. cm.$^{-2}$ and Q_2 = 0.392 mC. cm.$^{-2}$, respectively. These values indicate that the two arrests are, perhaps, due to reduction of oxide (0.58 V) and deposition of hydrogen (0.15 V).

In the potentiodynamic sweep runs, composite peaks are observed; hence no quantitative information on the charging processes could be deduced by this method in this case.

High Tafel slopes (4RT/F) indicate again a barrier-layer film on the electrode. That this Tafel slope refers to the Kolbe reaction (C_2F_6 is identified as a product here) and not to O_2 evolution may be deduced from the potential at which the Tafel region is observed to commence, viz. 2.1 V. The Tafel region for the oxygen evolution reaction in acid solutions would normally commence at substantially lower potentials (see p.250) (63) as indicated by the current-potential relation for the oxygen evolution reaction on Pt in 1M H_2SO_4 shown for comparison in Fig. 11.

In summary, the results indicate that the mechanism for the Kolbe reaction on Pt in aqueous solutions of CF_3COOK + CF_3COOH is the same as that in the nominally anhydrous solutions, i.e., an initial discharge step (B), $CF_3COO^- \rightleftharpoons CF_3COO^{\bullet}(M) + e$, is followed by a rate-determining process of the type:

$$CF_3COO^{\bullet}(M) + CF_3COO^- \longrightarrow C_2F_6 + 2CO_2 + e$$

If coverage by $CF_3COO^{\bullet}$ in the above step is appreciable at high potentials, a barrier-layer film effect would again arise and if about half of the total metal-solution potential drop operates across this barrier-layer a Tafel slope of 4RT/F would be predicted for this mechanism and would be consistent with the experimental results.

Role of Oxide

In the foregoing discussion, it was concluded that adsorbed oxides originating from traces or excess of water present in solution of KTFA in TFA tend to inhibit the Kolbe reaction on Pt. This is corroborated by the family of curves shown in Fig. 66. Here each curve represents a given potential and is made up from three points each of which represents a charge-log[rate] relation at that potential for the three conditions studied, viz. (a) completely anhydrous solutions; (b) nominally anhydrous solutions and (c) aqueous solutions. At potentials lower than that (viz. 2.1 V) beyond which the Kolbe reaction proceeds at appreciable rates with a linear Tafel region, Q values are increased on going from nominally anhydrous to the aqueous solution, and the rates are correspondingly increased. This suggests that with increase in the amount of water present in the solution, $Q_{ox.}$ and the rate for the O_2 evolution reaction increases. However, on going from aqueous to the non-aqueous solutions at this potential, Q <u>decreases</u> but the rate <u>increases</u>; this indicates that with decreased amounts of water, Q_{total} decreases probably because of a decrease in $Q_{ox.}$ but the rate continues increasing due, perhaps, to the possibility that the process being observed now is a composite one, i.e., it involves some contribution

Figure 66

Platinum/1M KTFA in TFA: plots of Q vs. rate at various anodic potentials for completely anhydrous (Δ), nominally anhydrous (□), and aqueous solutions (o).

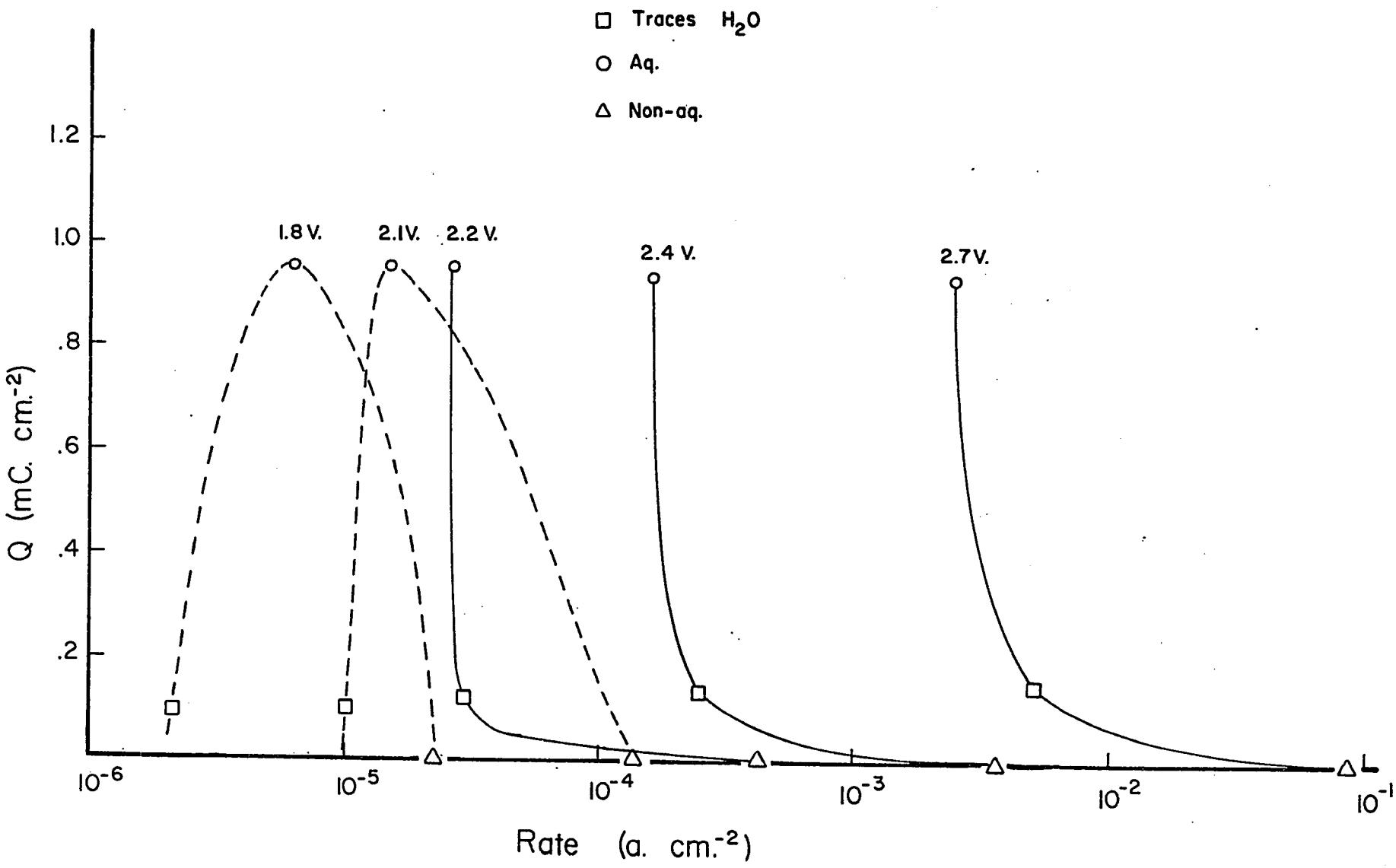
□ Traces H_2O
○ Aq.
△ Non-aq.
1.8 V.
2.1V.
2.2 V.
2.4 V.
2.7V.
1.2
1.0
.8
.6
.4
.2
Q (mC. cm.$^{-2}$)
10^{-6}
10^{-5}
10^{-4}
10^{-3}
10^{-2}
10^{-1}
Rate (a. cm.$^{-2}$)

from the Kolbe reaction and from O_2 evolution*. Only at potentials greater than 2.1 V at which the Kolbe reaction is known to be the major electrode process does the relation between the rate, Q and the water-content become more rationally explicable. At a given value of potential at these high potentials, and proceeding in the sequence aqueous ⟶ nominally anhydrous ⟶ completely anhydrous solutions, the rate is found to increase but Q_{total} decreases; these facts indicate that with increased water content in the solution, Q_{total} increases on account of the presence of larger amounts of surface oxide but the rate of the Kolbe reaction decreases correspondingly. This is consistent with the fact that the coulombic yields of Kolbe products in non-aqueous solvents studied by other workers (8) and in this laboratory previously (2) are usually much better than those in water, except at the highest anodic potentials in the latter case.

A Possible Oxide Pathway in the Aqueous Solution Reaction

In concluding the discussion of mechanisms at Pt in aqueous solutions, the following "oxide" pathway must be noted

---

*At the potentials involved here, the rate of evolution of products is too small to conduct a satisfactorily precise coulombic analysis, and at higher potentials the problem of solubility of C_2F_6 complicates quantitative measurements. However, the previous work (2) indicates substantial yields of the Kolbe product C_2F_6 at higher anodic potentials.

as a possibility since the present work (and see also ref. (3)) indicates appreciable coverage by adsorbed oxygenated species in the range of potentials over which the Kolbe reaction occurs. Instead of the direct ion discharge step of type B (p. 173), we can write an heterogeneous chemical oxidation of the type

$$PtO + CH_3.COO^- + H^+ \longrightarrow CH_3COO^\bullet(M) + PtOH \quad (F)$$

or

$$PtO + CH_3COOH \longrightarrow CH_3COO^\bullet(M) + PtOH$$

where "PtO" and "PtOH" are nominally sites of higher and lower degrees of surface oxidation at the Pt electrode interface but not necessarily of the stoichiometry formally indicated. The species $CH_3COO^\bullet(M)$ may then undergo further reactions down the sequence of steps of type C and type D, D', D" or E. The continuous anodic electrochemical process involved would then be steady-state re-oxidation of "PtOH" to "PtO" by the step

$$PtOH \longrightarrow PtO + H^+ + e \quad (G)$$

which could be coupled with step F in the steady-state.

This scheme has been included for completeness but it is regarded as an unlikely pathway since (a) the Kolbe reaction proceeds with rather similar electrochemical kinetic characteristics in non-aqueous medium to those for the reaction

in aqueous medium (31); hence, a radically different mechanism is unlikely in aqueous medium; (b) it proceeds at a faster overall rate in non-aqueous medium than in aqueous medium, other things being equal, and (c) no gas evolution in a differential manometer cell is found when CH_3COOK aq./CH_3COOK mixture is treated with platinum "dioxide". However, if a stable platinum oxide could be made chemically with the Pt.O ratio attainable on the surface of an electrode, the possibility of conducting a direct heterogeneous chemical oxidation of acetate could not be entirely excluded; at present, however, it is not possible to substantiate this tentative suggestion by any other conceivable experiment.

(ii) Gold in Trifluoroacetate-Trifluoroacetic Acid Solutions

Reaction in Completely Anhydrous Solutions (With Trifluoroacetic Anhydride)

Several features of the experimental results for the Kolbe reaction on gold are similar to those for Pt in this solution (compare Tables II and III). For example, somewhat high Tafel slopes (0.160 V) in the post-transition region are observed; again, absence of hysteresis in the ascending and descending i-V curves and low residual potentials in both cases are to be noted (compare Figs. 11 and 12). However, the evidence from the non-steady state measurements indicates

a qualitatively different behaviour on the two metal anodes. In contrast to the case of platinum, the presence of some electro-active adsorbed intermediates is indicated on gold. Thus, an arrest is observed on open-circuit e.m.f. decay on gold; C values calculated from these open-circuit decay profiles lie between 90 μF. cm.$^{-2}$ and 140 μF. cm.$^{-2}$ depending on the initial polarisation potential V_i (Fig. 23). These C values suggest the presence of some adsorbed intermediates; this inference is not, however, unambiguous since these C values are only marginally larger than the $C_{d.l.}$ values. A low value of the residual potential (0.4 V) indicates the absence of an oxide; this suggests, rather indirectly, that the added trifluoroacetic anhydride was effective in removing the last traces of water from the solution. An arrest is observed in the forced decay profiles (see photograph in Fig. 29) indicating, again, the presence of an electro-active intermediate on the electrode. However, the magnitude of $C_{max.}$ associated with this arrest is again only marginally larger than the $C_{d.l.}$ values and hence is not unambiguous evidence for deduction of the presence of adsorbed intermediates (Figs. 26,27). However, the value of Q (0.084 mC. cm.$^{-2}$) calculated from these arrests, although small, is by no means negligible (Table III). This Q value indicates that either

the electrode is partially covered by a rather small-sized ad-species or it is substantially covered by a bulky ad-species. The only species that may possibly be adsorbed on the electrode in this solution are $CF_3^\bullet$ and $CF_3COO^\bullet$. The possibility of $CF_3^\bullet$ being the ad-species is excluded on the grounds that it would be expected to be electro-inactive, by analogy with the case of platinum in this solution (see p. 189). Hence it may be concluded that $CF_3COO^\bullet$ is indicated as the ad-species, the values of Q expected, even when the electrode is substantially covered, would tend to be small; significant coverage of the electrode (i.e., as deduced from the somewhat high Tafel slopes and associated barrier-layer film) and small Q values (0.084 mC. $cm.^{-2}$) are indeed experimentally observed.

The presence on the electrode of bulky $CF_3COO^\bullet$ radicals (and of these radicals only) is also suggested by other experimental evidence. The shifts in $C_{max.}$ and $V_{C_{max.}}$ with increasing $i_{cath.}$ used in the forced discharge transient are in the theoretically-expected direction (46), i.e., increasing $i_{cath.}$ shifts $C_{max.}$ to higher values and $V_{C_{max.}}$ to more cathodic values (Figs. 26,27)*. This indicates that perhaps only one adsorbed species is present on the electrode (see section 2, this chapter). This again, suggests the absence of any co-adsorbed oxide and hence emphasizes the fact that, addition of small amounts of $CF_3CO.O.COCF_3$ did consume the

*This shift of $V_{C_{max.}}$ is again (cf. p. 207) much larger than that observed for the oxide species alone in H_2SO_4 solution and hence supports the presence of the Kolbe ad-species.

very last traces of water from the solution. In the cathodic reduction, more irreversibility than that observed with oxide alone on Pt is encountered and seems to be indicative of the presence of a species, e.g., $CF_3COO^{\bullet}$, different from surface oxide, as argued for other cases above. This may be seen by comparing the effect of $i_{cath.}$ on $V_{C_{max.}}$ for the present case (Fig. 26) and for the case of an oxide (Fig. 67). For a given increment in $i_{cath.}$ used in the transients, the shifts in $V_{C_{max.}}$ values to more cathodic potentials are substantially more pronounced when the electrode is covered by the "Kolbe species" (Fig. 26) than when it is covered by an oxide (Fig. 67).

An examination of the plot of Q *vs.* V_i (Fig. 29) shows that Q increases with increasing V_i. It may be noted that in the Kolbe region (V_i = *ca.* 2.25 V - Fig. 29) the Q value for the completely anhydrous solution is smaller than the Q values for the solutions containing traces or excess of water. This again suggests (assuming in both cases that the electrode is geometrically at full coverage at the given V_i) that the adsorbed radicals involved in the completely non-aqueous case are on the *average* much bulkier than those involved in solutions containing traces or excess of water. From this, a *tentative* conclusion may be drawn that in completely anhydrous solution, the species adsorbed on the electrode are *only* $CF_3COO^{\bullet}$ whereas in solutions containing traces or excess of water, co-adsorption by less bulky oxide

Figure 67

Platinum/1M H_2SO_4; a plot of $V_{C_{max.}}$ (or $E_{C_{max.}}$) vs. $i_{cath.}$

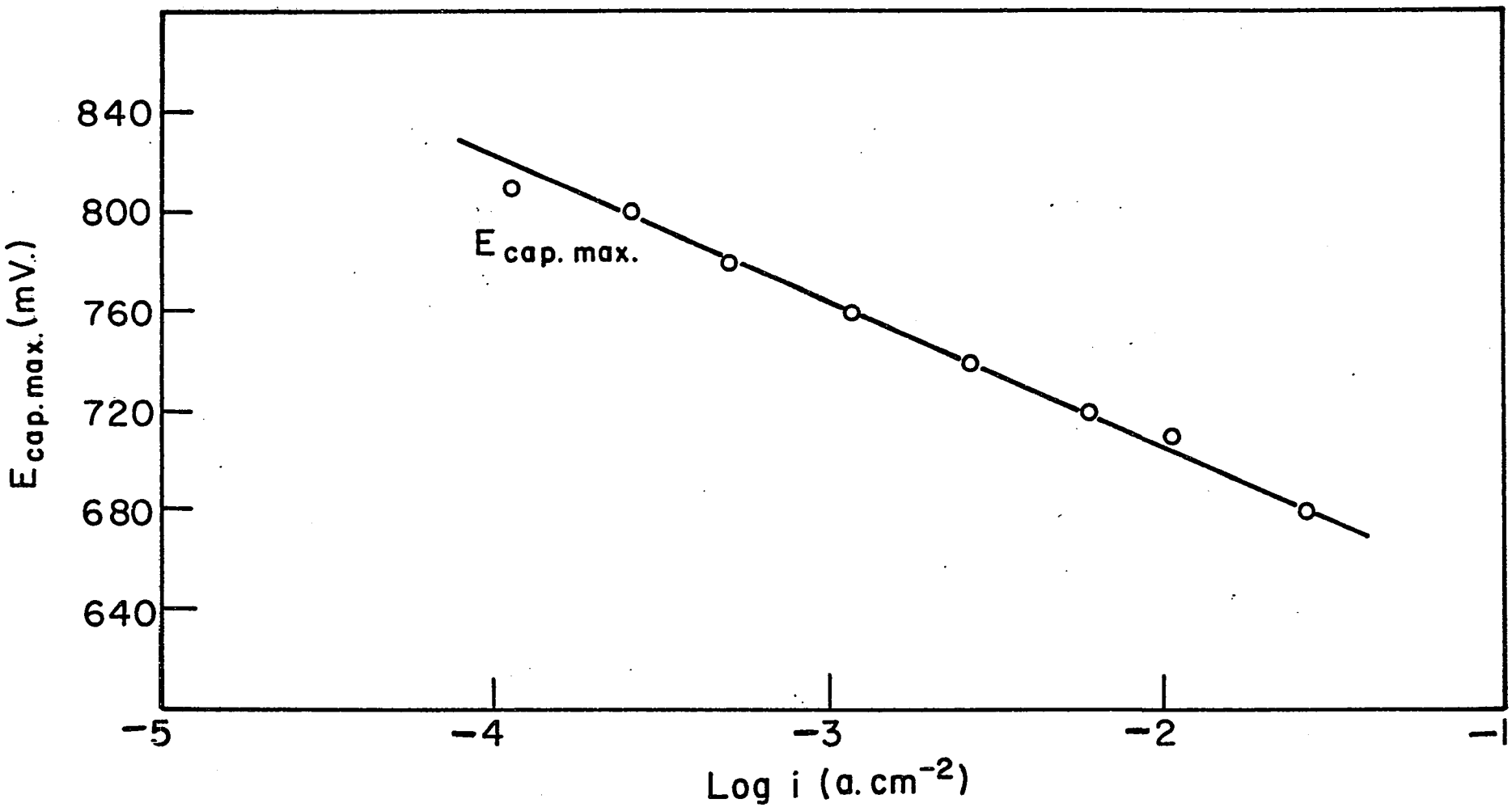
840
800
760
720
680
640
$E_{cap.max.}$ (mV.)
$E_{cap.\ max.}$
−5
−4
−3
−2
−1
Log i (a. cm^{-2})

species may be suspected with a consequent increase in the Q values. This point will be further elaborated, in relation to other experimental evidence, when mechanisms are discussed for the Kolbe reaction on gold in solutions of 1M KTFA in TFA containing traces or excess of water. In Fig. 29, three photographs showing comparatively the magnitude of arrests are also presented. It may be seen that the arrests expressed as $i_{cath.} \times \tau$ become larger with increasing amounts of water present in the solutions.

Hence it may be concluded that in completely anhydrous solutions, the Kolbe reaction proceeds on an electrode covered by an effective barrier-layer film of adsorbed $CF_3COO^{\bullet}$. A sequence of arguments closely analogous to those for the case of platinum in TFA solutions may easily be developed and the mechanism may be deduced in the following way.

An initial discharge step

$$CF_3COO^{\bullet} \rightleftharpoons CF_3COO^{\bullet}(M) + e \qquad (B)$$

would be followed by

$$CF_3COO^{\bullet}(M) + CF_3COO^{\bullet}(M) \longrightarrow C_2F_6 + 2CO_2 \qquad (D')$$

or

$$CF_3COO^{\bullet}(M) + CF_3COO^{-} \longrightarrow C_2F_6 + 2CO_2 + e \qquad (E)$$

Since the presence of a barrier-layer film of $CF_3COO^{\bullet}$ has been concluded, step B, which implies $CF_3COO^{\bullet} \longrightarrow 0$,

cannot be the rate-determining process. Step D', if the r.d.s., would give a Tafel slope equal to RT/F when $\theta_{CF_3COO^\bullet}$ is f(v) and a limiting current when $\theta_{CF_3COO^\bullet} \longrightarrow 1$; neither of these possibilities is compatible with the experimentally observed Tafel slope (0.16 V) on an electrode covered by a barrier-layer film. Step E, if rate-determining, gives a slope of 2RT/3F (not at all close to the experimental Tafel slope) under conditions of <u>low coverage</u> (which is, again, experimentally untenable); the only remaining possibility to be considered is E being the r.d.s. when $\theta_{CF_3COO^\bullet} \longrightarrow 1$. The predicted Tafel slope in this case is 2RT/F. If the presence of an effective potential barrier involving a film of $CF_3COO^\bullet$ is invoked again, the experimental slope of 0.16 can be reconciled with the predicted value. (See section 2, this Chapter). The argument for the barrier-layer film in this case, it is to be noted, is not so clear cut as in the other cases discussed above since b is not so anomalously high.

<u>Reaction in Nominally Anhydrous Solutions</u>

The experimental evidence for this case has been summarised in Table III.

In solutions presumably containing traces of water, the features of the steady-state current-potential relation are characteristically different from those associated with the current-potential relations for completely anhydrous solutions

(Fig. 12). Again C_2F_6 is the product of the reaction. The presence of traces of water seems to give rise to a hysteresis between ascending and descending current-potential relations; a characteristic inhibition inflexion appears around 1.8 V; also, the value of the rest potential increases to 0.9 V. All these features suggest the presence of a co-adsorbed surface oxide. The value of the Tafel slope (0.175 V). suggests, in this case also, the presence of a film having some characteristicsof a barrier layer.

On open-circuit decay of the anode potential, an arrest is observed. The values of capacity calculated from the open-circuit decay profiles depend on the initial polarisation potential. For example, the d.l. capacity (ca. 60 μF. cm.$^{-2}$) is observed when V_i = 2.5 V; however, when V_i = 1.8 V, the value of $C_{max.}$, 225 μF. cm.$^{-2}$ suggests the presence of an oxide (or other species) on the electrode (Fig. 24). The residual potential is ca. 0.9 V, which again suggests that the electrode surface is partly covered by an oxide. The presence of an appreciable arrest in the forced decay profile (see photograph in Fig. 29) indicates the presence of some electro-active ad-species. The appreciable values of C (Fig. 31) indicate that even traces of water in the solution give rise to ad-species with which these high values (ca. 500 to 1500 μF. cm.$^{-2}$) of pseudo-capacity are associated. Although

the shifts in $V_{C_{max.}}$ with increasing $i_{cath.}$ are in the predicted direction (Fig. 30), the shifts in $C_{max.}$ values themselves are not systematic which suggests that perhaps more than one species is adsorbed, as argued previously.

Important evidence suggesting co-adsorption (with an electro-active "Kolbe species", i.e., $CF_3COO^{\bullet}$) of an oxide is as follows: in the presence of traces of water, the overall rate at a given potential is lower than that in the completely anhydrous solution (Fig. 12); however, the value of Q (= 0.175 mC. cm.$^{-2}$) is twice as large, suggesting that a part of this charge is associated with a species which originates from water and inhibits the Kolbe reaction, e.g., a surface oxide.

When the relation between Q and V_i is examined, it is found that Q increases with V_i (Fig. 29). However, in the Kolbe region (>2.25 V), Q has a greater value in this solution than in completely anhydrous ones. Assuming that the electrode is completely covered in both these cases, (since barrier-layer films are indicated because the Tafel slopes are >2RT/F, this assumption is reasonable), higher Q values suggest the presence, on the average, of less bulky ad-species. Since the only possible ad-species that may be present are $CF_3COO^{\bullet}$ and an oxide ($CF_3^{\bullet}$ is excluded since it would probably be electro-inactive as argued previously), higher Q values for a given coverage suggest some contribution from co-adsorbed oxide.

From the foregoing discussion, it may be concluded that in nominally anhydrous solutions of 1M CF_3COOK in CF_3COOH the Kolbe reaction proceeds on a gold electrode covered by an effective barrier-layer film of $CF_3COO^{\bullet}$ with some co-adsorbed oxide. The mechanism of the reaction, it is suggested, is hence the same as for the closely analogous case of platinum (see pp. 197) in nominally anhydrous TFA solutions.

Reaction in Aqueous Solutions

The experimental evidence for this case has been summarised in Table III. C_2F_6 is again the product with oxygen.

In general, in aqueous solutions, co-adsorption by an oxide is substantially greater than in the nominally aqueous media with a consequently increased inhibition of the Kolbe reaction. This is supported by the following evidence.

(a) In the steady-state current-potential relations (Fig. 12), larger hysteresis between ascending and descending curves is observed; a higher rest potential (1.25 V) and a lower rate at a given potential, compared with the rate in completely and nominally anhydrous solutions under corresponding conditions, are found.

(b) The values of both the pseudo-capacity (2500 $\mu F. cm.^{-2}$) (Fig. 25) obtained from open-circuit e.m.f. decay profiles and the residual potential (1.3 V) are higher than in the non-aqueous case.

(c) Very high values of Q are obtained from the forced decay profiles (1.09 mC. cm.$^{-2}$) and very high values (2250 to 7500 μF. cm.$^{-2}$) of $C_{max.}$ (Fig. 34) are found.

(d) Any definite trend of shifts in $C_{max.}$ with increasing $i_{cath.}$ used in the cathodic transients is difficult to establish (Fig. 33); hence, the presence of more than one species is suspected, e.g., an oxide co-adsorbed with $CF_3COO^{\bullet}$ radicals.

(e) In the plot of Q vs. V_1 (Fig. 29), very high Q values at higher potentials suggest co-adsorption of appreciable amounts of an oxide.

Here again an effective barrier-layer film of $CF_3COO^{\bullet}$ is suggested by the high values (0.17 V) of the Tafel slopes. The mechanism for the Kolbe reaction in this case is hence regarded as the same as in the case of the nominally anhydrous solutions discussed above. However, the co-adsorption by the oxide and the consequent decrease in rate (at a given potential) is more pronounced in this case than in the other.

Role of Oxide

It has been concluded in the foregoing discussion that the role of oxide, which originates from traces or excess of water present in the solutions, in the Kolbe reaction on gold (as on Pt) is a purely inhibitory one. This is corroborated by the following further evidence:

(a) In Fig. 68 a family of curves of Q *vs.* rate has been shown for the three types of solutions studied. Each curve is plotted for a given value of potential in the potential range over which a Tafel line for the Kolbe reaction is obtained, i.e., *ca.*>2.1 V. Each curve is drawn through three points where each point represents a value of Q (obtained from the forced-decay profiles) plotted against the corresponding rate at the given potential (obtained from the steady-state current-potential relations) for the completely anhydrous, the nominally anhydrous and the aqueous solution, respectively. It is to be noted that at a given potential, proceeding in the sequence completely anhydrous ⟶ nominally anhydrous ⟶ aqueous solution, an *increase* in Q and a *decrease* in rate arises. This shows rather directly that with increased Q associated with increased co-adsorption by oxide (arising from increasing amounts of H_2O in the solution) the rate correspondingly decreases, i.e., the surface oxide plays an inhibitory role. The effects are larger at higher anodic potentials.

(b) In Fig. 69, a family of curves is shown which illustrates the same point in a different way. Each of the three solid lines represents the Q *vs.* rate relation covering the whole Tafel region (and a small upper part of the transition region) for completely anhydrous, nominally anhydrous and aqueous solutions, respectively. Dotted lines represent the corres-

Figure 68

Gold/1M KTFA in TFA: plots of Q vs. rate at various anodic potentials for completely anhydrous (△), nominally anhydrous (□) and aqueous (○) solutions.

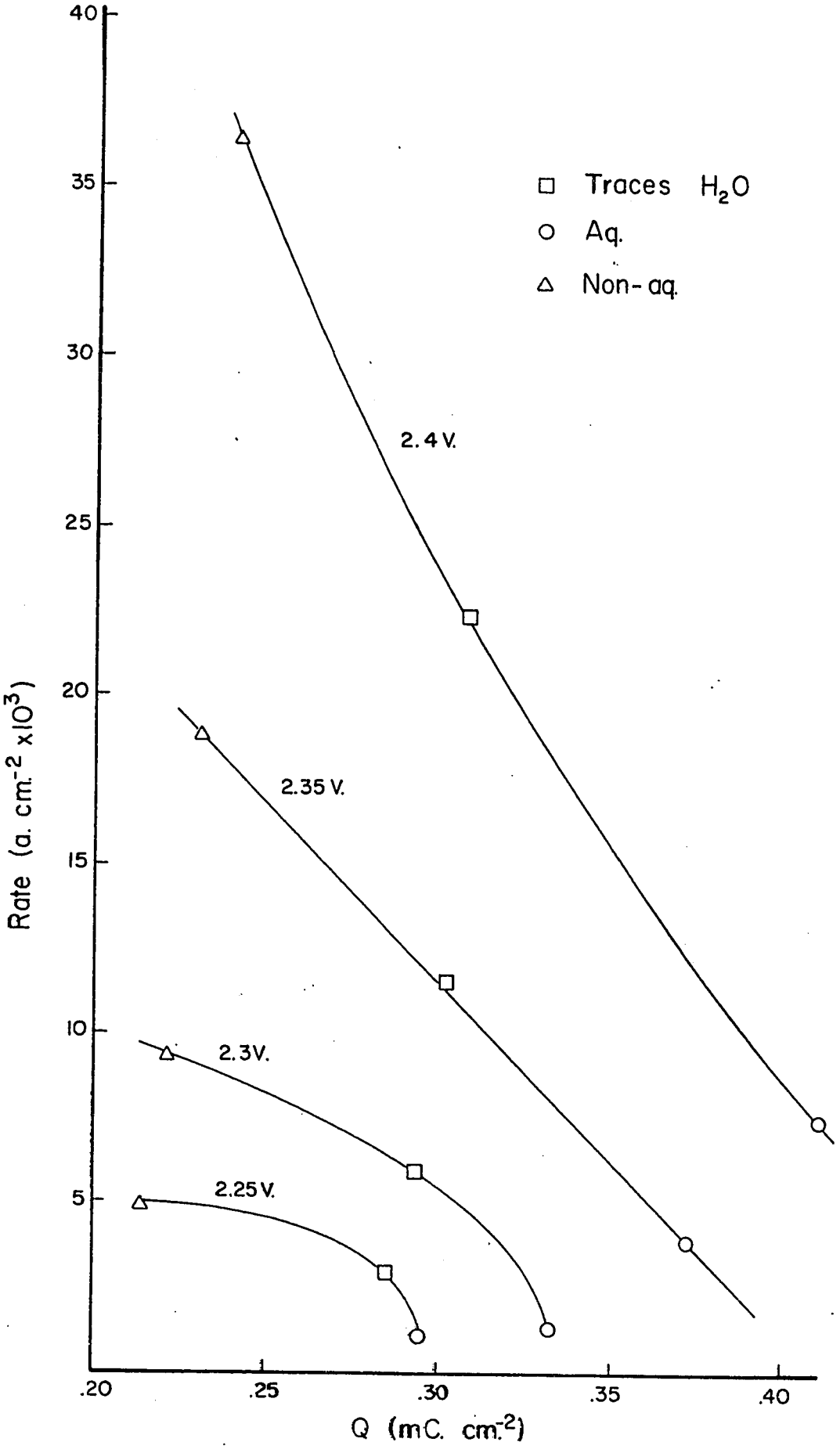
40
35
30
25
20
15
10
5
Rate (a. cm.$^{-2}$ x10^{3})
□ Traces H_2O
○ Aq.
△ Non-aq.
2.4 V.
2.35 V.
2.3V.
2.25 V.
.20
.25
.30
.35
.40
Q (mC. cm.$^{-2}$)

Figure 69

Gold/1M KTFA in TFA: plots of Q vs. rate for completely anhydrous (o—o), nominally anhydrous(•——•) and aqueous(▲——▲) solutions: the dotted lines represent the corresponding relations in which the rates have been "normalised" to appropriate potentials.

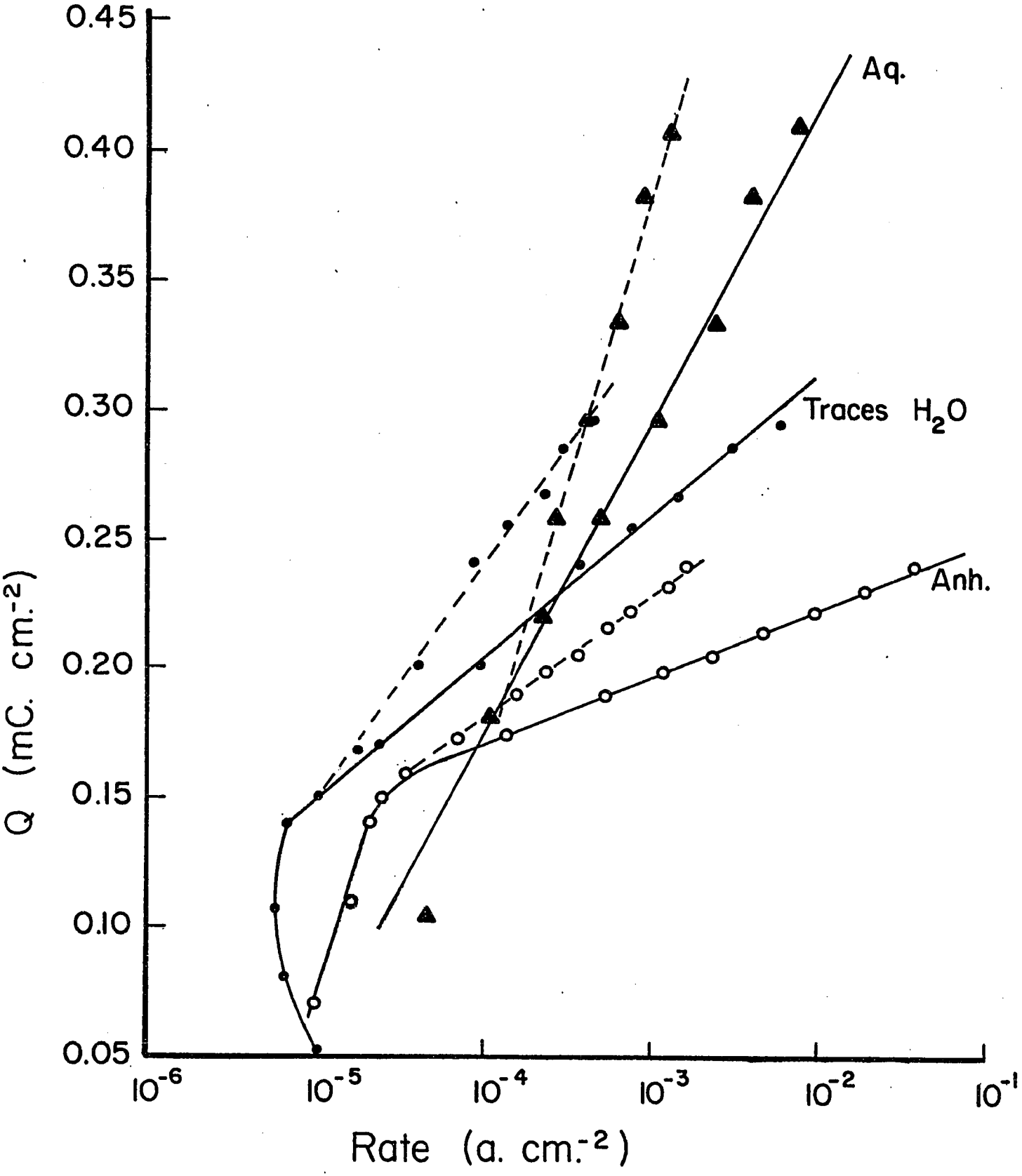
0.45
0.40
0.35
0.30
0.25
0.20
0.15
0.10
0.05
Q (mC. cm.-2)
Aq.
Traces H2O
Anh.
10-6
10-5
10-4
10-3
10-2
10-1
Rate (a. cm.-2)

ponding rates that would arise if they were empirically normalised w.r.t. potential to some arbitrary potential which is chosen to be that corresponding to commencement of the Tafel region (compare Fig. 65). Hence each dotted line represents the increase in rate with increasing Q (Q in turn increases due to increasing V_i) when no contribution to the increase in rate arises from increasing potential through the $e^{V/b}$ factor. It is to be noted that the value of Δ rate/ΔQ decreases with increasing amounts of water present in the solution, i.e., with increasing amounts of H_2O in the solution, an increasing portion of the total Q arises from a species which does not contribute to an increase in rate of the Kolbe reaction, and perhaps even inhibits it by rendering unavailable the sites required for it, and/or changing the activation energy of reaction steps.

Again, any possible pathways for the Kolbe reaction involving the oxide as a direct reactant species must be rejected for reasons similar to those discussed for the case of platinum (see page 211).

(iii) Platinum in Potassium Acetate-Acetic Acid Solutions Reaction in Anhydrous Solutions ("Vacuum Run")

The experimental evidence for this case has been summarised in Table IV.

In the completely anhydrous solutions, a Tafel slope of 0.14 V is obtained which is only marginally higher than 2RT/F. The rest potential (0.2 V) suggests the absence of an oxide and hence that the experiments made in the "vacuum cell" were effectively conducted under very anhydrous conditions; this conclusion is supported by the complementary evidence that addition of controlled small amounts of H_2O to the solution raised the value of the rest potential to 1.1 V (Table I). The hysteresis and the transition region observed (Fig. 13) in this case are believed to arise from some trace impurities in the solutions and <u>not</u> to the fact that the electrode perhaps may be completely covered. This conclusion is based on the following experimental evidence:

(a) The Tafel slopes observed are not high enough to suggest the presence of an effective barrier-layer film. The minimum value of Tafel slopes which may suggest that a part of the metal-solution potential drop operates across an effective barrier-layer film has been chosen, rather arbitrarily, to be 5RT/2F (apparent $\beta = 0.4$) in the present work.

(b) The values of C ($< 100 \mu F.\ cm.^{-2}$) and Q ($15 \mu C.\ cm.^{-2}$) obtained are too small to suggest the presence of an electro-active ad-species (Table IV).

(c) The possible presence of an electro-inactive ad-species is excluded on the grounds that such a species would be strongly adsorbed and hence a substantial fraction of the total metal-solution potential difference would fall across such a barrier-layer film of irreversibly adsorbed electro-inactive species; this, in turn, would tend to result in high Tafel slopes. However, such an effect with adsorbed $CH_3^{\bullet}$ radicals would be expected to be less than with $CF_3^{\bullet}$ radicals owing to the smaller dipole moment.

On open-circuit decay of the anode potential, a short arrest is observed on platinum in completely anhydrous solutions. However, the values of $C_{max.}$ are only of the order of $C_{d.l.}$ and no residual potential is observed; this suggests the absence of any adsorbed intermediates. This conclusion is supported by the following two additional facts: (a) the values of C obtained from the forced-decay profiles are again of the order of $C_{d.l.}$; and (b) the values of Q obtained from these transients are negligible (15μC. cm.$^{-2}$) (Fig. 37).

In the potentiodynamic profiles, no peaks are observed; however, a normal separation between the cathodic and anodic sweeps arises and the values of C, calculated at the point of maximum separation, are only of the order of $C_{d.l.}$

again. The "peak" current (measured at the centre of the sweep range) vs.$(dV/dt)^{\frac{1}{2}}$ plot gives a straight line (Fig. 59) indicating a non-charging process. It appears that this effect may be associated with formation of impurities possibly formed in the closed cell by the cyclic polarisation. The potentiodynamic profiles, thus indicate again (in a somewhat negative way) the absence of any electro-active adsorbed intermediates.

In summary, all the experimental evidence presented indicates the absence of any electro-active or electro-inactive adsorbed intermediates; also, a Tafel slope (0.14 V) only marginally higher than 2RT/F is experimentally observed. The examination of Table VIII clearly shows that the experimentally-observed conditions of $\theta \longrightarrow 0$ and $b = 2RT/F$ are satisfied only when an initial rate-determining discharge step [i.e., $CH_3COO^- \rightleftharpoons CH_3COO^{\bullet}(M)+e$] is followed by any of the subsequent radical-removing steps having higher rate constants than that of the discharge step. Thus, the mechanism of the Kolbe reaction in this case seems to be one involving initial discharge as the r.d.s. The facts and their interpretation in this case are simpler and more unambiguous than in the other cases discussed.

Reaction in Aqueous Solutions

The experimental evidence for this case has been summarised in Table IV.

In aqueous solutions there is a substantial hysteresis between ascending and descending i-V relations (Fig. 13); also the magnitude of the rest potential (1.25 V) immediately suggests, in a preliminary way, the presence of oxide as one of the ad-species. Several Tafel regions are observed. The values of the Tafel slopes in the "Kolbe" region ($>$ 2.2 V) are substantially higher than 2RT/F and hence suggest the presence of a barrier-layer film. The value of b is 0.26 V in the potential region 2.2 V to 2.5 V and 0.165 V beyond 2.5 V; this change of b value in this case suggests, perhaps, that the fraction of the total metal-solution potential drop that operates across the barrier-layer film of the ad-species is smaller above 2.5 V than below this potential. This may perhaps be associated with a change in the conducting properties or composition of the film of ad-species at higher fields. The exact reason for this change of b value at 2.5 V is, however, difficult to interpret. Similar comments also apply to the b value (0.2 V) associated with the Tafel region observed between the potentials 1.8 V to 2.2 V below the potential for commencement of the Tafel region for the Kolbe reaction (ca. 2.2 V).

On open-circuit decay of anode potential no arrest is observed and the C values calculated from these profiles are of the order of $C_{d.l.}$. However, a residual potential (0.79 V), is observed and is indicative of the presence of an adsorbed species. On forced decay from this residual potential, two appreciable arrests are observed in the cathodic discharge curve showing that the ad-species, with which this residual potential is associated, is an electro-active species. Very high values of $C_{max.}$ ($\underline{\sim}$ 6000 μF. cm.$^{-2}$) are associated with these arrests; the exact values of the $C_{max.}$ depend on the initial polarisation potential and are of relatively minor significance (Fig. 36). The values of $V_{C_{max.}}$ for the main arrest are around 0.6 V (Fig. 36) which again suggests the presence of an oxide. The values of $V_{C_{max.}}$ for the second arrest are around 0.25 V which suggests (but not unambiguously) that this arrest perhaps is associated with the adsorption of hydrogen. The ratio of charges Q_1 ($V_{C_{max.}}$ = 0.6 V) and Q_2 ($V_{C_{max.}}$ = 0.25 V) associated with the two peaks is equal to 1.46; this value of the ratio Q_1/Q_2 suggests that the arrest with $V_{C_{max.}}$ = 0.6 V is perhaps a "modified" (mixed) oxide-reduction arrest and the one with $V_{C_{max.}}$ = 0.25 V is perhaps a slightly displaced H-adsorption arrest. The ratio Q_1/Q_2 (= 1.48) may alternatively suggest that perhaps only a part of the electrode is covered by oxide since for a smooth Pt

electrode completely covered by oxide the ratio of $Q_{Ox.}/Q_H$ is already ca. 4 at V_i = 2.0 V (76) and would be expected to be still higher at a value of V_i = 2.5 V comparable with that attained in the Kolbe reaction.

The forced-decay profiles also show appreciable arrests. In this case, the detailed significance of the cathodic transients has been examined by polarising the electrode at two different values of initial polarisation potential, V_i; one of the V_i values (1.0 V) was chosen to lie well below the Kolbe region, whereas the second value of V_i (2.5 V) was well in the Faradaic Kolbe region. This approach was chosen to characterise the co-adsorbed oxide that may be present in the Kolbe region by the indirect procedure of proving its presence at much lower potentials, i.e., potentials at which the presence of oxide can be established unambiguously.

When V_i = 1.0 V, significant arrests are observed in the forced decay profiles. Two large and one small $C_{max.}$ with $V_{C_{max.}}$ = 0.5 V, 0.225 V, and 0.025 V, respectively, are observed (Figs. 38,39). The values of charge associated with these arrests are Q_1 = 0.15 mC. cm.$^{-2}$ ($V_{C_{max.}}$ = 0.5 V), Q_2 = 0.22 mC. cm.$^{-2}$ ($V_{C_{max.}}$ = 0.225 V), Q_3 = 0.17 mC. cm.$^{-2}$ ($V_{C_{max.}}$ = 0.025 V), respectively. From the $V_{C_{max.}}$ values, it seems likely that $Q_1 = Q_{oxide}$ and Q_2 and Q_3 are associated with the usual two hydrogen peaks for platinum; the ratio $Q_{Ox.}/Q_H$,

then, is equal to 0.38. The fact that the surface oxide species may be present only in relatively small quantities, as is suggested by the $Q_{Ox.}/Q_H$ ratio = 0.38 [normally it is ca. 0.7] (63), is not surprising since the V_i value is small (1.0 V). The values of $C_{max.}$ for the oxide arrests range between 1250 μF. cm.$^{-2}$ and 1500 μF. cm.$^{-2}$, depending on the $i_{cath.}$ used (Figs. 38,39); these $C_{max.}$ values are of the magnitude usually observed in the reduction of surface oxides on platinum.

The three capacity maxima tend to merge into one another at higher $i_{cath.}$ values (Fig. 38); this is the reason why the effect of $i_{cath.}$ on the value of $C_{max.}$ and $V_{C_{max.}}$ does not exhibit a consistent trend (Fig. 39).

When the V_i = 2.5 V, two large arrests are observed. The $V_{C_{max.}}$ values for these arrests are 0.5 V and 0.2 V; by analogy with the arguments developed in the discussion on cathodic forced decay from the residual potential (p.232), it may be concluded that these two arrests are due to a "modified" (mixed) oxide reduction process ($V_{C_{max.}}$ = 0.5 V) (see below) and a hydrogen adsorption process ($V_{C_{max.}}$ = 0.2 V) respectively. The magnitude of $C_{max.}$ (Figs. 42,43) for the "oxide" reduction peak ($V_{C_{max.}}$ = 0.5 V) is between 4500 μF. cm.$^{-2}$ and 5000 μF. cm.$^{-2}$; these high values of $C_{max.}$ are quite commonly observed when appreciable coverage by ad-species is involved.

The ratio Q_1/Q_2 (for V_i = 2.5 V) is equal to 1.86 where Q_1 is associated with the "modified" (mixed) oxide arrest ($V_{C_{max.}}$ = 0.5 V) and Q_2 is due to the slightly displaced H-adsorption peak ($V_{C_{max.}}$ = 0.2 V); if the peak at $V_{C_{max.}}$ = 0.5 V were entirely due to an oxide, the Q_1/Q_2 ratio to be expected would be greater than 4 (76a). Hence Q_1 refers either to partial coverage of the electrode by oxide (with part of the surface bare) or to the substantial coverage by a bulky "substituted" oxide [since $V_{C_{max.}}$ is very close to the value observed for pure oxide on Pt in H_2SO_4 (63)]. This substituted oxide may be composed of $CF_3COO^{\bullet}$ with some co-adsorbed oxide (Fig. 65). The latter possibility is more plausible for the following reasons.

(a) If it were assumed that only oxide is present on the electrode surface, the electrode would be expected to be completely covered by this oxide at the V_i (= 2.5 V) used. Thus, a higher ratio (> 4) of Q_1/Q_2 would be expected. It is impossible to conceive that at these high potentials an oxide would be present on a part of the surface with a significant fraction remaining bare.

(b) If it were assumed that only oxide is present on the electrode, it would be difficult to explain the high Tafel slopes observed since the known presence of an oxide on Pt does not result kinetically in a barrier-layer film, at least in the anodic oxygen evolution reaction (80).

(c) If oxide were the <u>only</u> species present on the electrode, the mechanism by which the Kolbe reaction could proceed under these conditions would be only the one involving the initial discharge step as the rate-determining process. It will be shown below, however, that the initial discharge step <u>cannot</u> be rate-determining in this case; hence a subsequent step, which must normally involve <u>some</u> coverage by a Kolbe species must be rate-determining.

(d) In the cathodic reduction, more irreversibility than that usually observed with oxide on Pt is encountered. This can be seen by comparing the effect of $i_{cath.}$ on $V_{C_{max.}}$ for the present case (Fig. 43) and for the case of the surface oxide on Pt (Fig. 67). For a given increment in the $i_{cath.}$ used in the transients, the cathodic shifts in values of $V_{C_{max.}}$ are substantially more pronounced when the electrode is covered by the "Kolbe" species supposedly involved in the present case (Fig. 43) than when it is covered by an oxide (Fig. 67). Hence the electro-active adsorbed species in the present case consists, at least partly, of a species other than oxide.

Hence it may be concluded that the Q_1 is associated with substantial coverage by a species such as $CH_3COO^{\bullet}$ together with some co-adsorbed oxide. The conclusions that <u>both</u> $CH_3COO^{\bullet}$ and a co-adsorbed oxide are present on the electrode and that the low values of Q_1/Q_2 ratio are <u>not</u> due to the fact

that the entire electrode surface may perhaps be covered by the bulky $CH_3COO^{\bullet}$ species alone, is supported by the following further evidence:

(a) The presence of co-adsorbed oxide that would arise from water in the aqueous solutions, would be expected to decrease the rate of the Kolbe reaction at a given potential*. This indeed is experimentally observed.

(b) The presence of more than one species associated with the arrest for the "modified" (mixed) oxide is also suggested by the effect of $i_{cath.}$ on $C_{max.}$ and $V_{C_{max.}}$. Increasing $i_{cath.}$ shifts both values of $V_{C_{max.}}$ to more cathodic potentials due to "overpotential" effects (46) (Fig. 43); however, the effect of $i_{cath.}$ on the values of $C_{max.}$ themselves is more revealing. Increasing $i_{cath.}$ shifts one $C_{max.}$ (i.e., for the H-adsorption peak at $V_{C_{max.}} = 0.2$ V) to higher values as predicted (46) (Fig. 43); however, the dependence of the second $C_{max.}$ (i.e., the one for the "substituted" oxide peak with $V_{C_{max.}} = 0.5$ V) on $i_{cath.}$ is not a systematic one (Fig. 43), thus suggesting that more than one species may be present, e.g., $CH_3COO^{\bullet}$ with an oxide.

---

*The possibility of any mechanism for the Kolbe reaction involving oxide directly as one of the reactant species may be excluded on the basis of arguments developed for the case of Pt in TFA solutions (p. 211).

(c) If the bulky $CH_3COO^\bullet$ radical were the only adsorbed species present, the ratio Q_1/Q_2 would be expected to be less than unity. This, it will be recollected, is not experimentally observed.

In the foregoing discussion, it has been assumed that the Kolbe ad-species present on the electrode (together with the co-adsorbed oxide, of course) in the present case is $CH_3COO^\bullet$ and not $CH_3^\bullet$. The possibility of $CH_3^\bullet$ being the ad-species in the present case is excluded on the basis of the following considerations.

(a) If $CH_3^\bullet$ were the adsorbed species, it would be expected to be adsorbed on the platinum anode through the formation of a "Pt-C" bond, since C is the electron deficient atom. "Pt-C" bonds are known to be extremely stable (77). Hence $CH_3^\bullet$ might be expected to behave as an electro-inactive radical. If $CH_3^\bullet$ were an electro-inactive radical, as supposed above, it would most likely be adsorbed also on Pt in anhydrous acetate solutions (cf. the case of Pt in anhydrous TFA solutions). Since no barrier-layer of electro-inactive $CH_3^\bullet$ radicals is indicated by the results for the anhydrous solutions (where it is most likely to be involved), there is no reason to believe that such a radical is the ad-species in the present case of aqueous acetate solutions.

(b) However, if it is now assumed (for the purposes of discussion)

that $CH_3^\bullet$ were perhaps an electro-active species (unlike $CF_3^\bullet$) and was co-adsorbed with oxide in the present case, a separate peak for the reduction of $CH_3^\bullet$ would be expected to appear in the cathodic transients and potentiodynamic profiles since $CH_3^\bullet$ is quite different from an oxide and would be expected to be reduced at a different potential. However, no such separate peak for the reduction of the Kolbe species is observed. Only one reduction peak appears in cathodic transients (Fig. 44) and one in potentiodynamic profiles (Figs. 61, 62, 63) around 0.5 V* suggesting that the Kolbe species involved is very similar to the co-adsorbed oxide in its reduction behaviour, i.e., $CH_3COO^\bullet$ is the ad-species and it is adsorbed on the substrate metal through "Pt-O" bonds.

Hence, from the foregoing discussion, it may be concluded that the electrode, in the present case, is substantially covered by a barrier-layer film of $CH_3COO^\bullet$ together with some co-adsorbed oxide (see Fig. 64).

A plot of Q *vs.* V_1 (Fig. 44) shows that Q increases with increasing V_1 up to 2.0 V but above 2.0 V, Q becomes insensitive to any further increase in V_1. This again suggests that the Kolbe reaction, which commences at potentials greater than *ca.* 2.2 V, is proceeding on a completely covered electrode.

---

*The hydrogen peaks at more cathodic potentials are excluded from the present argument.

The values of Q and $V_{C_{max.}}$ obtained from the charging peaks in the potentiodynamic profiles corroborate the above conclusions. The general behaviour of the potentiodynamic profiles is depicted in Fig. 61 in which peaks for Pt in potassium acetate and sulphuric acid solutions are compared. The general similarity of the shapes of the peaks, and the potentials at which they appear, strongly suggests that the peaks for acetate solutions are "modified" peaks for oxygen and hydrogen deposition and desorption processes. The profiles in Fig. 61 may also be compared, for identification purposes, with the schematic diagram in Fig. 1.

If Q_A is the charge for the oxide reduction peak in the potentiodynamic profiles, and Q_B the charge for the hydrogen deposition peak, Q_A/Q_B ratios may be compared for several relevant profiles (Table VI). It may be seen in Table VI that the ratio Q_A/Q_B ($\doteq$ 1.5) for the case of Pt in aqueous CH_3COOK solutions is noticeably lower than the Q_A/Q_B ratio, for the case of Pt in H_2SO_4 (ca. 2.4). This Q_A/Q_B ratio, it may be recalled, has the same significance as the Q_1/Q_2 ratio discussed in the case of the cathodic transients; thus, for example, the value of the ratio Q_A/Q_B (= 1.85) obtained at a slower sweep rate (dV/dt = 0.73 V $sec.^{-1}$) is, in fact, identical with the Q_1/Q_2 ratio obtained from the cathodic transients (V_1 = 2.5).

Since the ratio Q_A/Q_B for Pt in H_2SO_4 solution is increased by 57.7% over that for Pt in acetate solution (measured

at the same dV/dt), it may be concluded once again that in the aqueous acetate solutions the surface coverage indicated by the peak with $V_{C_{max.}} = 0.55$ V is associated with species which are on the average bulkier than the oxide species, so that $CH_3COO^{\bullet}$ co-adsorbed with oxide may be the species involved. Any possibility of a part of the surface being bare or covered by $CH_3^{\bullet}$ is excluded on the basis of arguments elaborated previously in the foregoing discussion.

A comparison of $C_{max.}$ [where in this case $C_{max.} = i_{max.}/(dV/dt)$] values for the peaks in the potentiodynamic profiles reveals a similar trend. Thus the value of $C_{max.}$ for the oxide reduction peak at Pt in H_2SO_4 is almost twice that for Pt in aqueous CH_3COOK in the same reduction region, whereas the $C_{max.}$ values for the hydrogen deposition peaks in the two cases are of comparable magnitude for the same range of potentials scanned and for similar sweep rates [Table VII (B)]. This again suggests that for the case of Pt in aqueous CH_3COOK solution, the reduction peak is, in fact, one for a reduction process involving a "modified" (mixed) oxide (see Fig. 64).

From the foregoing discussion, it may be concluded that the Kolbe reaction on Pt in aqueous CH_3COOK solutions proceeds on a surface covered by a barrier-layer film of $CH_3COO^{\bullet}$ together with appreciable co-adsorbed oxide (hence the initial discharge step cannot be rate-determining); the high Tafel

slopes observed can then be explained on the basis discussed for the closely analogous case of Pt in nominally aqueous TFA solutions (p. 197).

(iv) Gold in Potassium Acetate-Acetic Acid Solutions

The experimental results for this case have been summarised in Table V.

Reaction in Anhydrous Solutions

The reaction in anhydrous solutions in the present case was not carried out in vacuo and the solutions thus were susceptible to slight contamination by diffusion of traces of atmospheric moisture. That these minute traces of moisture were indeed present in the solutions when the measurements were carried out is indicated, in a preliminary way, by:

(a) Hysteresis between the ascending and descending i-V relations (Fig. 14).

(b) The rest potential of ca. 1.3 V.

(c) The residual potential of ca. 1.28 V.

On forced decay from the residual potential, two arrests are observed which manifest themselves as two $C_{max.}$ in the C-V profiles (Fig. 45). The values of the two $V_{C_{max.}}$ are 0.78 V ($C_{max.}$ = 1150 μF. cm.$^{-2}$) and 0.44 V ($C_{max.}$ = 2050 μF. cm.$^{-2}$); these values of $V_{C_{max.}}$ suggest that the two $C_{max.}$ are associated with the reduction of two oxides with different formal stoichiometry. The large Q values (0.839 mC. cm.$^{-2}$)

again suggest the presence of appreciable amounts of adsorbed oxide and the absence of any significant amounts of bulky adsorbed Kolbe species. The C and Q values obtained from the forced decay profiles, again, are very high (Fig. 46* ; Table V). The $V_{C_{max.}}$ values are in the range 0.18 V to 0.88 V depending on the $i_{cath.}$ used in the transients (Figs. 46, 47). The effect of $i_{cath.}$ on $V_{C_{max.}}$ is in the predicted direction (Fig. 47); however, the shifts in $C_{max.}$ values with increasing $i_{cath.}$ do not show a systematic trend perhaps due to co-adsorption with oxide of small amounts of Kolbe ad-species. The conclusion that these high Q and C values are associated with the presence of substantial amounts of adsorbed oxide and <u>not</u> a Kolbe ad-species is supported by the following arguments.

(a) If the Q and C values were associated with substantial amounts of $CH_3COO^{\bullet}$ or $CH_3^{\bullet}$, a barrier-layer film would be encountered by the charge transfer process, resulting in Tafel slopes $> 2RT/F$; this has been consistently observed in all previous cases in the present investigation, as mentioned in the foregoing discussion. The fact that the experimental Tafel slope in the present case is equal to 0.11 V indicates the absence of any such barrier-layer film and hence of adsorbed

*The sharp $C_{max.}$ peaks in Fig. 46 are usually indicative of a bulk type layer of the ad-species, e.g., oxide.

"Kolbe" species.

(b) When the plot of Q vs. V_i is examined, it is found (Fig. 49) that Q increases with increasing V_i below the potential of commencement of the Tafel region for the present case (1.9 V); however, at 1.9 V, with increasing V_i, Q begins to decrease. If Q were associated with a Kolbe ad-species, it would tend to increase with V_i well into the Kolbe region ($>$2.1 V).

Hence it may be concluded that the electrode is substantially covered by adsorbed oxide originating presumably from traces of water in solution. Since the presence of any adsorbed "Kolbe" species is not indicated, the r.d.s. must be such as involves a coverage by Kolbe species approaching zero. The only possible step fulfilling this requirement is the initial discharge step (step B, Table VIII). If the initial discharge step were rate-determining, the predicted value of the Tafel slope would be 2RT/F (Table VIII), in excellent agreement with the experimental value of 0.11 V(Table V) (cf. the case of Pt in anhydrous acetate solutions for which similar conclusions were reached; p. 227).

Reaction In Aqueous Solutions

The characterisation of the products of electrolysis in this solution shows that the Kolbe reaction does not proceed significantly on gold in aqueous solution (1M CH_3COOK + 1M CH_3COOH). This is in agreement with the conclusions of

previous investigators*(3,7,8). Only oxygen could be detected as a reaction product. (C_2F_6 is, however, a product at gold in aqueous TFA - see section 3(ii) in this Chapter and reference 2).

Although Kolbe products could not be detected, it was considered that an electrochemical investigation of gold in this solution might reveal some information which could be relevant to the study of the Kolbe reaction in a complementary way.

A comparison of the steady-state i-V relations obtained in non-aqueous and aqueous solutions (Fig. 14) immediately reveals that the two relations refer to two different reactions. Thus, the rate at a given potential is <u>higher in the aqueous</u> than in the non-aqueous medium, whereas in all the other cases examined, (Figs. 11,12,13), the presence of traces or excess of water diminishes the rate. This suggests that in the present aqueous solution the measured current density refers to the rate of a process different from the one proceeding in other cases discussed. Thus the i-V relations confirm the conclusions drawn from analysis of the products of electrolysis.

---

*Sugino and co-workers (60) mention very briefly that they obtained Kolbe products from electrolysis of aqueous acetate solution on gold. The details of their work, however, have not been published and were not available even through personal communication.

The Tafel region observed in this case (Fig. 14) is associated with the oxygen evolution reaction but the Tafel slope observed in this case (0.09 V) is, however, substantially greater than that observed for the oxygen evolution reaction on gold (0.045 V) in acid solutions (73).

Several features of the experimental results indicate the presence of substantial amounts of surface oxide and are summarised below.

(a) The rest potential is 1.25 V.

(b) A brownish deposit on the electrode was visually observed and an unusual amount of "noise" on the signals in open-circuit experiments was encountered possibly because of the presence of a thick resistive oxide film.

(c) Extremely long arrests having a small or zero slope ("infinite" capacity - see photograph in Fig. 53) are observed in cathodic transients; an appreciable increase in Q values with increasing V_i (Fig. 53) is found which is consistent with film growth mechanisms.

(d) Two capacity maxima with values of $V_{C_{max.}}$ lying between 1.08 V and 1.85 V suggest perhaps the presence of two oxides of distinguishable stoichiometry (Fig. 50); appreciable values of $C_{max.}$ (Fig. 50) arise.

When the effect of $i_{cath.}$ on $C_{max.}$ and $V_{C_{max.}}$ values

is examined, the shifts (Fig. 51) are found to follow the predicted trend (46). This probably indicates (cf. pp. 184) that only one species, i.e., oxide, is present on the electrode.

Hence it may be concluded that in this solution, the gold electrode is covered by a substantial oxide film and the Faradaic process proceeding on the oxide surface is simply oxygen evolution.

(v) Summary of Mechanistic Conclusions

Mechanistic conclusions are summarised in the Table IX given below.

Table IX

Summary of mechanistic conclusions.

Table IX. SUMMARY OF MECHANISTIC CONCLUSIONS

Electrode/Solution	Water Content	b	Identity of Adsorbed Species	Rate-Determining Step (r.d.s.)
Pt in 1M KTFA/TFA	(i) None	0.215V	A barrier-layer film of $CF_3^{\bullet}$	$CF_3^{\bullet}(M)+CF_3COO^- \longrightarrow C_2F_6+CO_2+e$
	(ii) Traces	0.22V	A barrier-layer film of $CF_3COO^{\bullet}$ + some co-adsorbed oxide	$CF_3COO^{\bullet}(M)+CF_3COO^- \longrightarrow C_2F_6+2CO_2+e$
	(iii) Excess	0.25 V	A barrier-layer film of $CF_3COO^{\bullet}$ +some co-adsorbed oxide	$CF_3COO^{\bullet}(M)+CF_3COO^- \longrightarrow C_2F_6+2CO_2+e$
Au in 1M KTFA/TFA	(i) None	0.16V	A barrier-layer film of $CF_3COO^{\bullet}$	$CF_3COO^{\bullet}(M)+CF_3COO^- \longrightarrow C_2F_6+2CO_2+e$
	(ii) Traces	0.175V	A barrier-layer film of $CF_3COO^{\bullet}$ + some co-adsorbed oxide	$CF_3COO^{\bullet}(M)+CF_3COO^- \longrightarrow C_2F_6+2CO_2+e$
	(iii) Excess	0.17V	A barrier-layer film of $CF_3COO^{\bullet}$ + some co-adsorbed oxide	$CF_3COO^{\bullet}(M)+CF_3COO^- \longrightarrow C_2F_6+2CO_2+e$
Pt in 1M CH_3COOK/CH_3COOH	(i) None	0.14V	None	$CH_3COO^- \longrightarrow CH_3COO^{\bullet}(M)+e$
	(ii) Excess	0.26V 0.165V	A barrier-layer film of $CH_3COO^{\bullet}$ + some co-adsorbed oxide	$CH_3COO^{\bullet}(M)+CH_3COO^- \longrightarrow C_2H_6+2CO_2+e$
Au in 1M CH_3COOK/CH_3COOH	(i) Traces	0.11V	A barrier-layer film of $CH_3COO^{\bullet}$ + some co-adsorbed oxide	$CH_3COO^{\bullet}(M)+CH_3COO^- \longrightarrow C_2H_6+2CO_2+e$
	(ii) Excess	0.09V	Oxide	-----only O_2 evolution

4. INHIBITION OF THE OXYGEN EVOLUTION REACTION AND RELATED PROBLEMS

(i) General

In the foregoing discussion it was concluded that the presence of co-adsorbed oxide on the electrode, originating from traces or excess of water in the solutions, results in partial or complete (e.g., for the case of gold in aqueous acetate solutions) inhibition of the Kolbe reaction. However, the important and related problem that the Kolbe reaction usually proceeds in preference to oxygen evolution in aqueous acetate solutions on Pt and Ir at higher potentials (>ca. 2.2 V), has not been considered. An attempt will therefore be made here to examine the various factors that may be involved in this phenomenon.

(ii) Inhibition of Oxygen Evolution

(a) Hypothesis

From the foregoing discussion, it has been concluded that an effective barrier-layer of $RCOO^{\bullet}$ radicals may exist on the Pt electrode when the Kolbe reaction is proceeding in aqueous acetate solutions. This, it may be suggested, not only can cause an anomalously high Tafel slope for the Kolbe reaction itself, but would also have a similar effect in any discharge of species from water to form oxygen. The Tafel slope for

such a process involved in oxygen evolution would thus be raised, so that at the high potentials at which the Kolbe reaction proceeds at moderate or high rates, the oxygen evolution reaction would hence proceed only much more slowly than it would (at those same potentials) in the absence of the Kolbe species. Hence the efficiency of the Kolbe reaction is higher than would be expected by comparison between the Tafel parameters for the two reactions considered separately. This may be schematically represented as follows.

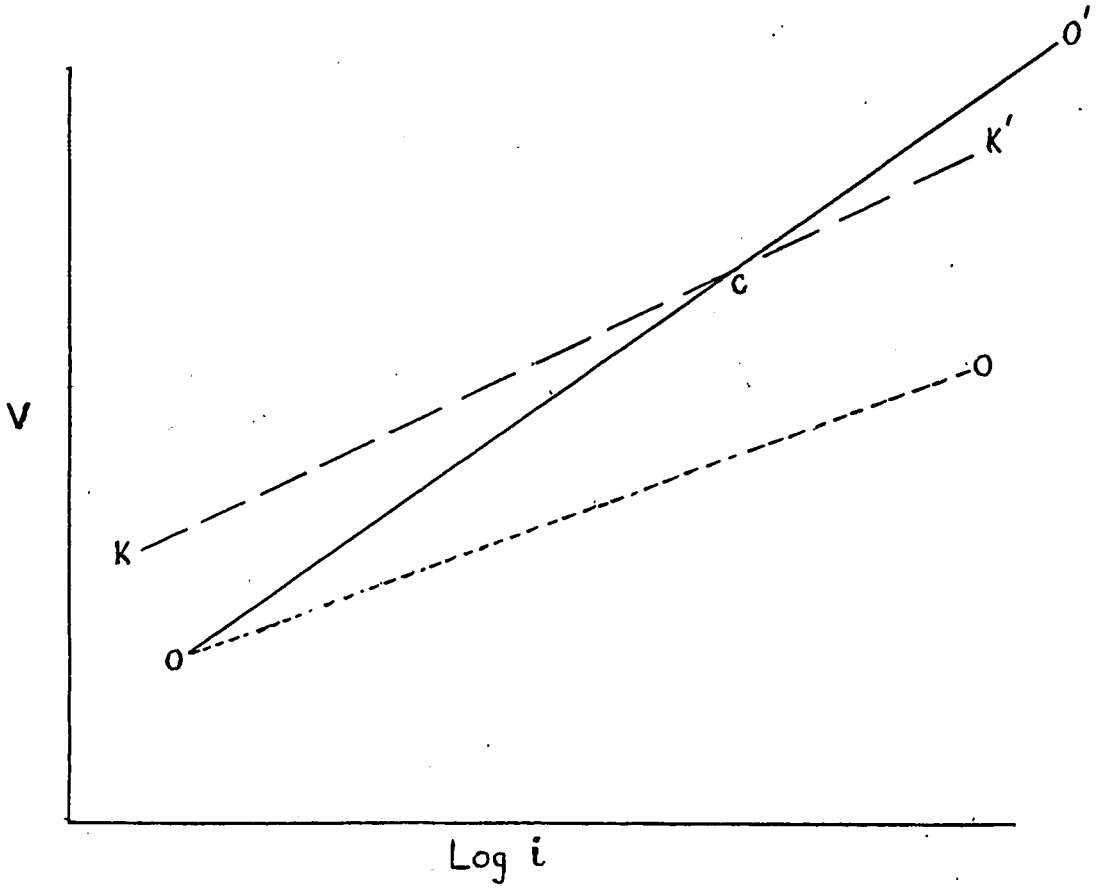

KK' is the Tafel line for the Kolbe reaction; 00 is the Tafel line for the normal oxygen evolution reaction, i.e., in the absence of a barrier-layer film of adsorbed radicals (e.g., for Pt in H_2SO_4); 00' is the expected Tafel line for the oxygen evolution reaction in the presence of a barrier-layer film of adsorbed RCOO' radicals on the electrode. It may be seen that at potentials higher than those represented by point C, the crossing point of KK' and 00', the Kolbe reaction would be expected to be the preferred process. In the absence of such an effect it is difficult to explain why oxygen evolution should <u>not</u> be the major process at higher potentials on Pt or Ir in aqueous acetate solutions, when the normal Tafel line for the oxygen evolution reaction in acid solutions (i.e., in the absence of any adsorbed barrier-layer films on the electrode) commences at a lower potential and has a lower slope than the one for the Kolbe reaction (see Figs. 11 and 13).

A second effect may occur in a different way and arise from the effect of one adsorbed species on another and on the kinetics of two processes tending to occur simultaneously. Thus, co-adsorbed RCOO species ("substituted surface oxide") may change the energy of adsorption of intermediates ("OH" or "O") (33) in the oxygen evolution reaction. Two types of effect may then arise; (a) the steady-state coverage of such species may be

modified and hence the rate of the oxygen evolution reaction could become changed; and (b) the presence of co-adsorbed species such as RCOO• may raise the activation energy for steps in the oxygen evolution reaction, e.g., by weakening bonding of the adsorbed species to the surface (69).

(b) Relation to Various Problems

The above considerations may also be useful for considering certain other important aspects of the Kolbe reaction, e.g., (a) the effect of the anode material, (b) effect of the potential of the working electrode, and (c) effect of the concentration of the electrolyte, etc., on the Kolbe reaction.

(α) Anode Material

It is well-known that the Kolbe reaction proceeds inefficiently in aqueous medium at electrodes on which the presence of multi-layer oxides is unambiguously established, e.g., Ni (3,7), Au (3,7), Fe (85), MnO_2 (7), PbO_2 (7,60). This is perhaps associated with the fact that the formation and presence of appreciable oxide inhibits the adsorption of RCOO• radicals (through metal-oxygen bonds) or R• radicals. In the absence of adsorbed RCOO• or R• "barrier-layer" films, the Tafel line for the oxygen evolution reaction has a normal

slope (80) (represented by line 00); any enhancement of this slope to give a line 00' and consequently a crossing-point C is therefore not possible. In other words, even at the highest potentials, oxygen evolution would be expected to be the predominant process because the Tafel line for the oxygen evolution reaction commences at a lower potential and has a lower slope than the one for the Kolbe reaction.

In non-aqueous media even on these electrode materials, oxygen evolution is excluded and the only possible reaction is the one involving Kolbe species. In terms of the above diagram, the Tafel regions corresponding to 00 and 00' lines are never involved, and indeed it has been observed experimentally that even on electrodes covered by some oxide layer (60), the Kolbe reaction proceeds with good efficiency in non-aqueous media, e.g., at PbO_2 electrode in acetate/glacial acetic acid solutions (60), and at gold anodes in nominally anhydrous CH_3COOK/glacial CH_3COOH solutions in the present work. A consequence of the arguments developed above is that on electrodes covered predominantly by oxides, since R$^\bullet$ and RCOO$^\bullet$ cannot be easily adsorbed, the Kolbe reaction in non-aqueous media must proceed with initial discharge as the r.d.s; any other step, if rate-determining, would imply some coverage by R$^\bullet$ or RCOO$^\bullet$. In the present investigation, it has been observed that on gold in nominally anhydrous potassium acetate solutions (see Table V),

the Kolbe reaction does, in fact, proceed on an oxide-covered electrode with the initial discharge step as the probable rate-determining stage (p.241). At present, insufficient data are available to test more thoroughly the various points made in this discussion.

(β) Anode Potential

It has been experimentally observed that the Kolbe reaction proceeds with increasing efficiency as the anode potential is raised (or with increased anodic current density in galvanostatic measurements) in aqueous solutions (3,8,14, 18,25,85). This is easily understood in terms of the above diagram: the higher the anode potential, the greater will be the separation between KK' and OO', i.e., at higher potentials the rate of the Kolbe reaction will be increasingly greater than that of oxygen evolution reaction.

(γ) Concentration of the Electrolyte

It has usually been observed that increased concentration of the electrolyte in aqueous acetate solutions results in an increase of the coulombic efficiency of the Kolbe reaction (3, 8,14,18,25,85). Increased bulk concentration, $(C_R)_b$, of the reactant part of the electrolyte would be expected to increase the surface concentration, $(C_R)_s$ of the reactant species; the $(C_R)_b$ is related to $(C_R)_s$ by the isotherm

$$(C_R)_s = (C_R)_b \exp\left[-\frac{\Delta\bar{G}^\circ_R}{RT}\right]$$

where $\Delta\bar{G}^\circ_R$ is the standard electrochemical free energy of adsorption of R and will be defined for appropriate standard states for R in the bulk and in the surface layer.

If the Kolbe reaction and the oxygen evolution reaction were proceeding in the same potential region and with comparable rate constants, the increase in coulombic efficiency for ethane formation with increased acetate concentration* in aqueous solution would be simply due to increased surface concentration of the reactant species, R. However, when the Tafel line for the oxygen evolution reaction commences at a lower potential and has a lower slope than the one for the Kolbe reaction, the above explanation for the effect of the concentration of the electrolyte would not be valid. Another explanation which seems plausible is that at higher bulk acetate concentrations, the surface concentration of the reactant species increases with a consequently increased barrier-layer film effect for the oxygen evolution reaction; this would tend to bring the point C down on the potential axis (see the above diagram)

*This effect of concentration will, of course, only change the rate (at a given overpotential) at concentrations greater than <u>ca</u>. 0.5 M where the ψ_1 potential tends to become independent of concentration, so that the increase of $(C_R)_s$ is no longer cancelled by diminishing ψ_1 (40).

with a consequently more pronounced separation of KK' and OO' at higher potentials in favour of the Kolbe reaction.

(δ) Tafel Slope on Gold in Aqueous Acetate Solutions

A matter related to the above considerations is the interpretation of the Tafel slope, observed in the case of oxygen evolution on gold in 1M CH_3COOK solution in water (see Table V) where no Kolbe reaction occurs. In the acetate solution, some adsorption by $RCOO^{\bullet}$ radicals may take place giving rise to an effective barrier-layer on the electrode with a consequent increase in the Tafel slope to 0.09 V from the usual value of 0.045V. This increase in the Tafel slope for the oxygen evolution reaction is perhaps still not high enough to shift OO to OO' to such an extent that OO' crosses KK' (see above diagram) at some easily accessible potential; since point C thus will not be easily reached, no Kolbe reaction would be expected. However, if very high concentrations (e.g., >10 M) of CH_3COOK were used and if a potentiostat were used which could control the potential of the electrode to values much higher than those usually reached (ca. 2.0 V) in this case, the possibility of achieving rates beyond the point C on the line KK' (see diagram above) and hence observing the Kolbe reaction would perhaps not be entirely excluded. However, this tentative suggestion has yet to be verified experimentally.

(iii) Inhibition Inflexion

In the potentiostatic steady-state log[i]-V relations for gold in nominally anhydrous 1M CF_3COOK/CF_3COOH solutions, an inhibition inflexion is observed in the potential region, ca. 1.6 V to 1.8 V. This inhibition inflexion is indicative of a co-adsorbed inhibiting species (62); however, it is not always observed when the presence of a co-adsorbed inhibiting species is suggested by other evidence. This inflexion behaviour would tend to be observed only when both i (i.e., the rate) and θ (i.e., the coverage) were dependent on potential in the same potential region. In such a case, the rate i could be expressed as

$$i = k\, e^{\alpha VF/RT}\, e^{-k'VF/RT} = e^{(\alpha - k')VF/RT}$$

where k' is a coefficient expressing the potential dependence of θ and α is a transfer coefficient determining the potential dependence of the rate in the usual way. When $k' > \alpha$, an inversion in the log[i]-V line, i.e., an inhibition inflexion will be observed (Fig. 12) as treated previously (62). However, if k is finite but smaller than α, only a change of slope in the log[i]-V line would be observed; an inhibition inflexion is actually a limiting case of this change of slope, i.e., when the slope changes in sign and the kinetics hence exhibit an inversion.

Complete inflexions of the type observed in anodic reactions which proceed at lower potentials (0 - 1 V E_H) e.g., formate and hydrocarbon oxidations, are not usually observed in the Kolbe reaction but some changes of slope of the kind referred to above do arise. The absence of the first effect is understandable when it is noted that initial coverage of the Pt electrode by oxide species has already occurred at potentials up to 1.0 - 1.2 V E_H and only secondary changes of the oxide film proceed at potentials higher than this range. Hence the absence of primary inflexion effects is accounted for.

5. COMPARISON WITH RECENT WORK

A brief critical assessment of recent work on the electrochemistry of the Kolbe reaction (2,3,11,60) is presented in this section of the thesis in relation to the present results. No attempt has been made, however, to review such recent work on the Kolbe reaction as involves considerations only of the organic aspects of this reaction (81,82,83).

Pande and Shukla (11) have reported some studies on the Kolbe reaction in aqueous solutions of the sodium salts of the carboxylic acids with the general formula $C_nH_{2n+1}CCONa$. The Kolbe reaction in sodium acetate solutions was not studied. These workers reported some potential *vs.* current plots;

however, they failed to discuss logically the mechanisms they proposed in terms of expected Tafel relations. The mechanisms proposed by these authors were based solely on the nature of reaction products obtained with little reference to the electrode processes, adsorbed intermediates and kinetic behaviour involved. Moreover, these authors seem to have overlooked all the relevant work on the Kolbe reaction done since 1936, especially the excellent work of Clunius and co-workers (28, 29,30) and also that of Wilson and Lippincott (31).

Dickinson and Wynne-Jones (3) carried out electrolysis of aqueous acetate solutions and studied the mechanism of the Kolbe reaction on Pt, Ir, and Au anodes in these solutions. They observed high Tafel slopes ($> 2RT/F$) on Pt, which is in agreement with the present work and the related previous work of Conway and Dzieciuch (2,6). On gold, they observed the evolution of oxygen only; this, again is consistent with the present work.

However, Dickinson and Wynne-Jones suggested a mechanism which is seemingly not consistent with the electrochemical kinetic analysis of the reaction. A brief discussion of their conclusions is given below.

According to Dickinson and Wynne-Jones, at low current densities, OH radicals are discharged at, and subsequently removed from, the electrode (Pt or Ir) in preference

to acetate radicals, resulting in the predominant evolution of O_2 with little participation of the Kolbe reaction. Above a critical current density, discharge (and subsequent decomposition and desorption) of acetate radicals is favoured over discharge of OH radicals, resulting in the occurrence of the Kolbe reaction and inhibition of O_2 evolution. It is postulated that at higher current densities at which the Kolbe reaction proceeds more efficiently, acetate radicals are discharged on an electrode already fully covered in the steady-state by acetate radicals. When the second acetate radical becomes discharged at a site already occupied by a previously discharged acetate radical, a situation of instability results, it is claimed, which is only remedied by the desorption of both the radicals from the electrode in the form of a Kolbe coupling product. On Au and Ni, it was found that the Kolbe reaction did not occur even at the highest current densities used (> 30 mA. cm.$^{-2}$); only oxygen evolution took place.

The experimental Tafel slopes reported by these authors are as follows for electrodes at which the Kolbe reaction proceeds.

	Metal	Tafel Slope		Transition Region
		Lower	Upper	
1.	Pt	170 mV	130 mV	Well-defined
2.	Ir	Not well-defined	120 mV	Well-defined

These authors did not put forward a scheme of consecutive elementary processes (cf. 2) that might be involved in the overall Kolbe reaction involving transfer of two electrons.

Although not stated explicitly, it is implied in the discussion of Dickinson and Wynne-Jones that the rate-determining process is the chemical desorption of two methyl radicals from the "same" site. Since it is supposed that the electrode is fully covered with acetate radicals, it follows that the initial discharge step ($CH_3COO^- \rightleftharpoons CH_3COO^\bullet + e$) and the subsequent heterogeneous step producing methyl radicals on the electrode surface ($CH_3COO^\bullet \longrightarrow CH_3^\bullet + CO_2$) must have rate constants greater than that for the final methyl radical recombination step which results in the formation of the Kolbe product C_2H_6 by desorption of two methyl radicals ($CH_3^\bullet + CH_3^\bullet \longrightarrow C_2H_6$). In the reaction sequence proposed by Dickinson and Wynne-Jones, the detailed mechanism of production of C_2H_6 from discharged CH_3COO^- ions was not examined. It is stated that the C_2H_6 arises from discharge of two acetate species at the same site through the intermediate formation of $CH_3^\bullet$ radicals. However, kinetically it seems necessary and preferable to separate

this process into two steps involving the decomposition of the $CH_3COO^{\bullet}/M$ ($\longrightarrow MCH_3^{\bullet} + CO_2$) and the subsequent recombination of $CH_3^{\bullet}$ radicals, viz.

$$2CH_3\dot{M} \longrightarrow 2M + C_2H_6$$

Then if the rate constant for the desorption step were greater than that for either of the first two steps we have suggested above, the electrode would not be fully covered with methyl radicals. Thus, in general, in terms of their mechanism, appreciable coverage will tend to arise if the rate constant for the "desorption" process is less than that for the discharge step at all potentials, i.e., the former step is rate-determining. A deduction of the Tafel slope for the reaction under these conditions (i.e., fully covered electrode with desorption as the rate-determining step) would predict a trend towards a limiting current (infinite Tafel slope) and not the finite Tafel slopes observed by Dickinson and Wynne-Jones. Hence, the conclusions of these authors do not seem to be consistent with the electrochemical kinetic analysis of the problem. Nevertheless, the experimental contributions in this work have advanced the knowledge of the electrochemical behaviour of the Kolbe reaction in important ways.

The difficulty arises here that in the work of Dickinson and Wynne-Jones, the overall process was not discussed in terms

of all the kinetically distinguishable elementary processes which seem likely to be involved nor were the consequences quantitatively evaluated in terms of the theoretically predictable parameters of electrode kinetics.

Similar comments may be made about the work of Sugino and co-workers (60), who carried out potentiostatic studies on the Kolbe reaction, both in aqueous and non-aqueous media. These authors reported current-potential relations (and not the usual log[current]-potential relations) but did not discuss, even qualitatively, the way in which these relations could be used in a diagnostic manner (i.e., through Tafel slopes and coverage effects) in determining the rate-determining step in a sequence of elementary consecutive processes involved in the overall, two electron, Kolbe reaction. Most of the evidence of these authors is concerned with the analysis of the products formed (cf. 11) under various experimental conditions in the Kolbe decarboxylation. Although these authors arrived at conclusions which support the free-radical theory for the Kolbe reaction, they did not, however, discuss the mechanism of the reaction in terms of electrochemical kinetic theories of possible consecutive processes involved in the overall reaction. Obviously, a combination of both approaches is desirable.

Conway and Dziecuich (2) applied modern electrochemical approaches to the study of the Kolbe reaction in

anhydrous and aqueous trifluoroacetic acid which was chosen to minimise side oxidation reactions of the R group. They have made an analysis, both theoretical and experimental, of the various possible consecutive steps involved in the overall Kolbe reaction and deduced the associated Tafel slopes for various conditions of adsorption of the possible intermediates. They approached the study of this organic electrode process with the purpose of studying the electrochemical behaviour of the adsorbed intermediates and relating, in a quantitative way, a variety of complementary data that can be obtained by such studies. The high values of Tafel slopes ($> 2RT/F$) and appreciable values of charge and capacity observed by these authors are, in general, consistent with the more detailed potentiostatic investigations reported in the present thesis. However, the following comments may be made about the work of these authors.

(i) The electrochemical measurements reported by these authors were carried out under galvanostatic conditions. The galvanostatic measurements, as it may be recalled (Chapter I), are not as satisfactory as controlled-potential techniques used in the present investigation for examining the behaviour of adsorbed intermediates and the current-potential relation.

(11) The role of surface oxide in the Kolbe reaction was not established in an unambiguous way in the work of Conway and Dziecieuch. This has been attempted in the present investigation by (a) making the TFA solutions very anhydrous by adding small amounts of trifluoroacetic anhydride; and (b) carrying out the experiments with Pt in anhydrous acetic acid solutions under vacuum; (c) by examining the reaction of PtO_2 with aqueous (1M CH_3COOK + 1M CH_3COOH) solution.

Eberson (68) has reported some investigations of the Kolbe reaction which involve some fundamental conceptual errors. He failed to appreciate that this reaction is a special type of <u>heterogeneous</u> reaction and not a homogeneous reaction. His calculations of the "thermodynamic potentials" for various possible steps in the overall Kolbe reaction are therefore invalid. This fundamental error in Eberson's paper has not been realised by Leung and co-workers (84) who quoted Eberson in their recent paper (84). Leung and co-workers presented Tafel relations but did not discuss their kinetic significance.

Fleischmann, Petrov and Wynne-Jones have reported (35) an investigation of the Kolbe reaction by a potential pulse technique. These authors conclude that ethane formation proceeds by a second-order reaction between acetate radicals. The report of their work (35) was, however, too brief to merit any further discussion.

Any conclusions regarding the identity of adsorbed species based on electrolytic preparation of some organic compounds are not unambiguous since substitution by both $CH_3^{\bullet}$ and $CH_3COO^{\bullet}$ radicals has been reported in the literature (32,86, 87,88). These investigations, however, are quite useful in explaining the formation of side products in the Kolbe electrosynthesis. In cases in which the Kolbe coupling reaction has been reported to fail, a more extensive oxidation of the adsorbed radicals giving rise to a carbonium ion has been indicated (89); e.g., a reaction sequence of the type

$$RCOO^- \longrightarrow RCOO^{\bullet} \longrightarrow R^+ + CO_2 + e$$

is believed to proceed.

CLAIMS TO ORIGINAL RESEARCH

(i) Potentiostatic steady-state log[i]-V relationships have been examined for platinum and gold electrodes in very anhydrous 1M KTFA/TFA and 1M CH_3COOK/CH_3COOH solutions and in these solutions containing traces or excess of water. A comparison of the log[i]-V relations for ascending and descending directions of potential change in solutions containing various amounts of water has been carried out and the behaviour observed is discussed in relation to the presence of adsorbed intermediates.

(ii) Potentiodynamic, non-steady-state i-V relations have also been examined. In cases where charging peaks are observed in the potentiodynamic profiles, the pseudo-capacity C and charge values associated with various peaks have been quantitatively related to the possible identifies of adsorbed intermediates involved in the Kolbe reaction and thence to the mechanism of the Kolbe reaction itself.

(iii) Differential galvanostatic transient methods have been applied to the study of the Kolbe reaction. The differentiated cathodic charging profiles were obtained by applying a cathodic pulse galvanostatically at various potentiostatically-maintained initial anodic potentials. The C-V profiles have been calculated from these transients and values of $C_{max.}$ and $V_{C_{max.}}$, and the effect of $i_{cath.}$ on these quantities has been qualitatively

related to the identity of the adsorbed intermediates, and thence to the reaction mechanisms in suitable cases.

(iv) The possibility of relating the residual potential and the rest potential empirically to the type of ad-species involved, has been proposed.

(v) Experimental data and derived conclusions have been presented which lead to an evaluation of the role in the kinetics, of (a) electro-inactive ad-species, $CF_3^{\bullet}$ and (b) "substituted" oxide species, $RCOO^{\bullet}$, which have been considered and discussed at the appropriate places in the thesis.

(vi) A variety of evidence has been presented which indicates rather strongly that the presence of co-adsorbed oxide is not only not necessary for the Kolbe reaction to proceed but is, in fact, a species which can inhibit the Kolbe reaction.

(vii) Various types of rate *vs.* charge plots have been introduced which show the relation between the rate of the overall Faradaic process and the coverage by ad-species present on the electrode in the potential region to which the rate and the charge refer. These plots are used in the derivation of conclusions on the nature of the ad-species.

(viii) A comparative way of plotting the potentiostatic steady-state $\log[i]$-V plots has been introduced in which the rates at a given potential for a given electrode can be compared in

various solutions which differ from one another only in regard to the amount of water present. Such a family of comparative plots, when supported by evidence from the transient studies in the corresponding solutions, can yield a direct method of testing whether or not the ad-species arising from the presence of water in the solutions participate as a reactant in the Kolbe reaction or only as an inhibiting species.

(ix) An hypothesis has been proposed which seems to provide a plausible explanation for the intriguing phenomenon of inhibition of oxygen evolution at higher potentials on platinum and iridium in aqueous acetate solutions. The relation of the proposed hypothesis to several important problems of a general nature has also been examined.

(x) Mechanisms for the overall Kolbe reaction on Pt and Au in very anhydrous 1M KTFA/TFA and 1M CH_3COOK/CH_3COOH solutions and for these solutions in the presence of traces or excess of water, have been proposed. The mechanistic proposals are based on (a) kinetic analyses of the potentiostatic steady-state log[i]-V relations; (b) indications of the identity of the ad-species as derived from complementary evidence of various kinds, and (c) knowledge of the products of electrolysis as indicated in the previous literature and confirmed in this laboratory. A critical comparison with recent related work reported by other investigators has also been presented.

APPENDIX

Immediately following the completion of the main body of the present thesis, two important papers by Fleischmann, Mansfield and Wynne-Jones (90) on the mechanism of the Kolbe reaction appeared in the literature. These authors have applied a new theoretical and experimental approach to the problem of the Kolbe reaction. A repetitive potential pulse technique [cf. (31)] was used and an attempt was made to develop the essential non-steady-state theory for the production of Kolbe and other products under the conditions that obtain in the above technique. Also a study of the behaviour of oxides at the surface of platinum electrodes in aqueous acetate solutions was carried out. On the basis of the investigations reported, these authors proposed that in the production of ethane on platinum in aqueous acetate solutions, initial discharge of the acetate ions is the rate-determining step. This conclusion requires, however, further discussion and some relevant points are recorded below.

(1) If the initial discharge step were rate-determining, as these authors conclude, then its rate-constant k_1 would have to be appreciably smaller (taking into account the appropriate units for the various k's) than the rate constants for the subsequent steps (in their scheme) with the result that the coverage θ would tend to zero. In that case, it is difficult

to see how their equation [14]* (90, pp. 524), which it is supposed explains high Tafel slopes for a rate-determining discharge step under "Temkin" conditions (see footnote on pp. 534, ref. 90), can be meaningful for the mechanism used in deriving it.

(ii) If, for the sake of argument, it is assumed that initial discharge is <u>not</u> the r.d.s., then the derivation of equation [14] (90, pp. 524) involves an assumption that in reaction [1] (in <u>their</u> scheme) the back reaction can be completely neglected. This, however, is not a generally acceptable assumption in the kinetics of consecutive reactions. These authors suppose that because the overall Kolbe reaction is "highly irreversible", <u>all</u> steps in it are irreversible so that rates of any such steps in the backward direction (prior to the rate-determining step) can be neglected. It is believed that this is not necessarily true.

---

*That is $\Omega\, d\theta/dt = k_1 C_{A^-}(1-\theta) - k_{5b} C_{A^-}\theta - k_{5a}\theta^2$ where Ω is the saturation coverage (moles cm^{-2}) of the surface; θ is any fractional coverage; C_{A^-} is the concentration of the acetate ions; k_1 is the rate constant for the initial discharge step, $CH_3COO^- \xrightarrow{K_1} CH_3COO(M)+e$; k_{5a} is the rate constant for the recombination step, $2CH_3^{\bullet}(M) \xrightarrow{K_{5a}} C_2H_6$; k_{5b} is the rate constant for the electrochemical desorption step, $CH_3^{\bullet}(M) + CH_3COO^- \xrightarrow{K_{5b}} C_2H_6+CO_2+e$.

(iii) There is another inconsistency in the second (Part II) paper of these authors; assuming, as they do, that initial discharge of acetate ions is the r.d.s., the numerical value of k_1 would be expected to be much <u>smaller</u> than that of k_{5a} (the rate constant for $CH_3^{\cdot}$ recombination; k_1 and k_{5a} refer to <u>their</u> scheme), which is at variance with their own observations after allowing for the difference of units of k_1 and k_{5a} (ref. 90, pp. 535, Table I). This particular criticism is not invalidated by the fact that the estimated values of rate constants quoted in Table I (90, pp. 535) involve some complicating uncertainties which these authors acknowledge, since the difference is seemingly beyond the range of anticipated errors.

(iv) There are also some qualitative discrepancies, it seems, between the theoretically expected current-time transients (90, Figs. 3, pp. 528) and the corresponding experimental plots (90, Fig. 2, pp. 528). This suggests that the theory presented may need some modification before it can explain the experimental behaviour. The authors, however, do state that there are difficulties in obtaining quantitative information from these plots.

(v) The authors state that, in general, "an anodic oxidation may go <u>via</u> a surface compound formed on the surface of the electrode from the solvent. In the case of water, this may

be adsorbed hydrogen or hydroxyl radicals as well as a number of oxides, a peroxide, or adsorbed oxygen on an oxide layer. Alternatively, the oxidation may proceed on the layer, the layer itself, rather than the platinum, forming the inert substrate" (90, pp. 511). This statement is contestable and in the present thesis an attempt has been made to show that in several cases oxide is co-adsorbed with RCOO• on the electrode and is in fact an inhibiting species. Moreover the concept of the electrode surface being only an "inert" sink or source of electrons does not seem in general to be entirely acceptable since the electrode surface usually behaves as an active interface for electrochemical, heterogeneously-catalysed processes, in this case for the electrode reaction itself.

(vi) Related to the point above, it is also implied that complete oxidation of acetate is the type of reaction which proceeds on the Pt metal "substrate" while the Kolbe reaction is "restricted to the surface covered by the oxide layer". The present results show that the Kolbe reaction can not only proceed on a surface free of an oxide layer (e.g., see the in vacuo acetate runs and anhydrous TFA experiments), but does so with a greater efficiency than in aqueous media (see Figs. 11, 12 and 13 in the present thesis) when oxide films are present. Also these authors mention that in non-aqueous

medium, oxide may still be present. The present results show that this is unlikely and other related work with Pt in acetonitrile shows that very small amounts of surface oxide, when present, can be detected by the differential galvanostatic method.

(vii) These authors argue that the formation of methyl radicals before the formation of ethane in their measurements is supported by the fact that trinitroxylene is formed (32) from trinitrotoluene in the presence of sodium acetate (90, pp. 536).

The fact that only poor yields in the electrolytic methylation have been reported (32) suggests that this perhaps may be only a minor side reaction; in this connection it is important to note that much higher yields have been reported for anodic acetoxylations of various organic substrates (88).

Finally however, it must be emphasised that Fleischmann, Mansfield and Wynne-Jones (90) have introduced, in an elegant way, a number of new ideas and approaches to the field of electro-organic chemistry which seem most promising for the further development of the subject.

REFERENCES

1. M. Faraday, Phil. Trans., 123, 23 (1833); 124, 77 (1834).
2. B.E. Conway and M. Dzieciuch, Can. J. Chem., 41, 21, 38, 55 (1963).
3. T. Dickinson and W.F.K. Wynne-Jones, Trans. Faraday Soc., 58, 382, 388, 400 (1962).
4. M. Faraday, Pogg. Ann., 33, 438 (1834).
5. H. Kolbe, Liebig Ann., 69, 257 (1849).
6. M. Dzieciuch, Ph.D. Thesis, Ottawa (1962).
7. S. Glasstone and A. Hickling, J. Chem. Soc., 1878 (1934); Chem. Rev. 25, 407 (1939).
8. D.A. Fairweather and O.J. Walker, J. Chem. Soc., 3111 (1926).
9. S.N. Shukla and O.J. Walker, Trans. Faraday Soc., 27, 722 (1931).
10. G. Preuner and E.B. Ludlam, Z. Physikal. Chem., 59, 682 (1907).
11. G.S. Pande and S.N. Shukla, Electrochimica Acta, 4, 215 (1961).
12. K. Hopfgartner, Monatsh., 32, 523 (1911).
13. J. Salause, Bull. Soc. Chim. France, 37, 522 (1925); Compt. rend., 180, 662 (1925).

14. K. Sugino, T. Sekine, N. Sato, J. of Elec. Tech., 1, 112 (1963).

15. C.E. Svadkovskaya and S.A. Voitkevitch, Uspekki Khimii, S.S.S.R., 29, 161 (1960).

16. H. Hofer and M. Moest, Analen., 323, 285 (1902).

17. S. Glasstone and A. Hickling, J. Chem. Soc., 820 (1936).

18. N.J. Allen, "Organic Electrode Processes," Rheinhold Publishing Corporation, New York, 1958, pp. 95-115.

19. C. Schall, Z. Electrochem., 3, 83 (1896).

20. F. Fitcher, Trans. Electrochem. Soc., 75, 309 (1939).

21. F. Fitcher, ibid., 56, 8 (1929).

22. F. Fitcher and R. Zumbrunn, Helv. Chim. Acta, 10, 869 (1927).

23. F. Fitcher and H. Buess, Helv. Chim. Acta, 18, 445 (1935).

24. S. Glasstone and A. Hickling, Trans. Electrochem. Soc., 75, 333 (1939).

25. B.C.L. Weedon, Quart. Rev., 6, 380 (1952).

26. A. Crum-Brown and J. Walker, Analen., 261, 107 (1891).

27. S.N. Shukla and O.J. Walker, Trans. Faraday Soc., 28, 457 (1932).

28. P. Holeman and K. Clusius, Z. Physikal. Chem., 358, 261 (1937).

29. K. Clusius and W. Schanzer, Z. Physikal. Chem., 192A, 273 (1943).

30. W. Schanzer and K. Clusius, Z. Physikal. Chem., 190A, 241 (1941).

31. C.L. Wilson and W.J. Lippencott, J. Am. Chem. Soc., 78, 4290 (1956); J. Electrochem. Soc., 103, 672 (1956).

32. L.F. Fieser, R.C. Clapp and W.H. Daudt, J. Am. Chem. Soc., 22, 2052 (1942).

33. J. O'M. Bockris, J. Chem. Phys., 24, 817 (1956).

34. B.E. Conway, Trans. Roy. Soc. (Can.), 49, 19 (1960).

35. M. Fleischmann, I.N. Petrov, and W.F.K. Wynne-Jones, Proceedings of the First Australian Conference on Electrochemistry, Pergamon Press, 500 (1965).

35a. M.A.V. Devanathan and M. Selvaratnam, Trans. Faraday Soc., 56, 1820 (1960).

36. J.O'M. Bockris, "Modern Aspects of Electrochemistry," Butterworths Scientific Publications, New York, 1959, Vol. 1, Chapter IV.

37. R. Parsons, Trans. Faraday Soc., 47, 1332 (1951).

38. E. Breiter, C.A. Knorr and W. Volkl, Z. Electrochem., 59, 681 (1955).

39. T.P. Bowden, Proc. Roy. Soc., 125A, 446 (1929).

40. B.E. Conway, "Theory and Principles of Electrode Processes", Ronald Press, New York, 1965.

41. J.A.V. Butler and G. Armstrong, Proc. Roy. Soc., 137A, 604 (1932).

42. F. Will and C.A. Knorr, Z. Electrochem., 64, 258 (1960).

43. H.A. Laitinen and G. Enke, J. Electrochem. Soc., 107, 773 (1960).

44. A. Sevcik, Coll. Czech. Chem. Comm., 13, 349 (1948).

45. M. Breiter, Electrochim. Acta, 8, 457 (1963); see also, A. Kutschker and W. Vielstich, ibid., 8, 985 (1963); S. Gilman, J. Phys. Chem., 82, 78 (1963).

46. B.E. Conway, E. Gileadi and H.A. Kozlowska, J. Electrochem. Soc., 112, 341 (1965).

47. A. Slygin and A.N. Frumkin, Acta Physicochim. U.R.S.S., 3, 719 (1935); ibid., 5, 819 (1936).

48. B.E. Conway, E. Gileadi, and M. Dzieciuch, Electrochim. Acta, 8, 143 (1963).

49. B.E. Conway and P.L. Bourgault, Can. J. Chem., 37, 292 (1959); Trans. Faraday Soc., 58, 593 (1962).

50. F.P. Bowden and E.K. Rideal, Proc. Roy. Soc., (London), 120A, 59, 80 (1928).

51. A.N. Frumkin and A.I. Slygin, Acta Physicochim. U.R.S.S., 4, 991 (1936).

52. M.A.V. Devanathan, J.O'M. Bockris, and W. Mehl, J. Electroanal. Chem., 1, 143 (1959-60).

53. H.A. Kozlowska and B.E. Conway, J. Electroanal. Chem., 2, 109 (1964).

54. E. Gileadi, Ph.D. Thesis, Ottawa (1962).

55. B.E. Conway and E. Gileadi, Can. J. Chem., 42, 90 (1964).

56. E. Gileadi and B.E. Conway, J. Chem. Phys., 39, 3420 (1963).

57. J.O'M. Bockris, B.E. Conway and W. Mehl, J. Sci. Inst., 33, 400 (1956).

58. J. O'M. Bockris, Disc. Faraday Soc., 1, 229 (1947).

59. B.E. Conway and P. Bourgault, Can. J. Chem., 37, 292 (1959); Trans. Faraday Soc., 58, 593 (1962); also J.J. McDonald and B.E. Conway, Proc. Roy. Soc. (London), 269A, 419 (1962).

60. N. Sato, T. Sekine and K. Sugino, Extended Abstracts of Electro-organic Division of The Electrochemical Society Meeting, San Francisco (May 9-13, 1965), Abstract No. 167.

61. P. Dolin and B. Ershler, Acta Physicochim., U.R.S.S., 13, 747 (1940).

62. D. Gilroy and B.E. Conway, J. Phys. Chem., 69, 1259 (1965).

63. D. Gilroy and B.E. Conway, in course of publication.

64. F.D. Rossini, et al., "Selected Values of Chemical Thermodynamic Properties", U.S. Govt. Printing Office, Washington D.C.

65. B.E. Conway and J.O'M. Bockris, J. Chem. Phys., 26, 532 (1957).

66. B.E. Conway, E. Beatty and P.A.D. DeMaine, Electrochim. Acta, 7, 39 (1962).

67. J.O'M. Bockris and A.M. Azzam, Trans. Faraday Soc., 48, 145 (1952).

68. L. Eberson, Acta Chim. Scand., 17, 2004 (1963).

69. B.E. Conway and E. Gileadi, Trans. Faraday Soc., 58, 2493 (1962).

70. J.G.N. Thomas, Trans. Faraday Soc., 57, 1603 (1961).

71. J.O'M. Bockris and E.C. Potter, J. Electrochem. Soc., 99, 169 (1952).

72. H. Gohr and E. Lange, Z. Electrochem., 63, 673 (1958).

73. J.J. MacDonald and B.E. Conway, Proc. Roy. Soc. (London), A269, 419 (1962).

74. R.E. Meyer, J. Electrochem. Soc., 107, 847 (1960).

75. L. Young, Anodic Films, Academic Press, New York, 1961.

76. S. Gilman, Trans. Faraday Soc., 61, 2546 and 2561 (1965).

76a. S. Gilman, Electrochimica Acta, 9, 1025 (1964).

77. G.E. Coates, "Organo-Metallic Compounds", Methuen and Co. Ltd., London (1956).

78. J.A.V. Butler, Proc. Roy. Soc., London, A157, 423 (1936).

79. J.O'M. Bockris and R. Parsons, Trans. Faraday Soc., 47, 914 (1951).

80. J.O'M. Bockris and A.K.M. Huq, Proc. Roy. Soc. London, A237, 227 (1956).

81. F.F. Rawlings, G.W. Thiessen and Dean Peterson, Electrochem. Tech., 3, 154 (1965).

82. R.F. Garwood, C.J. Scott and B.C.L. Weedon, Chemical Communications, 1, 14 (1965).

83. L. Eberson, Acta Chem. Scand., 17, ~~1196~~ 2004 (1963).

84. M. Leung, J. Herz and H.W. Salzberg, J. Org. Chem., 30, 310 (1965).

85. C.J. Brockman, "Electro-Organic Chemistry", John Wiley & Sons, Inc., New York (1926).

86. W.B. Smith and H. Gilde, J. Am. Chem. Soc., 81, 5325 (1959).

87. W.B. Smith and H. Gilde, J. Am. Chem. Soc., 82, 659 (1960).

88. C.L. Wilson and T. Hayashi, Abstracts of papers presented at 126th meeting of The American Chemical Society, New York, N.Y., pp. 78-80 (1954).

89. E.J. Corey, N.L. Bauld, R.T. Lalonde, J. Casanova, Jr., and E.T. Kaiser, J. Am. Chem. Soc., 82, 2645 (1960).

90. M. Fleischmann, J.R. Hansfield and W.F.K. Wynne-Jones, J. Electroanal. Chem., 10, 511, 522 (1965).

91. B.I. Podlovchenko, O.A. Petry, A.N. Frumkin, and H. Lal, J. Electroanal. Chem., 11, 12 (1966).